DESIGN OF VIRAL VECTORS FOR IMPROVED GENE DELIVERY

IVY HO AI-WEI
(MSc, Leicester University, UK)

A THESIS SUBMITTED FOR

THE DEGREE OF DOCTOR OF PHILOSOPHY

DEPARTMENT OF PHYSIOLOGY

NATIONAL UNIVERSITY OF SINGAPORE

2004

ACKNOWLEDGEMENTS

First and foremost, I am grateful to Dr. Paula Lam for supervising this project and for her endless support, guidance, advice and friendship.

I would like to extend my gratitude to Prof. Hui Kam Man for valuable ideas and discussions throughout the duration of this project.

I would also like to thank Dr. Wang Nai-dy for his support and contributions to this project.

I would also like to acknowledge Dr. R Müller (Institute of Molecular Biology and Tumor Research, Germany) for providing us with the plasmids CMV.GN and 8GalcycA, Dr. PD Nisen (University of Texas Southwestern Medical Center, Dallas, TX) for providing us with the glial specific promoter, Dr. MV Clement (National University of Singapore, Singapore) for providing the cDNA for FADD, and Dr. Thomas J (Department of Neurosurgery, Singapore General Hospital) for providing us with the primary glioma biopsy.

This research is supported by grants from the Singapore Biomedical Research Council, Singapore National Medical Research Council and Singhealth Cluster Research Grant.

My sincere appreciation to past and present members of the lab, especially Gan Shu Uin and Gao Hui, who have provided immense support during trying moments. Thanks also to members of the Laboratory of Cancer Genomics for the fun and laughter; I have enjoyed our many excursions together.

Finally, I would like to express my deepest gratitude to my family and friends for their support and encouragement.

TABLE OF CONTENTS

SUMMARY

The major challenge of cancer gene therapy trial is the ability to target transgene expression to a particular tumor cell type. As uncontrolled proliferation is a common characteristic of malignant tumor cells, an attractive strategy for cancer gene therapy would be the use of vectors carrying therapeutic genes that can be activated upon cellular replication. This strategy may be of special clinical relevance for brain tumor therapy. One of the clinical pathology of glioma is its highly invasive and diffuse nature, thus render complete surgical resection impossible. In this study, we have attempted to design vectors by the incorporation of regulatory elements that allow proliferation-dependent gene expression.

We have constructed a HSV-1 amplicon viral vector whereby the transgene expression is controlled by cell cycle events. The strategy adopted is based on a G_0/G_1 specific transcriptional repressor protein, CDF-1, that interacts with regulatory elements on the cyclin A promoter. In non-dividing cells, the activation of the cyclin A promoter by an upstream transactivator, Gal4/NF-YA fusion protein, is prevented by the presence of the CDF-1 protein. In actively proliferating cells, transactivation could take place due to the absence of CDF-1. Our results demonstrated that when all of these cell cycle-specific regulatory elements are incorporated *in cis* into a single HSV-1 amplicon plasmid, the reporter luciferase activity is greatly enhanced. As a further safety mechanism, the transgene cassette is placed under a glial cell-specific promoter for glial cell specific transcription since most recurrent brain tumors originate from glial-derived cells. When these amplicon plasmids are packaged into infectious but replication-defective HSV-1 amplicon viral vectors, the luciferase reporter expression could be regulated in a glial cell specific and proliferation-dependent manner in a variety of human glioma cell lines. These viral vectors are also demonstrated to be effective at delivering therapeutic genes to actively proliferating tumor cells in glioma xenografts.

In addition, we have screened the phage display library for a glioma-specific sequence with the aim of identifying molecules that target to glioma cells. We have isolated a novel human glioma-specific peptide, MG11, which could target exogenous DNA specifically to a wide array of human glioblastoma cells, *in vitro* and *in vivo*. The isolation of this MG11 peptide provides the means to conjugate therapeutic agents for targeting. The combination of these two strategies would ensure only those rapidly proliferating glioma cells that express the receptor for the MG11 peptide would be infected by the amplicon vector, thus greatly facilitate the expression of therapeutic gene to glioma cells. More importantly, the amount of viruses needed to achieve a therapeutic response would be significantly reduced; hence, potential side effects could be correspondingly minimized.

In summary, we have designed an HSV-1 amplicon based gene delivery system that is (i) capable of incorporating a large transgene capacity; (ii) stable; (iii) safe; (iv) regulatable; (v) capable of targeting to glioma cells.

LIST OF TABLES

LIST OF FIGURES

ABBREVIATIONS

Ad	Adenovirus
ANOVA	Analysis of variance
BAC	Bacterial artificial chromosome
BBB	Blood-brain barrier
bp	Base pair
CDE	Cell cycle-dependent element
CDF-1	Cell cycle-dependent factor 1
CHR	Cell cycle genes homology region
CMV	Cytomegalovirus
EGFR	Epidermal growth factor receptor
FACS	Fluorescence activated cell sorter
FADD	Fas-associated protein with death domain
FasL	Fas ligand
GBM	Glioblastoma Multiforme
gC	Glycoprotein C
GCV	Ganciclovir
GFAP	Glial fibrillary acidic protein
GFP	Green fluorescent protein
H&E	Hematoxylin and Eosin
HSV-1	Herpes Simplex Virus Type 1
HSV-tk	Herpes simplex virus thymidine kinase gene
i.c.	Intracranial
i.v.	Intravenous
ICP	Infected cell protein
IE	Immediate early
kb	kilobase
kDa	kiloDalton
MOI	Multiplicity of infection
MRI	Magnetic resonance imaging
NF-YA	Nuclear factor Y subunit A
PFU	Plaque forming unit
PHx	Partial hepatectomy
PI	Propidium iodide
pRb	Retinoblastoma protein
RLU	Relative light unit
RR	Ribonucleotide reductase
r.t.	Room temperature
s.c	Subcutaneous
SCID	Severe combined immunodeficient
SEM	Standard error of mean
TMZ	Temozolomide
TU	Transduction unit
TU/ml	Transduction unit per ml
TUNEL	Terminal-dUTP nick end labeling

LIST OF PUBLICATIONS

Publications

1. Ivy AW Ho, Kam M Hui and Paula YP Lam. (2004). Glioma-specific and cell cycle-regulated Herpes Simplex Virus Type 1 amplicon viral vector. Hum Gene Ther 15(5): 495-508.

2. Ivy AW Ho, Paula YP Lam and Kam M. Hui. (2004). Identification and characterization of novel human glioma-specific peptides to potentiate tumor-specific gene delivery. Hum Gene Ther 15(8): 719-732.

3. Ivy AW Ho, Kam M Hui and Paula YP Lam. (2005). Targeting proliferating tumor cells via the transcriptional control of therapeutic genes. Cancer Gen Ther. *In press.*

Oral/Poster Presentations

1. Ivy AW Ho, Paula YP Lam and Kam M. Hui. (2004). Identification and characterization of novel human glioma-specific peptides to potentate tumor-specific gene delivery. International Society for Cancer Gene Therapy 2004 Singapore Conference, 21st-22nd February, Singapore. Oral presentation, 2nd prize.

2. Ivy AW Ho, Kam M. Hui and Paula YP Lam. (2004). Selective induction of apoptotic cell death mediated by FasL using the HSV-1 amplicon viral vector. International Society for Cancer Gene Therapy 2004 Singapore Conference, 21st-22nd February, Singapore. Poster presentation.

3. Paula YP Lam, Jenn-Hui Khong, Kar Sian Lim, Ivy Ho and Kam M Hui. (2004) Transcriptional targeting to liver cells. International Society for Cancer Gene Therapy 2004 Singapore Conference, 21st-22nd February, Singapore. Poster presentation.

4. Ivy AW Ho, Kam M. Hui and Paula YP Lam. (2003). A novel molecular strategy to target proliferating tumor cells. Keystone Symposium on Molecular Targets for Cancer Therapeutics, 19th March-24th March, Banff, Alberta, Canada. Poster presentation.

5. Ivy AW Ho, Kam M. Hui and Paula YP Lam. (2002). Development of a cell cycle-regulated and cell type-specific HSV-1 amplicon viral vector. The 4th Annual meeting of the American Association of Gene Therapy, Boston, USA. Poster presentation.

Patents

1. Compositions and methods for treatment disease. Application No. 2004901220. March 2004.

2. Materials and methods relating to the treatment of gliomas. Application No. 0405482.1. March 2004.

Chapter 1

Introduction

1.1 Brain tumors

Tumors of the central nervous system (CNS) are the most prevalent neoplasm of childhood and also one of the leading cancer-related causes of death in adults (Alemany et al., 1999). Recent World Health Organization (WHO) classification grades the astrocytic tumors into pilocytic astrocytoma (grade I), fibrillary astrocytoma (grade II), anaplastic astrocytoma (grade III) and glioblastoma multiforme (GBM) (grade IV), with GBM being the most malignant and lethal subtype of brain tumor (Kleihues et al., 2002). GBM are highly heterogeneous, consisting of pleiomorphic cells and microvascular infiltrations, as well as regions of pseudopalisading necrosis. Glioma cells can also be detected at the perivascular and intrafascicular regions (Holland, 2000). Genetic abnormalities of GBM consist of various deletions, amplifications, and point mutations leading to activation of signal transduction pathways downstream of tyrosine kinase receptors, such as epidermal growth factor receptor (EGFR) and platelet-derived growth factor receptor (PDGFR). Other aberrations frequently observed in GBM include mutations in the *p53* tumor suppressor gene, amplification of *cyclin dependent kinase 4 (CDK4)*, loss of the *retinoblastoma (pRb)* gene as well as mutation in the *INK4a-ARF* locus, which encodes two gene products ($p16^{INK4a}$ and $p14^{ARF}$) involved in cell-cycle arrest and apoptosis (Castro et al., 2003a; Lam and Breakefield, 2001; Ng and Lam, 1998).

GBM that develop *de novo* are known as primary glioblastomas, while those that progress from low grade anaplastic astrocytoma are known as secondary glioblastoma (Figure 1.1). Although both tumor types eventually manifest as GBM, the molecular pathway leading to the development of GBM is different. Primary glioblastoma are characterized by the amplification of the transmembrane receptor *EGFR* (Louis and Gusella, 1995; von Deimling et al., 1993) and the *mouse double minute 2 (mdm2)* genes (Biernat et al, 1997). The frequency of *EGFR* amplification correlates with the progression of tumorigenicity, with 3 % of amplifications detected in low-grade astrocytoma and 40 % in high-grade GBM. A common mutation of the *EGFR* gene in human gliomas consists of an in-frame deletion of

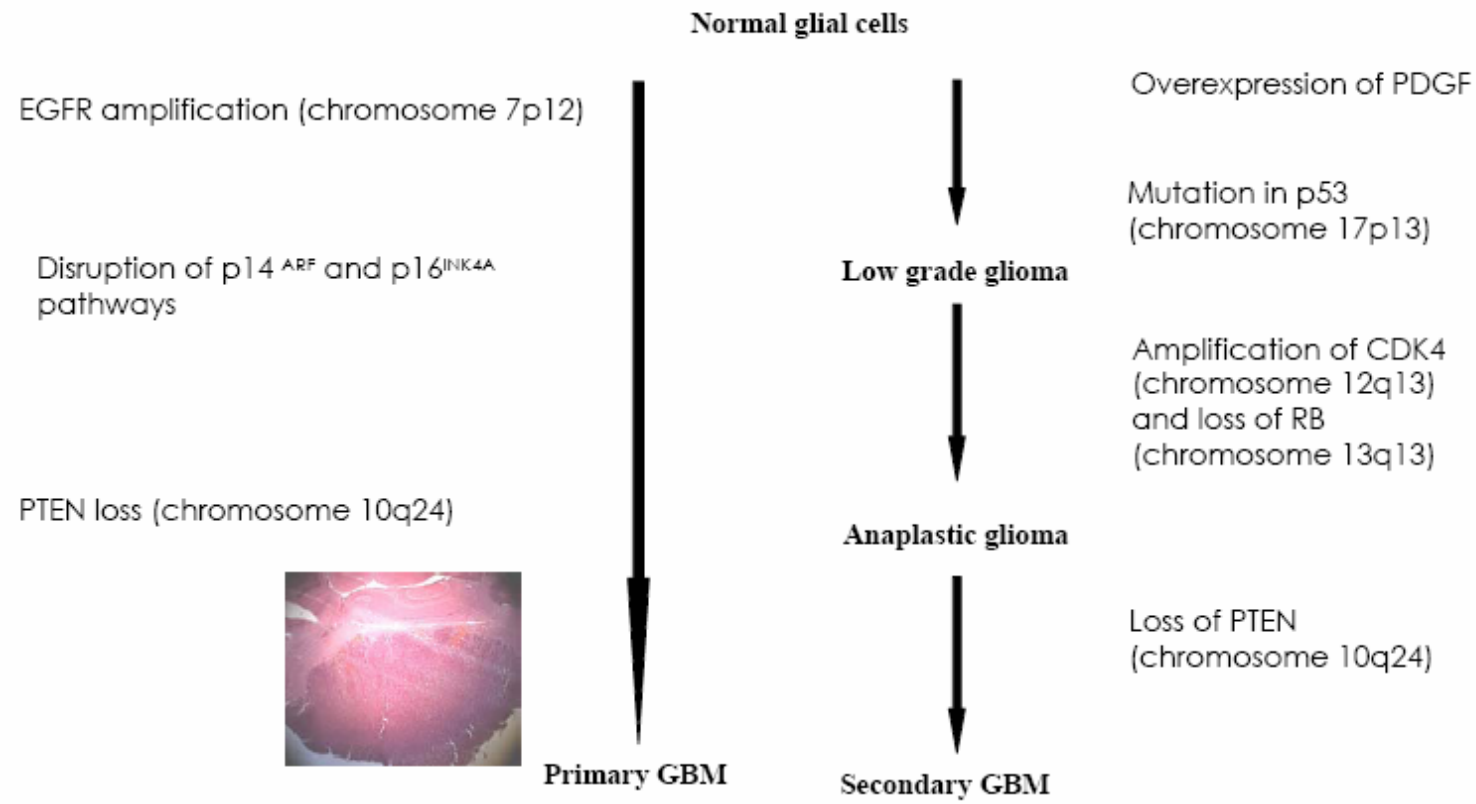

Figure 1.1. Pathways to gliomagenesis.
GBM can arise *de novo* as in the case of primary GBM, or progress from low grade astrocytoma to high grade astrocytoma through the acquisition of additional mutations. H&E pictures showed the typical phenotype of human glioma cells implanted into the brain of immunodeficient mice.

exons 2-7 from the extracellular domain. As a result, constitutively phosphorylated delEGFR enhances cellular proliferation and reduces apoptosis of human glioma cells (Nagane et al., 1996). Overexpression of mdm2 has been observed in more than 50 % of primary GBM, and is a characteristic of primary GBM that lacks a p53 mutation (Biernat et al., 1997). Interestingly, mutation in p53 or loss of heterozygosity (LOH) of chromosome 17p, which is a characteristic of secondary GBM, is almost never found in these primary GBM (von Deimling et al., 1993). In addition to *p53* mutation, which is present in more than 30 % of astrocytoma (Nigro et al., 1989; Sidransky et al., 1992), and LOH of chromosome 17p (von Deimling et al., 1993), the level of PDGFR-α is also elevated in secondary GBM (Castro et al., 2003b; Dunn et al., 2000; Sidransky et al., 1992).

In Asian countries such as Singapore, the incidence of astrocytic tumors represent only one third or less compared to that of the western countries (Das et al., 2002). The genetic profiles of Asian glioma patients do not appear to follow the conventional molecular pathways that define either primary or secondary GBM. In these studied cases, p53 was frequently detected to be overexpressed and did not present as mutually exclusive to the aberrant *EGFR* gene. Thus, molecular pathway leading to the development of GBM may be different in these patients. The trend may also be influenced by the small number of patients being studied as a result of lower rate of occurrence.

Two of the frequent abnormalities observed in GBM are the inactivation of the cell cycle regulators pRb and p16, and the amplification of cyclin D1 and cdk4 (Fueyo et al., 1996; Ueki et al., 1996) (Figure 1.1). p16 specifically inhibits the binding of cdk4 to cyclin D1, thus preventing the phosphorylation of the pRb protein and the subsequent progression of the cell cycle. Another common mutation is the LOH of chromosome 10 (von Deimling, 1997, 1993), the location of the tumor suppressor gene MMAC (mutated in multiple advanced cancers)/PTEN (phosphatase and tensin homologue deleted from chromosome 10), which is mutated in 30 % of malignant gliomas (Li et al., 1997; Steck et al., 1997) (Figure 1.1).

MMAC/PTEN is dependent on its lipid phosphatase activity to inhibit the phosphatidylinositol-3'-kinase (PI3K)/Akt pathway through the dephosphorylation of phosphatidylinositol-(3, 4, 5)-triphospate. Restoration of its activity leads to suppression of the neoplastic phenotype in glioma cells (Cheney et al., 1998).

1.2 Invasiveness of glioma cells

The prognosis of brain tumors, in particular GBM, remains dismal despite advances in neurosurgical techniques, radiation and drug therapies (Kleihues et al., 2002; Walter et al., 1995). One of the major difficulties encountered include single cell invasion of surrounding histologically normal brain parenchyme, forming perineuronal and perivascular satellitosis (Holland 2000), and migration through the white matter tracts to regions distant from the original tumor mass. These invasive cells can be found in normal brain tissues up to 4 cm beyond the visible tumor mass (Silbergeld and Chicoine, 1997), with 80 % of cases appearing in the opposite hemisphere (Figure 1.2). Despite therapeutic interventions, the infiltrating tumor cells continue to proliferate, leading to recurrences (Burger et al., 1983; Gaspar et al., 1992) (Figure 1.3) most frequently a few centimeters beyond the margins of resection (Damek and Hochberg, 1997).

1.3 Current treatment regime for brain tumors

Current therapy for glioma includes a combination of surgery, radiotherapy and chemotherapy, with majority of the tumor mass removable by surgical resection. Surgical debulking of the tumor mass reduces intracranial pressure and extends the survival of patients, enabling them to receive further treatment. Since majority of the tumor mass has been removed, the amount of therapeutic agents required to efficiently eradicate residual tumors is correspondingly decreased. Residual tumor can be removed by exposure to radiation or through chemotherapy. Radiation therapy is usually confined to the residual tumor mass and 2 cm of surrounding normal tissues (Castro et al., 2003a). If the tumor is well defined, measures less than 5 cm in diameter, and is surgically accessible, interstitial radiation therapy or brachytherapy, where

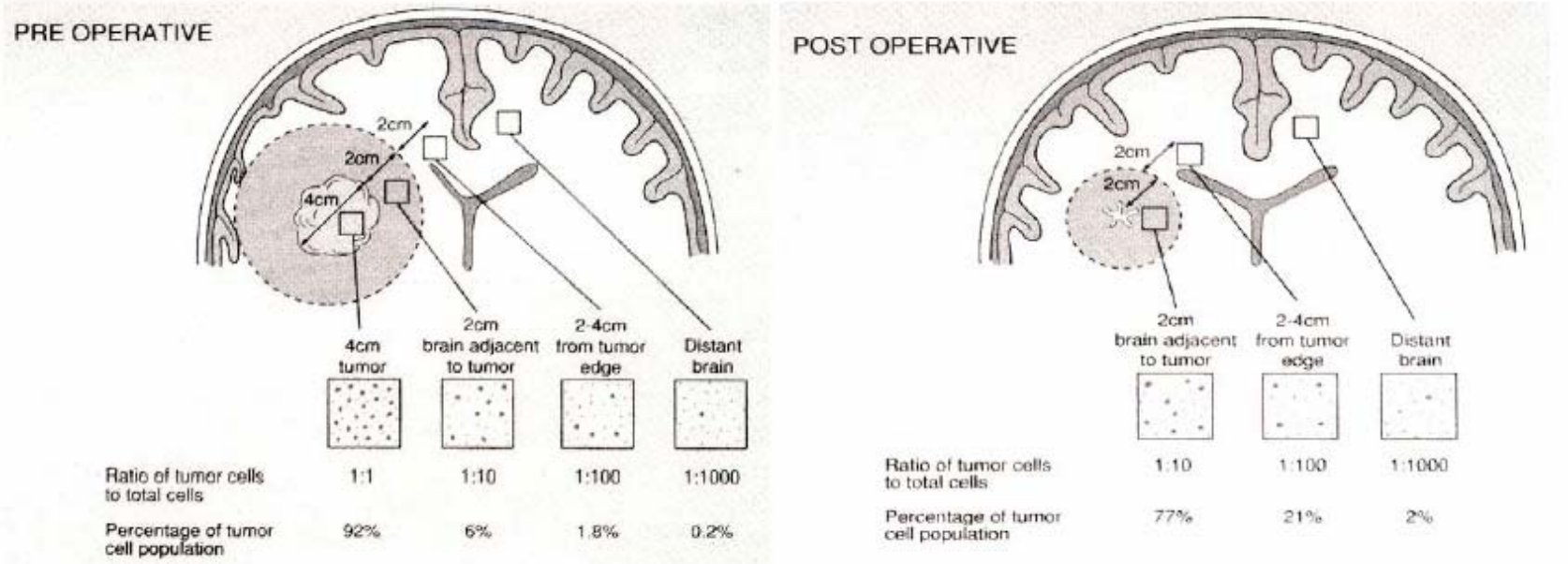

(Enam *et al.*, 1998)

Figure 1.2. A model predicting the rate of recurrences after surgical resection.
This model predicts that as the tumor mass is surgically removed, the distant infiltrated tumor cells have a higher chance to develop into recurrences at regions distant away from the original tumor mass.

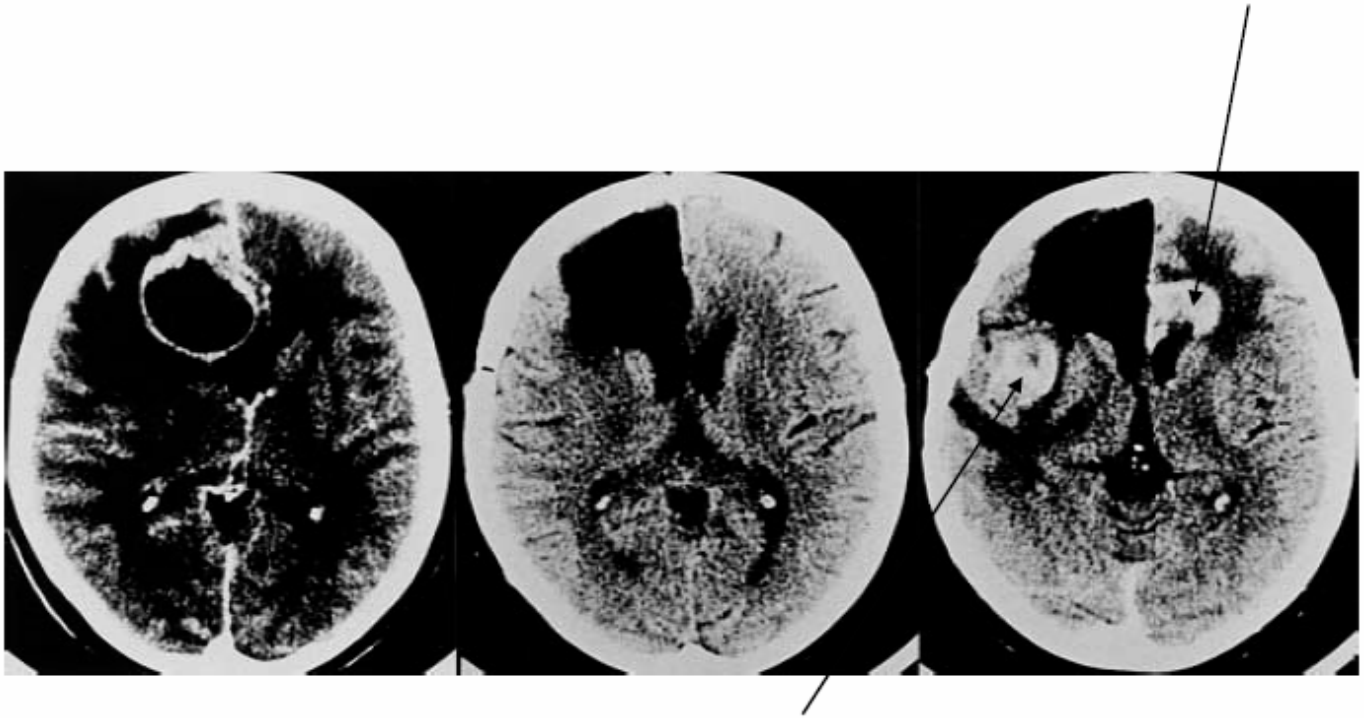

(Giese and Westphal, 2001)

Figure 1.3. MRI scans of a patient with GBM illustrating the spread of the disease.
Left panel: Tumor mass was observed in the left hemisphere. Middle panel: Complete surgical resection was performed followed by conventional radiotherapy. Right panel: Multifocal, recurrent tumors were detected near surgical resected region after ten months. Arrows indicate recurrent tumors.

radioactive pellets are implanted into the tumor mass, can be employed to kill the cancerous cells, yet sparing the normal brain tissues (Castro et al., 2003a). Chemotherapy can be used on its own or in combination with surgery and radiotherapy. However, the drawback is that most GBM are refractory to treatment with chemotherapeutic drugs, which damages the bone marrow of patients, and also, most chemotherapeutic drugs are not able to pass through the blood brain barrier (BBB).

1.3.1Why do current therapies fail?

Although current combination therapy increases the median survival time of patients, these malignant gliomas are eventually lethal. Lack of defined tumor edge and inaccessibility of the tumor to resective surgery when the tumor is located at or near critical areas renders complete surgical resection virtually impossible. In addition, gliomas are very heterogeneous. Within a tumor, most cells have varying subsets of genetic alterations as mentioned earlier (section 1.1), and some tumor cells may temporarily exit the cell cycle, thus making them resistant to therapy that targets proliferating cells (Lam and Breakefield, 2001; Ng and Lam, 1998). Moreover, cells within the GBM can have different sensitivity to chemotherapeutic drugs, giving rise to chemo-resistant clones (Castro et al., 2003a). Conventional chemotherapy lacks tumor specificity and is only effective against actively proliferating cells (Drewinko et al., 1981). Quiescent cells that survive chemotherapy will eventually re-enter the cell cycle resulting in relapse of the tumor. Residual tumor cells cannot be efficiently controlled by radiation therapy due to the high occurrence of radioresistant glioma cells (Leibel et al., 1994). In addition, the presence of efflux pumps such as P-glycoproteins, organic anion transporters, and multidrug resistance-associated proteins in the BBB acts as a barrier against efficient delivery for most drugs (Castro et al., 2003a).

1.3.2 Gene therapy of gliomas

One of the formidable tasks of intracranial gene delivery is the difficulty in achieving gene delivery to > 5 % of the tumor mass. It would be advantageous if the transduced cells are

able to exert a therapeutic effect on neighboring nontransduced tumor cells ("bystander effect"). One of the strategies for targeting glioma cells is the utilization of the pro-drug activation system. These prodrugs are nontoxic, and can be administered systemically and readily cross the BBB. This approach is called "suicide" gene therapy as the transduced cells convert the non-toxic prodrug into a toxic nucleoside analog, allowing it to be incorporated into the replicating DNA, thus killing the cells (Ilsey et al., 1995). The Herpes simplex virus type-1 (HSV-1) thymidine kinase (tk)/ganciclovir (GCV) system is one of the well-characterized prodrug activation systems. On its own, GCV is non-toxic to both non-transduced cells and non-proliferating cells. However, in proliferating cells, phosphorylation of GCV by tk converts it into a toxic metabolite which inhibits DNA replication, thus leading to cell death (Matthews and Boehme, 1988). Bystander effect is achieved when phosphorylated GCV passes through gap junctions between adjacent cells thus killing non-transduced cells (Culver, 1992; Elshami et al., 1996; Freeman et al., 1993; Moolten and Wells, 1990; Takamiya et al., 1993). Other prodrug activating systems such as the *Escherichia coli* (*E. coli*) cytosinedeaminase/5-fluorocytosine (CD/5FC), cytochrome P450 2B1/cyclophosphamide (CPA) (Jounaidi et al., 2004), *E. coli* nitroreductase/CB1954 (Bridgewater, 1995; 1997), and purine nucleoside prodrugs activated by viral thymidine phosphorylase (Hughes et al., 1998), have been demonstrated to have selectivity towards tumor cells (Aghi et al., 2000).

In addition to inducing bystander effect, tumor cells can be eradicated by the introduction of apoptotic genes, thus increasing the chances of immune recognition of tumor antigens. One of the commonly used tumor suppressor genes for the therapy of gliomas is p53, which plays a central role in the regulation of cell growth and apoptosis (Ravi et al., 1998). p53 activates the transcription of a series of downstream apoptosis effector genes such as bcl-2, bax, p21 and others. Mutations in p53 are found in more than 50 % of human tumors. Loss or mutation of p53 has been shown to promote genomic instability leading to deregulated

proliferation of tumor cells, apoptosis, and enhanced angiogenesis in tumor progression (Albertoni et al., 1998; Ravi et al., 1998).

Other promising novel therapeutic genes for glioma therapy include genes that target angiogenenic factors. A tumor nodule cannot derive nutrients through diffusion when its tumor size exceeds 1-2 mm^3; additional growth requires generation of new blood vessels, or angiogenesis (Folkman, 1972). GBM has many characteristics of an angiogenesis-dependent tumor. The rate of tumor growth and neovascularization increases as gliomas progress from low-grade astrocytoma to high-grade GBM. This correlates with the level of vascular endothelial growth factor (VEGF), where the level is highest in GBM (Plate and Risau, 1995). Strategies employing anti-angiogenic factors have been used for the treatment of gliomas, for instance, antisense VEGF (Saleh et al., 1996) , transforming growth factor β (TGF) (Paul and Kruse, 2001), dominant-negative vascular endothelial growth factor receptor 2 (Flk-1) (Millauer et al., 1994), and platelet factor 4 (Tanaka et al., 1997).

1.4 Criteria of an ideal delivery vector system

The success of gene therapy is highly dependent on the effectiveness of a vector to deliver the therapeutic genes in a specific and controllable manner. An ideal vector would be one that incorporates a large transgene capacity that allows for the insertion of multiple regulatory or transgene cassettes. In addition, the expression of heterologous genes in mammalian cells for therapeutic purposes using this vector should meet the following criteria: vector exhibits no background gene activity in the "off-state" but rapidly achieves high levels of expression upon induction; the system should not respond to endogenous activators or interfere with cellular regulatory pathways; has a minimum immunological profile; and expression levels of a given gene is regulatable in a stable and controlled manner. Furthermore, the vector has to be targeted to specific cell types. One of the greatest challenges to cancer gene therapy is the lack of tumor specificity, which frequently causes side effects as well as limits the therapeutic

dosage. Targeting the vector to a specific cell type would restrict the amount of DNA required to achieve therapeutic responses while minimizing toxicity to non-target cells.

1.5 Delivery Modalities

The dismal prognosis for malignant glioma patients in spite of improvement in current therapeutic modalities has resulted in the exploration of new approaches to therapy, such as using viral or non-viral vehicles to deliver "weapons" for eradication of tumor cells. Each of these approaches has its pros and cons relating to its specificity and efficacy (Table 1.1). Non-viral vectors plasmid DNA complexed with liposome or polymers. Gene transfers to the brain using non-viral vectors have been demonstrated by Schwartz et al. (1996) and Brooks et al. (1998). Although transgene expression can be detected in the striatum, the efficiency of gene transfer still lags behind that of the viral delivery system, which is more efficient at delivering genes to cells than any synthetic reagents devised so far. Different viruses have different abilities to target certain cell types. Retroviruses and adenoviruses (Ad) are the two most commonly used viral vectors for gene delivery. Retroviruses confer stable transgene expression due to its propensity to integrate into the host genome; however, the random insertion might activate the transcription of oncogene or proto-oncogene, which might be deleterious. Retrovirus selectively infect only dividing cells, thus making this vector a promising choice for use in brain tumor therapy. Retrovirus was also employed in a phase III clinical trials for glioma therapy (Rainov, 2000). Adenoviruses have the advantage of infecting both dividing and non-dividing cells and are able to confer transient high level of gene expression. However, Ad vector has been shown to induce host immune response, which is detrimental to the gene delivery process and the recipient. Alternatively, adeno-associated vector (AAV) is non-pathogenic and non-cytotoxic, and can integrate into specific sites on the genome of both dividing and non-dividing cells. The limitation of AAV is its relative small size, which can incorporate only ~ 4 kb of transgene. In comparison, advantages of the HSV-1 amplicon vector include its large insert capacity, low toxicity and low immunogenicity, however, the transgene expression is relatively instable, and production

Table 1.1 Vectors and delivery systems for gene therapy

Vectors	Advantages	Disadvantages
Non-viral vectors	• easy to produce	• low gene transfer efficiency • transient gene expression
Retrovirus	• stable gene expression due to viral genome integration • only infect dividing cells	• random insertion of viral genome, may possibly cause mutagenesis; • limited transgene capacity (~8kb)
Adenovirus	• transient high level of gene expression • infect dividing and nondividing cells	• host immune response • limited transgene capacity (~8kb)
Adeno-associated Virus	• integrate into genome of dividing and nondividing cells • nonpathogenic • noncytotoxic	• difficult to obtain high titer of pure virus • helper virus required for propagation • limited transgene capacity (~4kb)
HSV-1 Recombinant	• large transgene capacity • transduce dividing and nondividing cells	• immunogenic, some toxicity • instability of transgene expression
Amplicon	• as above • low toxicity and low immunogenicity	• vector production depends on transfection of cells • instability of transgene expression

of viruses is dependent on transfection, therefore, it is difficult to obtained high titer vector for clinical purposes. Ad (Kumar-Singh and Farber, 1998; Lieber et al., 1997; Morsy et al., 1998; Thomas et al., 2000), lentiviruses (LV) (Baekelandt et al., 2002), retrovirus (Culver et al., 1992; Rainov, 2000; Rainov and Kramm, 2001), AAV, and HSV-1 have been used for delivering therapeutic genes to the brain with varying success.

1.5.1 HSV-1 vectors

1.5.1.1 Biology of HSV-1 vectors

HSV-1 is an enveloped virus containing 150 kb of double-stranded (ds) DNA encoding approximately 80 genes (Roizman and Sears, 1996). The virion consists of four components; (1) a lipid envelope that contains glycoproteins which are responsible for receptor-mediated entry (Burton et al., 2001; Rajcani and Vojvodova, 1998; Spear, 1993); (2) the tegument which contains some of the viral regulatory proteins such as the virion host shut-off (vhs) protein and the VP16 transcriptional activator; (3) the icosadeltahedral capsid and (4) the core containing dsDNA (Burton et al., 2001) (Figure 1.4). The tegument proteins are responsible for the induction of viral gene expression e.g. VP16 (Batterson and Roizman, 1983), or for switching-off host protein synthesis following infection e.g., vhs (Kwong et al., 1988; Read and Frenkel, 1983). The viral genome consists of long and short unique segments (U_L and U_S) flanked by repeated sequences (Roizman and Sears, 1996) (Figure 1.4). The approximately 80 genes encoded by the viral genome can be divided into non-essential and essential genes, depending on whether their functions are required for viral replications *in vitro*. The non-essential genes can be deleted in the construction of gene delivery vectors, hence allowing the insertion of exogenous DNA and at the same time, reducing cytotoxicity resulting from expression of viral proteins (Krisky et al., 1998).

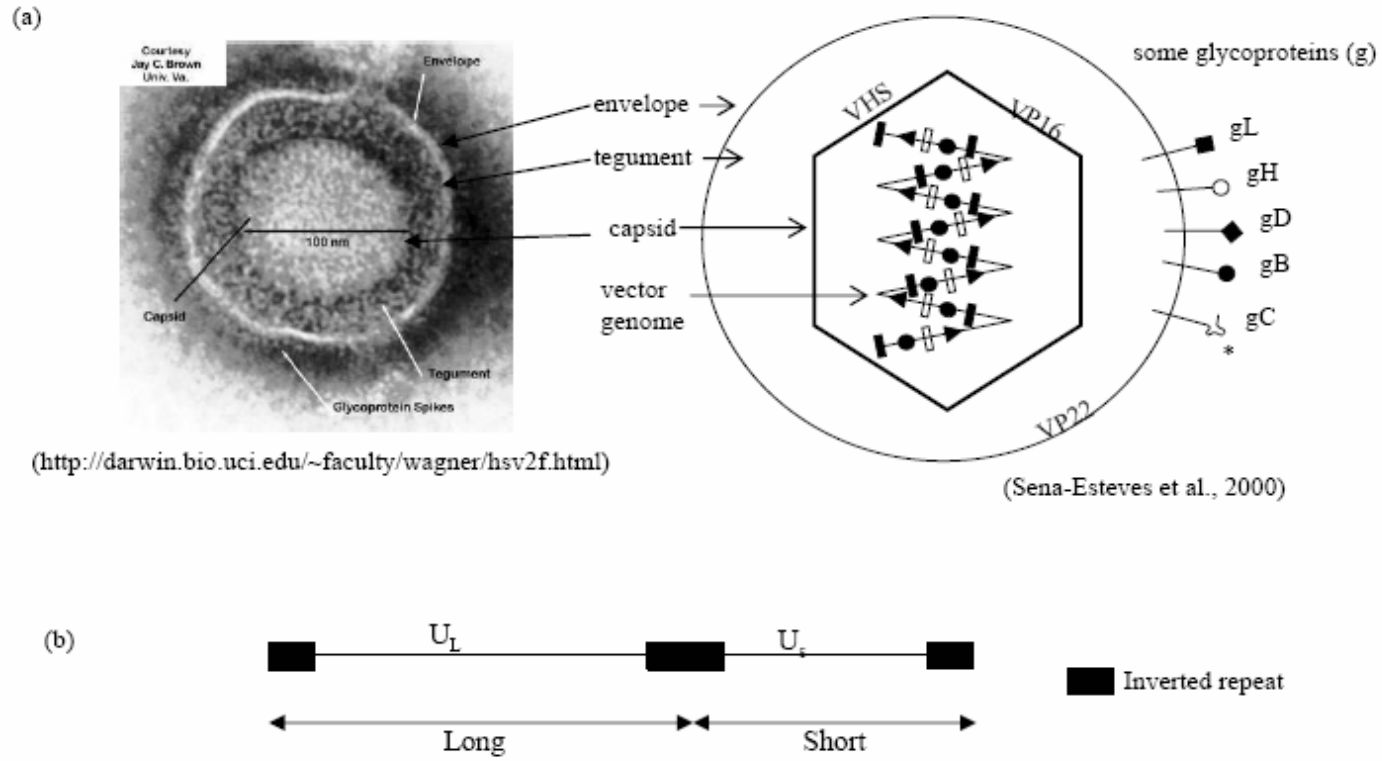

Figure 1.4. Herpes Simplex Virus Type-1
(a) The HSV-1 particle consists of cell surface glycoproteins, lipid envelope, the tegument protein and the capsid which contains the 150 kb of dsDNA. (b) The genome of the HSV-1 can be divided into long and short unique elements, each flanked by inverted repeat sequences.

HSV-1 is neurotrophic; in neurons, HSV vectors are transported from the nerve terminal into the cell body by retrograde transport. The virion enters the cell by fusion of the envelope with the cell plasma membrane through the envelope glycoproteins, notably glycoprotein D (gD) and B (gB). The viral DNA is subsequently deposited in the nucleus. Immediately after viral entry into the cells, both the viral DNA and the VP16 tegument protein are transported to the nucleus (Roizman and Sears, 1996). The lytic pathway of HSV-1 infection is characterized by sequential expression of immediate early (IE), early (E), and late (L) gene products. VP16 induces the expression of the IE gene products, *ICP0*, *ICP4*, *ICP22*, *ICP27* and *ICP47* (Wysocka and Herr, 2003). Both *ICP4* and *ICP27* genes are required for the expression of the E and L genes thus, the replication of the virus in cell culture (DeLuca et al., 1985; Sacks et al., 1985). Expressions of these IE genes initiate the transcription of the E genes and the L genes (Roizman and Sears, 1996; Sacks et al., 1985). However, during latency, the viral genome remains as an episomal element with no IE, E or L genes expressed. During this phase, only a set of nontranslated transcripts, namely the latency-associated transcripts (LAT) are produced in the infected cells (Burton et al., 2001). The viruses remain dormant for a long period of time until changes in the host-virus interaction occur. As a result, viral infection might be reactivated, and the transcription of the viral genome resumes in the lytic phase.

1.5.1.2 HSV-1 vectors as gene delivery vehicles

HSV-1 vectors are attractive vehicles for gene therapy due to their broad host range, large transgene capacity, and their ability to transduce both non-dividing and dividing cells. Vectors that are based on HSV-1 are attractive for gene delivery to the brain because HSV-1 can efficiently infect neuronal cells as well as other cell types, and can persist indefinitely in neurons (Lachmann, 2004). There are three types of HSV-1 vectors, the recombinant HSV-1, the replication competent HSV-1, and the replication defective HSV-1 amplicon vectors.

1.5.1.2.1 Recombinant HSV-1

Recombinant HSV-1 vectors contain the full viral genome with mutations in one or more viral genes. First generation HSV-1 vectors contained a mutation in the VP16 transactivator which prevents it from interacting with the IE genes (Ace et al., 1989). However, when administered at high concentration, these first generation vectors were capable of undergoing full productive replication. Further attempts at reducing the virulence were introduced, by constructing temperature-sensitive deletion mutants that were devoid of *ICP4* and contained a mutation in *ICP0* (Preston et al., 1997; 1998). These viruses could be propagated in the presence of a complementing cell line that expressed ICP0 at 31 °C. Samaniego et al. (1997; 1998) further attempted to modify the vectors by deleting other IE gene products. The mutant virus, *d109*, carries multiple deletions of the IE genes, *ICP0*, *ICP4*, *ICP22*, *ICP27* and *ICP47*. Deletion of these IE genes allowed the incorporation of 30-50 kb of foreign DNA into the vector genome. These replication defective virus mutants could thus be packaged in complementing cell lines expressing these gene products (ICP0, ICP4 and ICP27) *in trans*.

1.5.1.2.2 Replication competent HSV-1

The first replication competent oncolytic HSV-1 vector was constructed in 1991 (Mineta et al., 1994; Varghese and Rabkin, 2002) for the treatment of glioma. This replication competent HSV-1 was generated from a single mutation of its viral enzymes that are involved in nucleotide metabolism, such as TK (Martuza et al., 1991) and ribonucleotide reductase (RR) (also known as *ICP6*) (Mineta et al., 1994; Boviatsis et al., 1994b), which is required for the conversion of ribonucleotides to 2'-deoxyribonucleotides that provide the precursors for both DNA synthesis and repair (Kolberg et al., 2004). These viral enzymes are upregulated in cancer cells in contrast to normal postmitotic cells. One such mutant, hrR3, which contains a deleted RR gene, selectively replicates in cells that contain high levels of RR, such as tumor cells. The hrR3 also harbors an insertion of the *lacZ* gene into the *ICP6* locus which allows the tracking of the virus. This mutation in the *ICP6* locus reduces neurovirulence (Cameron et al., 1988; Yamada et al., 1991). HrR3 has been used for the treatment of gliomas because it

also contains the TK gene. The efficacy of hrR3 has been shown to be specific for gliosarcoma tumor cells, hence not affecting the postmitotic neural cells (Boviatsis et al., 1994a; Mineta et al., 1994; Spear et al., 2000).

Second generation replication competent HSV-1 vectors, such as G207 (MGH-1) were constructed with multiple deletions or mutations to enhance safety. G207 contains deletion in both copies of the *γ34.5* gene, a virulence factor that suppresses the total shut-off of protein synthesis (Chou and Roizman, 1992), as well as inactivation of *ICP6*. These modifications prevent reversion and ensure that G207 only replicates in cells that contain RR. No adverse effect could be detected when 10^7 plaque forming units (pfu) of G207 were injected directly into the ventricles of mice and non-human primates (Hunter et al., 1999; Sundaresan et al., 2000; Varghese et al., 2001). In fact, G207 has been found to be effective against a variety of solid tumors, including melanoma, breast, colon, gallbladder, gastric, head and neck, ovarian, pancreatic and prostate cancers (Varghese and Rabkin, 2002). HSV1716, another replication competent HSV-1 with deletion in the *γ34.5* gene, was also used for the treatment of glioma in a proof of principle study (Papanastassiou et al., 2002). Direct injection of this virus into glioma has been shown to prolong the survival of patients in clinical trials (Harrow et al., 2004).

1.5.1.2.3 Replication defective HSV-1 amplicons

The HSV-1 amplicons are plasmid-based vectors that consist of (1) sequences from bacteria such as the origin of replication and the *β-lactamase* gene, (2) sequences from HSV-1, including a packaging signal (*pac*) and an origin of DNA replication (ori_s), allowing them to be packaged as concatemers into virions in the presence of HSV helper functions (Spaete and Frenkel, 1982; Spaete and Frenkel, 1985), (3) multiple cloning sites for insertion of foreign DNA, and (4) a reporter gene, such as enhanced green fluorescent protein (eGFP) for titering of vector stocks (Figure 1.5). These vectors have broad host range and yet retain the neurotrophic properties of HSV-1. Since they are largely devoid of any viral sequences

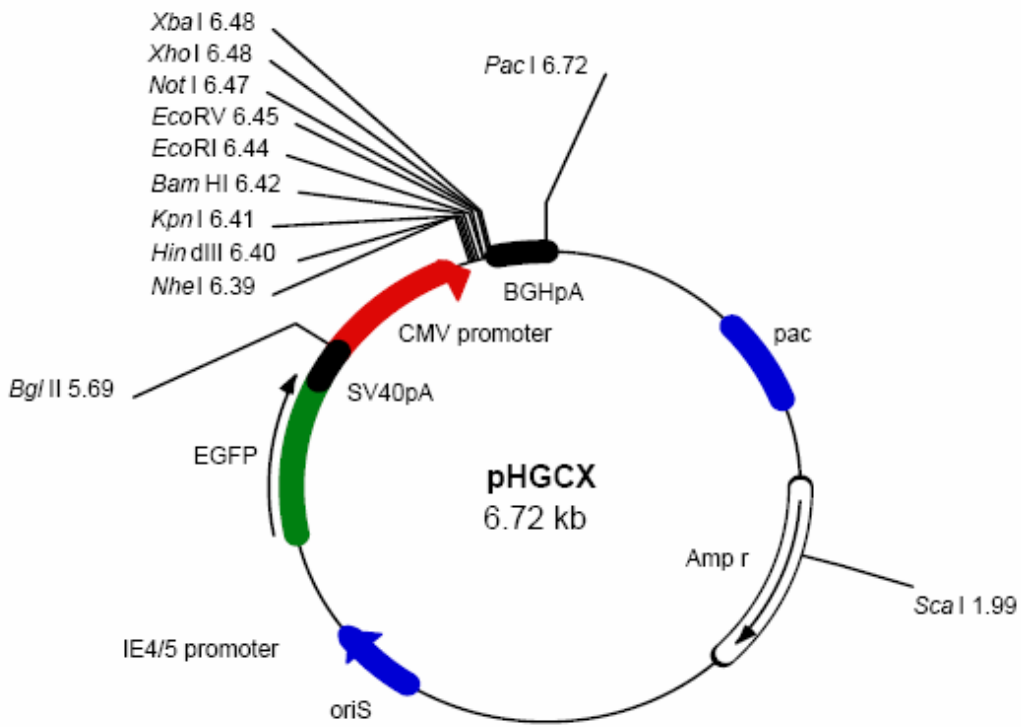

Figure 1.5. HSV-1 amplicon vector.
HSV-1 amplicon vector is plasmid based and contains the essential genes for the plasmid to propagate efficiently in bacteria. The only viral elements present on the vector is the Ori_S and the *pac* signal.

except for *pac* and *ori*$_s$, theoretically, these vectors can accommodate transgenes of up to 150 kb (Oehmig et al., 2004). As DNA replication occurs by the rolling circle mechanism, the resulting virions contain multiple copies of the recombinant DNA including the transgene, up to the maximum limit for packaging (Oehmig et al., 2004). The amplicon DNA is packaged into virions using helper virus-based or helper virus-free packaging systems (Oehmig et al., 2004). First generation amplicons were packaged in the presence of helper virus. The resulting virions were contaminated with the helper virus particles, consequently, these viruses are cytotoxic due to the presence of immune responses elicited against the *IE* genes encoded on the helper virus. A recent improvement is the introduction of the helper virus-free packaging system (Fraefel et al., 1996). Amplicons can be packaged by cotransfection with either a set of 5 overlapping cosmids (cos6Δa, cos14, cos28, cos48Δa and cos56) (Cunningham and Davidson, 1983; Fraefel et al., 1996) or a bacterial artificial chromosome (BAC) (Saeki et al., 1998; Stavropoulos and Strathdee, 1998; Saeki *et al,*, 2001) that represent the HSV-1 genome with the *pac* deleted (Figure 1.6). Cunningham and Davidson (1983) showed that when a set of overlapping cosmids that represent the entire HSV-1 genome was transfected into cells, the cosmids formed an infectious replication-competent virion through homologous recombination. However, when *pac* was deleted, the reconstituted viral genome was not packaged, yet still conferred all the required helper functions *in trans*. The generation of a packageable replication-competent HSV-1 would require six recombination events and is therefore, rare. In 1996, Fraefel et al. developed the helper virus-free packaging system by co-transfecting the amplicon plasmid DNA together with 5 overlapping cosmids that constitute the entire HSV-1 genome but lack the *pac* signal. The resulting viruses are free of contaminating helper virus. In an attempt to simplify the packaging procedure, Saeki et al. (1998) cloned the HSV genome as an F-plasmid-based BAC. However, replication-competent helper viruses were detected at a frequency of 10^{-4} to 10^{-6}, possibly resulting from recombination events between the BAC and the amplicon plasmid (Saeki et al., 1998). By deleting *ICP27* and adding a "stuffer" sequence from *ICP0* to the BAC (fHSVΔpacΔ27 0+), the resulting amplicon stocks were virtually free of contaminating replication-competent

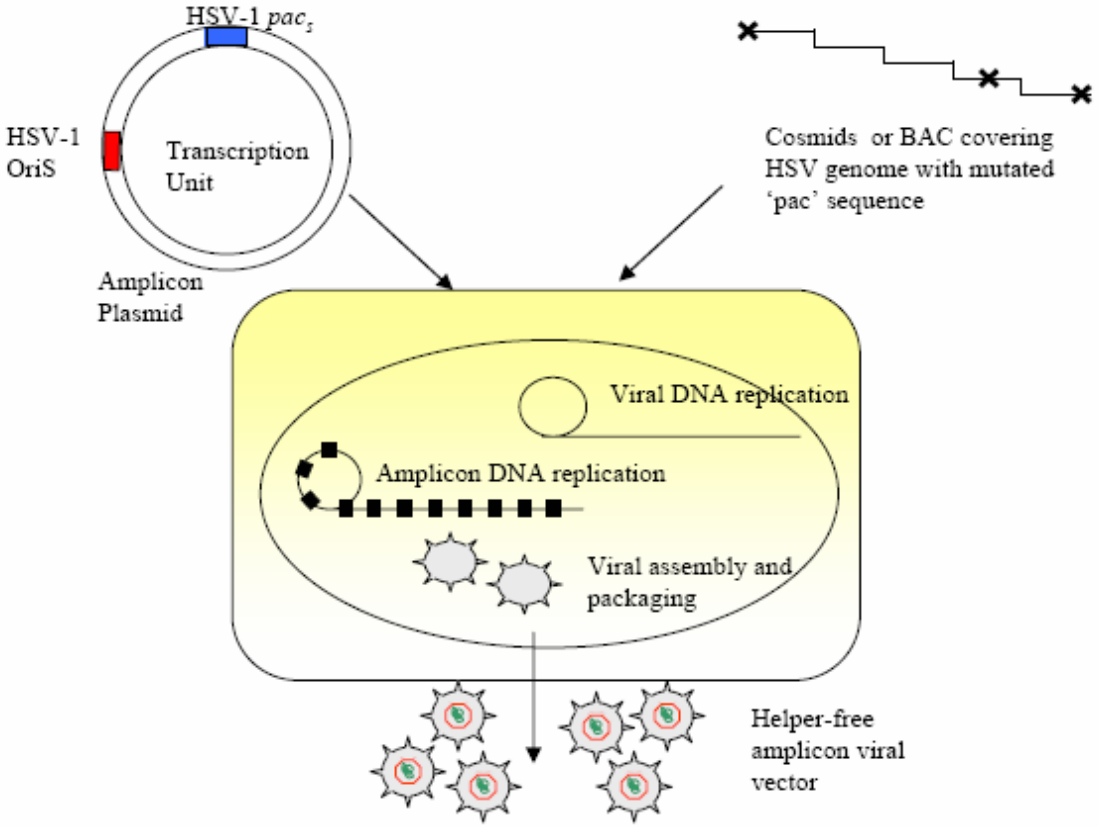

Figure 1.6. Helper virus free packaging system.
The amplicon plasmid is packaged by either co-transfection with a set of overlapping cosmids that span the entire HSV genome or BAC sequence, with the *pac* signal deleted. The amplicon DNA is packaged in a rolling-circle mechanism, allowing it to be packaged as concatamer in a HSV virions. The final product is free from contaminating helper virus.

helper viruses and achieved titers of up to 3-10 x 10^8 transduction unit (TU)/ml (Saeki et al., 2001; Saeki et al., 2003). In comparison to the recombinant HSV, helper virus-free amplicons essentially do not have any toxicity or antigenicity due to their lack of viral genes (Constantini et al., 2000). In addition to accommodating transgenes of up to 150 kb, the amplicon can be retained for months in non-dividing cells (Wang et al., 1999; Song et al., 1997; Zhang et al., 2000), and have high infectivity for cells of the CNS and relatively high titers (10^8 TU/ml) (Sena-Esteves et al., 2000). The large transgene capacity, low immunogenicity, and broad host range makes this vector an ideal gene delivery vehicle.

1.6 Transcriptional regulation system

One of the pitfalls of current cancer gene therapies is the lack of tumor specificity. Restricting transgene expression to tumor cells would minimize toxicity to normal tissues; therefore, it is important to regulate expression of therapeutic genes to specific cell types. An added benefit would be the activation of the transgene expression during particular circumstances. Two approaches have been widely adopted.

1.6.1 Tetracycline-regulated system

The tetracycline regulatable system is one of the most commonly used methods employed for regulating transgene expression (Gossen and Bujard, 1992). Unlike other drug regulatory systems, the tetracycline-regulatable system is more versatile. The vectors can be designed to be activated either in the presence or absence of tetracycline or its derivatives. The tetracycline-repressible system is based on the tetracycline repressor (tetR), which is a prokaryotic dimeric DNA binding protein that binds to the tetracycline operator (tetO) of the tet-resistance operon (Toniatti et al., 2004). In this system, the VP16 transactivator is fused to tetR, generating a chimeric tetracycline-repressed transactivator (tTA). In the absence of tetracycline, tTA binds with high affinity and specificity to the tetracycline-regulated promoter. To achieve inducible transient gene expression, the tetracycline-inducible system

(TiRS) could be adopted. In the presence of tetracycline, the chimeric transactivator binds to tetO, thus stimulating transcription.

1.6.2 Dimerizer-regulated system

The dimerizer-regulated system is based on the interaction of two subunits with a small molecule that contains distinct binding sites. A classical example of the dimerizer-regulated system utilizes the small molecule rapamycin which mediates binding of FK506 binding protein 12 (FKBP12) and the FKBP rapamycin-binding (FRB) domain of the FKBP rapamycin-associated protein (FRAP) (Pollock and Clackson, 2002). Fusion of FKBP to zinc-finger homeodomain fusion (ZFHD1) generates the DNA binding region; while the activator domain is comprised of FRB with NF-κB p65 protein. In the presence of rapamycin, the ZFHD1/FKBP chimeric protein binds to the FRB/p65 protein, forming a complex that would activate transgene expression.

1.6.3 Limitations of inducible systems

The drawback with all these systems is the reliance on exogenous pharmacological inducers. The major concern with the tetracycline regulatable system is the possibility of developing resistance to the antibiotic. Regulating the effective dosage level of an exogenous factor *in vivo* also poses a challenge. To circumvent the problem of relying on exogenous stimulation for regulating gene expression, it would be advantageous to regulate transgene expression that is dependent on endogenous cellular factors.

1.7 Strategies to target dividing, recurrent tumor cells

As uncontrolled proliferation is a common characteristic of malignant tumor cells. Therefore, an attractive strategy for cancer gene therapy would be the use of vectors carrying therapeutic genes that can be activated upon cellular replication. This strategy may be of special clinical relevance for brain tumor therapy since GBM is highly diffused and invasive, and complete surgical resection of the tumor mass is practically impossible. Two different strategies have

been designed for the construction of such a cell cycle-regulatable transcription system (Jerome and Müller, 1998; Nettelbeck et al., 1999).

1.7.1 Gal4/p56^{lck} system

In the first strategy, a melanoma-specific promoter drives an artificial heterodimeric transcription factor consisting of the Gal4 DNA-binding domain fused to the N-terminal domain of human p56^{lck}, a CD4-associated tyrosine kinase (Jerome and Müller, 1998). The transactivating subunit consists of the HSV VP16 fused to the interacting domains of human CD4 transcribed from a cell cycle-regulatable promoter. As a result, only in proliferating melanoma cells will both subunits be expressed and form a complex through the CD4-p56^{lck} interaction, thus activating transcription of the transgene (Jerome and Müller, 1998). The extent of cell type-specificity and cell cycle-regulation of transgene expression was shown to be in the range of 10-fold and 5-fold, respectively. Though the feasibility of this system is well established, it is nevertheless dependent on the specific protein dimerizations between fusion proteins of VP16-CD4 and Gal4/p56^{lck}. Binding of this heterodimeric transcription factor to Gal4 binding sites will then lead to transcriptional activation through the strong VP16 activation domain.

1.7.2 Gal4/NF-YA system

The second approach does not depend on the heterodimerization of chimeric transcription factors. Rather, transcriptional activation following DNA-binding takes place in a single step (Nettelbeck et al., 1999). A chimeric transcription factor (Gal4/NF-YA), consisting of the transactivation domain of the A subunit of nuclear factor Y (NF-YA) and the DNA binding domain of Gal4, is expressed from a tissue-specific promoter. This fusion protein (Gal4/NF-YA) can subsequently bind to a second promoter, consisting of the regulatory region of the cyclin A promoter downstream of the multiple Gal4 binding sites, and transactivate the transgene expression. The authors have shown the feasibility of a dual specific transcriptional regulation system that is discussed further in section 3.4.

The disadvantage of employing the above co-transfection of plasmid DNA for clinical application is due to its low efficiency and specificity. It would not be feasible for the co-transfections of two independent DNA plasmids-transduced cells to receive an optimum ratio of promoter and transactivator, thus resulting in sub-optimal activity and/or specificity.

1.7.2.1 Current strategy

The strategy described in our present study presents a more efficient alternative approach where a single-vector system combining both the transcriptional activator and the transgene reporter cassettes is assembled to confer cell cycle-dependent transgene expression. This is particularly advantageous in brain tumor gene therapy since cellular proliferation is a rare event in the normal brain tissues. In contrast, malignant brain tumor cells divide rapidly leading to the invasion of surrounding normal brain parenchyma.

1.8 Aims of this study

The aim of this study is to develop a better gene delivery system to target recurrent brain tumors occurring at or near the resected regions. This can be accomplished by the development of a cell cycle-regulated and cell type-specific viral vector whereby the transgene encoded by this vector will be activated only in actively proliferating glioma cells.

Specifically, the aims are:

1) To generate and characterize a cell cycle-regulated HSV-1 amplicon viral vector;
2) To evaluate the therapeutic efficacy mediated by this vector *in vitro* and *in vivo*;
3) To develop strategies that target transgene expression specifically to glioma cells by
    (i) employing a tissue specific promoter;
    (ii) isolating glioma-specific peptides for targeting purpose;
4) To better characterize the dual specificity vector *in vivo* by
    (i) examining the immunogenicity in an immunocompetent mouse model;
    (ii) determining the stability of the virions;

(iii) determining the transduction efficiency of the virions; and

(iv) investigating the sensitivity of the virions to chemotherapeutic drugs.

Chapter 2

Materials and Methods

2.1 Materials

2.1.1 Geniticin

Source: Invitrogen Life Technologies, Grand Island, NY

Stock concentration: 50 mg/ml.

Dissolved in Phosphate buffered saline (PBS), filter sterilized, aliquoted, and stored at -20 °C.

2.1.2 Puromycin

Source: Invitrogen Life Technologies

Stock concentration: 1 mg/ml

Dissolved in PBS, filter sterilized, aliquoted and stored at – 20 °C.

2.1.3 Dulbecco's modified Eagle's medium (DMEM) culture medium

DMEM is supplemented with 10 % fetal bovine serum (FBS) (Hyclone Laboratories, Logan, UT), 100 U/ml penicillin (Invitrogen Life Technologies), 100 μg/ml streptomycin (Invitrogen Life Technologies), and 2 mM L-Glutamine (Sigma-Aldrich Corp., St. Louis, MO).

2.1.4 Cells-freezing medium

Cells-freezing medium was prepared by adding tissue culture grade dimethyl sulfoxide (DMSO) (Sigma-Aldrich Corp.) to fetal bovine serum (FBS) to a final concentration of 10 %.

2.1.5 Lovastatin

Source: Merck, Singapore

Stock concentration: 25 mg/ml

Dissolve 25 mg of lovastatin into 500 μl of 95 % ethanol. This is followed by addition of 400 μl of 1N NaOH. Adjust to pH 7.2 using 1N HCl. Dilute the solution to 4 mg/mg (10 mM) using ddH_2O. Aliquot and store away from light at –20 °C.

2.1.6 Mevalonate

Source: Sigma-Aldrich Corp.

Stock concentration: 1M

Dissolve in ddH_20 to a final concentration of 1 M. Store away from light at –20 °C.

2.1.7 Dithio-DL-threitol (DTT)

Source: Sigma-Aldrich Corp.

Stock concentration: 1M

Dissolve 3.08 g of DTT in 20 ml of 10 mM sodium acetate (pH 5.2). Filter sterilize and aliquot. Store at -20 °C.

2.1.8 RNase A (DNase Free)

Source: Sigma-Aldrich Corp.

Stock concentration: 20 mg/ml

Dissolve in PBS. Store as aliquots at -20 °C.

2.1.9 Propidium iodide (PI) solution

Source: Sigma-Aldrich Corp.

Stock solution: 100 µg/ml

Dissolve PI in PBS containing 0.1 % Triton X-100. Store at -20 °C covered with tin foil.

2.1.10 Sucrose solution

Dissolve 25 g or 30 g in 100 ml of PBS to a concentration of 25 % and 30 % respectively. Filter sterilize and store at 4 °C.

2.1.11 Solution I for DNA extraction

Prepare by adding 50 mM Glucose, 10 mM EDTA, and 25 mM Tri-HCl, pH 8.0 to ddH_20. Autoclave and store at 4 °C.

2.1.12 Lysis solution for DNA extraction

Prepare by adding 200 mM NaOH, and 1% SDS to ddH_20. Freshly prepared before use.

2.1.13 Neutralizing buffer for DNA extraction

Neutralizing buffer contains 5 M potassium acetate solution, pH 5.5. Prepare by adding 11.5 ml of glacial acetic acid and 28.5 ml of ddH_20 to 60 ml of 5 M potassium acetate. The resulting solution is 3 M with respect to potassium and 5 M with respect to acetate.

2.1.14 Lysis buffer for isolating Hirt's DNA

Lysis buffer is freshly prepared by dissolving 0.6 % SDS, 10 mM EDTA pH8.0, 10 mM Tris-Cl, pH 7.5, in ddH_20.

2.1.15 Tris-EDTA (TE)

Dilute 10 mM Tris (pH 8.0) and 1 mM EDTA (pH 8.0) in ddH_20. Sterilize by autoclaving.

2.1.16 Cesium chloride/TE/ ethidium bromide (EtBr) solution

1.16 g/ml of cesium chloride was dissolved in this 8 ml of TE, followed by addition of 1 ml of EtBr solution

2.1.17 TE-saturated Butanol

TE was added to butanol with intermittent mixing until two phases are observed. Butanol should be in the upper phase.

2.1.18 Diethylpyrocarbonate (DEPC) water

Add 0.2 ml of DEPC to 100 ml of ddH_20. Shake vigorously and incubate overnight in a fume hood. Inactivate remaining DEPC by autoclaving.

2.1.19 Preparation of temozolomide (TMZ)

Stock concentration: 100 mM

Dissolve temozolomide in DMSO to give a concentration of 100 mM. Store at room temperature (r.t.).

2.1.20 Ampicillin

Source: Sigma-Aldrich Corp.

Stock concentration: 100 mg/ml

Dissolve in sterile ddH_20. Filter sterilize and store at -20 °C in aliquots.

2.1.21 Kanamycin

Source: Sigma-Aldrich Corp.

Stock concentration: 30 mg/ml

Dissolve in sterile ddH_20. Filter sterilize and store at -20 °C in aliquots

2.1.22 Chloramphenicol

Source: Sigma-Aldrich Corp.

Stock concentration: 34mg/ml

Dissolve in ethanol. Filter sterilize and store at -20 °C in aliquots

2.1.23 Luria broth (LB)

Mix 10 g Bacto-Tryptone, 5 g Bacto-Yeast extract and 10 g sodium chloride in 900 ml of ddH_20. Adjust pH to 7.0 with sodium hydroxide. Sterilize by autoclaving.

2.1.24 SOB (1L)

Mix 20 g Bacto-Tryptone, 5 g Bacto-Yeast extract, 0.5 g NaCl and 2.5 ml of 1M KCl in 900 ml of ddH_20. Adjust pH to 7.0 with NaOH. Sterilize by autoclaving. Add 10 ml of 1M Mg_2Cl before use.

2.1.25 *Escherichia coli* strain ER2537

Escherichia coli strain ER2537 was purchased from New England Biolabs (Beverly, MA). The genotype of the strain is [F' lacIq Δ(lacZ) M15 proA+B+/fhuA2 supE thi Δ(lac-proAB) Δ(hsdMS-mcrB) 5 (rk- mk- McrBC-)]

2.1.26 5-bromo-4-chloro-3-indolyl-β-D-galactoside (X-Gal)

Source: Bio-Rad Laboratories

Stock concentration: 40 mg/ml

Dissolve X-Gal in dimethyl sulfoxide to a final concentration of 40 mg/ml.

2.1.27 Isopropyl β-D-thiogalactoside (IPTG)

Source: Invitrogen Life Technologies

Stock concentration: 50 mg/ml

Dissolve IPTG in ddH_20 to a final concentration of 50 mg/ml.

2.1.28 Tris-buffered saline (TBS)

TBS contains 100 mM Tris-Cl (pH 7.5) and 0.9 % NaCl in ddH_2O.

2.1.29 Peptides

Source: Mimotopes, Victoria, Australia

The poly-L-lysine-SIPVKFNKP-MG11 ((K_{16})-MG11) and poly-L-lysine-SIPVKFNKP-H42 ((K_{16})-H42) peptides were synthesized and purified. The peptides were dissolved in 0.15 M NaCl at 1 mg/ml and stored in small aliquots at -20 ºC. The purity of both peptides was > 90%.

2.1.30 Protein lysis buffer

Protein lysis buffer contains 50 mM Tri-Cl (pH7.6), 0.1 % Triton X-100, and 150 mM NaCl in ddH_2O. Add 1x protease inhibitor before use.

2.1.31 Luciferase assay buffer

Mix 25 mM Glycylglycine (pH7.8), 15 mM $MgSO_4$, 4 mM EGTA and 15 mM potassium phosphate (pH 7.8) in ddH_2O. Store at 4 °C.

2.1.32 Luciferin buffer

Mix 25 mM Glycylglycine (pH7.8), 15 mM $MgSO_4$, 4 mM EGTA in ddH_2O. Store at 4 °C.

2.1.33 Luciferin

Source: Roche Diagnostics GmbH, Mannheim, Germany

Stock concentration: 10 mM

Dissolve 10 mg of luciferin powder in 3.57 ml of 25 mM Glycylglycine (pH 7.8). Aliquot and store at -20 °C in the dark.

2.1.34 Preparation of Ponseau S

Source: Sigma-Aldrich Corp.

Stock concentration: 1%

Dissolve 1 % of Ponseau S (w/v) in 5 % acetic acid (v/v).

2.1.35 Resolving gel (10%)

10 % (10 ml) gels were cast by mixing 3.3 ml of 30 % acrylamide mix (30 % acrylamide/0.8 % bisacrylamide) with 2.5 ml of 1.5 M Tris-Cl pH 8.8, 4 ml ddH_20 , 50 µl of 20 % SDS, 100 µl 10 % ammonium persulfate (APS) (Amersham Biosciences AB, Uppsala, Sweden) with 10 µl of N, N, N', N'-tetramethylethylenediamine (TEMED).

2.1.36 Stacking gel (5%)

0.83 ml of 30 % acrylamide mix with 0.63 ml of 1 M Tris-Cl pH6.8, 3.4 ml of ddH_20, 25 µl of 20 % SDS and 50 µl of 10 % APS with 6 µl of TEMED.

2.1.37 Protein loading buffer

Protein loading buffer is prepared by mixing 62.5 mM Tris-Cl pH 6.8, 10 % glycerol, 2 % SDS, 100 mM DTT, 0.0005 % bromophenol blue in ddH_2O.

2.1.38 SDS electrophoresis buffer

Mix 25 mM Tris-base, 192 mM glycine (electrophoresis grade) and 0.1% SDS in ddH_2O.

2.1.39 Protein transfer buffer

Mix 25 mM Tris, 190 mM glycine and 20 % methanol in ddH_2O

2.1.40 Western hybridization blocking buffer

Blocking buffer contains 5% nonfat milk, 10 mM Tris pH7.5, 100 mM NaCl, 0.1% Tween-20

2.1.41 Polyacrylamide gel electrophoresis (PAGE)

6 % PAGE gel was prepared by adding 12 ml of 30 % acrylamide (29 % acrylamide/1 % bisacrylamide), 6 ml of 10 X TBE, 360 µl of 10 % APS, 36 µl of TEMED to 42 ml of ddH_20. The gel was allowed to polymerize at r.t.

2.1.42 Binding buffer for isolation of nuclear extract for Electromobility shift assay (EMSA) (Wu et al., 2001)

Binding buffer for EMSA was freshly prepared by adding 2.5 % glycerol, 5 mM $MgCl_2$, 0.2 mM EDTA, 0.05 % NP-40, 250 ng of poly(dA-dT) (Amersham Biosciences AB) and 100 fmol of biotin-labeled probe to a final volume of 20 µl.

2.1.43 Buffer A for isolation of nuclear extract (Wu et al., 2001)

Buffer A contains 10 mM Hepes pH 7.9, 10 mM KCl, 1.5 mM $MgCl_2$, 1 mM EDTA, 1 mM EGTA in ddH_20. Add 1 mM DTT and 1 mM phenylmethelsolfonyl fluoride (PMSF) before use. Sterilize by filtration and store at 4 °C.

2.1.44 Buffer C for isolation of nuclear extract (Wu et al., 2001)

Buffer C contains 20 mM Hepes pH 7.9, 400 mM NaCl, 1 mM EDTA and 1 mM EGTA in ddH_20. Add 1 mM DTT and 1 mM PMSF before use. Sterilize by filtration and store at 4 °C.

2.1.45 Tris-Acetate EDTA buffer (TAE)

Mix 40 mM Tris-Acetate, Glacial acetic acid and 1 mM EDTA in ddH_2O

2.1.46 Fixative

Concentration: 4 % of Paraformaldehye (Sigma-Aldrich)

Paraformaldehyde is dissolved in PBS in a heated water bath set at 65°C, with constant stirring.

2.1.47 Blocking buffer for Immunohistochemistry

PBS containing 0.1 % Tween 20 and 10 % goat serum.

2.1.48 Antibodies

For ELISA:

Monoclonal mouse anti-human FADD (Zymed Laboratories) Cat no: 35-8000

Polyclonal rabbit anti-human FADD (Calbiochem-Novabiochem Corp) Cat no: 341282

For western hybridization:

Monoclonal mouse anti-human FasL, clone G247-4 (BD Pharmingen) Cat no: 37720

Monoclonal mouse anti-human Fas, clone 13 (BD Pharmingen) Cat no: F22120

Monoclonal mouse anti-human FADD (BD Pharmingen) Cat no: F36620

Monoclonal mouse anti-cyclin A antibody (BF683) (Santa Cruz Biotechnology) Cat no: sc239

Monoclonal mouse anti-β tubulin antibody clone 5H1 (BD Pharmingen)

Rabbit anti-human caspase 8 (BD Pharmingen) Cat no: 559932

Goat anti-rabbit HRP conjugated (Dako Cytomation) Cat no: P0448

Goat anti-mouse HRP conjugated (Dako Cytomation) Cat no: P0447

For immunohistochemitry and immunofluorescence:

Goat Anti-human GFAP (C-19) (Santa Cruz Biotechnology) Cat no: sc-6170

Monoclonal rat anti-mouse CD8, clone 53-6.7 (BD Pharmingen), Cat no: 550281

Monoclonal rat anti-mouse CD4, clone RM4-5 (BD Pharmingen), Cat no: 550280

Monoclonal rat anti-mouse CD11b, clone M1/70 (BD Pharmingen), Cat no: 550282

Polyclonal rabbit anti-luciferase (Sigma-Aldrich Corp.) Cat no: L0159

Alexa-Fluor 647 goat anti-mouse IgG (Molecular Probes)

Alexa-Fluor 350 goat anti-rabbit IgG (Molecular Probes)

Biotin-conjugated goat anti-rat IgG, (BD Pharmingen), Cat no: 559286

Streptavidin-HRP prediluted for IHC (SAv-HRP) (BD Pharmingen), Cat no: 550946

For FACS analysis:

Anti-BrdU-FITC conjugated (BD Pharmingen), Cat no 347583

2.1.49 Animals

All Balb-C nu/nu (nude) and severe combined immunodeficient (SCID-CB-17) mice were purchased from Animal Resource Center, Western Australia. Immunocompetent Balb-C mice were purchased from Laboratory Animal Center, National University of Singapore, Singapore.

2.2 General Methods

2.2.1 Tissue culture

2.2.1.1 Cell lines

A549 (lung adenocarcinoma), HeLa (human cervical carcinoma), HepG2 (human hepatocellular carcinoma), HK1 (nasopharyngeal carcinoma), NIH3T3 (mouse fibroblast), KZ2 (melanoma), KOSC-3 (head and neck carcinoma), M059K (human glioma), PC-3 (human prostate adenocarcinoma), Saos-2 (osteosarcoma), T98G (human glioma), U87MG (human glioma), U373MG (anaplastic astrocytoma), and WT18 (lymphoma) were obtained from American Type Culture Collection (Rockville, MD). CNE2 cells are derived from undifferentiated human nasopharyngeal carcinoma (gift from Prof. HM Wang, Cancer Institute, Guangzhou, People's Republic of China). Gli36, SF767 and U251MG human gliomas were kindly provided by Dr. AT Campagnoni (UCLA School of Medicine, Los Angeles, CA) and Dr. DF Deen (Brain Tumor Research Center, UCSF, School of Medicine, CA), respectively. dGli36 cells which overexpresses a truncated mutant EGFR commonly found in human gliomas was a gift from Dr. M Sena-Esteves (Children's Hospital of Philadelphia, Philadelphia, PA). The African green monkey kidney 2-2 cells, which are VERO-derived cells, constitutively express the HSV-1 ICP27 proteins was kindly provided by Dr. R Sandri-Goldin (UCLA) (Smith et al., 1992).

2.2.1.2 Culture conditions of cell lines

All cell lines, except PC-3, were grown in DMEM culture medium. dGli36 cells were grown in DMEM culture medium in the presence of puromycin (1 μg/ml). PC-3 was cultured in F12K culture medium (Invitrogen Life Technologies, Grand Island, NY). Vero 2-2 cells were cultivated in the presence of 500 μg/ml of Geniticin. All cells were maintained at 37 °C in a humidified incubator with 5 % CO_2.

Normal human astrocytes purchased from Cambrex Bio Science Walkersville, Inc., (Walkersville, MD) were cultured in Astrocyte Basal Medium supplemented with

recombinant human EGF, insulin, ascorbic acid, GA-100, L-glutamine and FBS as recommended by the supplier (Cambrex Bio Science Walkersville, Inc., Walkersville, MD).

Primary glioma biopsy was kindly provided by Dr. Thomas, J. (Department of Neurosurgery, Singapore General Hospital, Singapore) with patient's consent. Tissues were immediately kept in DMEM with 10 % FBS. To obtain single cell suspension, the tissues were digested for 5 min with 0.25 % trypsin, followed by washing twice with DMEM culture medium. The cells were plated onto a single well of a twenty four-well plate (Nunc, Roskilde, Denmark), and incubated at 37 °C in a humidified incubator with 5 % CO_2.

2.2.1.3 Subculturing of cells

Subculturing of cells was carried out using 0.25 % trypsin-EDTA. Briefly, when the cells reach a confluency of ~ 80 %, the medium was discarded and the cell monolayer was washed gently with PBS. After removing the excess PBS, appropriate amount of 0.25 % trypsin-EDTA was added for approximately 3 to 5 min until most of the cells became resuspended. This was followed by resuspending the cells in complete medium and centrifugation for 5 min at 1000 rpm (Beckman Coulter, Palo Alto, CA). The pelleted cells were then resuspended in appropriate medium and divided into individual flasks.

2.2.1.4 Cryopreservation of cells

For cryopreservation, cells were trypsinized and pelleted as above. Cell pellet was resuspended in cell freezing medium (section 2.1.4) and stored in liquid nitrogen using cryovials (Nunc).

2.2.1.5 DNA transfections

NIH3T3, U251MG, SF767, HepG2 and PC-3 were transfected in six-well plates using LipofectAmine (Invitrogen Life Technologies) according to the manufacturer's instructions. Briefly, 3 μg of plasmids were mixed with 8 μl of LipofectAmine in OptiMEM (Invitrogen

Life Technologies) for 45 min at r.t. DNA/LipofectAmine complexes were added to 3 x 10^5 cells per well in a six-well plate (Nunc) and incubated for an additional 6 h at 37 °C. Cells were subsequently rinsed with PBS twice and replenished with fresh culture medium.

Other cell lines namely Gli36, dGli36, and HeLa (3 x 10^5 cells /6-well plate) were transfected using a novel cationic lipid NCC4. When compared with LipofectAmine, NCC4 has been reported to give more than 2-fold increase in luciferase gene activity in certain cell lines (Gao and Hui, 2001). Briefly, 3 µg of DNA was mixed with 20 µl of liposomes in 1 ml of sodium lactated Ringer's buffer (B. Braun Melsungen AG, Melsungen, Germany) and the complexes were allowed to form for 15 min at r.t. The DNA/liposome complexes were added to each well and incubated for another 15 min at r.t. After adding 1 ml of sodium lactated Ringer's buffer, the cultures were incubated for additional 2 h incubation at 37 °C. Cells were subsequently rinsed with PBS and replenished with fresh culture medium. All transfection reactions were performed in triplicates.

2.2.1.6 Synchronization of cells and cell cycle analysis

For synchronization at G_1, cells were washed twice with PBS. Depending on the cell lines, fresh medium was supplemented with 0.1 %-0.5 % FBS and 40-50 µM of lovastatin was added. After 48 h, cells were harvested by trypsinization, and resuspended in 500 µl of cold 70 % ethanol. After an overnight fixation at 4 °C, cells were washed with PBS thrice, before resuspending in 100 µl of PBS containing RNase A (2 mg/ml) and PI (100 µg/ml). The samples were kept on ice for an hour before FACS analysis was performed using Cell Quest and Modfit software (BD Biosciences, San Jose, CA).

G_1-arrested cells were stimulated into the cell cycle by removing medium containing lovastatin, followed by two washes with PBS. Cells were then replenished with DMEM containing 10 % FBS and 5 mM mevalonate for additional 48 h.

2.2.2 Packaging of HSV-1 amplicon vector using helper virus-free system

2.2.2.1 BAC fHSVΔpacΔ27 0+ packaging

Packaging of HSV-1 amplicons into HSV-1 virions was performed as described previously. Briefly, 3 x 10^6 Vero 2-2 cells were cotransfected with 1.8 µg of amplicon DNA, 0.3 µg of pEBHICP27 helper plasmid, and 3 µg of BAC fHSVΔpacΔ27 0+ in OptiMEM (Saeki et al., 2003), using the LipofectAmine procedure. After 6 h of transfection, cells were replenished with fresh medium and incubated for an additional 60 h.

2.2.2.2 Cosmids C6Δa48Δa packaging

For packaging of HSV-1 amplicons using cosmids (Fraefel et al., 1996), five overlapping cosmids (cos 6Δa, cos 14, cos 28, cos 48Δa and cos 56) were digested with *Pac*I enzyme and purified. For transfections, 3 x 10^6 Vero 2-2 cells were plated the previous day to achieve a confluency of 80-90 % on the day of transfection. The transfection mixture contains 6 µg of *Pac*I digested DNA from cosmids set C6Δa48Δa (Cunningham and Davidson, 1993) and 2 µg of amplicon DNA. After 6 h of transfection, the cells were replenished with fresh complete medium and incubated for an additional 60 h.

2.2.2.3 Harvesting of virions

Sixty hours post-transfection, the cells were scraped into the medium using cell lifter (Corning Enterprises, Corning, NY); the suspension was frozen and thawed three times in liquid nitrogen and sonicated for 17 sec at 3.5 setting (550 Sonic Dismembrator). The cellular debris was removed by centrifugation for 10 min at 1000 rpm (Beckman Coulter). After centrifugation, the supernatant was transferred to a clean 50 ml centrifuge tube and stored at -80 °C.

2.2.2.4 Sucrose gradient ultracentrifugation

The crude viral lysate (CVL) harvested were filtered through 0.45 µm sterile filter (Millipore, Billerica, MA). The filtered CVL was added to pre-cleaned ultraclear tubes (30 ml; Beckman

Coulter) followed by addition of 25 % sucrose/PBS solution. Five ml of 25 % sucrose/PBS was carefully pipetted onto the bottom of the centrifuge tubes, and cold complete medium was added to a final volume of 30 ml. This was followed by ultracentrifugation at 25 000 rpm at 4 °C for 4 h with a Beckman SW28 swingout rotor. After completion of centrifugation, the supernatant was carefully decanted, and the pellet resuspended in 100 µl of Hank's Balanced Salt Solution (HBSS) overnight at 4 °C. The next day, the purified virus was transferred to a clean microcentrifuge tube, aliquoted and stored at -80 °C.

2.2.2.5 Determination of viral titer

To determine viral titers (TU/ml), 1 x 10^5 Vero 2-2 cells were plated per well in twenty four-well plate (Nunc) one day before experiments. On the day of experiment, 1 µl of viral stocks was diluted 1000- and 5000-fold in culture medium and added to duplicate wells. The volume of infection was maintained at 300 µl. The cells were incubated for 18 h in 37 °C. At the end of 18 h, green fluorescent cells were counted using a fluorescence microscope (Nikon Instech Co., Kanagawa, Japan) equipped with an ocular lens fitted with a 10 x 10 counting grid and counted under 100x (10 x objective lens and 10x ocular lens) magnification. About three to four random fields selected from each well were included for counting. The titer of the virus was calculated using the formula, TU/ml = number of green cells multiplied by the amplification factor and the dilution factor; where the amplification factor under a 100 x magnification is 190.

2.2.2.6 Amplicon vector transduction

For vector transduction, 3 x 10^5 dGli36 cells per 60-mm-well in triplicate were incubated for 6 h at 37 °C with various amplicon viral vector stocks so as to achieve a constant multiplicity of infection (MOI). At the end of 6 h, cells were washed twice and fresh medium containing 10 % FBS was added to proliferating cells. Synchronization of cells and subsequent luciferase assays were performed as described above.

2.2.3 Nucleic acid isolation

2.2.3.1 Isolation of plasmid DNA-mini alkaline lysis method

The plasmid DNA isolation from transformants was carried out using QIAprep Spin Miniprep Kit (Qiagen GmbH, Hilden, Germany). The plasmid DNA was extracted by alkaline lysis method following manufacturer's instruction. Briefly, bacterial cultures were incubated in 4 ml of LB containing the appropriate drug selection overnight at 37 °C with 225 rpm shaking. The next day, the bacterial cells were pelleted by centrifugation at 4000 rpm for 10 min. The pellet was resuspended in 250 µl of buffer P1 (25 mM Tri-HCl, 10 mM EDTA, 250 µg/ml RNase) follow by adding 250 µl of lysis buffer P2 (200 mM NaOH, 1 % SDS) for 5 min, r.t. This was followed by addition of 350 µl of neutralizing buffer N3. After centrifugation at 13 000 xg for 10 min using a tabletop centrifuge, the plasmid DNA solution was transferred to a new column and subjected to an additional round of centrifugation at 13 000 xg for 1 min. The column was washed once by adding 700 µl of buffer PE. Residual buffer PE was removed by further centrifugation at 13 000 xg for 1 min. Plasmid DNA was then eluted by the addition of 30 µl of buffer EB (10 mM Tri-HCL, pH 8.5).

2.2.3.2 Isolation of plasmid DNA, BAC and cosmid DNA-by alkaline lysis method

Large scale plasmid extractions were carried out using QIAGEN maxi plasmid kit (Qiagen GmbH). The plasmid DNA was extracted by alkaline lysis following the manufacturer's instructions. Briefly, a single colony was picked and inoculated into 5 ml LB medium and incubated at 37 °C for 8 h. After 8 h, the log-phased bacterial culture was transferred into 400 ml of LB medium containing appropriate antibiotics and further incubated for 16-18 h at 37 °C with shaking. Cosmids were inoculated into SOB medium. The bacterial cells were pelleted by centrifugation at 4000 rpm for 10 min (Kendro Laboratory Products, Asheville, NC). The pellet was then resuspended by adding 10 ml of Buffer P1 (25 mM Tri-HCl, 10 mM EDTA, 250 µg/ml RNase). This was followed by adding 10 ml of lysis buffer P2 (200 mM NaOH, 1 % SDS) and incubating at room temperature for 5 min with gentle mixing. Ten

ml of cold neutralization buffer P3 (3 M KOAc, pH 5.5) was added and the mixture was incubated on ice for 20 min. The chromosomal DNA and cellular proteins were then removed by centrifugation at 10 000 rpm for 30 min at 4 °C. The supernatants were then filtered through a sterile cotton mesh before being loaded into a buffer QBT (750 mM NaCl; 50 mM MOPS (free acid) pH 7.0; 15 % (v/v) isopropanol and 0.15 % Triton-X100) equilibrated QIAGEN-tip 500 and allowed to flow through the resin by gravity. The QIAGEN-tip was washed twice by adding 30 ml of buffer QC (1 mM NaCl; 50 mM MOPS pH 7.0; 15 % isopropanol). Plasmid DNA was eluted by adding 15 ml of buffer QF (1.25 mM NaCl; 50 mM Tris-HCl pH8.5 and 15 % isopropanol) to the QIAGEN-tip. The DNA was then precipitated by adding 10.5 ml of r.t. isopropanol and centrifuged at 10 000 rpm for 30 min at 4 °C. This was followed by washing the pellet in 5 ml of room temperature 70 % ethanol and centrifugation at 10000 rpm for 10 min at 4 °C. The DNA was then air dried and resuspended in TE buffer.

2.2.3.3 Isolation of total RNA from cultured cell lines

To isolate RNA from tumor cell lines, the cell monolayer was rinsed with PBS twice and After scraping into 1 ml of PBS, the cells were pelleted by centrifugation at 2000 rpm for 5 min at 4 °C. The pellet was then resuspended thoroughly using 1 ml of Trizol solution (Invitrogen Life Technologies) and incubated at r.t for 5 min. This was followed by addition of 200 µl of chloroform, and the phases were mixed by vigorous shaking and allowed to incubate at room temperature for 5 min before centrifugation. After centrifugation at 12 000 xg for 15 min at 4 °C, the clear upper phase was transferred to a clean microcentrifuge tube and 500 µl of isopropanol was added. The mixture was incubated at room temperature for 10 min before being centrifuged at 12 000 xg for 10 min at 4 °C. The pellet was washed with 1 ml of 75% ethanol and then centrifuged at 7500 xg for 5 min at 4°C. The pellet was dried at 60 °C using a heat block before resuspending in an appropriate amount of 0.1 % DEPC-treated water at 65°C for 10 min. The RNA was stored at -80°C until use.

2.2.3.4 Isolation of total RNA from tumor tissues

Freshly extracted tumor nodules from mice were immediately frozen in liquid nitrogen until used. RNA was extracted according to the method described in section 2.2.3.3.

2.2.3.5 Quantification of nucleic acid concentration

The DNA or RNA concentration was determined by using an Ultrospec 3000 UV/visible spectrophotometer (Amersham Biosciences AB, Uppsala, Sweden). The samples were diluted 100-fold and the readings were taken at wavelength of 260 nm and 280 nm.

2.2.3.6 Extraction of viral DNA from brain tissues

Viral DNA was recovered from brain tissues using Hirt's method (Hirt, 1967) with slight modifications. Briefly, the tissues were grind into powder in liquid nitrogen using mortar and pestle. Five hundred microliter of lysis buffer (section 2.1.14) was incubated with the tissues for 20 min at RT. This is followed by the addition of 125 µl of 5M NaCl and incubation at 4 °C overnight. The next day, the extract was subjected to centrifugation at 13 000 xg at 4 °C for 30 min. The supernatant was recovered and extracted with phenol, phenol-chloroform and chloroform. DNA was precipitated with isopropanol, rinsed with 70 % ethanol and dissolved in 35 µl of TE buffer.

2.2.4 Protein isolation and analysis

2.2.4.1 Total cell lysate

Cells were harvested by rinsing the monolayer with PBS and scrapping the cells to 1 ml of PBS. The cells were pelleted by centrifugation at 2000 rpm for 10 min. The pellet was either subjected to three cycles of freezing and thawing, or lysed in protein lysis buffer or 10 min on ice. The cell debris was removed by centrifugation at 13 000 xg for 10 min at 4 °C. The supernatant was transferred to a clean tube, aliquoted and stored at -80 °C until used.

2.2.4.2 Determination of protein concentration

Protein concentration was determined spectrophotometrically using Bradford method with protein binding dye (Bio-Rad Laboratories). For measurements, 5 µl of protein sample were added to 795 µl of PBS and 200 µl of the dye. Readings were recorded at wavelength of 595nm.

2.2.4.3 Assay for luciferase activity

Cells were harvested from 6-well plates at the respective time point following transfection, washed, resuspended in 120 µl of Tris-HCl (pH 7.8), and freeze-thawed three times. Cell debris was discarded following centrifugation at 14 000 xg at 4 °C for 10 min. One hundred µl of the supernatant collected was used for assaying luciferase activity using the Auto-Lumat LB952 luminometer (EG&G Berthold, Bad Wildbad, Germany). Five µl of the supernatant collected was used for the determination of protein concentration using the Bio-Rad protein assay dye reagent (Bio-Rad Laboratories, Hercules, CA) with the Ultrospec 3000 UV/visible spectrophotometer (Amersham Biosciences AB).

2.2.4.4 Assay for FasL protein expression

Cells were harvested from 24-well plates at the respective time point following infection. Supernatant was concentrated with Centricon (Millipore) with 10 kDa cut-off. FasL protein expression was determined using ELISA (Oncogene Research Products, San Diego, CA) according to manufacturer's instructions.

2.2.4.5 Assay for FADD protein expression

Cells were harvested from 24-well plates at the respective time point following infection. The cell monolayer was rinsed twice with PBS followed by centrifugation at 2000 rpm for 5 min. The pellet was lysed in lysis buffer containing 50 mM Tris-Cl (pH 8.0), 0.1 % Triton X-100 and 0.1 mM NaCl for 10 min at 4 °C. Cell debris was removed by centrifugation at 14 000 xg

for 10 min at 4 °C. Supernatant was collected and 1 µl was used for the determination of protein concentration. For the detection of FADD protein expression, the sandwich ELISA method was adopted. 0.25 µg/ml of mouse anti-FADD monoclonal antibody were coated on a flat-bottom 96-well plate (Nunc) and incubated at 4 °C overnight. Excess antibody was removed by rinsing thrice in washing buffer containing PBS with 0.1% Tween 20 (Invitrogen Life Technologies). All subsequent washing steps were carried out at r.t. The coated wells were incubated in blocking buffer [0.1 % Tween-20 and 1 % BSA (Sigma-Aldrich Corp.) in PBS] for 1 h at r.t. 0.1 µg/ml of cell lysate were added to each well and incubated at r.t. for 1 h, followed by three rounds of rinsing in washing buffer. Rabbit anti-FADD polyclonal antibody was diluted to a final concentration of 2 µg/ml in blocking buffer and added to each well. After rinsing for five rounds in washing buffer, wells were incubated with HRP conjugated goat anti-rabbit antibody (diluted to a final concentration of 2 µg/ml in blocking buffer) for 30 min, followed by incubation in detection reagent (R&D Systems Inc., Minneapolis, MN) for a additional 30 min. Colorimetric development was aborted by the addition of stop buffer containing 2 N sulfuric acid (R&D Systems Inc.). Absorbance reading was analyzed at wavelength of 450 nm using Spectrafluor Plus (Tecan USA Inc., Research Triangle Park, NC).

2.2.4.6 SDS-polyacrylamide gel electrophoresis (SDS-PAGE)

The 10 % SDS-PAGE gel was cast using the Mini-PROTEAN III gel apparatus (Bio-Rad Laboratories). The gels were prepared following the method outlined by Ausubel et al. (1987). The resolving gel was allowed to set at r.t for 30 min. A 5 % stacking gel was prepared and loaded onto the resolving gel. The protein samples were boiled in 1 x loading buffer (section 2.1.37) before loading onto the gel. The gel was run at 180 V for 1.5 h in 1 x SDS electrophoresis buffer. A pre-stained high molecular weight protein marker (14.2 kDa – 200 kDa; Invitrogen Life Technologies) was run as a reference. After electrophoresis, the proteins were transferred from gel to polyvinylidene difluoride (PVDF) membrane at 20 V

constant voltages for 30 min at r.t in transfer buffer. To determine the efficiency of transfer, the blots were stained with Ponseau S (Sigma-Aldrich Corp.). Excess stain was removed by rinsing in water.

2.2.4.7 Western hybridization

The membrane was placed into blocking buffer (section 2.1.40) for 1 h at r.t. The primary antibody was diluted in blocking buffer according to manufacturer's recommendation. Following blocking, the membrane was incubated in the primary antibody for 1 h at r.t. Excess antibody was removed by washing the membrane in wash buffer for 30 min with agitation, and changing the buffer every 10 min. Secondary antibodies conjugated to horseradish peroxidase (HRP) were diluted in blocking buffer according to manufacturer's recommendation. The membrane was then incubated in the secondary antibodies for 1 h at r.t with agitation. To remove unbound secondary antibodies, the membrane was washed in washing buffer for 30 min with agitation. Detection of positive signal was achieved using SuperSignal West Pico Substrate (Pierce, Rockford, IL).

2.2.4.8 Hematoxylin and Eosin (H&E) staining

The H&E staining was performed by incubating the sections in Harris' hematoxylin (Sigma-Aldrich Corp.) for appropriate duration followed by rinsing in running water until blue color was observed. The sections were then dipped into 70 % and 90 % ethanol for 30 s each followed by counterstaining with eosin for appropriate duration. This was followed by dehydrating the sections in 95 % ethanol for 1 min and 100 % ethanol twice of 1 min each. After dehydration, the sections were incubated in xylene twice at 5-min intervals. Excess xylene was drained from the sections before a drop of DPX (Sigma-Aldrich Corp.) was applied. The sections were then mounted with a coverslips and stored at r.t. until examined under the microscope.

2.2.4.9 Immunohistochemistry staining

Tissue sections were fixed in 4% paraformaldehye for 10 min, r.t., followed by three washes with washing buffer. To quench endogenous peroxidase activity, the sections were subjected to treatment with 0.3 % hydrogen peroxide for 5 min at r.t. followed by three washes. Nonspecific binding was removed by incubating the sections in blocking buffer (refer 2.1.47), for 30 min at r.t. Primary antibody was diluted 1:100 in blocking buffer, added to the sections, and incubated for 30 min r.t., followed by three washes with washing buffer. HRP-conjugated secondary antibody was applied to the sections and incubated for another 30 min, r.t. This was followed by 3 washes of 5-min each. Colorimetric development was visualized after the addition of 3, 3' diaminobenzidine (DAB) substrate solution (Sigma-Aldrich Corp.).

2.2.4.10 Immunofluorescence staining

To determine the localization of transgene expression, cells were first plated on coverslips and then infected with viral vectors for 6 h. The cells were then replenished with fresh medium containing 10 % FBS. After 24 h, the cells were rinsed with PBS twice and fixed using 4% paraformaldehyde at r.t. for 10 min. Excess fixative was removed by agitating cells with washing buffer containing PBS with 0.1% Tween 20 at r.t. for 10 min. All subsequent steps that required rinsing were carried out at r.t. The cells were permeabilized using 0.1 % Triton-X 100, rinsed for 10 min, and incubated in blocking buffer [0.1 % Tween 20 and 10 % goat serum (Sigma-Aldrich Corp.) in PBS] for one hour. This was followed by an overnight incubation with diluted primary antibodies (final concentration of 2 µg/ml in blocking buffer) at 4°C. Cells were subsequently rinsed thrice at 5 min intervals and incubated with diluted secondary antibody (final concentration of 2 µg/ml) for an hour. The cells were mounted and examined using a LSM 510 Meta confocal microscope (Carl Zeiss Microscopy, Göttingen, Germany) with appropriate filters.

2.2.5 Recombinant DNA techniques

2.2.5.1 Electrophoresis of plasmid DNA or PCR fragments

Electrophoresis of plasmid DNA and PCR fragments was carried out as described by Sambrook et al., (1989). 0.7 % agarose gels were prepared with DNA grade agarose (Invitrogen Life Technologies) in 1 x TAE buffer and were run in 1 x TAE buffer.

2.2.5.2 Purification of DNA fragments

The DNA and PCR fragments were purified from agarose gel using Gel purification kit (Qiagen GmbH) according to manufacturer's instructions. Briefly, DNA or PCR fragments were excised from the agarose gel using a scalpel and put into a clean 1.5 ml microcentrifuge tube. Three volume of buffer QG was added to the agarose gel piece and incubated at 50 °C for 10 min. After solubilization, the DNA solution was transferred to a column and subjected to centrifugation at 13 000 xg for 1 min using a tabletop centrifuge. The column was rinsed once with buffer PE, excess PE was removed by an additional round of centrifugation. DNA or PCR fragments were eluted in 30 µl of buffer EB (10 mM Tris-Cl, pH 8.5).

2.2.5.3 Removal of nucleotides

Excess restriction enzymes or oligonucleotides were removed from reaction solution using the Nucleotide Removal Kit (Qiagen GmbH) according to manufacturer's instructions. Briefly, reaction solution was added to nucleotide removal column and centrifuged at 6000 xg for 1 min. This is followed by rinsing the column with buffer PE and centrifuging at 6000 xg for 1 min. Excess buffer PE was removed by a further centrifugation at 13 000 xg for 1 min. DNA was eluted with 30 µl of buffer EB (10 mM Tris-Cl, pH 8.5).

2.2.5.4 Restriction endonuclease digestions

The restriction endonuclease digestions reactions were performed as recommend by the manufacturer (New England Biolabs).

2.2.5.5 Dephosphorylation

For cloning of inserts with identical restriction ends, the calf intestinal alkaline phosphatase (CIAP) was used to remove the overhanging phosphate group to prevent self ligation of the vector. After restriction digestion with appropriate enzymes, the vector and the insert DNA was purified. The purified vector DNA containing the single restriction ends was then transferred to a clean microcentrifuge tube and 1 U of CIAP (New England Biolabs) was added to a final volume of 20 µl. The reaction was incubated at 37 °C for 1 h. After completion of the reaction, the CIAP was heated inactivated at 65 °C for 20 min, and the treated DNA was then purified as mentioned in 2.2.5.2.

2.2.5.6 Ligation reaction

The ligation reaction was carried out in a vector to insert ratio of 1:1 to 1:3. The ligation reactions were performed in a final volume of 10 µl containing 1 x ligation buffer (Invitrogen Life Technologies), appropriate amount of vector and insert DNA, and 1 Weiss Unit of T4 DNA ligase (Invitrogen Life Technologies) and ddH_20. The ligation reaction was incubated at 16 °C overnight.

2.2.5.7 Transformation of bacterial cells by the heat shock method

The competent bacterial cells, STBL-2 (Invitrogen Life Technologies), were thawed and kept on ice. 10 ng of supercoiled DNA or $1/10^{th}$ of ligation product was added to 50 µl of the cells and kept on ice for 20 min. The cells were heat shocked by placing in a 42 °C water bath for 25 sec, and then immediately on ice for additional 2 min before addition of 950 µl LB. The cells were incubated at 30 °C for 90 min with gentle agitation. 100 µl of the transformed cells were plated on to LB agar plate containing 100 µg/ml of ampicillin (Sigma-Aldrich Corp.).

2.2.5.8 Polymerase Chain Reaction (PCR)

For the cloning of DNA fragments, *pfu* DNA polymerase (Stratagene Cloning Systems, La Jolla, CA) was used to amplify target sequences, since it exhibited the lowest error rate than

most thermostable DNA polymerase. To amplify DNA fragments, reaction mix containing 1 x *Pfu* buffer, 2.5 mM MgCl, 10 mM dNTPs, 50 pmol of forward and reverse primers, and 2.5 Unit of *Pfu* DNA polymerase were added to a final volume of 25 µl. The reaction starts with an initial denaturation at 95 °C for 5 min. This is followed by incubating the sample at 95 °C for 30 sec. Annealing temperature of the PCR primers to the template varies, but generally falls between 50-60 °C. Annealing reaction was carried out for 1 min. The extension reaction is programmed at 72 °C, and the duration is dependent on the size of the desired PCR product. Standard PCR reaction is repeated for 30 cycles with a final extension at 72 °C for 10 min. After the completion of the reactions, the samples were kept on ice. If desired, the PCR products were analyzed using agarose gel electrophoresis.

2.2.5.9 Reverse Transcriptase-PCR (RT-PCR)

The first strand complementary DNA (cDNA) was synthesized using 1 or 2 µg of total RNA as template. cDNA was synthesized using random hexanucleotide primers (Invitrogen Life Technologies) and oligo-dT_{12-17} primers, in the presence of Superscript II reverse transcriptase (Invitrogen Life Technologies) at 42 °C for 45 min. The RNA samples were pretreated with 1 U of RNase free DNase (Invitrogen Life Technologies) by incubating at 37 °C for 15 min followed by 70 °C for 5 min to remove contaminating genomic DNA. DNase I was subsequently removed by extracting with phenol and chloroform. The RT-PCR reaction was prepared in a final volume of 25 µl using 1 µl of the first strand cDNA as template. PCR reaction was performed as described in section 2.2.5.8.

2.2.6 Cell viability assay using trypan blue exclusion assay

To determine the viability of cells following infection, the monolayer of infected cells were rinsed with PBS and harvested at particular time points post infection. Equal volume of cell suspension was mixed with 0.4 % of trypan blue solution (Sigma-Aldrich Corp.). Cells were visualized under phase contrast microscope (Nikon). Cells that are still intact will exclude

trypan blue and appear as clear under the microscope. Assays were performed in triplicate. The number of viable cells was expressed as a percentage of the total cells.

2.2.7 Terminal deoxynucleotide transferase dUTP Nick End labeling (TUNEL) assay

dGli36 cells (3 x 10^5) was plated on cover slips and infected with pC8-FasL or pC8-FADD (MOI of 1.0) for 6 h. The cells were then replenished with fresh medium containing 10 % FBS or medium supplemented with 50 μM lovastatin. TUNEL staining of apoptotic cells was performed according to manufacturer's protocol (Roche Diagnostics). Briefly, after 72 h, cells were rinsed with PBS twice and fixed using 4% paraformaldehyde at room temperature for 1 hr. Excess fixative was removed by rinsing in PBS, followed by treatment with PBS containing 0.1 % Triton X-100 and 0.1 % sodium citrate for 2 min on ice to permeabilize the cells. After washing with PBS to remove excess permeabilizing solution, cells were incubated for 1 hr at 37 °C in TUNEL reaction mixture containing terminal deoxynucleotidyl transferase (TdT) and TMR red-labeled dUTP, which preferentially labels DNA strand breaks generated during apoptosis. Excess reaction mixture was removed by rinsing with PBS. A fluorescence microscope with appropriate filters Was used for visualization.

2.2.8 Animal models

2.2.8.1 Establishment of subcutaneous (s.c.) tumor model

After removal of trypsin, tumor cells are resuspended in PBS. Each mouse, either Balb-C nu/nu or CB-17 SCID, was inoculated with 2 x 10^6 tumor cells in total volume of 100 μl. The tumor cells were injected into the mouse using 1-ml syringe connected to a 27-G needle. Tumor volume was calculated using the formula: tumor volume (mm^3) = 0.52 x (width [mm^2] x (length [mm]) (Bergers et al., 1999).

2.2.8.2 Establishment of intracranial (i.c.) tumor model

For intracranial tumor model, mice were injected with 1 or 2 x 10^6 cells resuspended in a maximum volume of 10 μl of PBS. The tumor cells was stereotactically inoculated into the caudate putemen region [bregma (0,0), 2.0 mm lateral, 2.5 mm depth] using stereotaxic equipment (Stoelting Co, Wood Dale, IL). Tumor growth was monitored by magnetic resonance imaging (MRI), H&E staining, and loss of body weight.

2.2.8.3 Establishment of dGli36-SCID8 cells

The formation of s.c. dGli36-derived tumor is not consistent in SCID mice. To establish a more consistent derivative, dGli36 cells was serially passaged in SCID mice. When the tumor reached a volume of approximately 45 mm^3, the tumor was harvested into cold DMEM containing 10 % serum. The tissue suspension was treated with 0.25 % trypsin solution at 37 °C for 10 min, and passed the mixture through a 1 ml serological pipette followed by flame-polished pasteur pipette. The suspension was subjected to centrifugation at 100 x g for 5 min. The pellet was resuspended in cold DMEM containing 10 % serum. The recovered cells were grown in culture for one passage after which the cells were reinoculated into SCID mice. The cells were passaged in SCID mice three times before used. *In vitro* and *in vivo* growth kinetics was determined. The growth rate of dGli36-SCID8 was similar to dGli36 cells. *In vivo*, dGli36-SCID8 consistently forms s.c. tumors in both SCID and nude mice. The morphology of dGli36-SCID8 resembles that of the parental dGli36 cells. Transfection and infection efficiency is comparable.

2.2.9 Statistical analysis

Statistical analysis was performed using Prism 3.0 (Graphpad Software Inc., San Diego, CA) and Instat (Graphpad). Paired Student's *t* test was used when comparing two related experimental groups. Unpaired Student's *t* test was used when comparing experimental data from 2 unrelated groups. One way analysis of variance (ANOVA) followed by Bonferroni Multiple Comparisons Test were used for comparing statistical significance for more than 2

groups. p value < 0.05 was considered statistically significant. The Kaplan-Meier survival analysis was used to calculate the percentage of survival as a function of time, the survival curves were compared using the logrank test.

Chapter 3

Characterization of the cell cycle-regulated HSV-1 amplicon vector

3.1 Background

Currently, one of the greatest challenges to cancer gene therapy is the ability to regulate transgene expression with minimal adverse effects. Tissue-specific or tumor-specific promoters have been employed to target transgene expression to particular cell types (Shibata et al., 2000; Ueno et al., 2001). However, tissue-specific promoters are generally weak inducers of transgene expression. Moreover, the essential upstream control region that governs gene expression from a particular promoter can span several kb; this represents a major hindrance in the construction of the transcriptionally-mediated targeted vector systems (Agha-Mohammadi and Lotze, 2000). To circumvent the problem of relying on exogenous stimulation for gene expression regulation, endogenous cell cycle regulation has recently been introduced as a new concept (Nettelbeck et al., 1999). As hyperproliferation is a characteristic of most malignant tumor cells, the transduction of cell cycle-regulated viral vectors carrying therapeutic genes into the tumor region could represent promising tools for cancer gene therapy.

3.1.1 Cell cycle regulation

The eukaryotic cell cycle is divided into four phases, namely, G_1, S, G_2 and the M phase. Nonproliferating quiescent cells, reside in the G_0 phase, and enter into the cell cycle when stimulated by mitogenic factors. The cells may proceed to DNA replication, to pause or to exit the cell cycle in G_1 phase. DNA replication takes place in the S phase, cell division at the end of the G_2/M phase. This complex process is controlled by two major checkpoints, the G_1/S checkpoint (Figure 3.1) and the G_2/M checkpoint, both of which are critical for maintaining genomic integrity. The regulatory molecules that are involved in the G_1/S transition are cyclin D, cyclin E, cdk (cdk2, cdk4 and cdk6), the protein phosphatase cdc25A, transcription factor E2F, pRb, and cdk inhibitors (p15, p16, p21, and p27). The Rb-E2F pathway is the major regulator of cellular progression from G_1 to S phase. In fact, inactivation of Rb occurs in 20-30 % of GBM (He et al., 1995; Henson et al., 1994; Ueki et al, 1996).

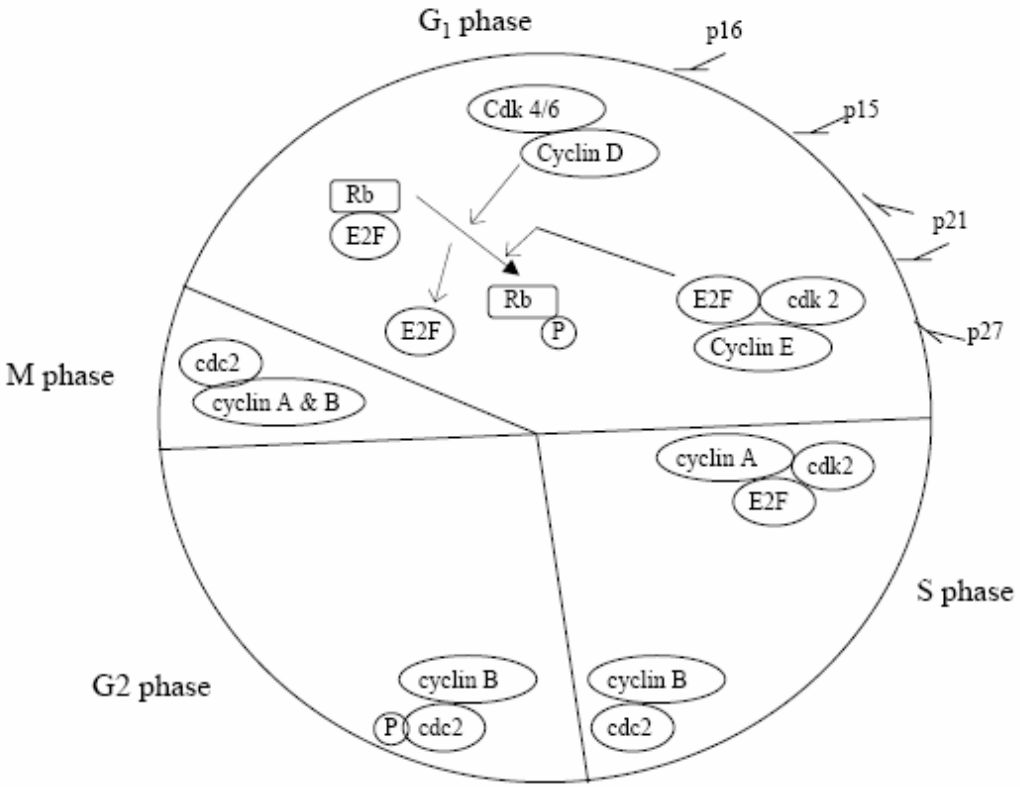

Figure 3.1. Summary of cell cycle regulation.
The G_1 phase of the cell cycle is primarily regulated by the Rb-E2F pathways. Altered expression of Rb, cyclin D, cdk4/6, p16, p15 and p21 have been observed in gliomas.

3.1.1.1 Transcriptional repression mediated by E2F

Transcriptional repression is a major mechanism that regulates gene expression during the cell cycle. In mammalian cells, a specific set of cell cycle genes that are transcribed around the G_1/S border is regulated by factors of the *E2F* family, a heterodimeric transcription factor composed of members of the *E2F* and *DP* multigene families. In G_0 and early G_1, the E2F/DP-1 complex is bound to pRb, and is hence inactive. As cell cycle progresses, pRb is hyperphosphorylated by G_1-specific cdk4/6, leading to dissociation from E2F/DP-1, which generates free E2Fs and thus enables the activation of E2F-regulated genes. Several genes expressed in late G_1/early S phase have been shown to be regulated through an E2F-mediated mechanism. These genes are involved in cell cycle regulation, for instance, *cdk2*, *cdk4*, *cyclin A*, *D* and *E*; and DNA synthesis, such as *proliferating cell nuclear antigen* (*PCNA*) and *RR* (Black and Azizkhan-Clifford, 1999). The presence of E2F binding sites on these genes enables the binding of E2F during late G_1/early S phase of the cell cycle. These genes are generally repressed by E2F during G_0/G_1 and activated at late G_1/early S phase.

3.1.2 Cyclin A

Cyclin A is one of the genes that are regulated by the transcription factor, E2F. Cyclin A is a cell cycle regulatory protein that functions in the S phase and M phase of the mammalian cell cycle. Transcription of c*yclin A* is regulated; its mRNA levels increase at the G_1/S boundary and reach peak levels in S phase (Pines and Hunter, 1990). Cyclin A was first identified in sea urchin embryos (Evans et al., 1983) and was found to interact and activate cdc 2 (Pines and Hunter, 1990) and cdk2 (Swenson et al., 1986). During S phase of the cell cycle, cyclin A forms a complex with cdk2, this interaction then leads to phosphorylation and activation of the cellular DNA replication factor (Dutta and Stillman, 1992; Elledge et al., 1992). Cdk2 dissociates from cyclin A as the cells progress into G_2/M phase, allowing cyclin A to interact with cdc2.

3.1.3 Regulation of the cyclin A transcription

The short promoter sequence of *cyclin A* has been shown to harbor most regulatory elements required for cell cycle-regulation and efficient transcription (Henglein et al., 1994; Huet et al., 1996; Zwicker et al., 1995b). The *cyclin A* promoter does not contain a TATA-binding site, instead it comprises of an inverted CCAAT box binding site and four Sp1 sites, an ATF site and two overlapping sites for the murine G_1/S-specific transcription factor Yi (Figure 3.2). A single AP-1 site and two NF-Y/CBF sites are also found on the promoter (Henglein et al., 1994). Analysis of other S/G_2 phase specific promoter sequences revealed a conserved regulatory region that is shared among *cyclin A, cdc25C, cdc2,* and *B-myb* (Figure 3.3).

These promoters are controlled by transcriptional repression through two contiguous protein binding sites termed "cell cycle-dependent element" (CDE) and "cell cycle genes homology region" (CHR). The CDE and CHR region in these promoters are highly conserved (Figure 3.3). The CDE region is occupied by repressor proteins during G_0/G_1, but this repression is released in G_2. It has been found that mutation of either CDE or CHR abolished the repression in G_0 (Zwicker et al., 1995b). Interestingly, genomic footprinting of the *cyclin A* promoter depicted a cell cycle-regulated protein binding to the G residues of the CDE element in the major groove, and the A residues of the CHR element in the minor groove. This cell cycle-regulated protein was termed "cell cycle dependent factor-1" (CDF-1).

3.1.4 CDF-1

The *cdc25C* promoter was used as a model system to study transcriptional regulation of gene expression controlled by the CDF-1 repressor protein (Zwicker et al., 1995a). The *cdc25C* promoter contains three functionally important NF-Y binding sites upstream of the CDE/CHR element. The CDE element does not interfere with basal transcription from the core promoter (Lucibello et al., 1995); however, its function is dependent on a stretch of upstream activating sequences (UAS) that is required for transcriptional activation. A second major transactivator is the Sp-1 transcription factor, which interacts with two sites further upstream of the

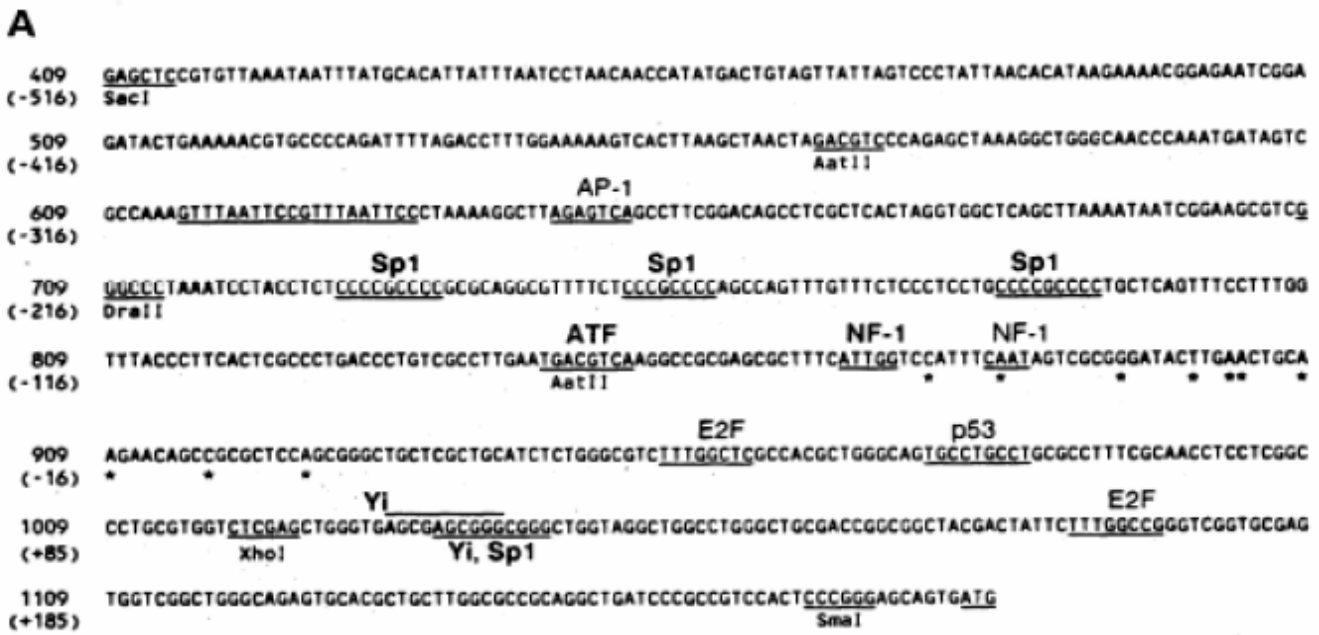

(Henglein *et al.*, 1994)

Figure 3.2. Cyclin A promoter sequence.
Asterisks indicate major transcription start points (± 2 bp). Numbers in parentheses refer to the 3' most start site (position 9258 as +1. A 10-bp repeat and the translation start site are underlined. Consensus (bold) or near-consensus transcription factor binding sites are indicated and underlined.

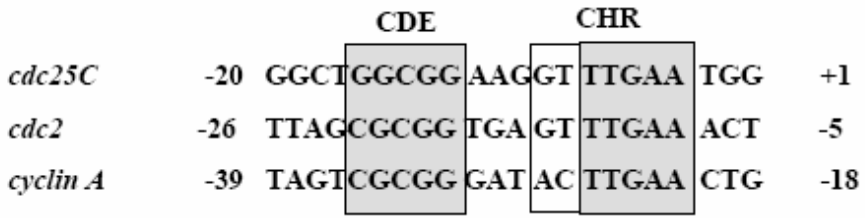

CDE	N	N	T/G	G/C	G	C	G	G	N A/G
CHR	N	G/A	T/C	T	T	G	A	A	N N

Figure 3.3. Sequence alignment of the CDE/CHR regulatory region in the *cdc25C*, *cdc2* and *cyclin A* promoter.
Box region represents the core CDE and CHR sequence. Shaded color highlights the conserved sequence. Underlined sequences represents core sequence. From Zwicker et al., 1995b.

CCAATT-box binding factor (CBF)/NF-Y binding sites. Repression of gene expression mediated by CDF-1 is specific for a subset of transactivators. Significant regulation is observed with three different activation domains, namely, the glutamine rich *Oct-2*, *Sp1* and the serine/threonine/glutamine-rich domain of the human NF-Y (Zwicker et al., 1997). In fact, the most significant repression was seen with the A subunit of NF-Y. Binding of NF-YA to nucleosomes induces DNA bending, resulting in the opening of the chromatin structure of the proximal promoter. In contrast to NF-YA, no significant transactivation was detected with *VP16*, *Myc* and the serine/threonine rich *ITF-2*. Replacing the UAS of *cdc25C* resulted in partial or complete abrogation of cell cycle regulated repression.

CDF-1, a G_0/G_1 phase-specific repressor protein, was found to bind with similar efficiency to *cdc25C*, *cdc2* and *cyclin A*, and this binding is dependent on the presence of intact forms of CDE and CHR (Liu et al., 1997). In fact, CDF-1 binds cooperatively to these two elements. There is much evidence indicating that CDF-1 is the major repressor of *cyclin A* promoter. As demonstrated by DNA binding assays, the affinity of E2F for the *cyclin A* CDE is lower compared to its affinity for promoters that harbor the E2F-binding sites, such as *B-myb*. Moreover, as mentioned above, the transcriptional repression of the *cyclin A* promoter is highly dependent on the CHR region. Mutation or deletion of the CHR sequence completely abolished the CDF-1 mediated repression. Similar to *cyclin A*, the CHR element from the *cdc25C* promoter only interacts with CDF-1, but not E2F (Liu et al., 1997).

One of the factors implicated in cell cycle-regulated repression is E2F, which can form DNA binding repressor complexes through its interaction with pocket proteins, such as pRb. *B-myb, p107 and orc-1* are among the promoters controlled by transcriptional repression through E2F sites. The distinction between transcriptional repression mediated through E2F and CDF-1 is evident from the repression of the *B-myb* promoter, which requires a second regulatory element downstream of E2F site, termed CHR or DRS. Liu et al. (1997) showed that CDF-1

does not bind to the *B-myb* promoter under conditions where a strong interaction is seen with the *cdc25C, cdc2* and *cyclin A* promoters.

CDF-1 is distinct from E2F whereby it neither contains DP1 nor forms a complex with pocket proteins (Liu et al., 1997). Liu *et al*. (1998) demonstrated that E2F does not play a significant role in the repression of the *cyclin A* promoter in G_0/G_1 cells. Constructs which contained mutations in the CDE element, abolishing the binding of E2F but not affecting CDF-1 activity, demonstrated that repression of the *cyclin A* promoter in G_0 cells was not affected (Liu *et al*., 1998). However, when the cells progressed to late G_1, interaction of E2F with the CDE element was clearly observed (Liu et al., 1998). In the G_0/G_1 phase, CDF-1 occupies the CDE/CHR element, leading to repression of promoter activity. In late G_1/S, CDF-1 partially dissociates from CDE element; and the free E2F competes for the binding to CDE. At this stage of the cell cycle, complex formation of E2F with the CDE is comparable to the binding of CDF-1 to the CDE element. Promoter variants with mutations in the CDE leading to decreased interaction with E2F show a delay in derepression. In contrast, mutants which exhibit increased E2F binding are upregulated prematurely. This induces the onset of transcription and the subsequent inactivation of CDF-1 in S/G_2 phase, leading to maximum levels of gene expression.

3.1.5 Recombinant transcriptional activator (RTA) system

The construction of the RTA system is based on the modular structure of transcription factors which allows the DNA binding domain to interact with the transactivation domain derived from different proteins (Nettelbeck et al., 1999).

Essentially, this system is based on the CDF-1 transcriptional repressor protein, which is specifically expressed during the G_0/G_1 phase of the cell cycle (Liu et al., 1997). A chimeric transcription factor, consisting of the Gal4 DNA binding domain and the serine/threonine/glutamine-rich transactivation domain of the NF-Y subunit A (Gal4/NF-YA),

is expressed as a fusion protein. The Gal4 DNA binding domain can interact with another promoter, consisting of the minimal *cyclin A* promoter CDE/CHR regulatory element downstream of multiple Gal4 DNA binding sites. In non-dividing cells, the transactivation of the *cyclin A* promoter is repressed because the CDE/CHR element is occupied by the CDF-1 repressor protein thus abolishing transactivation via the upstream factors. Absence of CDF-1 repressor protein in dividing cells allows the binding of the chimeric transcription factor Gal4/NF-YA to the Gal4 binding sites located upstream of the minimal *cyclin A* promoter, hence driving the transcription of the reporter/therapeutic gene (Figure 3.4).

3.1.5.1 Methods for synchronizing cells at G_1 phase

Synchronization of cells at specific stages of the cell cycle is particularly useful for studying cell cycle-regulated events and to analyze proteins whose expression are dependent on cell cycle stages. The G_1 phase of the cell cycle averages between 8-16 h for most cell lines. To synchronize cells at G_0/G_1, cells may be subjected to serum free medium for 24-48 h (Ausubel et al., 1987) to allow the whole population to respond to serum withdrawal. However, some cells do not respond to serum withdrawal and require the use of drugs such as lovastatin and mimosine, to induce arrest. Another method of synchronizing cells at the G_0/G_1 is the depletion of amino acids, such as thymine and methionine, in the culture medium (Sallot et al., 1996; Wejde et al., 1993). However, tumor cells recalcitrant to synchronization using either serum withdrawal or amino acid depletion, in which case, lovastatin or mimosine can be used to arrest the cells.

Lovastatin inhibits 3-hydroxy-3-methylglutaryl-coenzyme A (HMG-CoA) reductase, resulting in depletion of mevalonate, which is a precursor of cholesterol synthesis (Bonapace et al., 1996). Mevalonate is also required for the isoprenylation of substrate molecules, such as p21 ras (Wejde et al., 1993). The ability of lovastatin to induce cell cycle arrest at early G_1 has been demonstrated in a variety of cell lines (Bonapace et al., 1996; Wilcken et al., 1997). Mimosine is an amino acid derived from plants. The target molecule of mimosine is

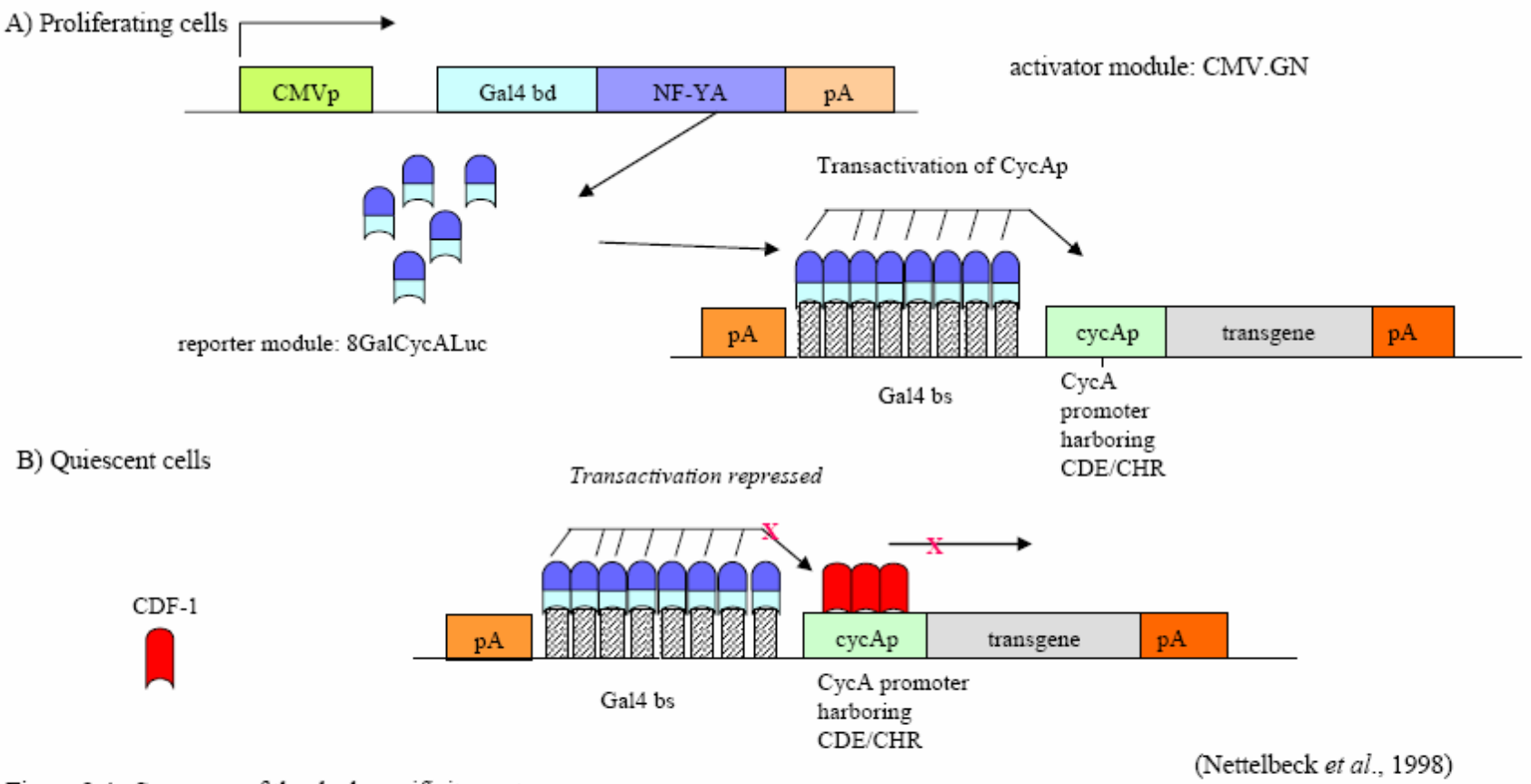

(Nettelbeck *et al.*, 1998)

Figure 3.4. Summary of the dual specificity system.

In proliferating cells, the chimeric transcription activator Gal4/NF-YA binds to the Gal4 DNA binding site (bs) on the reporter module, leading to the transactivation of the minimal cyclin A promoter (cycAp) and the subsequent activation of transgene expression. In quiescent or G_0/G_1 cells, the presence of the CDE/CHR specific repressor protein CDF-1 interacting with the minimal cyclin A promoter prevents the transactivation through the NF-YA. Therefore, transgene is not expressed.

unknown, but it has been shown to block cell cycle in late G_1 or at the G_1/S boundary. To avoid complications, we have decided to use lovastatin instead of mimosine to induce G_1 arrest since its mechanism is better understood.

3.1.6 Liver regeneration model

One of the best examples of studying cellular replication *in vivo* is the regeneration of liver following partial hepatectomy (PHx) (Higgins and Anderson, 1931). In this procedure, two-thirds of the liver is removed without affecting the remaining lobes. The remaining hepatic tissues will enlarge to compensate for the loss of tissue mass. The entire process of liver regeneration, which is largely due to the rapid proliferation of hepatocytes, takes approximately 5 to 7 days (Michalopoulos and DeFrances, 1997). Analysis of DNA synthesis showed that the replication of hepatocytes peaks at about 48 h after PHx, which correlates with the expression of cyclin A; cyclin A levels increase from 12 h onwards until 7 days post-PHx (Michalopoulos and DeFrances, 1997). We have chosen liver regeneration following PHx as a model to study the activation of transcriptional activity associated with the onset of DNA replication. In normal adult rodents, increasing numbers of hepatocytes enter S phase shortly after hepatectomy, thus providing a good system to study cell cycle-regulated transgene expression conferred by the cell cycle-regulated amplicon vector *in vivo*.

3.1.7 Aim of research

The strategy described in our present study presents a more efficient alternative approach where a single-vector system combining both the NF-YA transcriptional activator and the reporter modules is assembled to confer cell cycle-dependent transgene expression. This is particularly advantageous in brain tumor gene therapy since cell proliferation is a rare event in the normal brain. In contrast, malignant brain tumor cells divide rapidly leading to the invasion of surrounding normal brain tissues.

3.2 Methods

3.2.1 Construction of the cell cycle regulated amplicon plasmids

pHGCX (HSV-1 amplicon) vector was obtained from Dr. Y Saeki (Massachusetts General Hospital, Boston, MA). CMV.GN and 8GalcycA were obtained from Dr. R Müller (Institute of Molecular Biology and Tumor Research, Marburg, Germany). To construct pHGCX.GN, the Gal4 DNA binding domain (amino acids 1-147) and the murine NF-YA transcriptional activation domain (amino acids 1-261) in plasmid CMV.GN was inserted into the *Hin*dIII and *Bam*HI restriction enzyme sites of pHGCX. The 8GalLuc DNA fragment was released from plasmid 8GalcycA and subcloned into the *Nhe*I and *Bam*HI restriction enzyme sites of pHGCX, and the pre-existing CMV promoter was subsequently removed using *Spe*I and *Nhe*I to generate pIH8GalLuc plasmid. To generate pC8-36 plasmid, the 8GalLuc fragment was amplified by PCR using 8GalcycA plasmid as a template (the forward and reverse primers were 5'-CCTCTTCGCTATTACGCC and 5'-AAGAAGACAGTCATAAGTGCGG, respectively). The amplified DNA fragment was subcloned into the shuttle plasmid pGemT-easy (Promega, Madison, WI), released using *NotI* restriction enzyme sites, and inserted into pHGCX.GN. When this 8GalLuc cassette was inserted in the opposite orientation to Gal4/NF-YA, the resulting plasmid was named pC8-34. All plasmids were amplified in *E. coli* STBL-2 (Invitrogen Life Technologies) and DNA was extracted with a QIAprep spin miniprep Kit (Qiagen). All plasmids were verified by DNA sequencing (Applied Biosystem Inc., Foster City, USA).

3.2.2 Transfection of oligomers

For oligomer competition assay, oligomers (500 nM) were mixed with 3 µl of Oligofectamine (Invitrogen Life Technologies Life Technologies) in Opti-MEM for 15 min at r.t. The complexes were added to HeLa cells (3×10^5) and incubated for 4 h at 37 °C. The cells were then rinsed with PBS twice, followed by transfection of pC8-36 plasmids, using LipofectAmine reagents. Refer to section 2.2.1.5 for DNA transfections of cells.

3.2.3 Preparation of nuclear extract

HeLa cells (3 x 10^6) treated with lovastatin were rinsed with PBS twice, trypsinized and resuspended in 800 µl of buffer A (refer 2.1.43). After incubation on ice for 15 min, the cells were lysed in the presence of 50 µl of 10 % Nonidet P40 (NP-40). Each sample was vortexed briefly and centrifuged for 45 sec at 5000 xg at 4 °C to collect the nuclear pellet. The pellet was then resuspended in 100 µl of buffer C (refer 2.1.44). Samples were incubated for 10 min on ice followed by centrifugation at 14 000 xg at 4 °C to remove the insoluble materials; supernatant, containing the nuclear extract, was stored at -70 °C. The protein concentration was determined as described in section 2.2.4.2.

3.2.4 Labeling of oligonucleotide probes

Oligonucleotide probes were labeled at the 3' end, using terminal deoxynucleotidyl transferase enzyme in the presence of biotin-N4-dCTP (Pierce Biotechnology) according to manufacturer's conditions. The labeled oligonucleotides or probes were purified using the Nucleotide Removal Kit (Qiagen GmbH) according to the manufacturer's instructions.

3.2.5 Electrophorectic mobility shift assays (EMSA)

EMSA reactions were performed with the LightShift Chemiluminescent EMSA kit (Pierce Biotechnology) according to the manufacturer's instructions. Briefly, 5 µg of HeLa nuclear extract was incubated in 2 µl binding buffer (refer 2.1.42) containing 2.5 % glycerol, 5 mM $MgCl_2$, 0.2 mM EDTA, 0.05 % NP-40, 250 ng of poly(dA-dT) (Amersham Biosciences AB, Uppsala, Sweden). Biotin-labeled probe (100 fmol) was added in a total volume of 20 µl and the reaction mixture was incubated for 20 min at r.t. The double- stranded probe CDE (5'TTACTGGGCTGGCGGAAGGTTTGAATGGTCAATTACTGGGCTGGCGGAAGGTT TGAATGGTCAA-3'), was used (Liu et al., 1997). The random oligomer contains an irrelevant sequence. The protein-DNA complexes were then separated on native 6 % PAGE at r.t. Gels were transferred to Hybond N+ nylon membrane (Amersham Biosciences) followed by cross-linking at 120 mJ/cm^2, using a Stratalinker (Strategene). Detection and

visualization of the protein-DNA complexes were performed using a LightShift Chemiluminescent EMSA kit (Pierce Biotechnology) according to the manufacturer's instructions.

3.2.6 Hepatectomy

Animal work was performed under guidelines approved by the National Cancer Centre Animal Care and User Committee. Female BALB/c mice were purchased from the Laboratory Animal Unit of the National University of Singapore, Singapore. The mice were of age 6-8 weeks and submitted to a 12:12-hour light/dark cycle, housed five per cage, and allowed food and water. Animals to undergo hepatectomy were anesthetized with an intraperitoneal (i.p.) injection of ketamine/xylazine (70/10 mg/kg). A 70% PHx was performed through a midline incision as described by Higgins and Anderson (1931). Forty eight h after PHx, the animals were treated with an injection of virus (1 x 10^6 TU) via tail vein. Regenerated liver tissues and tissues from normal livers were removed and assayed for luciferase activities.

3.2.7 Isolation of single cells for FACS analysis

The liver tissues were harvested in cold DMEM containing 10 % serum. Liver tissues were then treated with 0.05 % collagenase solution at 37 °C for 10 min. This was followed by passing the mixture through a 1 ml serological pipette, followed by 18 G and 23 G needle. The suspension was subjected to centrifugation at 1000 x g for 5 min. The pellet was resuspended in cold DMEM containing 10 % serum. For cell cycle analysis, the pellet was resuspended in 70 % ethanol overnight followed by treatment with propidium iodide (refer to section 2.2.1.6).

3.3 Results

3.3.1 Construction of a cell cycle-regulatable HSV-1 amplicon viral vector

The HSV-1 amplicon plasmid, pHGCX, contains the gene encoding the eGFP under the control of the viral immediate early promoter (*IE* 4/5). The transgene of choice can be inserted into the multiple cloning sites (MCS) located downstream of the strong cytomegalovirus (CMV) promoter, as shown in Figure 3.5a. The activator plasmid, pHGCX.GN (Figure 3.5b), was constructed by subcloning the chimeric transcriptional activator module composed of the DNA-binding domain of Gal4 and the repressible activation domain of the A subunit of NF-Y into pHGCX. In the reporter plasmid, pIH8GalLuc (Figure 3.5c), the luciferase reporter gene was under the control of a minimal cyclin A promoter. Located upstream of the minimal cyclin A promoter was an eight-tandem repeats of the Gal4 DNA-binding sites, which allowed for the interaction of the Gal4 DNA binding domain encoded by the plasmid pHGCX.GN. In proliferating cells, the interaction between the activator- and the reporter- modules-containing plasmids, namely pHGCX.GN and pIH8GalLuc, respectively, will augment the expression level of the transgene. In addition to these basic constructs (pHGCX, pHGCX.GN and pIH8GalLuc) we have also incorporated both the activator module and the reporter module into our single-vector plasmids, pC8-36 and pC8-34 (Figure 3.5d and 3.5e). In the construct pC8-36, the activator module (Gal4/NF-YA) and the reporter module (8GalLuc) were constructed to be in the same direction as shown in Figure 3.5d. To ensure that any transgene activity observed was not due to read-through by the CMV promoter; the activator module (Gal4/NF-YA) and the reporter module (8GalLuc) of pC8-34 were constructed in opposite orientation to one another (Figure 3.5e). To exclude the possibility of promoter interference from the upstream CMV promoter, we have also constructed pC8-delcycA-Luc, whereby the minimal cyclin A promoter has been removed (Figure 3.5f).

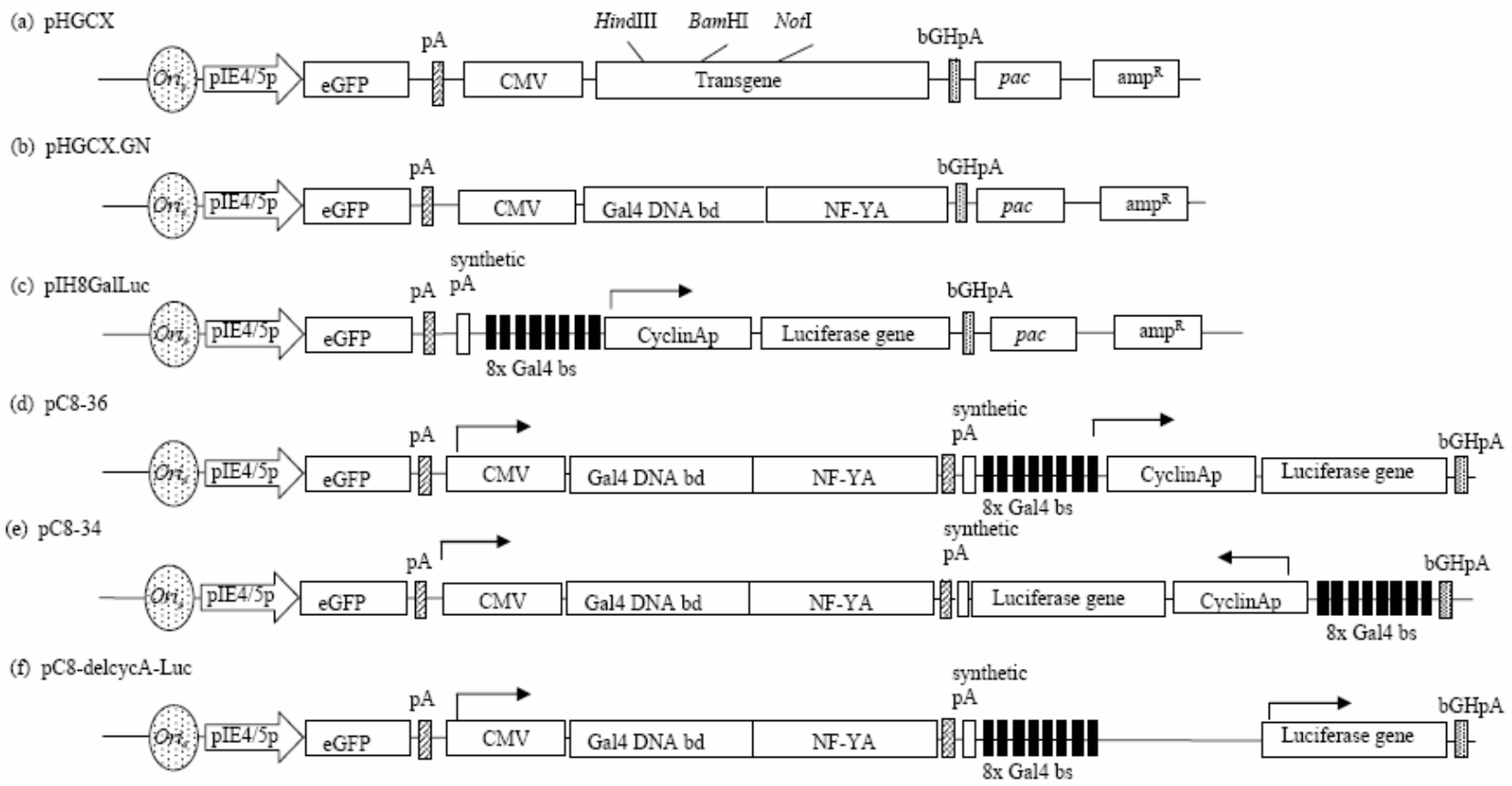

Figure 3.5. Constructs used in this chapter.
(a) pHGCX is the backbone HSV-1 amplicon vector. (b) pHGCX.GN contains the chimeric transcription activator Gal4 DNA binding domain and NF-YA transactivator. (b) pIH8GalLuc is the amplicon vector containing the Gal 4 DNA binding site, the minimal cyclin A promoter and the luciferase gene. (d) pC8-36 contains both the activator and the reporter module in the same orientation. (e) To prevent translational readthrough, the reporter module is cloned in the opposite orientation, generating pC8-34. (f) In pC8-delcycA-Luc, the minimal cyclin A promoter is deleted.

3.3.2 Enhanced transgene expression via a single-vector construct

For *in vivo* gene therapy purposes, it would be desirable to introduce a single-plasmid vector, pC8-36 and pC8-34, which contain of all the essential elements for cell cycle regulation. The transfection efficiencies of these single-vector constructs were compared with those obtained following the cotransfection of both the activator (pHGCX.GN) and reporter (pIH8GalLuc) plasmids in a 1:2 ratio (Figure 3.6). Transfection of the pIH8GalLuc plasmid was performed and served as negative control. The transfection efficiency among the various plasmid constructs in CNE2 cells was comparable (~ 50 %), as analyzed by counting the number of GFP positive cells. The level of luciferase expression in pC8-36 transfected cells (5720 RLU/μg) was 30-fold higher than that of pIH8GalLuc (189 RLU/μg), which served as negative control, and 4-fold higher than the co-transfection of both pHGCX.GN and pIH8GalLuc plasmids (1309 RLU/μg), which served as positive control. Luciferase activities mediated by pC8-delcycA-luc plasmid (183 RLU/μg) is similar to the negative control, pIH8GalLuc, indicating that transgene expression observed in pC8-36 is mediated by the transactivation of the cyclin A promoter by NF-YA, and not due to interference from upstream CMV promoter. Transgene expression mediated by pC8-34 (1175 RLU/μg), in which the activator and reporter modules are in opposite orientations, exhibited similar luciferase activities as the corresponding co-transfected plasmids. The lower level of luciferase activities observed in pC8-34 thus suggests the possibility of interference between CMV and cyclin A promoters.

3.3.3 Synchronization of cells at early G_1 phase using lovastatin

In order to evaluate the cell cycle regulatory abilities of our amplicon plasmid constructs, target cells were subjected to treatment with lovastatin for the induction of G_1 arrest. The cells were treated with escalating doses of lovastatin starting from 20 μM to a maximum of 120 μM concentration in the presence of 0.1 – 0.5 % serum for 24-48 h. The cell cycle distribution was determined using FACS analysis. The optimum concentration of lovastatin employed was selected based on the minimal toxicity and dosage required to achieve > 85 %

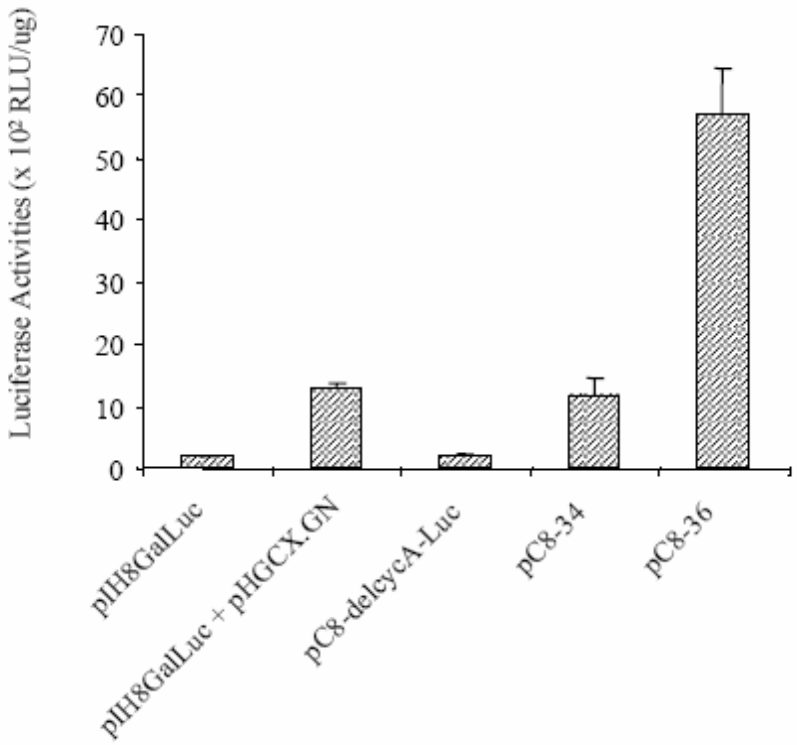

Figure 3.6. Single vector construct containing both activator and reporter module is much more efficient than co-transfection.

pIH8Galluc, pHGCX.GN, pC8-delcycA-Luc, pC8-34 and pC8-36 were transfected into CNE2. Luciferase expression was determined 24 h post-transfection. Data shown is an average of triplicate readings ± SEM.

of G_1 population. NIH3T3 cells were synchronized at the G_1 phase of the cell cycle in the presence of 40 μM lovastatin and 0.5 % serum for 48 h. This reduced the percentage of S phase cells from 28 % to ≤ 3 % as monitored by flow cytometry and represented in Figure 3.7.

3.3.4 Cell cycle-regulated transgene expression mediated by HSV-1 amplicon plasmid vectors in NIH3T3

To determine the cell cycle regulatory abilities of the amplicon vectors, NIH3T3 cells were transfected with pC8-36 and the control plasmid, pIH8GalLuc. The degree of cell cycle regulation was measured as a ratio of luciferase activity of the proliferating and G_1-arrested cells. Our results showed that luciferase activities were 9-fold higher in proliferating cells (21669 RLU/μg) in comparison to the corresponding G_1-arrested cell populations (2283 RLU/μg) (Figure 3.8a). No significant difference was observed in cells transfected with pIH8GalLuc. Immunoblotting against cyclin A antibody demonstrated the presence of cyclin A in proliferating cells and the reduction of cyclin A protein in the G_1-arrested populations (Figure 3.8). In contrast, the luciferase activities in both proliferating cells and G_1-arrested cells transfected with pHGCX-Luc remained similar (Figure 3.8b). These results indicated that the pC8-36 amplicon plasmid is able to confer cell cycle dependent transgene regulation.

3.3.5 Cell cycle-regulated transgene expression mediated by HSV-1 amplicon plasmid vectors in a series of cell lines in vitro

In addition to using the mouse fibroblast cell line, NIH3T3, we also examined if our constructs would allow for proliferation-dependent gene expression in various other tumor cell lines. The sensitivity of these cell lines to lovastatin was predetermined and the optimal growth-arrested condition was used for each cell line. Amplicon plasmids (pC8-36) were transfected into six human tumor cell lines of different origins, namely, Gli36 (glioma); HeLa (cervical carcinoma), PC-3 (prostate carcinoma), Saos-2 (osteosarcoma), SF767 (recurrent primary glioma) and U373MG (glioma) (Figure 3.9a; 3.9b 3.9c, 3.9d, 3.9e, and 3.9f, respectively). The ratio of luciferase activities between proliferating and G_1-arrested cells

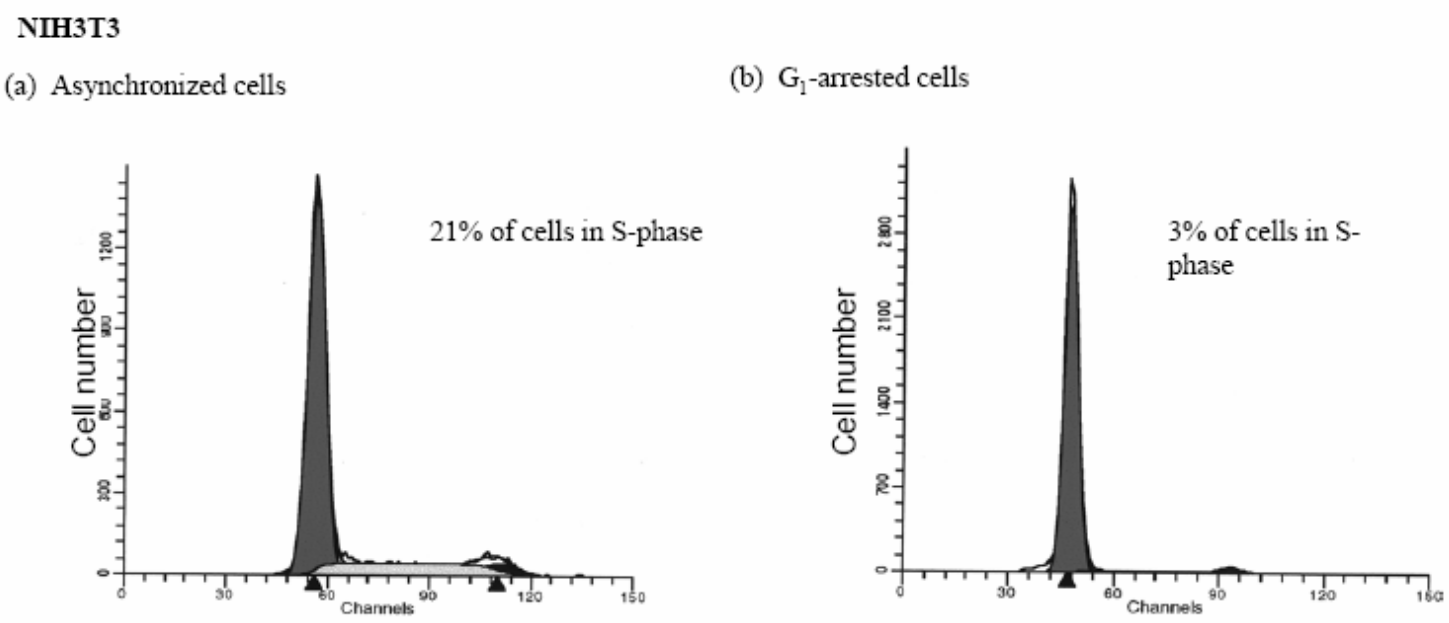

Figure 3.7. Cell cycle profile of NIH3T3.

(a) NIH3T3 cells were cultured in DMEM containing 10 % serum for 24 h. (b) To induce G_1 arrest, NIH3T3 cells were treated with 40 uM of lovastatin in DMEM containing 0.5 % serum for 48 h. Cells were harvested after the respective time points, and processed for FACS analysis.

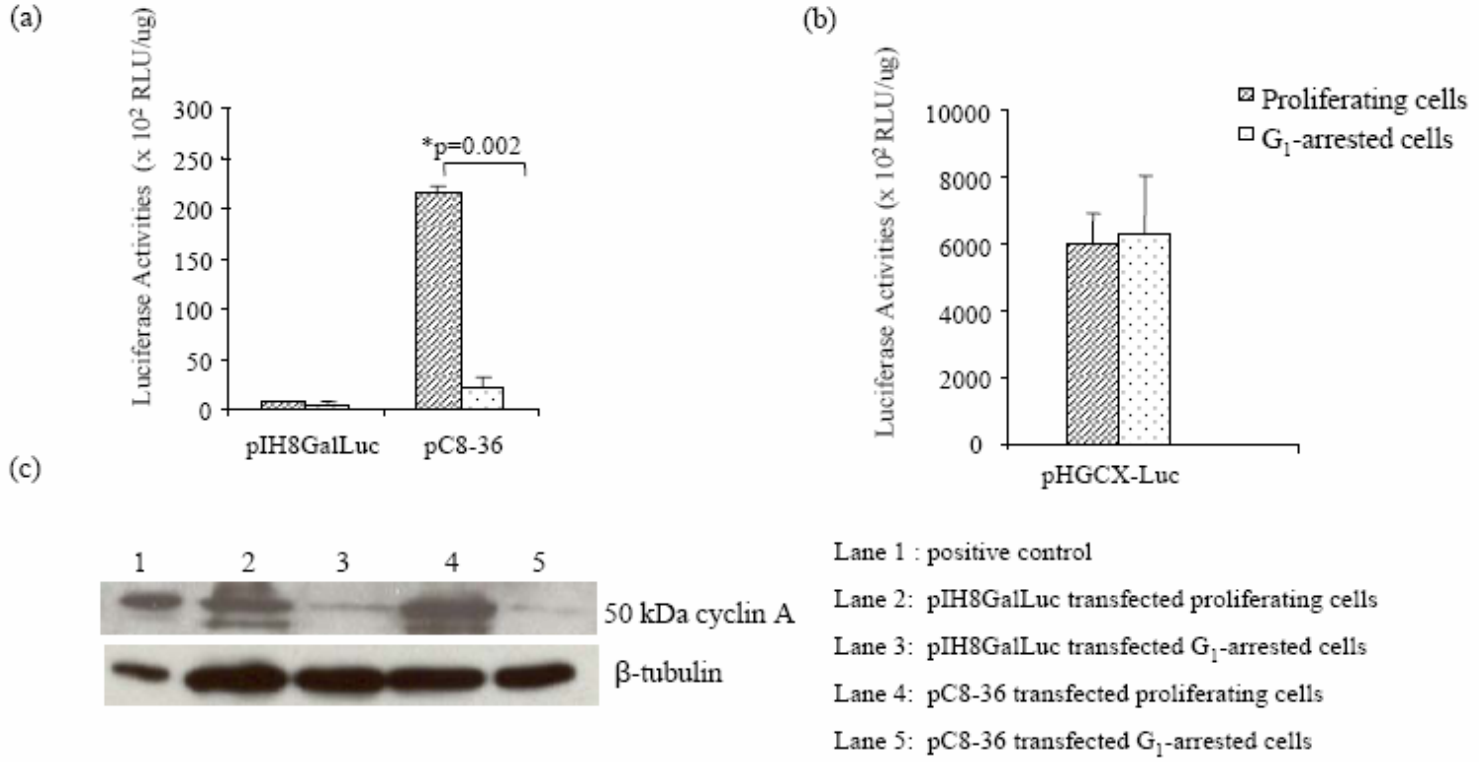

Figure 3.8. Cell cycle regulated Luciferase gene expression in NIH3T3.

(a) NIH3T3 were transfected with pC8-36 and pIH8GalLuc vector for 6 h. The transfection medium was changed into either complete medium (for proliferating cells) or medium containing lovastatin (for G_1-arrested cells), and incubated for 24h and 48 h, respectively. Luciferase activities were analyzed at the respective time points. (b) A similar experiment was performed on pHGCX-Luc-transfected cells. (c) The level of cyclin A protein expression was determined in proliferating and G_1-arrested cells transfected with pIH8GalLuc and pC8-36.

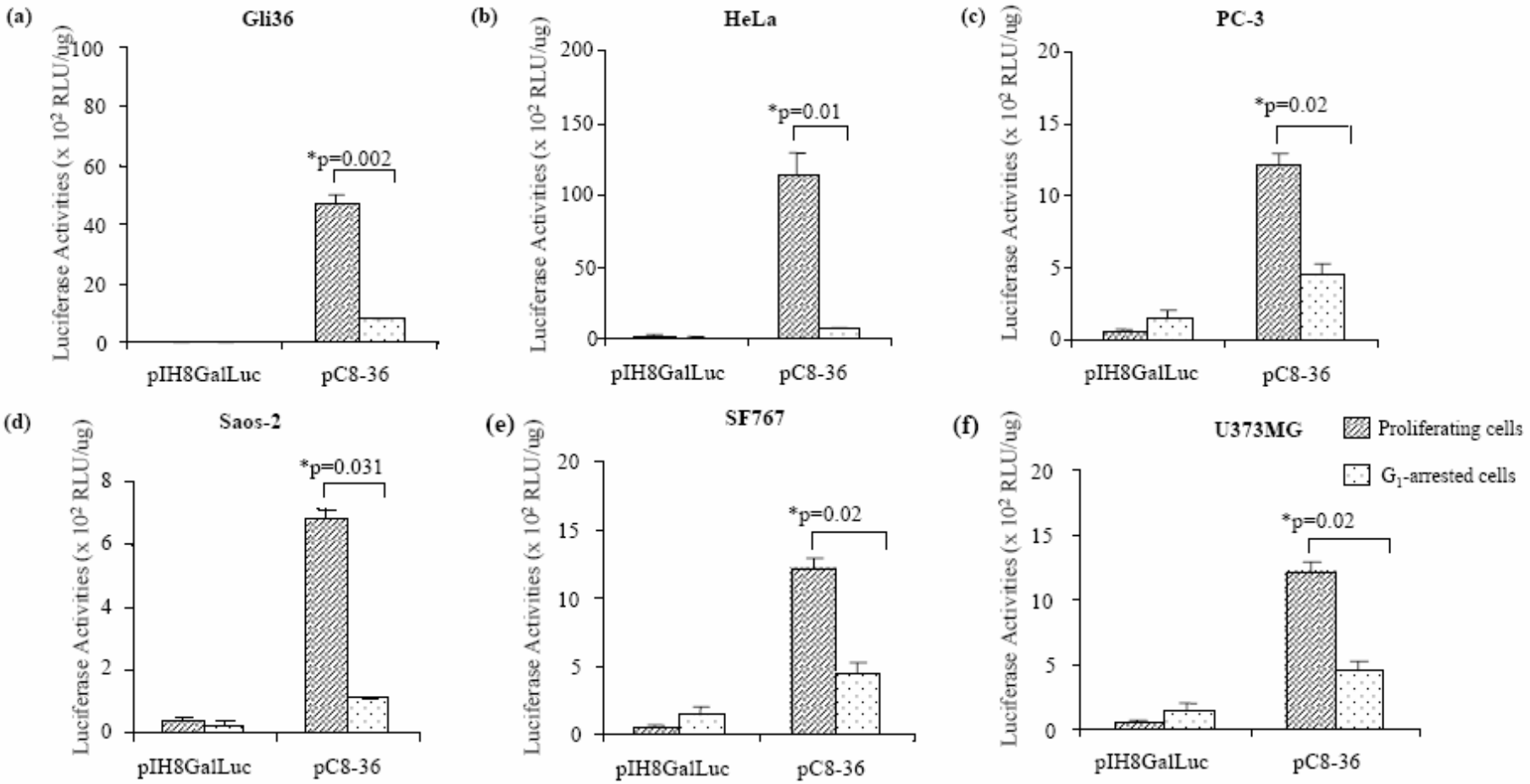

Figure 3.9. Analysis of cell cycle-regulated transgene expression in human tumor cell lines.
Luciferase expression was assayed at 24 h post-transfection for proliferating cells and at 48 h post-transfection for G_1-arrested cells in (a) Gli36; (b) HeLa; (c) PC3; (d) Saos-2; (e) SF767; and (f) U373MG, respectively. The data shown are averages of triplicates $\pm$ SEM.

was enhanced by a minimum of 3-fold to 16-fold, depending on the cell type, in pC8-36 transfected cells. In contrast, only background level was observed in those transfected with pIH8GalLuc. We have also tested the cell cycle regulatory potential of pC8-34 in these tumor cell lines (data not shown). Except for PC-3 cells, all cell lines exhibited better cell cycle regulation ability when transfected with pC8-36 than pC8-34 constructs, thus supporting our previous data (Figure. 3.6) that there might be a down-regulation of the cell cycle regulatory elements due to promoter interference. Taken together, our results demonstrate that our novel amplicon plasmid vectors (pC8-36 and pC8-34) could be regulated in a cell cycle-dependent manner in both normal fibroblasts and tumor cells.

3.3.6 Interaction of the CDE/CHR regulatory region with CDF-1 repressor protein

To confirm that the cell cycle-dependent transgene regulation mediated by pC8-36 amplicon plasmids shown in the transfection experiments above is a result of CDF-1-mediated repression of the CDE/CHR regulatory region, competition assays were performed. Oligonucleotides that span the CDE/CHR region of the cdc25C promoter (CDE oligomer) were used as it was previously demonstrated that cyclin A promoter binds the CDF-1 repressor protein with similar efficiency as the cdc25C promoter (Liu et al., 1998; Liu et al., 1997). HeLa cells were transfected with either CDE oligomer or a random oligomer with the same number of nucleotides, followed by the pC8-36 amplicon plasmid. These transfected cells were cultured with or without lovastatin to represent proliferating and G_1-arrested cell populations, respectively. The extent of cell cycle regulation was then measured as a ratio of luciferase activity of the transfected cells in the proliferating status versus the G_1-arrested status. When HeLa cells were transfected with the CDE oligomer, the extent of cell cycle regulation was reduced by half when compared to cells that were transfected with either pC8-36 alone or in the presence of the random oligomer (Figure 3.10). This result suggested that the level of cell cycle-regulated transcription is dependent on the CDE/CHR-mediated repression site on the cyclin A promoter.

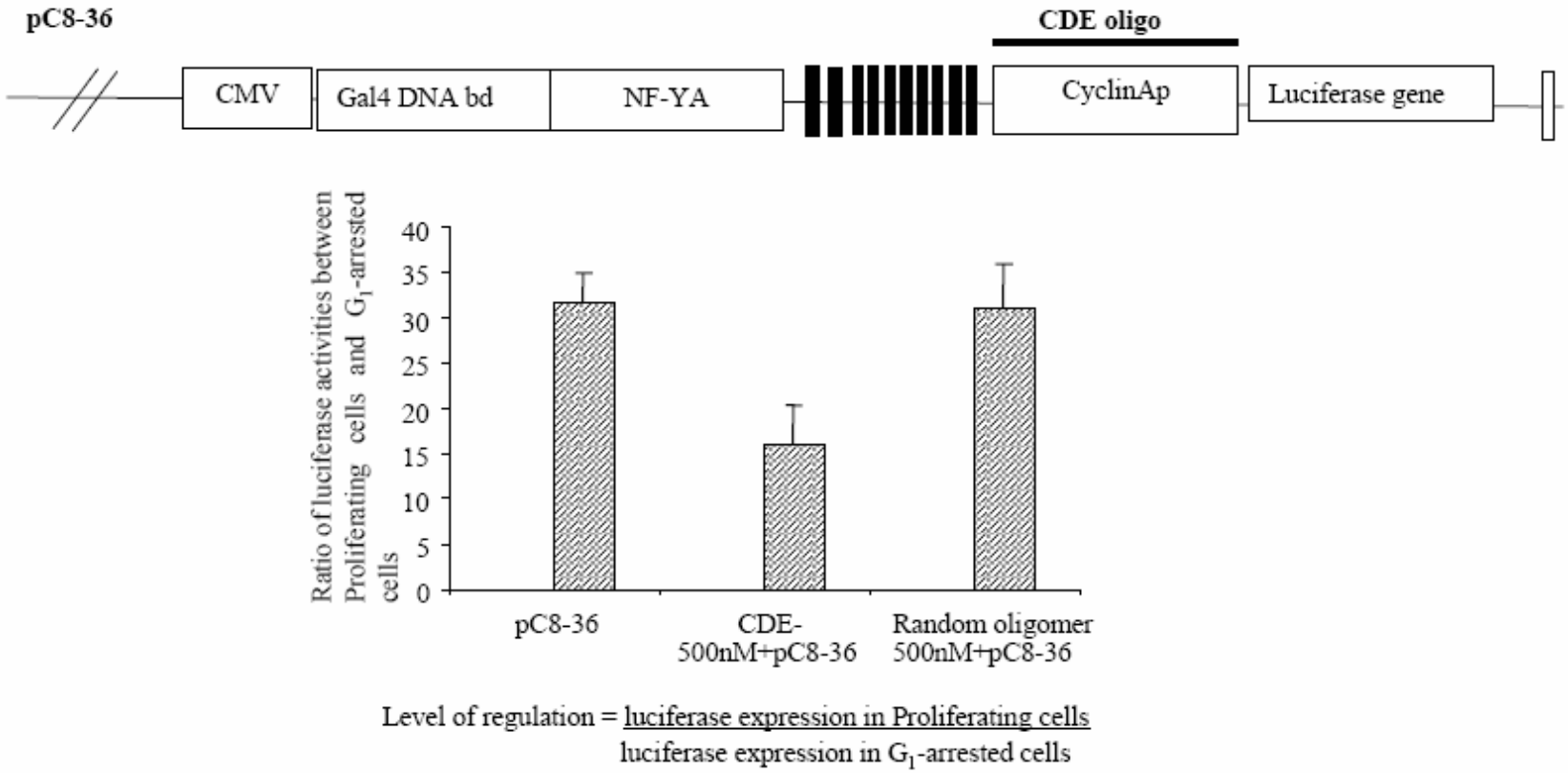

Figure 3.10. Cell cycle-dependent transgene regulation can be abolished in the presence of competitor. HeLa cells were transfected with pC8-36, pC8-36 with CDE oligomer, and pC8-36 with random oligomer. Luciferase expression was analyzed for proliferating cells and G_1-arrested cells. The level of regulation is expressed as a ratio between the two different populations of cells. Each ratio, as represented by bar column, is derived from an average of triplicates.

3.3.7 Cell cycle mediated transgene activity can be abolished in the presence of competitor

To further investigate whether the CDF-1 repressor protein would interact with the CDE oligomer described above, nuclear extracts of G_1-arrested HeLa cells were analyzed by EMSA using CDE oligomer as a probe. The results clearly showed the presence of CDF-1 binding activity in the presence of CDE oligomer (Figure 3.11). The CDF-1 binding activity could be specifically competed in the presence of increasing ratio of probe to unlabelled competitor. This binding activity was absent when the random oligomer was employed as a probe (Figure 3.11). Taken together, these data confirmed the specific interaction of CDF-1 to sequences containing the CDE/CHR motif.

3.3.8 Transgene expression can be switched on in resting cells

To determine if the cell cycle-regulatable amplicon plasmids can be reactivated in resting cells, luciferase assays were performed in cells transfected with pC8-36 and the pIH8GalLuc amplicon plasmids in the proliferating, G_1-arrested and the G_1-released cell populations. Both NIH3T3 and HeLa cells have been chosen as controlling their cell cycling events is easier compared with other cell lines tested. Cells transfected by either pC8-36 or pIH8GalLuc were analyzed (24 h post transfection) for luciferase expression in the proliferating cell populations. Transfected cells were also treated with lovastatin in 0.5 % serum for 48 h to induce G_1-arrest. After 48 h, a portion of the cells were harvested for analysis of luciferase transgene expression; while 10 % serum containing 5 mM mevalonate were added to the remaining cells for an additional 48 h followed by luciferase assay. Although the absolute values obtained with pC8-36 transfected NIH3T3 cells and HeLa cells were much lower as compared to Figure 3.8a and 3.9b, luciferase activities were still 15-fold higher in proliferating NIH3T3 cells and 35-fold higher in HeLa cells when compared to the respective G_1-arrested cell populations (Figure 3.12a and 3.12b). Only background level of luciferase expression could be detected in pIH8GalLuc-transfected cells (Figure 3.12a and 3.12b). The level of luciferase transgene expression is approximately 5-fold higher in these serum-stimulated cells as compared to G_1-arrested cells. It is also significantly higher than background level.

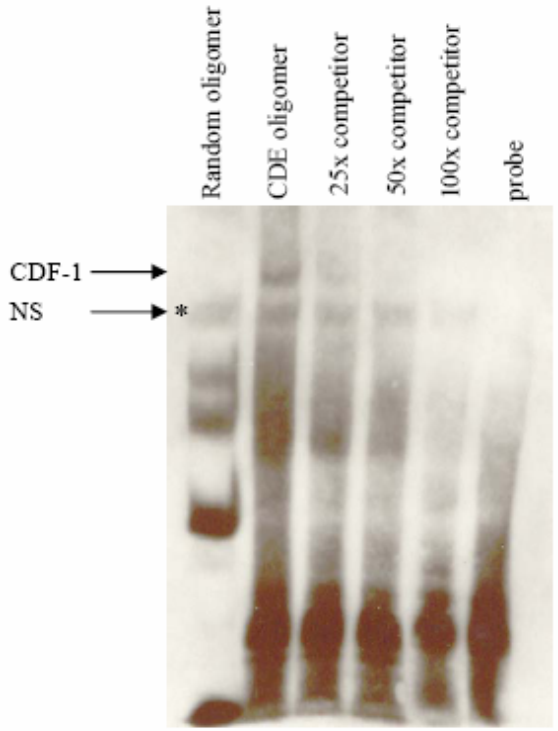

Figure 3.11. Interaction of the CDE/CHR regulatory region with CDF-1 repressor protein.
Nuclear extracts were incubated with biotin-labeled random oligomer; CDE oligomer or CDE probe in the presence of 25-fold, 50-fold and 100-fold excess of the unlabeled CDE oligomer. Bound protein complexes were separated using 6 % PAGE and detected by LightShift™ Chemiluminescent EMSA kit. *NS: non-specific band.

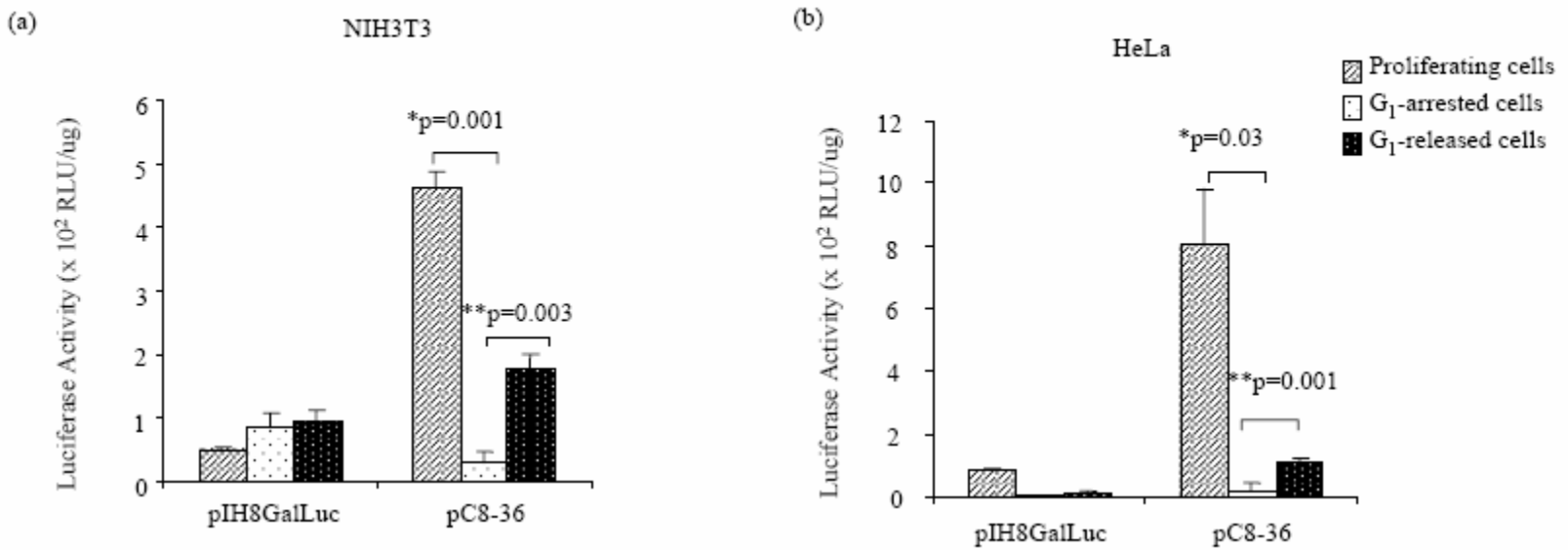

	G_0/G_1	S	G_2/M
Proliferating cells	73.20	18.72	8.08
G_1-arrested cells	94.53	2.56	5.15
G_1-released cells	85.28	9.57	2.91

Figure 3.12. Luciferase transgene expression can be switched on in resting cells transfected with pC8-36 amplicon plasmid.
(a) NIH3T3 and (b) HeLa cells were transfected with pIH8GalLuc and pC8-36. Luciferase expression was assayed for proliferating cells, G_1-arrested cells and G_1-released cells. The data shown are averages of triplicates ± SEM. Table shows the cell cycle profile of NIH3T3 in proliferating cells, G_1-arrested cells and G_1-released cells.

These luciferase activities correlated with the cell cycle distribution as measured by flow cytometry which indicates a decrease in the percentage of S phase cells in the G_1-arrested population, and the increase in the S fraction in the G_1-released cells (Figure 3.12). These results indicated that the regulation of the transgene expression could be activated as the G_1-arrested cells enter the proliferative stage of the cell cycle.

3.3.9 Packaging of amplicon viral vectors

To determine if the amplicon plasmids could be packaged into infectious HSV-1 amplicon virions, we have adopted the helper virus-free packaging system (Fraefel et al., 1996) (detailed in 2.2.2.1 and 2.2.2.2) to package our amplicon plasmid constructs. The titer obtained for the resulting packaged amplicon viral vectors ranged from 1×10^7 to 1×10^8 TU/ml after concentration through a sucrose gradient. The ability to package these amplicon plasmids into infectious amplicon viral vectors demonstrated that the functions of essential viral elements were not disrupted during the cloning procedure.

3.3.10 Analysis of cell cycle-dependent transgene expression in pC8-36 amplicon viral vectors

We next determined if these viral vectors were capable of conferring similar cell cycle-regulatable properties as determined in dGli36 cells transfected with pC8-36 amplicon plasmids (Figure 3.13). The dGli36 cells, which overexpressed the exogenous truncated mutant EGFR commonly found in human gliomas (Nagane et al., 1996), were employed in our system as these cells were capable of inducing tumor formation in immunodeficient mice more consistently than their parental derived Gli36 cells (unpublished observations). After 6 h of transfection (Figure 3.13a) or infection (Figure 3.13b) at an MOI of 1.0, similar number of cells (~50 %) was observed to be GFP positive. These cells were then replenished with either complete medium or treated with lovastatin to induce cell proliferation or G_1-arrest, respectively. Using luciferase gene reporter assay, the level of cell cycle regulation was observed to be much higher in pC8-36-infected cells (28-fold) in comparison to that of the

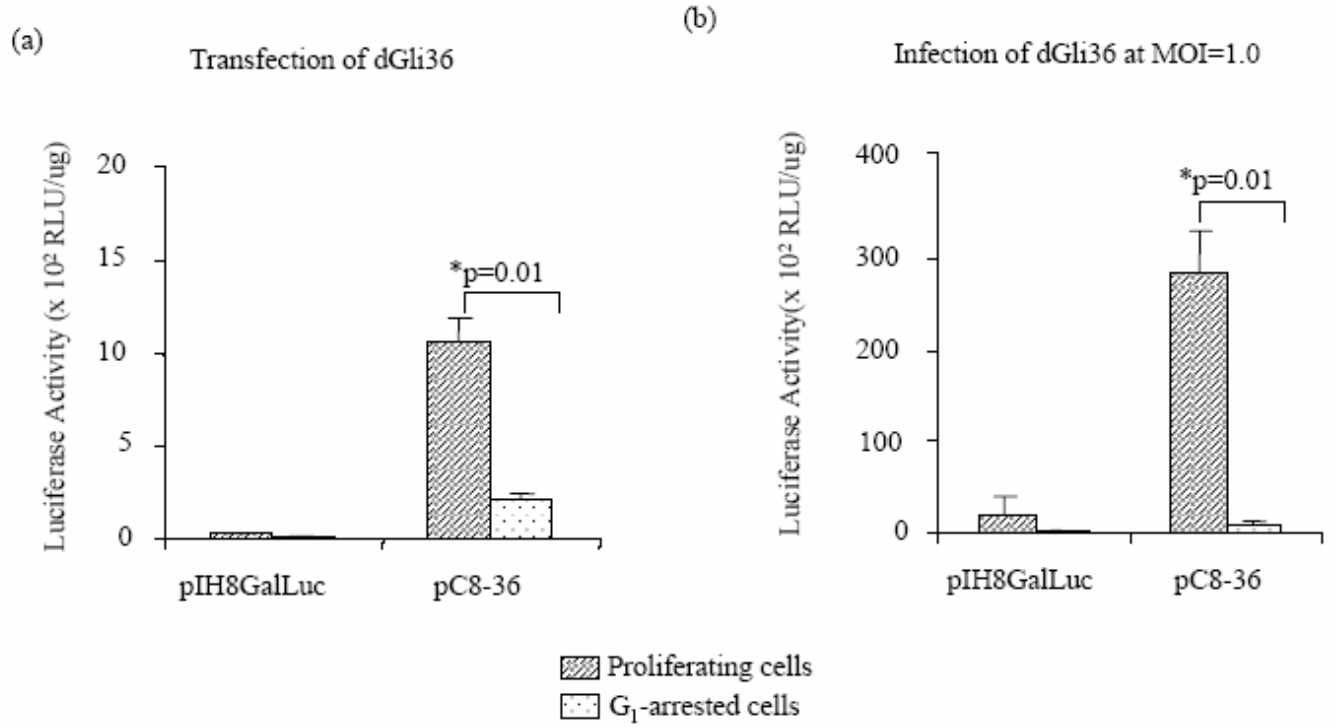

Figure 3.13. The effect of viral transduction on cell cycle regulated transgene expression.
Human glioma cells were either (a) transfected or (b) infected with pC8-36 and pIH8GalLuc. Luciferase expression was measured for both proliferating cells (24 h) and G_1-arrested cells (48 h) at the respective time-point post-transfection or infection. The data shown are averages of triplicate ± SEM.

transfected cells (6-fold) (Figure 3.13b and 3.13a, respectively). This result demonstrated that pC8-36 amplicon viral vector was capable of conferring cell cycle-regulated transgene expression to human glioma cells *in vitro*.

3.3.11 Effect of transduction of viral vector on the cell cycle profile

To determine whether infection of the amplicon viral vector will alter the cell cycle distribution, dGli36 human glioma cells were infected with pC8-36 at MOI of 1.0 for 6 h. Using FACS analysis, the percentage of cells at various stages of cell cycle was determine and compared with control uninfected dGli36 cells. No significant difference was observed after transduction with pC8-36 amplicon vector (Figure 3.14); demonstrating infection of viral vectors does not affect the cell cycling.

3.3.12 Transgene expression is dosage dependent

To analyze if the cell cycle regulatability is viral dosage dependent, dGli36 cells were infected with pC8-36 for 6 h at an MOI of 0.1, 1.0 and 2.0, which correspond to infection efficiency of 21.62 %, 92.93 % and 97.11 %. The amplicon viral vector, pIH8GalLuc, was used as negative control (as shown in Figure 3.15). Proliferating or G_1-arrested cells transduced by pC8-36 or control vectors at a specific MOI were analyzed as a mixed cell population (consisting of both transduced and non-transduced cells) for luciferase activities. For comparison purposes, the level of cell cycle regulation is then expressed as a ratio between the two different populations of cells. The ratio of luciferase expression was correspondingly increased by 10-fold and 2-fold when the MOI of pC8-36 amplicon viral vector was increased from 0.1 to 1.0 and from 1.0 to 2.0 (Figure 3.15). In contrast, this effect was not observed in the negative control. These data support that the level of cell cycle-regulated transgene expression mediated by pC8-36 vectors is viral dosage-dependent. Taken together, the higher level of cell cycle-regulated transgene expression observed is a consequence of more cells being infected with increasing MOI, which may result in a higher level of Gal4/NF-YA fusion protein for transactivation to occur.

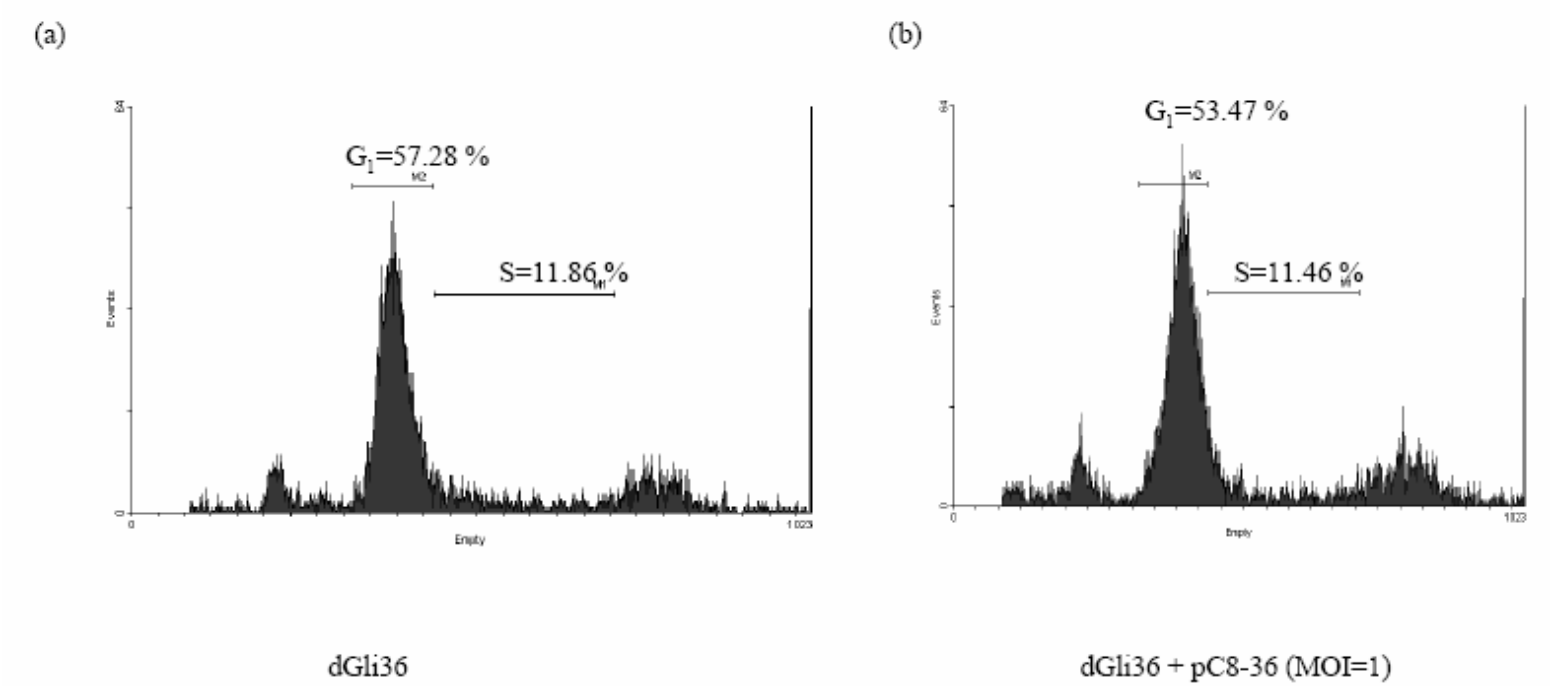

Figure 3.14. HSV-1 infection does not alter the cell cycle profile
Cell cycle profile of dGli36 (a) before and (b) after infection (asynchronized cells)

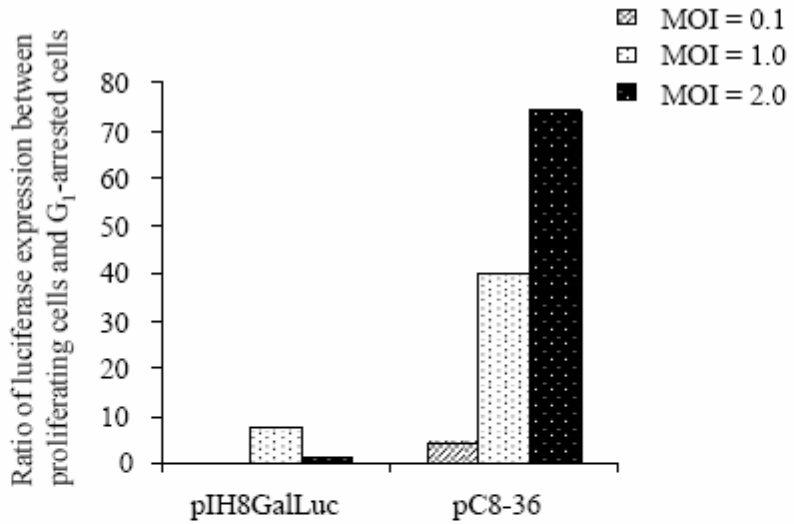

Figure 3.15. The effect of viral dose on the regulation of transgene expression.
The effect of different viral dosage on the regulation of transgene expression via cell cycling event is determined by monitoring the level of luciferase activities in the proliferating and G_1-arrested cells. This level of regulation is expressed as a ratio between the two different populations of cells. Each ratio, as represented by bar column, is derived from an average of triplicate infections at an individual MOI.

3.3.13 Transgene expression is restricted to proliferating cells in vivo

The liver is an excellent tissue for the study of growth regulation because of its potent regeneration capacity by a process of compensatory growth following surgical resection or toxic injury. Much of the investigation on the mechanisms of hepatic growth has been done in PHx animals *in vivo* and in hepatocytes in primary culture. Almost immediately after PHx, transcription factors are activated, followed by DNA synthesis *in vivo* in quiescent hepatocytes that have become "competent" to proliferation. Thus, we have chosen the normal liver regeneration following PHx as an animal model to study cell cycle-regulated transgene expression conferred by pC8-36 amplicon viral vectors *in vivo*. Female BALC/c mice were separated into three experimental groups consisting of the normal, sham-operated and those that underwent PHx. Following PHx, the resected liver lobes were weighed immediately. The kinetics of liver regeneration was monitored closely and it was noticed that the peak of the regeneration process occurred at day 2 following PHx (Figure 3.16a) and consisted of 33-45 % of S phase cells in comparison to 16-18 % in the normal mice group when analyzed by FACS analysis (Figure 3.16b, c). No significant difference in the percentage of S-phase cells could be observed in PHx mice injected with either pIH8GalLuc or pC8-36 amplicon viral vector ($p=0.113$), thus indicating that infection with viral vectors does not alter the cell cycle distribution *in vivo*. On Day 2 post PHx, hepatectomized, sham-operated and normal mice ($n = 5$) were injected with $1x\ 10^6$ TU of either pC8-36 or pIH8GalLuc amplicon viral vector through tail vein. The animals were sacrificed and luciferase activities were analyzed after 24h from the harvested liver tissues. Reporter luciferase activities were found to be significantly higher in livers of hepatectomized mice (one way ANOVA, $p=0.038$) (Figure 3.17) compared with those of the sham-operated and normal groups. These data indicated that luciferase expression conferred by pC8-36 amplicon viral vector is specifically switched on in actively proliferating hepatocytes during liver regeneration.

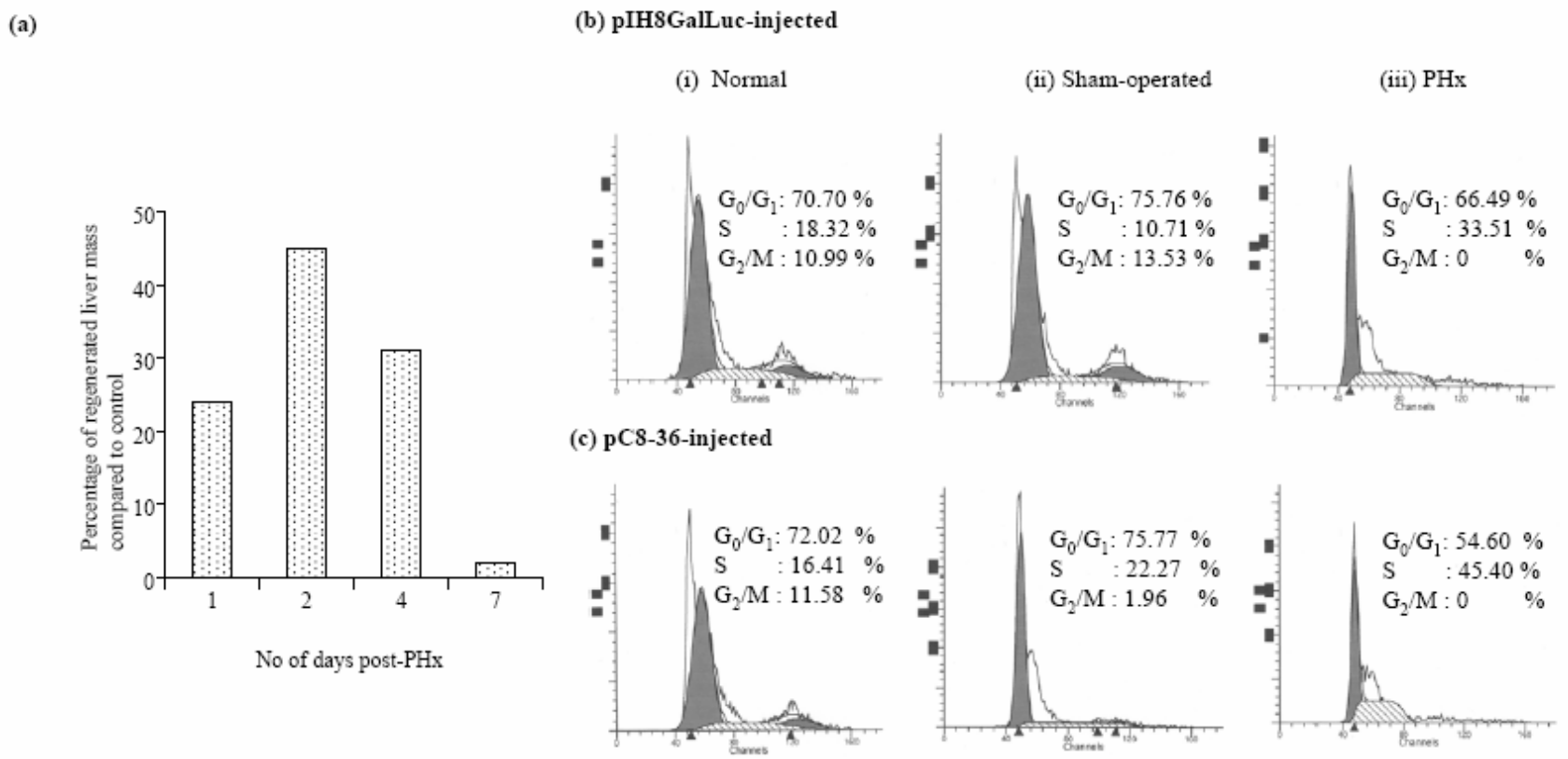

Figure 3.16. Kinetics of liver regeneration following PHx.
(a) Time course of liver regeneration. (b) and (c) FACS analysis demonstrating the cell cycle profile of (i) normal, (ii) sham-operated, and (iii) PHx liver in mice injected with either pIH8GalLuc or pC8-36, respectively.

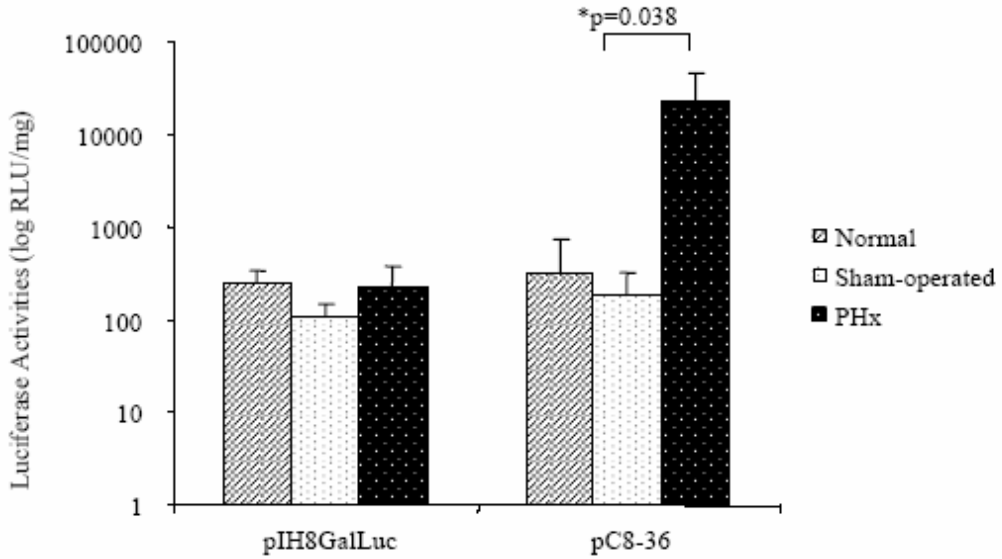

Figure 3.17 Transgene expression mediated by pC8-36 in PHx, sham-operated and normal mice.
1x 10^6 TU of pIH8GalLuc or pC8-36 amplicon viral vector was injected via tail vein into three groups of mice, namely normal, sham-operated and PHx. Luciferase activities were analyzed 24 h postinjection. Data shown represent averages of at least 5 mice ± SEM.

3.4 Discussion

In this study, we have engineered a novel HSV-1 amplicon viral vector that incorporates cell cycle-specific regulatory elements and demonstrated cell cycle-dependent gene regulation.

Nettelbeck et al. (1999) described a system whereby transcriptional activation following DNA-binding takes place in a single step as mentioned earlier (section 3.1.5). In that study, the cell type-specificity of transgene expression was in the range of 50-fold and the extent of cell cycle-regulation was approximately 20-fold in melanoma cells.

For the purpose of possible gene therapy, we have attempted to address the question whether cell cycle-dependent transgene regulation can be sustained if both the activator and the reporter modules were subcloned into a single plasmid vector, and whether the regulation of transgene expression via cell cycle event may be affected by the various genetic aberrations in cell cycle proteins such as p53, pRb, p16 and EGFR, that are frequently found in all types of cancer. Our results demonstrated that a single-vector system based on amplicon plasmids conferred 4-fold higher luciferase activities than a co-transfection of both plasmids containing the activator and the reporter modules (Figure. 3.6). The level of cell cycle-regulated transgene expression was further enhanced using a viral based vector system. Our results also showed that regardless of the origin of tumor cells, a common trend was observed in the augmentation of the ratio of luciferase activity in proliferating versus growth-arrested cells. Although both pC8-36 and pC8-34 amplicon plasmids displayed cell cycle-dependent transgene expression, pC8-36 plasmid exhibited higher cell cycle regulatory potential than pC8-34 plasmid ($p=0.02$), possibly due to the promoter context and positioning in the latter construct. Such transcriptional interference displayed by two promoters arranged in opposite orientations to each other has previously been reported (Eszterhas et al., 2002). Another phenomenon observed in our studies was that the extent of cell cycle regulation differed in different cell types. For example, prostate (PC-3) and cervical (HeLa) carcinoma cells, exhibited a 3- and 16-fold increase in the luciferase activities in proliferating versus G_1-

arrested cells (Figure. 3.9). This might suggest a possible variation in the transfection efficiencies between the two cell lines. Alternatively, the various genetic aberrations might still exert an effect on the extent of regulation but overall, did not appear to abrogate the ability to regulate in a cell cycle-dependent fashion. Further studies were performed to assess whether resting cells transfected with pC8-36 amplicon plasmid, on serum stimulation, would re-activate the transcription of the luciferase reporter gene. We have observed that luciferase transgene expression increased by approximately 5-fold in G_1-released cells in comparison to G_1-arrested cells in both NIH3T3 and HeLa cells transfected with pC8-36 amplicon plasmids (Figure. 3.12a and 3.12b). The differential transgene expression between G_1-arrested and G_1-released cells, though significant, is not as much as that observed between cells in the proliferating and G_1-arrested stage (15-fold and 35-fold differences in NIH3T3 and HeLa cells respectively; Figure. 3.12a and 3.12b). Our data have shown that transgene expression could be regulated in a cell cycle-dependent manner, which would be an important feature of our amplicon viral vectors when applied to a clinical setting.

The cDNA of CDF-1 was not isolated. In fact, several laboratories have attempted to isolate the cDNA encoding for CDF-1, but was not successful. It was suggested that CDF-1 might be a complex of proteins instead of a single protein (personal communications). Therefore, we are unable to demonstrate the requirement for CDF-1 using siRNA against CDF-1 or CDF-1 null cells, and the effect of overexpression of CDF-1 cDNA *in vitro*. However, Zwicker et al (1995) generated a series of mutant constructs with point mutation at position 7 within the CDE region and also alteration of the conserved sequence within the CHR region of cyclin A promoter. The differential luciferase activities between proliferating versus arrested NIH3T3 cells conferred by these mutants were almost abolished (ratio of luciferase activities between proliferating and arrested cells is 1.8 in both mutant constructs; in construct containing wild-type cyclin A promoter, the induction factor is 41.7-fold). Also, due to the unavailability of antibodies generated against CDF-1, we cannot correlate the level of transgene expression to the amount of active CDF-1 repressor proteins. However, two

different approaches were adopted to ensure that the increase in luciferase activity is likely to be a consequence of the loss of CDF-1 mediated repression in the G_1-fraction of the normally cycling cell population. Firstly, G_1-arrested HeLa cells were assayed for the presence of CDF-1 activity via EMSA (Figure 3.11). The specific binding of CDF-1 to sequences containing CDE/CHR motif correlates to the repressed cell cycle transcription when CDE oligomer is included in the co-transfection (Figure 3.10). In contrast, the failure of random oligomer binding to CDF-1 could explain the lack of competition resulting in a similar level of cell cycle regulation as the control, pC8-36 (Figure 3.10). Secondly, we hypothesized that if the cell cycle regulation observed in proliferating cells is due to the absence of CDF-1 proteins binding to CDE/CHR modules within the cyclin A promoter, then by introducing more copies of CDE/CHR elements, the extent of cell cycle-regulated luciferase activities would increase correspondingly. Indeed, our results showed that the level of cell cycle-regulated transgene expression appeared to be dependent on viral dosage (Figure. 3.15). There was also no significant change in the cell cycle distribution before and after dGli36 cells were transduced by pC8-36 amplicon viral vectors, as determined by FACS analysis (Figure. 3.14). These results suggested that the increased luciferase activity in proliferating cells are due to a direct action of CDF-1 on the cyclin A promoter rather than a more rapid cell cycle progression of G_1-arrested cells induced upon viral infection. At present, we do not know if the presence of HSV amplicon viral proteins may interfere with binding of CDF-1 to its cognate binding site. From studies by Zwicker et al. 1999, the expression of SV40 large T oncoprotein can dissociate CDF-1 repressor protein from its cognate DNA binding site, resulting in a deregulated transgene expression with respect to cell cycle event. So far, our results reflected a tight transgene expression mediated by HSV amplicon virus in a cell cycle-controllable manner. Nevertheless, further analysis is required to determine the precise effect of HSV viral proteins on CDF-1. Potential factors that may affect gene expression from HSV vectors would be the virion host shut-off function (Read and Frenkel, 1983), a component of the HSV virion that has been shown to cause translational shut-off and mRNA degradation of the host cells (Smibert et al., 1992). In addition, immediate early gene products (ICP4, ICP27

and ICP0) of HSV and the VP16 tegument protein have also been found to interfere with the integrity of tetracycline-regulated transgene expression (Herrlinger et al., 2000).

In summary, we have demonstrated the feasibility of employing a single viral vector in conferring transgene expression in a cell cycle-dependent manner. It would be of clinical importance to evaluate the efficacy of the system using therapeutic transgenes that would cause a direct cell killing effect, such as FADD or FasL. Once the therapeutic efficacy of this cell cycle-regulatable HSV-1 amplicon viral vector system is fully characterized, it may serve as a useful tool in cancer gene therapy.

Chapter 4

Application of the cell cycle-regulated amplicon vector

4.1 Background

4.1.1 Apoptosis

Apoptosis, also known as programmed cell death, is characterized by the activation of cysteine proteases, termed caspases, followed by induction of caspase-mediated cellular mechanisms, such as membrane shrinkage, chromatin condensation, and disintegration of dead cells into small pieces that can be phagocytosed (Jäättelä, 2004). Apoptosis can be divided into two pathways depending on whether it is triggered by internal or external signals. The intrinsic pathway, which is triggered by internal signals, can be activated in response to oxidative stress and irradiation (Choi and Benveniste, 2004). This pathway involved the release of cytochrome c from the mitochondria and subsequent activation of caspase-3 and 7 by the formation of apoptosome. The other pathway is dependent on external signals transduced by surface receptors and ligands binding. One of the best characterized molecules is the tumor necrosis factor (TNF) superfamily of cytokines including Fas ligand (FasL), TNF-α, and TNF-related apoptosis inducing ligand (TRAIL). Apoptosis is activated by the recruitment of death adaptor proteins, such as Fas-associated protein with a death domain (FADD) and TNF-receptor associated death domain (TRADD), to the receptors leading to activation of oligomerized pro-caspase 8 (Choi and Benveniste, 2004).

4.1.2 Fas and Fas Ligand

Fas (CD95/Apo-1) is a type I transmembrane protein that belongs to the TNF receptor superfamily (Cosman, 1994). The Fas receptor contains three cysteine-rich extracellular domains which function to engage FasL, and an intracellular death domain (DD) that interacts with the DD of adaptor proteins to initiate downstream apoptosis signaling.

FasL is a type II membrane protein (Kayagaki et al., 1995; Tanaka et al., 1995). Unlike the ubiquitous expression of Fas, FasL is express in activated T cells and natural killer (NK) cells of the “immune privileged” organs, such as the eye, the reproductive organs, and the brain (Choi and Benveniste, 2004). In the brain, FasL is expressed in both normal and disease

states. For instance, FasL is expressed in astrocytoma cells and in normal glial cells, microglial cells, and astrocytes (Saas et al., 1997). Expression of FasL in tumors has been implicated in the promotion of tumor evasion by eliminating host anti-tumor response mediated by Fas-positive effector lymphocytes (O'Connell et al., 1996; Shinohara et al., 2000). FasL can be cleaved by several metalloproteinases to generate soluble- and membrane-bound FasL (Kayagaki et al., 1995; Tanaka et al., 1998), with the latter having higher apoptotic-inducing effect (Schneider et al., 1998; Suda et al., 1997; Tanaka et al., 1998).

4.1.3 FasL-induced apoptosis

FasL binding induced the recruitment of FADD to the C-terminus of Fas receptor, leading to the establishment of the death-inducing signaling complex (DISC) (Figure 4.1). Clustering of FADD to Fas induced the recruitment of pro-caspase 8 to the death effector domain (DED) of FADD, resulting in proximity-induced proteolytic processing and autoactivation of pro-caspase 8. In type I cells, the activated caspase 8 initiates activation of downstream caspases, which eventually leads to the proteolysis of specific protein targets that is central to apoptosis. However, in type II cells which are not dependent on surface receptor-ligand interactions, the activation of caspase 8 is not sufficient to activate pro-caspase 3. Instead, caspase 8 cleaves Bid, a proapoptotic member of the Bcl-2 family of proteins, which in turns induced the release of cytochrome c from the mitochondria resulting in the activation of caspase 9 and Apaf-1, which then activates pro-caspase 3.

The activation and execution of apoptosis by Fas/FasL system is regulated in part by members of the Bcl-2 family of apoptosis regulators. The Bcl-2 family of apoptosis regulators consists of proapoptotic proteins, as well as antiapoptotic proteins. Bax, Bak, Bcl-x_s, and Bid are members of the proapoptotic homologues, whereas Bcl-2 and Bcl-x_L are antiapoptotic (Choi and Benveniste, 2004). This balance between the proapoptotic and the antiapoptotic proteins controls the susceptibility of the cell to apoptosis. In addition to Bcl-2 family of proteins, recruitment of FLICE-inhibitory proteins (FLIP) to the DISC and the

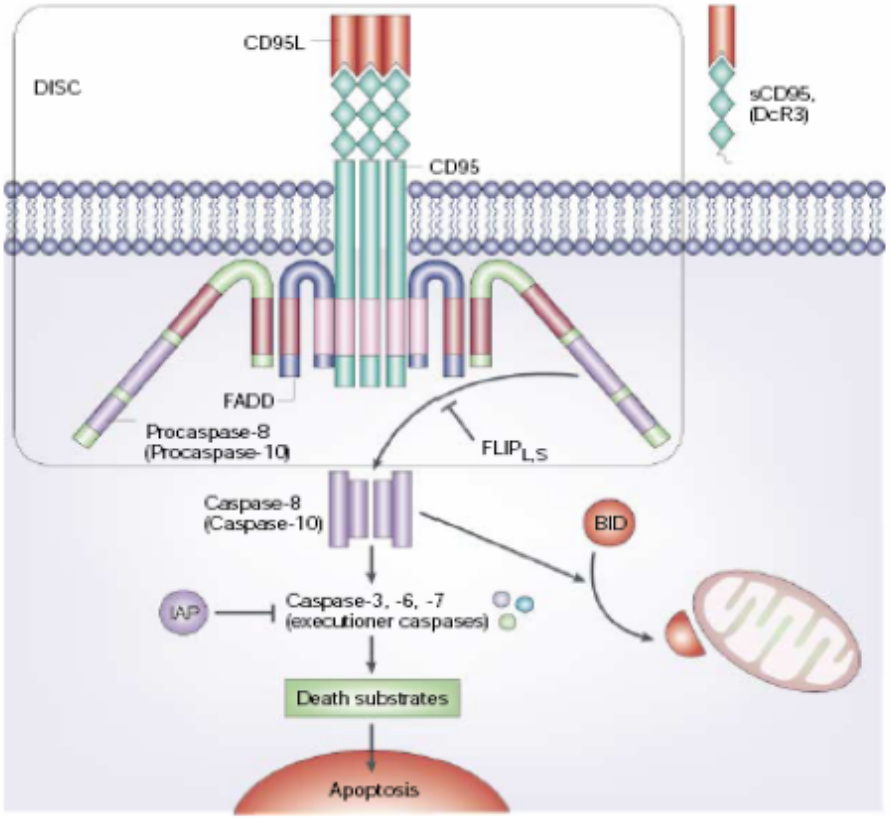

(Igney and Krammer,2002)

Figure 4.1 Fas/FasL mediated apoptosis
Binding of FasL (CD95L) to Fas receptor leads to the formation of the DISC. The procaspase 8 is recruited into the DISC by FADD, resulting in proximity-induced autoproteolysis of procaspase 8 into its active form. Activated caspase 8 subsequently cleaved downstream caspases and induced apoptosis.

presence of inhibitor of apoptosis (IAP) induced an inhibitory effect on the initiation of apoptosis.

4.1.4 Gene therapy using FasL and FADD

One of the major hurdles in glioma therapy is the acquisition of chemoresistant clones. Using death receptor as a therapeutic agent would circumvent this problem as direct activation of caspases would result in cell death. Crosslinking of Fas with anti-Fas antibody has been shown to induce apoptosis in human glioma cell lines (Kondo et al., 1998; Weller et al., 1994; Weller et al., 1995). Ambar et al. (1999) demonstrated that adenoviral mediated transferred of exogenous FasL into F98-glioma bearing rats prolonged the survival of the animals by 80 % when compared to the control group. In addition, Maleniak et al. (2001) showed that overexpression of the murine FasL in chemo-resistant primary glioma culture induced the cells to undergo apoptosis. Although the efficacy of FasL in tumor progression has been demonstrated by several groups, tumors with low or undetectable level of Fas expression are found to be resistant to Fas dependent cell death (Hao et al., 2001; Kondo et al., 1998; Weller et al., 1994). In addition, tumors that have dysfunctional DISC, arising from low level FADD and/or caspase 8 were also found to be resistant to FasL induced cell death.

4.1.5 Aims of this study

Several reports have indicated that neurons, astrocytes and oligodendrocytes express Fas receptor, thus are sensitive to Fas-mediated apoptosis. It is therefore crucial to restrict the expression of FasL in tumor tissues to avoid damaging normal brain cells. Since gliomas are very heterogeneous, with different clonal populations within a tumor mass responding differently to different therapeutic agents, exposure to more than one therapeutic modality might be advantageous.

The aims of this study are as follows:

(i) To examine the efficacy of the FasL and FADD apoptotic genes in the cell cycle regulatable amplicon vector *in vitro* and *in vivo*.

(ii) To determine whether co-expression of both FasL and FADD genes can enhance the apoptotic effect.

4.2 Methods

4.2.1 Construction of pIH8GalFasL, pC8-FasL

To construct pIH8GalFasL, the human FasL gene was PCR amplified using pHGCX-FasL plasmid as a template (the forward and reverse primers were FasLF; 5'-CCCAAGCTTGGCACCATGGCGCAGCAGCCC-3' and FasLR; 5'-CCGGGATCCCGCTCGGTGCCTGTAAC-3', respectively). The amplified DNA fragment was subcloned into the *Hin*dIII and *Xba*I restriction enzyme sites of 8GalcycA plasmid (Nettelbeck et al., 1999). The 8GalcycAFasL DNA fragment was then subcloned into the *Nhe*I and *Bam*HI restriction enzyme sites of pHGCX amplicon vector (Figure 3.5a) and the pre-existing CMV promoter was subsequently removed using *Spe*I and *Nhe*I to generate pIH8GalFasL plasmid. To construct the cell cycle-regulated FasL vector, pC8-FasL, the 8GalcycAFasL fragment was amplified by PCR using the primers 8GalF (5'-CCTCTTCGCTATTACGCC) and 8GalR (5'-AAGAAGACAGTCATAAGTGCGG), respectively. The amplified DNA fragment was subcloned into the shuttle plasmid pGemT-easy; released using *NotI* restriction enzyme sites and inserted into pHGCX.GN (Figure 3.5b), thus, generating pC8-FasL.

4.2.2 Construction of pIH8GalFADD and pC8FADD

For the construction of pIH8GalFADD and pC8-FADD amplicon plasmid, the human FADD cDNA fragment was PCR amplified from pCIneo-FADD (a kind gift from Dr. MV Clement, National University of Singapore, Singapore) using the primers FADD-ORF-F (5'-AAACCCAAGCTTGGGATGGACCCGTTCCTGGTGCTG-3') and FADD-ORF-R (5'-AGCTAGTCTAGACTATCAGGACGCTTCGGAGGTAGA-3'), followed by subcloning into the *Hin*dIII and *Xba*I restriction enzyme sites of 8GalcycA plasmid. Subsequent cloning procedures were similar to the construction of pC8-FasL amplicon plasmid vector. All plasmids were amplified in *E.coli* STBL-2 and DNA was extracted using QIAprep Spin Miniprep Kit. All plasmids were verified by DNA sequencing.

4.2.3 Real time RT-PCR

Total RNA was isolated from tumor mass using TRIzol (Invitrogen Life Technologies) method according to manufacturer's conditions. One μg of total RNA was used for 1st strand cDNA synthesis. cDNA was synthesized using random hexanucleotide primers (Invitrogen Life Technologies) and oligo-dT_{12-17} primers (Invitrogen Life Technologies), in the presence of Superscript II reverse transcriptase (Invitrogen Life Technologies). The expression level of FasL, FADD and the 18S rRNA was quantitated using QuantiTech™ SYBR Green PCR kit (Qiagen). The primer sequences for the amplification of FasL were FasL-F376-392 (5'-GGGCCTGGGGATGTTTC-3') and FasL-R505-488 (5'-TTTTTCAGGGGGTGGACT-3'); for FADD: FADD-F271-287 (5'-GCGCCTGGGGAAGAAGA-3') and FADD-R414-396 (5'-TGTCAGGTTGCGGGGGTAT-3'). For the amplification of 18S rRNA, the following primers were used, 18S-F (5'-CCTGCGGCTTAATTTGACTC-3') and 18S-R (5'-CGCTGAGCCAGTCAGTGTAG-3'). All PCR reactions were performed in duplicate. Standard curves for FasL, FADD and 18S rRNA were generated independently. The relative copy number of each sample was calculated according to the corresponding standard curve using RotorGene version 4.6 software. Normalization was performed in each sample by dividing the copy number of either FasL or FADD to that of 18S rRNA. The relative expression levels were calculated by arbitrarily designating the lowest normalized value to 1.

4.2.4 In vivo transduction

Four groups (n=6) of 6-8 weeks old CB-17 SCID mice were inoculated with 2 x 10^6 dGli36-SCID8 cells to form s.c. tumor. A total of 2 x 10^6 TU of viral vectors were administered intratumorally. Tumor volume was measured every 3-4 days and calculated according to Bergers et al (1999). Animals were sacrificed when the tumors in the control group were severely necrotic.

4.2.5 Statistical analysis

Data are presented throughout this study as means $\pm$ standard error of the mean. Statistical significance in the *in vitro* experiments was evaluated by unpaired t-test, $p < 0.05$ was considered significant. In the *in vivo* experiments, statistical significance was evaluated by one-way ANOVA, $p< 0.05$ was considered significant.

4.3 Results

4.3.1 Construction of a cell cycle-regulatable HSV-1 amplicon viral vector that contains the human FasL and FADD gene

We have previously constructed a HSV-1 amplicon vector, pC8-36, whereby the transgene expression can be regulated in a proliferation-dependent manner (Chapter 3). To determine whether the transcriptional activation mediated by the minimal *cyclin A* promoter is sufficient to elicit a biological response, the luciferase gene is replaced by either *FasL* (pC8-FasL, Figure 4.2b) or *FADD* (pC8-FADD, Figure 4.2d). In addition, we have also constructed the basic constructs, pIH8GalFasL (Figure 4.2a) and pIH8GalFADD (Figure 4.2c), which contain the minimal *cyclin A* promoter driving either the *FasL* or the *FADD* gene, respectively. Further descriptions of the cloning strategies can be found in section 4.2.1 and 4.2.2.

4.3.2 Cell death induced by FasL is regulated in a cell cycle-dependent manner

Recent publications suggested that FADD gene transfer may induce cell death regardless of the expression of Fas/APO-1 in the target cells (Juo et al., 1998; Kondo et al., 1998). To confirm if this is true in dGli36 human glioma cells, the human *FADD* cDNA was also employed to induce apoptosis. Similar experiments were performed for each of the therapeutic genes and results relating to FasL will first be discussed.

To determine if apoptosis mediated by FasL gene expression can be restricted to proliferating cells, dGli36 human glioma cell line was infected with pC8-FasL and the control vector, pIH8GaLFasL at MOI of 1.0. After 6 h of infection, the cells were replenished with fresh medium containing 10 % serum to induce proliferation or treated with medium containing 1 % serum with 50 μM of lovastatin to induce G_1-arrest, which decreased the percentage of S phase cells from approximately 52.8 % to 6.51 %. To determine the level of cell death induced by FasL expression, cytotoxicity assay was performed in dGli36 cells infected with pC8-FasL in both proliferating and G_1-arrested stage.

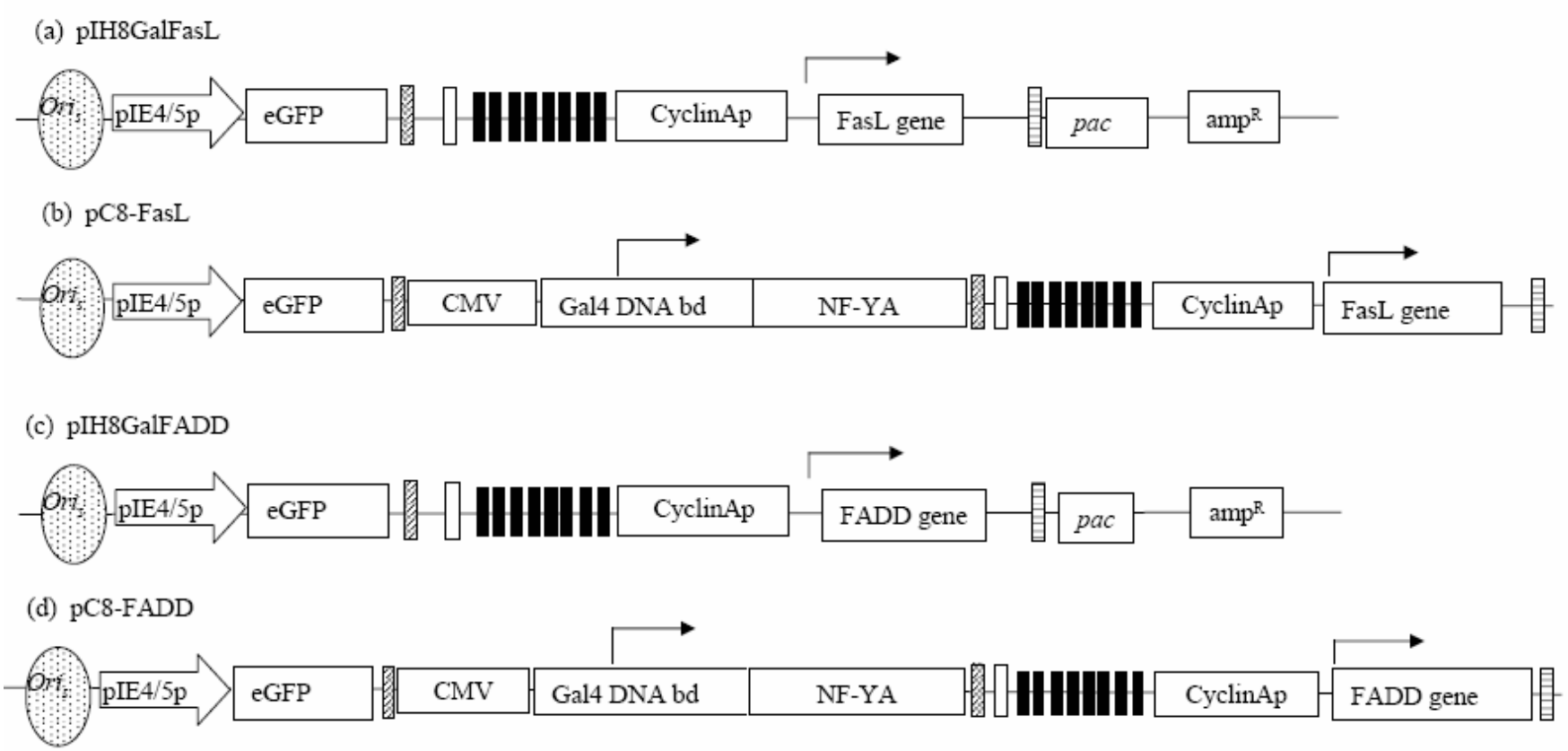

Figure 4.2. Cell cycle regulated amplicon vector constructs harboring either the FasL or the FADD gene

Approximately 41.2 % cell death was detected in proliferating dGli36 cells infected with pC8-FasL, which was 10-fold higher than that of the G_1-arrested population (4.2 %) ($p=0.032$; Figure 4.3a). In contrast, cell death was not observed in both proliferating and G_1-arested populations infected with pIH8GalFasL. Using TUNEL assay, pyknotic nuclei were only evident in proliferating cells overexpressing FasL and absent in G_1-arrested populations (Figure 4.3b). In comparison to pC8-FasL-transduced cells, apoptotic cell death was not detected in proliferating and G_1-arrested cells infected with pIH8GaLFasL. These results thus suggest that cell death mediated by pC8-FasL is dependent on proliferation.

4.3.2.1 Conditioned medium harvested from FasL transduced cells induces apoptosis

It is worth noting that some of the non-infected cells (as determined by the absence of GFP) were also TUNEL positive (Figure 4.4a), indicating that FasL might induced bystander effect in non-transduced cells. To determine whether conditioned medium harvested from FasL-transduced cells induces apoptosis, supernatant from both proliferating cells and G_1-arrested cells were collected after 72 h of infection with pHGCX-FasL, pIH8GalFasL, and pC8-FasL. Conditioned medium was then added to dGli36 cells and the percentage of apoptosis-induced was analyzed after 72 h. Approximately 40 % apoptosis was observed when dGli36 cells were treated with conditioned medium harvested from proliferating pHGCX-FasL-transduced cells (Figure 4.4b). Similar percentage of cell death was also observed in cells treated with conditioned medium harvested from G_1-arrested cells. In contrast, minimal cell death was observed in cells treated with pIH8GalFasL, thus confirming the lack of FasL expression from this control vector (Figure 4.4b). Approximately 38 % cell death was also observed in cells treated with conditioned medium harvested form pC8-FasL-transduced proliferating cells ($p=0.002$; Figure 4.4b). This data thus confirmed that the expression of FasL is regulated in a cell cycle-dependent manner.

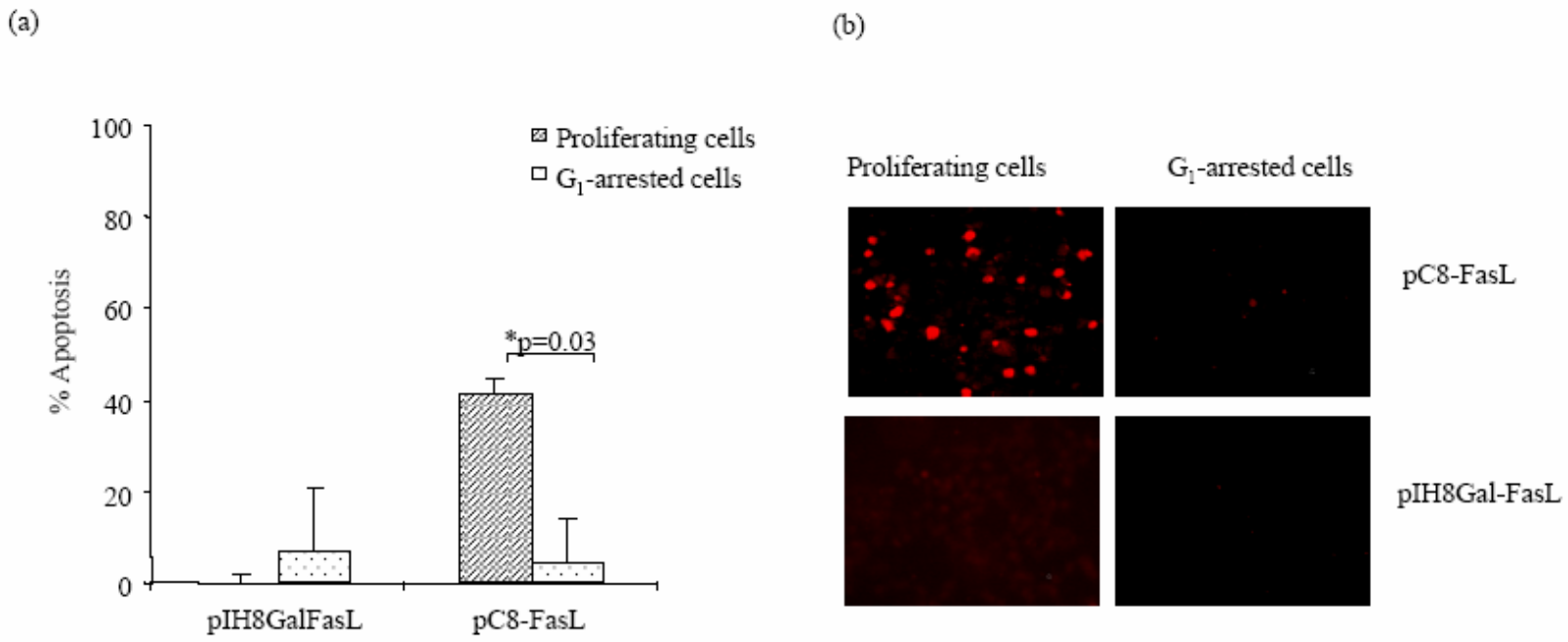

Figure 4.3 Apoptosis mediated by FasL is specific for proliferating glioma cells
(a) Cell cycle-regulated apoptosis was analyzed in the proliferating and the G_1-arrested populations infected with either pIH8GalFasL or pC8-FasL at 72 h post-infection. Percentage of apoptotic cells were determined using trypan blue exclusion assay. (b) Cell death mediated by pC8-FasL was confirmed using TUNEL assay.

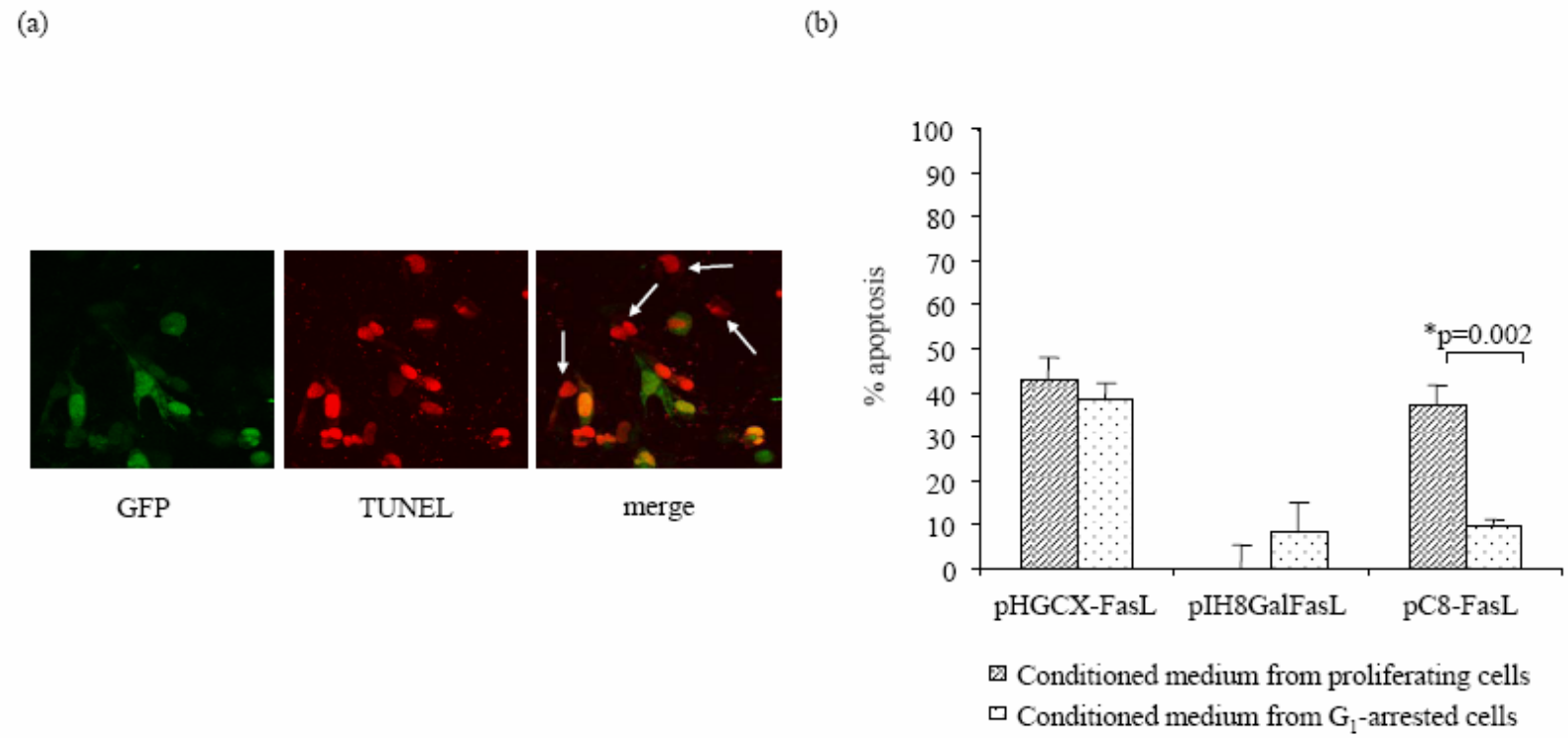

Figure 4.4 Conditioned medium harvested from FasL-transduced proliferating dGli36 cells induces apoptosis.
(a) "Bystander effect" was observed in cells infected with pC8-FasL. Arrows indicate cells that are TUNEL positive, but uninfected. (b) Conditioned medium harvested from pHGCX-FasL-, pIH8GalFasL- and pC8-FasL-transduced cells were added to dGli36 cells. Percentage of apoptosis was analyzed after 72 h. Data are presented in triplicate ± SEM.

4.3.3 Cell death induced by pC8-FADD is also cell cycle-dependent

Next, the level of cell death induced by pC8-FADD was also determined in dGli36 cells using trypan blue exclusion assay. Twenty two percent cell death was observed in the proliferating population in comparison to 4 % in the G_1-arrested population (p=0.019; Figure 4.5a). In contrast, minimal apoptosis was detected in the both proliferating and G_1-arrested cells infected with the control vector, pIH8GalFADD (Figure 4.5a). Similar to FasL, TUNEL positive cells were only detectable in proliferating cells infected with pC8-FADD (Figure 4.5b), while the G_1-arrested cells and the control cells did not exhibit any fluorescence. These results thus suggested that FasL and FADD gene expression mediated by the cell cycle-regulated HSV-1 amplicon vector was controlled in a proliferation dependent manner.

4.3.4 Expression of FasL and FADD are correlated to cell cycling events

To correlate the level of protein expression with the degree of cell death induced by FasL or FADD overexpression, cellular extracts were harvested from FasL- and FADD-transduced cells and analyzed using ELISA. FasL expression in the pC8-FasL-infected proliferating population is 4-fold higher than the corresponding G_1-arrested cells (Figure 4.6a). The slight increase in FasL expression observed in the G_1-arrested population and the pIH8GalFasL infected cells could be due to the combined effect of serum and lovastatin, which has been reported to induce apoptosis in some glioma cells (Jiang et al., 2004; Schmidt et al., 2001). The level of FADD expression in pC8-FADD-transduced proliferating dGli36 cells was 15-fold higher than that of the G_1-arrested cells and 5-fold higher than the control (Figure 4.6b). Collectively, these data indicate that the level of expression of FasL and FADD is regulated in a cell cycle-dependent manner, which correlates with their apoptotic-inducing activity.

4.3.5 Co-expression of FasL and FADD enhanced apoptosis

The effect of FasL and FADD overexpression in FasL-sensitive dGli36 cells have been demonstrated in Figure 4.3 and 4.5. To investigate whether co-expression of FasL and FADD are able to enhance the apoptotic index, dGli36 cells were infected with (i) pC8-36, (ii) pC8-

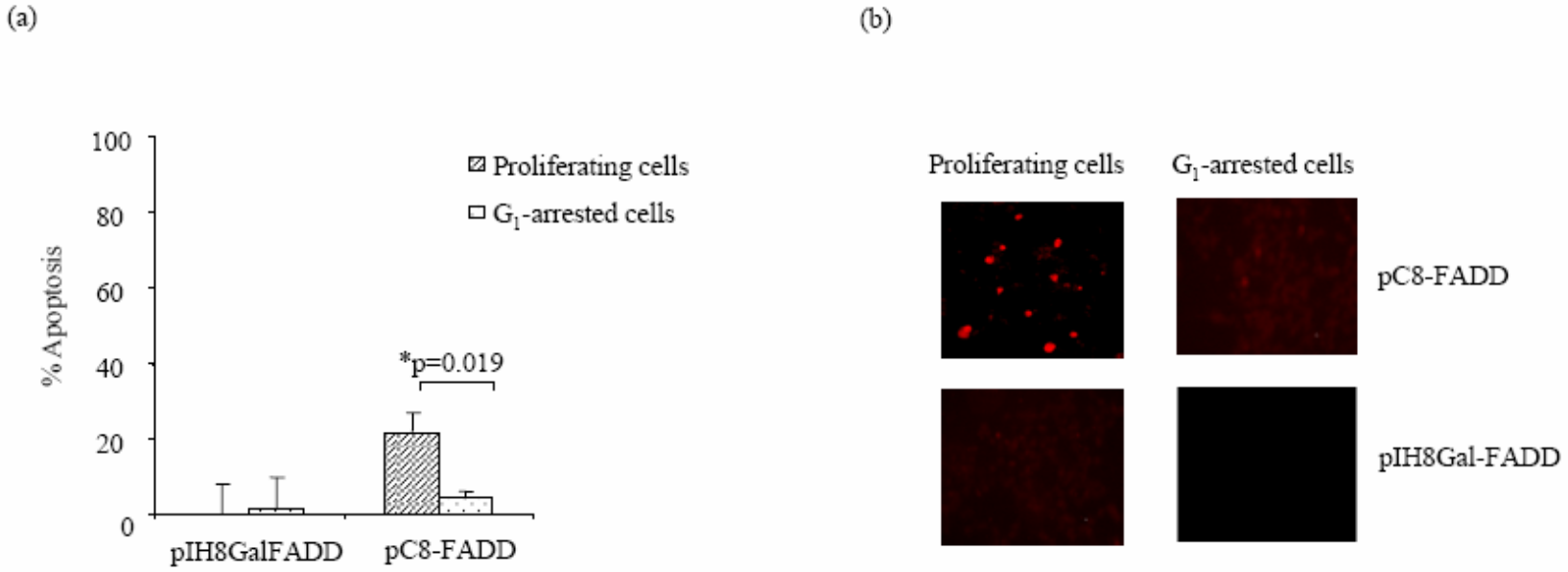

Figure 4.5. Apoptotic effect of FADD mediated by pC8-FADD is cell cycle-regulated.
dGli36 glioma cells was infected were pIH8GalFADD and pC8-FADD at MOI of 1.0. (a) Cell cycle-regulated apoptosis was analyzed in the proliferating and the G_1-arrested populations infected with pIH8GalFADD and pC8-FADD at 72 h post-infection. The percentage of apoptotic cells was determined using trypan blue exclusion assay. (b) Cell death mediated by pC8-FADD was confirmed using TUNEL assay.

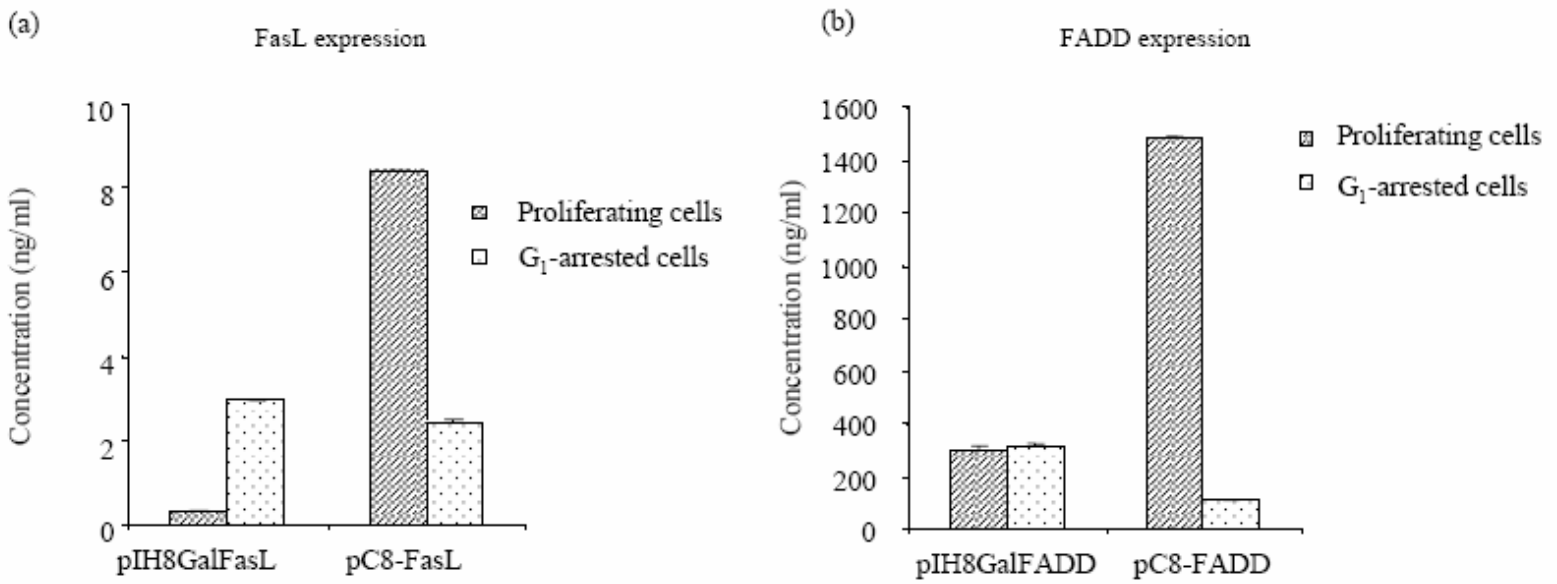

Figure 4.6. Expression of FasL and FADD mediated by pC8-FasL and pC8-FADD is cell cycle-regulated.
Cellular extracts from either proliferating cells or G_1-arrested cells infected with the respective vectors (MOI of 1.0) were harvested. The expression levels of exogenous (a) FasL and (b) FADD in dGli36 cells were analyzed using ELISA.

FasL, (iii) pC8-FADD, and (iv) 1:1 ratio of pC8-FasL and pC8-FADD at MOI of 1.0 for 6 h. The infected cells were either allowed to proliferate or induced to arrest in G_1. The percentage of apoptosis induced by either pC8-FasL or pC8-FADD in proliferating dGli36 cells was approximately 40 % and 30 %, respectively (Figure 4.7a). The percentage of cytotoxicity in the corresponding G_1-arrested cells was comparable to that observed in the control (12.49 %). When dGli36 cells were co-infected with pC8-FasL and pC8-FADD, the percentage of apoptosis increased by 20 % with respect to pC8-FasL and 30% with respect to pC8-FADD (Figure 4.7a). Cytotoxicity observed in these co-transduced (pC8-FasL and pC8-FADD) proliferating cells was significantly higher (60 %, $p=0.04$) than the corresponding G_1-arrested cells (10 %).

This effect of FasL and FADD were also tested on U373MG. In comparison to dGli36 cells, U373MG was not sensitive to pC8-FasL-induced cell death (Figure 4.7b). However, approximately 20 % of apoptosis could be observed when FADD was overexpressed (Figure 4.7b). Interestingly, the percentage of cell death was greatly enhanced when U373MG was co-infected with pC8-FasL and pC8-FADD (Figure 4.7b). The percentage of apoptosis in the co-infected cells was 38 % higher than pC8-FasL-infected (1.5 %) cells and 11 % higher than pC8-FADD-infected (19.9 %) cells. The lack of sensitivity of U373MG to FasL-induced cell death could be attributed to the absence of functional DISC components, such as the downregulation of the Fas receptor, FADD and caspase 8 proteins. Analysis of the cellular extracts obtained from U373MG and dGli36 cells indicated that FADD and caspase 8 are present in both cell lines (Figure 4.7c). However, the level of Fas receptor expression was only detectable in dGli36, and absent in U373MG (Figure 4.7c). This indicates that the lack of sensitivity to FasL-induced cell death in U373MG is due to the absence of or low level of Fas receptor. These results also suggested that the over-expression of FADD protein could interact with FasL through a yet undefined pathway, to bring about a greater cell killing effect.

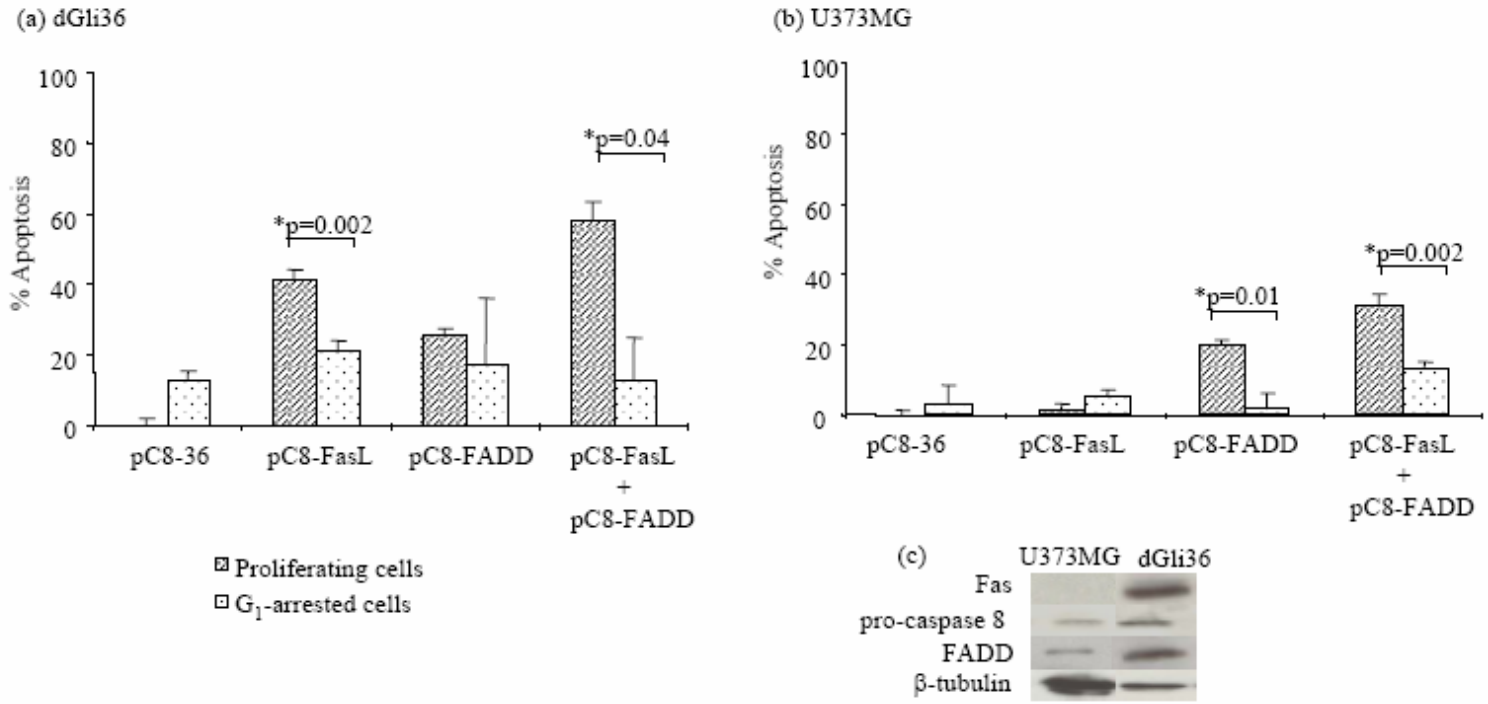

Figure 4.7. Combined effect of FasL and FADD overexpression was observed in glioma cells.
Combined apoptotic effect of FasL and FADD were analyzed in (a) dGil36 and (b) U373MG cells. The percentage of apoptotic cells was determined 72 h post-infection using trypan blue exclusion assay. Data shown are averages of triplicate experiments ± SEM. (c) Western blot hybridization indicates the presence or absence of the respective gene products in U373MG and dGli36 cells.

4.3.6 Expression profile of FasL and FADD

The apoptotic effect of pC8-FasL and pC8-FADD was also examined *in vivo*. The injection regime was predetermined *in vitro* according to the kinetics of FasL and FADD expression at various time points following infection with either pC8-FasL or pC8-FADD. Expression of FasL peaked on day 10 post-infection (Figure 4.8a), while the level of FADD expression peaked on day 3 (Figure 4.8b). Thus, repeated injection of pC8-FasL and pC8-FADD viral vectors will be administered every 10 days and 3 days respectively. The administration of the control vector will follow the injection regime of FasL, i.e. every 10 days.

4.3.7 FasL and FADD gene delivery in vivo suppresses tumor growth

dGli36-SCID8 (refer section 2.2.8.3) was used for the *in vivo* experiment because this cell line consistently forms s.c. tumor in immunodeficient SCID mice. Similar to dGli36 cells, this derivative is also sensitive to FasL- and FADD-induced apoptosis, and has more aggressive tumor growth kinetics in immunodeficient mice (data not shown). Tumor volume of 121 mm^3 (average of five animals) consistently formed at day three post implantation of dGli36-SCID8 cells into the flanks of SCID mice. When 1 x 10^6 of dGli36-SCID8 cells were intracranially implanted into immunoincompetent mice, the animals died within 10 days, three times faster than its parental dGli36 cells. In an attempt to ensure an optimal ratio between therapeutic vectors against tumor cells, we have chosen to administer the viral vectors the next day following tumor cells implantation. Palpable tumors were injected with 2 x 10^6 TU of (i) pC8-36, (ii) pC8-FasL, and (iii) pC8-FADD viral vectors. To investigate the combine effect of FasL and FADD *in vivo*, dGli36 tumors were also injected with both pC8-FasL and pC8-FADD (iv) viral vectors at a 1:1 ratio. Tumor volume was documented every 3-4 days. The tumor volume in animals treated with either pC8-FasL or pC8-FADD construct was significantly smaller than those in the control vector group ($p < 0.001$ and $p< 0.01$, respectively; Figure 4.9). In mice treated with pC8-FasL, the tumor volume ranges between 2 mm^3 and 19 mm^3, with 2 out of 5 animals completely devoid of any detectable tumor mass. The effect of pC8-FADD expression in dGli36-SCID8 tumor was comparatively weaker than

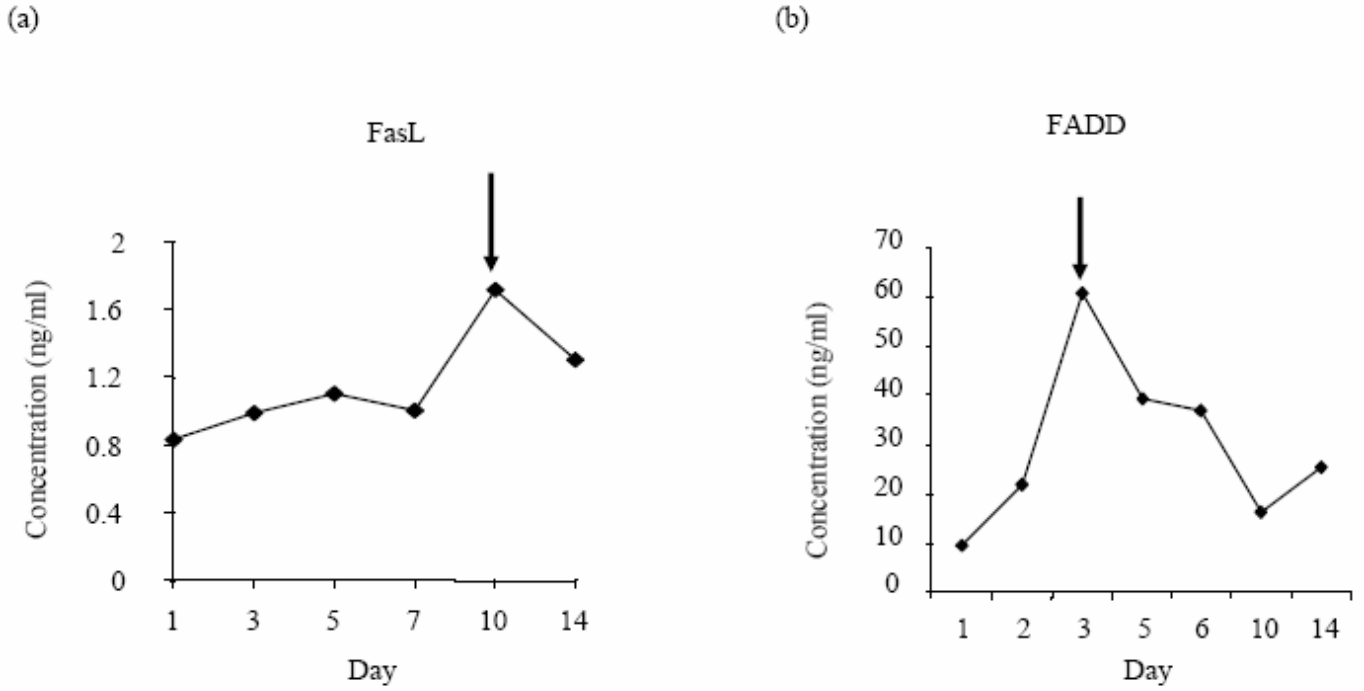

Figure 4.8. Expression profile of FasL and FADD *in vitro*.
The expression profile of (a) FasL and (b) FADD were determined in dGli36 cells infected with either pC8-FasL or pC8-FADD, respectively. Cell lysate were harvested at respective time points and the expression of the respective proteins were analyzed using ELISA.

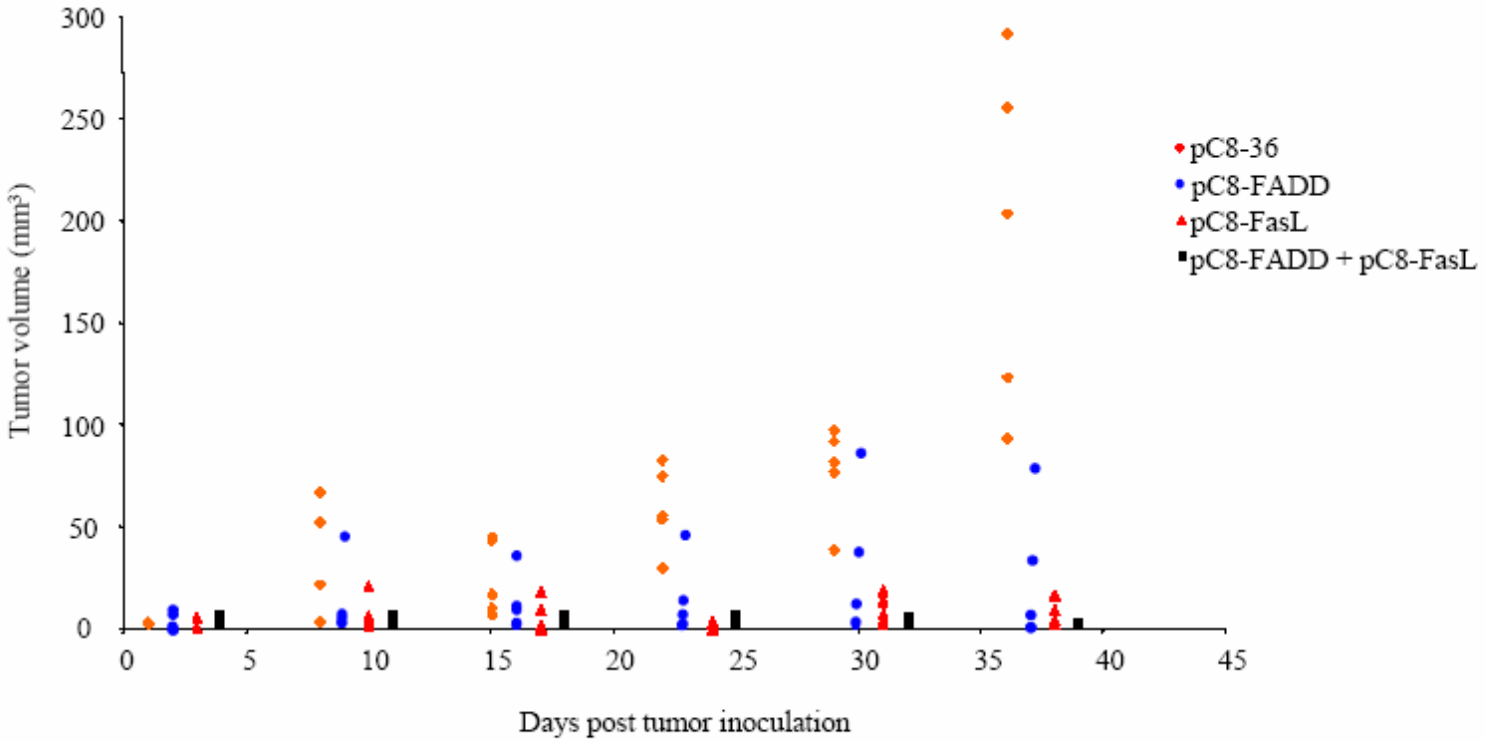

Figure 4.9. Suppression of tumor growth is observed *in vivo*.
To analyze the effect of overexpression of FasL or FADD, SCID mice harboring s.c dGli36-derived tumor xenograft were injected intratumorally with pC8-36 control vector, pC8-FasL, pC8-FADD, and pC8-FasL with pC8-FADD.

pC8-FasL, with tumor volume averages around 25 mm^3 (range, 2 mm^3 to 85 mm^3), with 2 out of 5 mice tumor free. Interestingly, effective suppression of tumor growth was observed in all mice co-injected with pC8-FasL and pC8-FADD. In comparison to other groups of mice, all mice in this treatment group were tumor free (Figure 4.9). During the early stages of the experiment, we noticed that tumor mass in this group of mice were consistently smaller (range, approximately 0.77 mm^3 to 4.21 mm^3) than any of the treatment groups, suggesting that co-expression of both FasL and FADD effectively enhanced the apoptotic index of the xenografts, thus preventing tumor growth. Although considerable differences were observed in the tumor volume among the treatment groups, this difference is not statistically significant.

4.3.8 Suppression of tumor growth is mediated by overexpression of exogenous Fas or FADD

To confirm that overexpression of FasL and FADD resulted in the suppression of tumor growth observed in all the animals, real time RT-PCR was performed on the dissected tumors (harvested at the end of the experiment from one extra mouse that contains palpable tumor) to quantitate the level of exogenous FasL and FADD mRNA expressions. As mentioned earlier in the Methods section 4.2.3, all samples were normalized to that of 18S rRNA. Subsequently, the differential mRNA expressions were expressed as a ratio between tumors injected with therapeutic vectors or control tumors injected with the backbone vectors. As shown in Figure 4.10, the mRNA level of FasL in tumor injected with pC8-FasL was 5-fold higher than those injected with the control vector. Interestingly, co-infection of pC8-FADD and pC8-FasL resulted in 20-fold increase in the FasL mRNA activities in comparison to the control tumor. Similarly, the level of FADD mRNA was also higher in tumors that were co-infected with FasL and FADD (2.2-fold higher than control) compared with FADD alone (0.62-fold higher than control). The level of FasL or FADD mRNA expression correlates with the suppression of tumor growth, such that the tumor volume in mice co-injected with FasL and FADD is the smallest, followed by pC8-FasL, pC8-FADD and lastly, the control vector. Taken together,

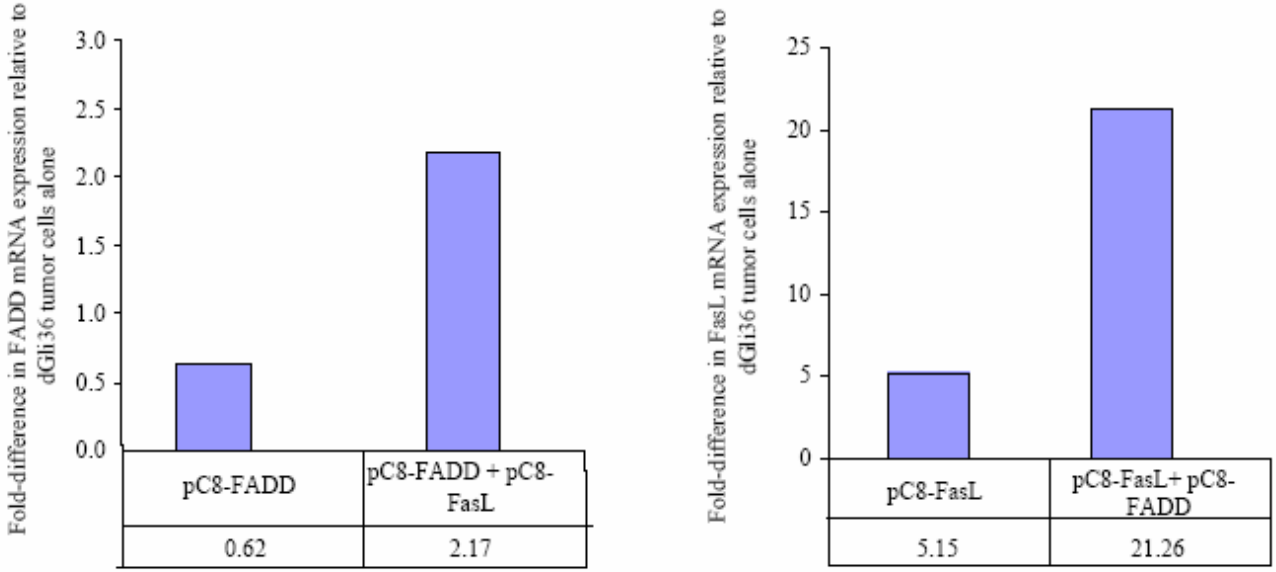

Figure 4.10 Differential mRNA expression of (a) FADD and (b) FasL in treated tumors compared with control.

these results demonstrated that therapeutic gene expression mediated by the cell cycle-regulated vector suppresses tumor formation *in vivo*.

4.4 Discussion

In this study, we incorporated the *FasL* and *FADD* gene into the cell cycle-regulated amplicon vector and demonstrated that the expression and function of these genes can be regulated according to cell cycling event.

The proapoptotic activity of FasL was analyzed in U373MG and dGli36 human glioma cells. Overexpression of FasL induced cell death in dGli36 cells, whereas U373MG is resistant to FasL expression (Figure 4.7). Most human glioma cells express Fas receptor and thus are sensitive to FasL-induced cell death. However, some glioma cells acquire mechanisms, such as the loss or downregulation of the Fas receptor expression, to evade Fas/FasL mediated cell death. Other possible mechanisms include mutations in the gene encoding the Fas receptor resulting in the failure of the receptor to be externalized (Karlsson et al., 2004); the presence of the soluble receptor that lack the transmembrane domain (sFas) (Cascino et al., 1996); present of the soluble decoy receptor DcR3 that binds to FasL (Roth et al., 2001); and the lack of FADD or caspase 8 (Karlsson et al., 2004). Using western blot analysis, we found that the expression level of the Fas receptor in U373MG is relatively low, although it expresses both pro-caspase 8 and FADD. This suggests that a functional Fas receptor is essential for the activation of apoptosis.

It has been reported that overexpression of the adaptor protein, FADD, induces apoptosis in FasL-insensitive cells (Chinnaiyan et al., 1995; Chinnaiyan et al., 1996; Grimm et al., 1996). However the effect of FADD overexpression on glioma cell lines has been controversial. Kondo et al. (1998) and Hao et al. (2001) reported that overexpression of FADD induces apoptosis in U373MG, while Knight et al. (2001) reported that enforced expression of FADD did not sensitize this cell to FasL-induced cell death. In our study, we observed an increase in the percentage of cell death in pC8-FADD-transduced U373MG when compared with the control vector (Figure 4.7b). Moreover, the percentage of apoptosis in U373MG increased by approximately 40 % when both FasL and FADD were co-expressed (Figure 4.7b). In contrast,

the effect of FasL and FADD co-expression in dGli36 cells is not as significant. It is possible that both molecules might synergistically enhanced apoptosis in U373MG (Figure 4.7b), while additively in dGli36 cells (Figure 4.7a). Alternatively, it is possible that the presence of exogenous FADD does not play that much a role in dGli36 cells which already express high level of Fas receptor. At present, we do not know what factors contribute to the tremendous enhancement observed in one glioma cell line (U373MG) but not the other (dGli36). However, we speculate that the different genetic profile of glioma cell lines, with different levels of pro-apoptotic or anti-apoptotic molecules, might play a role in this difference.

We noticed that a fraction of the TUNEL positive cells were not GFP positive, indicating that these cells were not transduced by our viral vectors (Figure 4.4a). We hypothesize that the cell death observed in non-transduced cells could be due to the binding of secreted soluble FasL to Fas receptor. This observation is confirmed when conditioned medium harvested from FasL-transduced proliferating cells induced apoptosis while those from the G_1-arrested cells do not (Figure 4.4b). FasL is processed by several metalloproteinases to yield both a soluble form and a membrane-associated form. It has been widely reported that FasL induce "bystander effect" in untransduced cells, possibly through the action of the soluble form. (Kayagaki et al., 1995; Powell et al., 1999; Schneider et al., 1998; Tanaka et al., 1998). The apoptosis observed in non-infected cells could be due to the binding of the oligomerized soluble FasL to the Fas receptor on untransduced cells.

The effect of FasL and FADD expression was examined in immunodeficient mice harboring s.c. dGli36-SCID8 glioma xenografts. We observed that 2 out of 5 animals injected with either pC8-FasL or pC8-FADD were completely devoid of tumor. These results indicated that FasL and FADD gene expression mediated by this cell cycle-regulated vector is able to suppress tumor growth *in vivo*. Sandler VM et al (2002) have recently demonstrated that HSV-1 amplicon vectors expressing enhanced green fluorescent protein (EGFP) can reliably infect neurons after it is injected into cortex, striatum and thalamus in rats, producing

sufficient numbers of infected neurons for electrophysiological experiments in acute brain slices. Expression of eGFP delivered by these HSV-1 amplicon viruses was detected for up to 5 weeks post-infection. Therefore the lack of complete regression of tumors is unlikely to be due to the instability of the amplicon DNA. Complete regression of tumors was not observed possibly due to the following reasons; firstly, the expression pattern of FasL and FADD were determined *in vitro*, which might not truly represent the *in vivo* condition. Secondly, the expression of the therapeutic genes is strictly dependent on cell division. It is possible that the expression of FasL was not activated due to the absence of proliferating cells in the injected region. In comparison to FasL or FADD alone, all mice injected with pC8-FasL/pC8-FADD were tumor free. However, the differences in tumor volume among each treatment group are not statistically significant. We speculate that in order to detect a statistically significant difference among each treatment group, we might have to use other glioma cells rather than dGli36. The presence of a functional Fas receptor in dGli36 cells might have masked the effect of the overexpression of both FasL and FADD. Instead, in U373MG, which lacks the Fas receptor, the effect might be more apparent, as demonstrated in the *in vitro* experiments (Figure 4.7b).

In summary, our study showed that FasL- or FADD-induced apoptosis in the cell cycle-regulated amplicon vector is activated specifically in proliferating cells *in vitro* and *in vivo*. Current combined treatment for glioma fails to remove tumor cells completely resulting in recurrences in majority of patients. Our vector can be employed as adjuvant therapy to complement surgery whereby the viral vectors can be injected directly into the tumor bed; this ensures that the transcription of the therapeutic gene is activated when the residual tumor cells start to proliferate. Since gliomas are very heterogeneous, the delivery of more than one treatment modalities could enhance the therapeutic index.

Chapter 5

Strategies for targeting therapeutic gene expression to glioma cells

5.1 Background

Lack of tumor specificity is a recurring problem in current gene therapy protocols. It is crucial to target therapeutic agents specifically to tumor cells in order to minimize damages to healthy tissues. This is especially important in the gene therapy for GBM since it has the tendency to invade into surrounding brain tissues, thus rendering complete surgical removal practically impossible. One way to overcome this difficulty is to design strategies that facilitate the expression of therapeutic genes specifically in glioma cells.

Two different approaches of targeting gene expression specifically to glioma cells will be presented in this chapter. Targeting can be achieved at the level of gene expression by the incorporation of tissue-specific transcriptional elements or during gene delivery by the modification of the gene delivery vectors.

5.1.1 Transcriptional targeting

One of the factors that influence the stability of transgene expression is the type of promoter used. Ubiquitous promoters such as CMV are frequently employed to drive therapeutic gene expression due to their high level of activity (Cooper, 2001). However, gradual inactivation of the ubiquitous viral promoters often results in the silencing of transgene expression *in vivo*. CMV-driven EGFP expression has been shown to decrease rapidly with time in cycling hepatocarcinoma cell lines (Gerolami et al., 2000). To overcome this problem, tissue-specific promoters have been adopted to restrict gene expression to selected cell populations (Shibata et al., 2000; Ueno et al., 2001). However, tissue-specific promoters may also be active in normal cells (Vandier et al., 1998). For instance, the used of the glial fibrillary acidic protein (GFAP) promoter to drive cytotoxic gene expression in glioma cells might result in unwanted toxicity in normal brain tissues (Vandier et al., 1998). These could be overcome by incorporating the GFAP promoter into the cell cycle-regulated vector described here to direct transgene expression specifically to rapidly proliferating glial cells.

5.1.1.1 GFAP

GFAP, which was first identified in patients with multiple sclerosis (Eng et al., 1971), is the most frequently used marker for glial cells. It is a major component of the intermediate filaments in the brain, and is expressed exclusively in cells of glial origin (Eng, 1985). GFAP is also responsible for modulating the shape and the stability of astrocytes (Eng et al., 2000). Elevated level of GFAP is detected during reactive gliosis resulting from injury or trauma to the brain (Eddleston and Mucke, 1993). Several studies have shown negative correlation between the level of GFAP expression and the proliferation state of the astrocytes. Increased level of GFAP has been correlated with changes in proliferation (Rutka et al., 1994), in extension of cellular processes (Rutka and Smith, 1993), and anchorage-independent growth (Rutka et al., 1994). Pekny et al (1998) demonstrated that the proliferation rate of primary astrocytes harvested form GFAP-/- mice was higher when compared with that from the wildtype mice.

5.1.1.2 GFAP promoter for transgene regulation

The regulatory region controlling the expression of the *GFAP* gene has been mapped to sequences 1.8 kb upstream of the transcriptional start site. Positive regulatory regions for the *GFAP* gene exist between -250 and -80 bp as well as between -1980 and -1500 bp upstream of the transcriptional start site (Besnard et al., 1991; Eng et al., 2000). The human *GFAP* promoter consensus sequence (hgcs), which confers glial cell specificity, is mapped to the positive regulatory regions of the *GFAP* promoter (Besnard et al., 1991; Masood et al., 1993; Rutka et al., 1997). Although the expression of GFAP is repressed in most GBM due to the methylation of the *GFAP* promoter, GFAP-negative glial cells nonetheless allow in functional GFAP promoter activities (Fukuyama et al., 1996). In 1998, Chen et al. incorporated three tandem-repeats of the *GFAP* enhancer element coupled to a tetracycline transactivator into an Ad vector to drive *lacZ* expression in glioma cells. This glial-specific enhancer element is located within the positive regulatory region (-1753 to -1489) upstream of the transcriptional start site. This study demonstrated that *GFAP* enhancer element was able to direct gene

expression in cells of glial origins. LacZ expression was detectable not only in GFAP-expressing glioma cells (U373 MG and U343 MG), but also in GFAP-negative glioma (T98G), medulloblastoma (DAOY) and neuroblastoma (SHEP, LAN-5, KCNR) cells (Chen et al., 1998). In contrast, lacZ expression was not observed in non-glial derived IMR90 fibroblasts (Chen et al., 1998).

Furthermore, the *GFAP* promoter was shown to confer gene expression particularly to astrocytic cells in transgenic mice (Brenner et al., 1994; Eng et al., 2000). When incorporated into Ad (Smith-Arica et al., 2000; Vandier et al., 2000), retrovirus vectors (Cortez et al., 2000), and lentivirus (Jakobsson et al., 2003), the *GFAP* promoter confers glial-cell specific gene expression *in vitro*.

Vectors that combine cell type-specific promoters with inducible expression have been developed to augment the activity of the transcriptionally weak *GFAP* promoter (Besnard et al., 1991). To enhance promoter strength, Ralph et al. (2000) inserted the tet-off transactivator (tTA) under the control of the GFAP promoter into an Ad vector system. Infection of primary hippocampal cultures demonstrated specific transgene expression in glial cell populations. Moreover, when the Ad-GFAP vector was delivered into adult rat hippocampus, it showed a similar pattern of glial cell specific expression (Ralph et al., 2000). McKie et al. (1998) further demonstrated astrocyte-specific gene expression mediated by GFAP-lacZ in a HSV-1 vector. To study the functions of astrocytes in the developing brain, Delaney et al. (1996) expressed the *HSV-tk* gene under the GFAP promoter in a HSV-1 vector. LacZ expression driven by the GFAP promoter has also been used to study the fate of astrocytes in embryonic neural grafts (Quintana et al., 1998). Gene therapy using FasL for systemic treatment of cancer is greatly hampered by the inherent toxicity to non-target FasL-positive cells. Several groups have constructed vectors that limit the expression of FasL *in vivo* by the incorporation of tissue-specific promoters, such as GFAP, smooth muscle-specific promoter, and prostate-specific promoter (Aoki et al., 2000; Morelli et al., 1999; Rubinchik et al, 2001).

5.1.1.3 One step closer to clinical trials

5.1.1.3.1 Effect of chemotherapy on the cell cycle-regulated amplicon vector

Chemotherapy is a well-established treatment for gliomas (Stewart, 2002). Chemotherapy can be used as a primary treatment regime, or as a post-operative treatment together with radiotherapy. The most commonly used chemotherapeutic drugs for the treatment of glioma are procarbazine, CCNU (lomustine), and vincristine (PCV) (Newlands et al., 2003). The effect of these agents on survival is limited and the responses to these drugs were short-lived (Georges et al., 1988; Rodriguez and Levin, 1987; Sandberg-Wollheim et al., 1991; Stewart, 2002). Moreover, these drugs cause damage to the bone marrow of patients. A low toxicity drug, temozolomide (TMZ), has been employed as an alternative for the treatment of recurrent gliomas (Chang et al., 2004a; Chang et al., 2004b; Yamini et al., 2004; Yung et al., 2000; Yung et al., 1999). TMZ is an alkylating agent that acts by methylating DNA at the N^7 and O^6 site on guanine and the O^3 site on adenine. The modification at O^6 sites leads to the insertion of thymine residue instead of cytosine opposite the methylguanine during DNA replication, thus leading to cell death (Clark et al., 1995; Takemoto et al., 2003). Chemotherapeutic drugs such as TMZ have been reported to arrest cells at G_2/M of the cell cycle (Hirose et al., 2001; 2004). It would therefore be important to determine whether transgene expression mediated by the cell cycle-regulated amplicon would be affected in TMZ-treated cells.

5.1.1.3.2 Stability of HSV-1 amplicon

For successful gene delivery *in vivo*, the gene delivery vehicle must be stable to confer reliable gene expression. The HSV-1 amplicon DNA is relatively stable in nondividing cells, but is lost after a few cell divisions (Johnston et al., 1997). Fraefel et al. (1996) demonstrated that the viral DNA can be detected for at least 1 month in the midbrain and striatum. In HSV-1 vector bearing the rat tyrosine hydroxylase (TH) promoter driving the *lacZ* reporter gene, lacZ expression can be detected up to 2 months in the substantia nigra pars compacta (Wang

et al., 1999). To overcome the problems associated with gene delivery, improvement in prolonging transgene expression *in vivo* needs to be explored.

5.1.1.3.3 Transduction efficiency of HSV-1 amplicon vector

Although promising results for the delivery of therapeutic agents to tumor cells have been reported *in vitro* and *in vivo*, the lack of widespread specific vector distribution is one of the major limitations for successful gene therapy. Even with the use of a prodrug activating system which has a potent bystander effect, such as the HSV-tk/GCV system or the CD/5-FC system, only 2 % of the tumor cells in the tumor mass are effectively transduced (Huber et al., 1994).

Gene delivery to the brain presents unique challenges due to the limited and risky access to the brain, the sensitivity to volumetric changes, and the difficulty of accessing the BBB and blood-tumor barrier (BTB) (Constantini et al., 2000; Lam and Breakefield, 2001). Most gene delivery to the brain involved direct stereotactic injections with restricted number of injections and volume. By this route of delivery, the vector is only taken up by cells in the immediate vicinity of the injection site. Spread of virus to other sites can be facilitated by slower injection rates, but still, not comprehensive. Other modes of administrations include the generations of vectors *in situ* by implantation of retrovirus packaging cells to produce viral particles which will infect residual dividing cells (Short et al., 1990) and the passage of vectors through the BBB and BTB by intra-arterial, intrathecal or intraventricular routes of injection (Constantini et al., 2000).

Despite promising preclinical efficacy of HSV-tk/GCV system, engraftment of retroviral producer cells harboring HSV-tk to GBM patients did not produce therapeutic benefits in a phase III clinical trial (Rainov, 2000). The elements of the Epstein Barr virus (EBV), *Epstein-Barr nuclear antigen 1* (*EBNA-1*) can confer episomal replication and retention, thus increase transgene stability. Hampl et al. (2003) demonstrated higher transgene expression in

tumors when tumor cells were converted into retrovirus producer cells by a HSV/ EBV/RV tribrid amplicon vector. Other methods to increase transgene delivery include multiple-sites injections (Qureshi et al., 2000); use of replication competent vectors (Martuza, 1991); protease digestion of the extracellular matrix (Kuriyama, 2000) and transport across the tumor vasculature (Nilaver et al., 1995; Rainov et al., 1995). However, all these methods lack demonstratable benefits in clinical trials, thus, indicating a need to improve gene delivery modalities.

5.1.1.3.4 Immunogenicity of HSV-1 amplicon

The most critical issue in the development of a gene delivery vector system is the potential adverse effect to patients. This issue has been brought into attention by the death of a patient after hepatic-arterial infusion during a gene therapy protocol for ornithine transcarbomylase (OTC) deficiency whereby the patient reacted to a massive immune response elicited by the Ad vector (Hsich et al., 2002; Verma, 2000).

The transduction of cells by gene transfer vectors involves the interaction of the vectors with the host immune system. This introduction of foreign gene products is often compared to microbial infection, in which the host first line of defense, i.e. innate immune response is activated. Thus, in both naive and immunized individuals infected with wild-type HSV-1 vectors, the complement cascade and macrophages are activated; NK cells, dendritic precursors, γδ T cells are recruited, activated and matured; also, chemokines and cytokines are generated and secreted (Chen et al., 2003; Wakimoto et al., 2003). Together, these molecules coordinate the lysis of virions and virus-infected cells, and also provide a link to effective adaptive immunity (Medzhitov and Janeway Jr, 1997; Wakimoto et al., 2003). Immune responses elicited by recombinant HSV-1 vectors can arise from the viral particle components, expression of viral gene products, cellular debris, and transgene expression (Bowers et al., 2003), with viral gene products as the major source of immunogenic antigens. Recombinant HSV-1 retains the ability to enter into latency phase in non-dividing cells,

where expression of viral genes except for the LAT is switch-off. To prevent reactivation from latency, multiple immediate early gene products that encode for transactivators, for instance *ICP0* and *ICP4* are mutated or deleted (Krisky et al., 1998).

The amplicon plasmids are dependent upon helper virus function to provide the essential replication machineries and structural proteins required for packaging into viral particles (Spaete and Frenkel, 1982). These helper viruses are similar to the recombinant HSV-1 vectors in that they retain majority of the HSV-1 genome. Therefore, the final stock of the helper virus-based packaging contains a mixture of varying ratios of helper and amplicon viral particles. Viral genomes from the helper viruses induce the activation of immune responses. Preferential purification of the amplicon vector from the helper virus is not possible since the physical properties of both entities are essentially similar (Olschowka et al., 2003). A recent improvement to the amplicon system is the development of the helper virus-free packaging system (Fraefel et al., 1996; Saeki et al., 2001; Saeki et al., 1998; Stavropoulos and Strathdee, 1998). This packaging system produces HSV-1 viruses that are virtually free from contaminating helper viruses with minimum toxicity or antigenicity (Constantini et al., 2000).

Olschowka et al. (2003) compared the induction of immune response in C57Bl/6 mice injected with HSV-1 amplicon viral vectors carrying *lacZ* gene (HSVlac), which were packaged using either the helper virus-dependent or the helper virus-free system. All injections including saline controls induced inflammation on day 1, indicating an activation of inflammatory responses due to the transient breach of the BBB. However, on day 5 post-inoculation, mRNA levels of the proinflammatory cytokines, chemokines and ICAM-1 adhesion molecules in helper virus-free amplicon groups were similar to saline-injected mice. In contrast, mice injected with helper virus-packaged HSVlac showed persistent elevated level of proinflammatory cytokines, chemokines and ICAM-1 adhesion molecules (Olschowka et al., 2003). This study demonstrates that helper virus-free amplicon

preparations exhibit a safer innate immune response profile, presumably as a result of the absence of helper virus gene expression.

Majority of humans are seropositive for HSV-1 (Baringer and Swoveland, 1973; Corey and Spear, 1986; Herrlinger et al., 1998). The presence of pre-existing antibodies is a concern in HSV-1 mediated gene therapy protocols. Neutralizing antibodies could prematurely eliminate the viral vectors, which could potentially inhibit the infection of target cells or even result in the elimination of transduced cells. The influence of pre-existing anti-HSV-1 immunity on HSV-1 vector-mediated transfer of transgenes such as HSV-*tk* or lacZ gene was studied in intracranial rat gliomas with and without prior immunization to HSV-1 (Herrlinger et al., 1998). Although the number of HSV-*tk*- and lacZ-positive cells was reduced in pre-immunized animals compared with non-immunized animals, the duration of transgene expression was similar between the two groups of animals. Further, there was no apparent increase in neurotoxicity caused by the inflammatory response within the brain associated with a pre-existing anti-HSV-1 immune response. These findings support the potential utility of recombinant HSV-1 vectors in treatment of brain tumors in humans who have circulating neutralizing antibodies to HSV-1.

5.1.2 Vector retargeting

Stereotactic injection of vectors to the brain is limited by the volume and number of injections. The ability to target gene delivery vector would enhance the safety profile of the vector. Identification of molecules that mediate the targeted delivery of therapeutic DNA or drugs to specific cell types would thus significantly reduce the amount of therapeutic agents required, and correspondingly, reduce unwanted toxicity to non-target cells.

There has been much progress in the field of vector targeting using different vector systems. Wu and Wu (1987) was the first to report the use of the glycoprotein asialoorosomucoid (ASOR) to specifically target the liver parenchyma. Retroviral vectors have been modified to

contain a chimeric envelope to target to breast cancer cells (Tai et al., 2003). As mentioned earlier in the introduction section, EGFR is frequently amplified or mutated in GBM, thus producing a constitutively active receptor in the absence of the EGF ligand (Mischel and Cloughesy, 2003). Vectors that target to this growth factor receptor have been designed. Doubly ablated Ad vectors, lacking both the coxsackievirus-adenovirus (CAR) receptor and the αv integrin binding capacities, together with bispecific single-chain antibodies that recognize both the EGFR or the epithelial cell adhesion molecule have been employed for specific gene delivery to primary human brain tumors (Samoylova et al., 2003; Van Beusechem et al., 2002). Fusion proteins consisting of peptide toxins fused to the human EGF (DAB 389EGF) has been demonstrated to selectively kill cells that overexpresses EGFR (Cohen et al., 2003). The overexpression of EGFR has been reported in esophageal squamous cell carcinoma (Sunpaweravong et al., 2004), non-small cell lung carcinoma (Hirsch et al., 2003) and various cancer (Oh et al., 2000). Therefore, it is not an ideal targeting molecule due to its lack of specificity.

5.1.2.1 Phage display technology

Identification of glioma-specific molecules would greatly facilitate the targeted delivery of therapeutic agents. Biopanning of the phage display library was employed to select for epitopes that are specific for human glioma cells. Phage display techniques have been used for selection on whole cells to identify peptide ligands directed against particular cell surface proteins (Barry et al., 1996; Campa et al., 2002; Liu et al., 2003; Parmley and Smith, 1989; Szardenings et al., 1997). Using this technique, peptides that bind to kidney, lung, skin, pancreas, intestine, uterus, adrenal gland, retina, fibroblast cells, myoblast, myotubes, human neutrophils, human laryngeal carcinoma cells, endothelial cells (Arap et al., 1998; Barry et al., 1996; Koivunen et al., 1999; Pasqualini et al., 2000; White et al., 2001), and human colorectal cell line (Rasmussen et al., 2002) have been identified. Recently, peptides that home selectively to the vasculature of various organs were isolated by the *in vivo* biopanning of peptide phage display libraries in mice (Arap et al., 2002a; Essler and Ruoslahti, 2002;

Pasqualini and Ruoslahti, 1996; Rajotte et al., 1998; Trepel et al., 2002), as well as in human (Arap et al., 2002b). The selected sequence can be used to target therapeutic agents (Arap et al., 1998) and diagnostic imaging radiolabels (Schumacher et al., 2002).

5.1.3 Aims of this study

The ability to direct transgene expression to specific cell types can significantly increase the efficiency of gene transfer. Two approaches were attempted with the aim to:

(1) control transgene expression specifically to rapidly proliferating glioma cells by the incorporation of the GFAP promoter to achieve transcriptionally regulated gene expression; and

(2) target HSV-1 amplicon vector to human glioma cells by first identifying glioma-specific peptide that would potentiate this targeted delivery.

5.2 Methods

5.2.1 Plasmid constructs

To generate a glial cell-specific and cell cycle-regulatable HSV amplicon vector, the GFAP enhancer element (-1753 to -1489) of the human GFAP promoter region together with the minimal hCMV promoter was first released from the parental plasmid, pBluescriptKS-GFAPtTA (kindly provided by Dr. P Nisen, University of Texas Southwestern Medical Center, Dallas, TX), using *Kpn*I and *Eco*RI, and subsequently cloned into the *Kpn*I and *Eco*RI sites in pHGCX (pHGCX-GFAP). Upon removal of the CMV promoter in pHGCX-GFAP using *Hin*dIII and *Bgl*II restriction enzyme sites, the entire DNA fragment encoding Gal4/NF-YA fusion protein and the 8GalLuc region of pC8-36 (Figure 3.4d) was inserted at the *Pme*I site, resulting in plasmid pG8-18. To generate pG8-FasL, the entire DNA fragment encoding Gal4/NF-YA fusion protein and the 8GalFasL region from pC8-FasL vector was excised, and inserted into pG8-18. All plasmids were amplified in *E.coli* STBL-2, and DNA was extracted using QIAprep Spin Miniprep. All plasmids were verified by DNA sequencing.

5.2.2 In vivo transduction

Two groups (n=5) of 6-8 weeks old CB-17 SCID mice were subcutaneously injected with either HeLa or dGli36 cells (5×10^6). A total of 2×10^6 TU of either pG8-18 or control pIH8GalLuc amplicon viral vectors was administered intra-tumorally when the tumor reached 80-100 mm^3 in volume. Animals in all the groups were sacrificed after 24 h and tumor nodules were meticulously harvested.

5.2.3 Determination of the efficacy of FasL in s.c. tumor

6-8 weeks old CB-17 SCID were subcutaneously injected with either HeLa or dGli36-SCID8 cells (2×10^6) and divided into 8 groups. One day following tumor inoculation, a total of 2×10^6 TU of either pG8-FasL or control vectors was administered intratumorally. Injections of viral vectors were repeated every 10 days until necrosis of tumor is observed in the control groups. Tumor volume is measured according to Bergers et al. (1999).

5.2.4 Determination of the efficacy of FasL in i.c. tumor

To maximize the effect of the therapeutic gene, 1 x 10^6 dGli36 cells were infected with various amplicon vectors at MOI of 2.0. The transduced cells were implanted stereotactically into the right hemisphere [bregma (0,0); lateral 2 mm; depth 2.5 mm] of immunodeficient nude mice. In general, tumor formation in these mice is marked by an observed loss of food intake and gait, resulting in a loss of body weight compared to the healthy mice. At each time point, the weight has been noted and survival kinetics on these animals were employed as a mean of evaluating the efficiency of treatment.

5.2.5 Treatment with TMZ

$3x10^5$ dGli36 cells were seeded one day before experiment. On the day of treatment, varying concentrations of TMZ were added directly to the medium and incubated for 1 hr at 37 °C. Following treatment, the cells were rinsed three times with PBS and replenished with complete medium. To determine the effect of TMZ on dGli36 cells, the cells were divided into two portions for assessing the cell cycle profile and cell death-induced by TMZ.

To assess the effect of TMZ on luciferase gene expression, cells were first infected with the respective amplicon vectors for 6 h. The transduced cells were divided into three portions; one portion of the cells was replenished with complete medium; the other portion of the cells was treated with lovastatin to induce G_1-arrest. The third portion of the cells was incubated in 75 μM of TMZ at 37 °C. After 1 h of treatment, the cells were rinsed with PBS twice, and replenished with complete medium containing 10 % serum.

5.2.6 Stability of pG8-18 viral vector

Six-week old SCID mice were used for this experiment. The mice were separated into 3 groups. The right side of the brain of the mice was inoculated with dGli36 (2 x 10^6) glioma cells. One day post implantation of tumor cells, pG8-18 (1 x 10^6 TU) viral vector, was inoculated into both the tumor bearing region and the normal side of the brain (left side).

Brains were harvested on day 4, day 10 and day 28 post inoculation. The harvested brains were prepared for extraction of viral DNA or protein.

5.2.7 Transduction efficiency of pC8-36 and pG8-18 viral vector

Six-week old SCID mice were separated into 4 groups of 2 animals each. The right side of the brains was inoculated with 10 µl of either pC8-36 (1 x 10^4 TU) or pG8-18 (1 x 10^4 TU) viral vector. Brains were harvested 1 day post injection. On the day of harvesting, mice were perfused through the heart with PBS. From 2 groups of animals, brains were harvested and single cell suspension obtained as follows. The brains were homogenized in 50 ml falcon tube with 12 ml of HBSS (Invitrogen Life Technologies) using a 5 ml serological pipette (Nunc), followed by 1 ml serological pipette and a flamed-polished pasteur pipette until no clumps were visible. 0.25 % trypsin was added to the cell suspension and incubated for 15 min at 37 °C, with mixing every 5 min. The homogenates were filtered through a 70 µm pore size nylon cell strainer (BD Biosciences). The filtrates were subject to centrifugation at 500 rpm for 15 min at 4 °C without brake (Beckman Coulter). Supernatant was removed and cell pellet resuspended in DMEM containing 10 % serum. The percentage of GFP positive cells was analyzed using FACS analysis. For the other 2 groups, the brains were fixed in 4 % paraformaldehyde solution overnight followed by 30 % sucrose for 48 h, and cryosections were performed. GFP positive cells were visualized using LSM 510 Meta confocal microscope (Carl Zeiss Microscopy, Göttingen, Germany) with appropriate filters.

5.2.8 Immunogenicity of HSV-1 amplicon vector

6 weeks old Balb/c mice were used for this experiment. The mice were separated into 4 groups of 2 animals each. The mice were inoculated at the right side of the brain with 10 µl of saline in group 1, AdGFP (1 x 10^2 pfu) in group 2, pC8-36 (1 x 10^4 TU) in group 3 and pG8-18 (1 x 10^4 TU) viral vectors in group 4. Brains were harvested on day 1 and day 4 post injections. On the day of harvesting, mice were perfused through the heart with PBS followed by 4 % paraformaldehyde. Brains were harvested and fixed in 4 % paraformaldehyde

overnight, followed by incubation in 30 % sucrose/PBS for 48 h, at 4 °C. Fixed tissues were then cryosectioned. Immunohistochemical staining was performed on consecutive sections.

5.2.9 Phage-display library biopanning

The phage display library employed for biopanning for glioma specific phage was the Ph.D. 12 library (New England Biolabs, Beverly, MA). Phages were selected for binding to human glioma cell lines by panning against intact cells in suspension. Glioma cell lines (dGli36, SF767, U87MG, U251MG, and U373MG) were grown in monolayers until confluent, and harvested by treating the cells with PBS containing 5 mM EDTA. The five glioma cell lines were mixed together in equal proportions to give a final cell number of 1 x 10^6. This was followed by incubating the cell mixture with 1 x 10^{11} pfu of M13 phage at 37 ºC for 2 h. The cells were washed once with PBS containing 0.1 % Tween-20 and nine times with PBS, followed by pelleting and resuspension to remove unbound phage. Bound phages were recovered by eluting with 0.2 M glycine, pH 2.2, containing BSA (1 mg/ml), followed by neutralization with 1 M Tris-Cl (pH 9.1). Recovered phages were amplified in ER2537 bacteria and subjected to two additional rounds of enrichment panning. These enrichment pannings were then followed by three rounds of subtraction panning against A549, CNE2, and HepG2 successively. The isolated phage clones were titered using ER2537 bacteria.

To determine the *in vitro* specificity of the recovered phage to glioma and nonglioma cell lines, 1 x 10^6 cells were incubated with 10^{12} pfu of the isolated phage clone at 37 °C for 2 h. Unbound phage was removed and bound phage was recovered and titered as mentioned.

5.2.10 Amplification of phage clones

ER2537 bacteria were employed for phage amplification. To 20 ml of log-phase bacteria culture, 1 x 10^{10} pfu of the phages were added and the mixture was incubated for 4.5 h at 37 °C in a shaking incubator. To precipitate the phages, a 1/6 volume of PEG8000/NaCl solution was added to the bacteria/phage mixture and precipitated at 4 °C overnight. The next

day, phages were harvested by centrifugation at 13 000 rpm for 10 min at 4°C. The resulting phage pellet was resuspended in 1 ml TBS. The phages were further precipitated by adding a 1/6 volume of the PEG/NaCl solution. After incubating for 1 h on ice, the phages were pelleted at 13 000 g for 10 min at 4 °C and resuspended in 200 µl of TBS containing 0.01% sodium azide. The amplified phages were titered and stored at 4 °C.

5.2.11 Titering of phage

To determine the titer, amplified phages were serially diluted in LB. Each of the diluted phage solutions was added to a log culture of the ER2537 bacteria. After incubating for 5 min at r.t. to allow infection to take place, 3 ml of melted 0.7 % agarose (45 °C) was added and the mixture was poured onto a LB agar plate containing 40 mg/ml of X-Gal, and 50 mg/ml IPTG. The titer of the phage solution was determined by counting the number of blue plaques after 24 h of incubation.

5.2.12 In vivo targeting of MG11 phage to tumor xenograft

For intracranial tumor, 2 x 10^6 dGli36 cells resuspended in 10 µl of PBS were stereotactically inoculated into the bregma region (2 mm lateral, 0.25 mm depth) of the right hemisphere of 6 week-old female nude mice. Phages were injected via tail vein 10 days post-inoculation of tumor cells, when the tumor volume was approximately 75 mm^3.

For s.c. tumor, 5 x 10^6 of either SF767, dGli36 glioma cells or CNE2 (nonglioma cells control) were suspended in 100 µl of PBS and injected into the right and left flanks of 6-week old SCID mice, respectively. Phage was injected via tail vein 7 days post-implantation of tumor when the tumor volume was approximately 100 mm^3.

Tumor bearing mice were randomized into two groups (5 per group), namely the control group and the experimental group. Control phage or phage bearing the glioma-specific sequence (1 x 10^{12} pfu), suspended in 400 µl of DMEM, was injected via tail vein into tumor-

bearing mice, and allowed to circulate for 24 h. After 24 h, mice were anesthesized and perfused through the heart with DMEM. Tumor and other organs were dissected and weighed. The tissues were homogenized in ice-cold DMEM containing protease inhibitor cocktail and 0.1 % BSA. After centrifugation to remove the tissue debris, bound phage was rescued by mixing the supernatant with 0.5 ml of ER2537 bacteria for 30 min at 37 °C. The supernatant containing phage was diluted in LB, after which aliquots were plated on LB agar plates containing X-Gal and IPTG. As control, unselected phage was administered at the same titer in the second group of animals.

5.2.13 Formation of peptide/DNA complexes

The formation and transfection of peptide/DNA complexes were carried out according to Patel et al. (2001) with slight modifications. Peptide/DNA complexes were prepared at a peptide:DNA ratio of 2:1 (w/w). Plasmid DNA was diluted to 10 μg/ml in Ringer's buffer (B. Braun Melsungen AG, Melsungen, Germany). The appropriate volume of peptide was also diluted in Ringer's buffer to give a final concentration of 20 μg/ml (peptide: DNA ratio, 2:1). The peptide was added dropwise to the DNA solution while vortexing gently. This mixture was allowed to incubate at r.t. for 30 min. After 30 min, the mixture was diluted to 4 μg of DNA per milliliter with DMEM in the presence of 100 μM of chloroquine, and added to cells.

5.2.14 Transfection of tumor cell lines

For transfection, 3 x 10^5 cells were seeded into each well of a six-well plate. After culturing overnight, the cells were washed twice with PBS. Freshly prepared peptide/DNA complexes were added into each well and incubated for 2 h at 37 ºC. For transfection performed in the presence of serum, FBS was added to a final concentration of 10 % immediately after the addition of peptide/DNA complexes. Reporter gene activity was assayed after 24 h or 48 h.

5.2.15 In vitro fluorescent peptide binding assay

For *in vitro* binding assay, 1 x 10^5 cells were seeded into each well of a 24-well dish. After culturing the cells overnight at 37 ºC, the cells were washed once with PBS, followed by incubation in blocking buffer containing PBS with 1 % BSA at r.t. for 1 h. The cells were washed twice with PBS. One hundred nanogram of Lissamine rhodamine-conjugated (K_{16})-MG11 peptide (Mimotopes, Victoria, Australia) was added to the blocking buffer containing 0.1 % sodium azide, and incubated with the cells at 37 ºC for 20 min. This is followed by five washes of PBS with 0.1 % Tween-20 at r.t. at 5-min intervals. The cells were then fixed in 4 % paraformaldehyde. After removal of excess paraformaldehyde, the cells were mounted. Images were captured digitally and analyzed with a LSM 510 Meta confocal microscope with appropriate filters.

5.2.16 In vivo fluorescent peptide binding assay

SF767-tumor bearing mice were randomized into two groups (2 per group). Fifty microliter containing 100 μg of Lissamine rhodamine-conjugated (K_{16})-MG11 or (K_{16})-H42 was injected intratumorally into each of two mice harboring the tumor, and allowed to circulate for 20 min. After 20 min, the mice were anesthesized and perfused through the heart with PBS followed by 4 % paraformaldehyde. The tumors were dissected and cryosectioned. The sections were then counterstained with the fluorescein isothiocyanate (FITC)-phalloidin and mounted. Images were examined using LSM 510 Meta confocal microscope with appropriate filters.

5.2.17 Statistical analysis

Data are presented throughout this study as means $\pm$ standard error of the mean. Statistical significance was evaluated and $p < 0.05$ was considered significant.

5.3 Results

For the ease of presenting data, the result section will be divided into two parts, namely 5.3.1 and 5.3.2, for transcriptional targeting and vector retargeting, respectively.

5.3.1 Cell type-specific and cell cycle-regulated transgene expression mediated by HSV-1 amplicon vectors in vitro

To achieve conditional gene expression in proliferating cells of a glial origin, the CMV promoter in pC8-36 amplicon plasmid (Figure 3.4d) was replaced by the glial cell-specific GFAP enhancer element cloned upstream of a minimal CMV promoter, thus generating pG8-18 (Figure 5.1).

To verify that the feature of cell cycle regulation was retained in this vector, an experiment similar to that described in section 3.3.5 (refer Figure 3.9) was performed. Our results demonstrated that when transfected with pG8-18 amplicon plasmid, the level of transgene expression was comparatively higher in proliferating glioma cells (dGli36, 1300 RLU/µg; U251MG, 228.91 RLU/µg; SF767, 689.98 RLU/µg) than in nonglioma cells (HeLa, 5 RLU/µg; HepG2, 75.36 RLU/µg) (Figure 5.2). In contrast, luciferase activities were minimal in pIH8GalLuc-transfected proliferating cells, as well as in pG8-18 transfected but growth-arrested cells. This observation was not due to differential transfection efficiency as these cell lines have been predetermined to yield similar numbers of GFP-positive cells 24 h posttransfection. We further investigated whether the variability in transgene expression was due to the lack of cellular protein required to confer glial cell-specific transgene expression. Immunohistochemical staining showed that unlike dGli36, SF767 and U251MG glioma cells, HeLa and HepG2 nonglioma cells did not express any detectable level of endogenous GFAP proteins (Figure 5.2). Thus, it appears that the pG8-18 amplicon vector was capable of conferring glial cell-specific transgene expression. Further, luciferase expression was shown, at a single-cell level, only in proliferating dGli36 cells transduced with the pG8-18 amplicon viral vector (Figure 5.3a). Confocal microscopy studies demonstrated that pG8-18-transduced

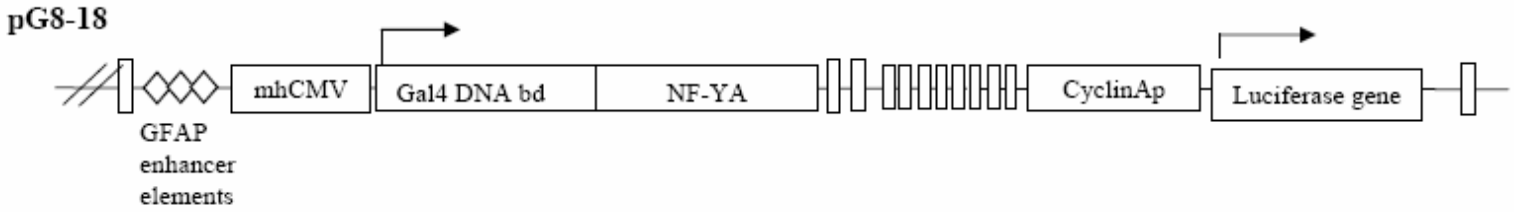

Figure 5.1 Diagram of glioma-specific and cell cycle-regulated vector.
pG8-18 vector containing three tandem repeats of the GFAP enhancer elements driving the minimal human CMV promoter upstream of the chimeric transcriptional activator, Gal4/NFYA.

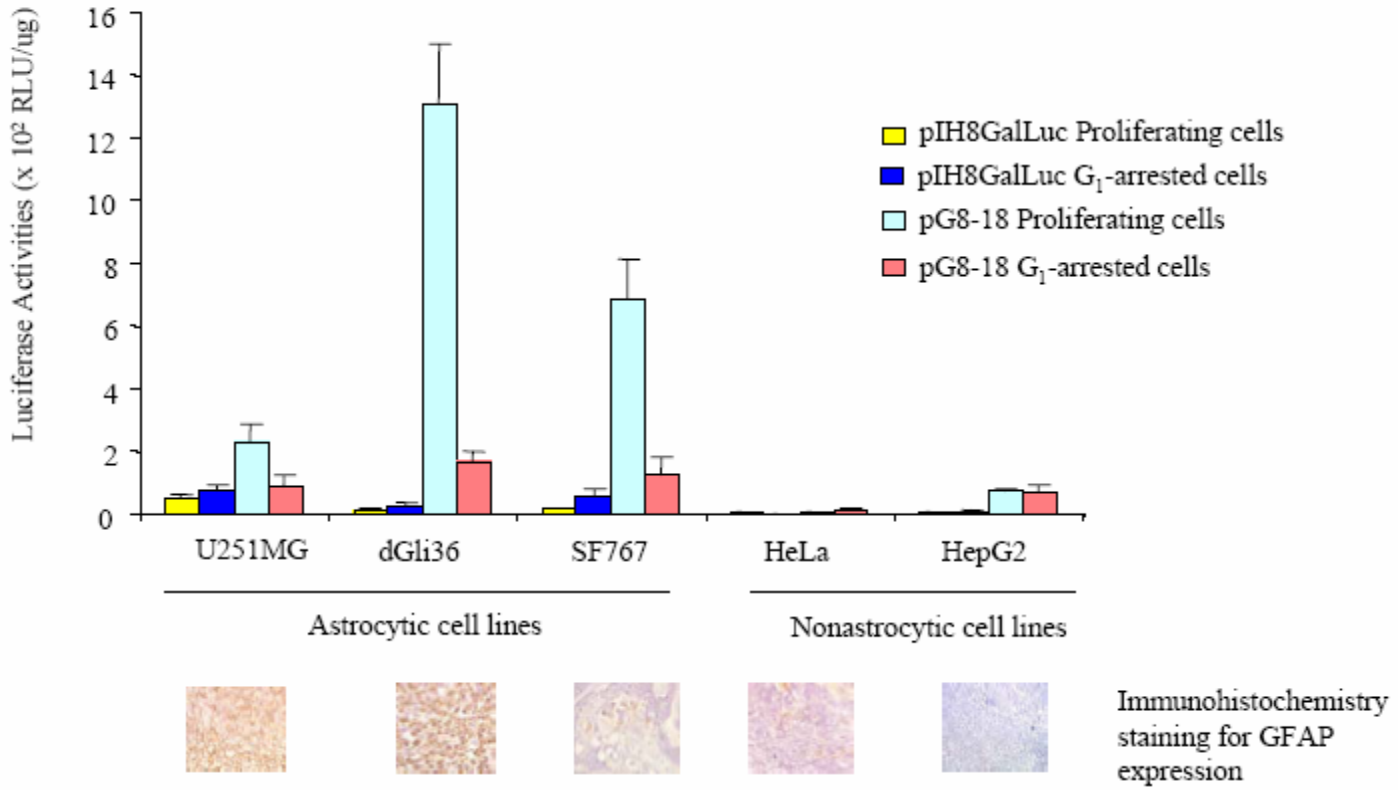

Figure 5.2. Glial cell-specific and cell cycle-regulated luciferase expression mediated by pG8-18 vectors in different tumor cells. Proliferation-dependent as well as glial-specific transgene expression was analyzed in pIH8GalLuc and pG8-18 (containing the three tandems GFAP enhancer repeats) transfected dGli36, U251, SF767, HepG2 and HeLa cells. Luciferase activities were determined 24 h and 48 h post-transfection for proliferating cells and G_1-arrested cells, respectively. Data shown are averages of triplicate $\pm$ SEM. Expression of GFAP was determined using immunohistochemisty staining in tumor tissues.

(a) dGli36

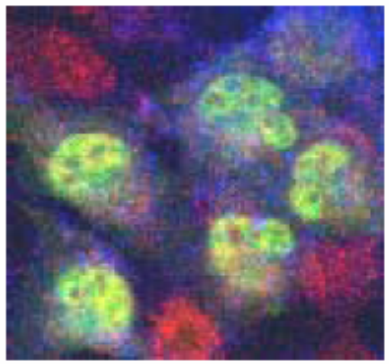

(b) HeLa

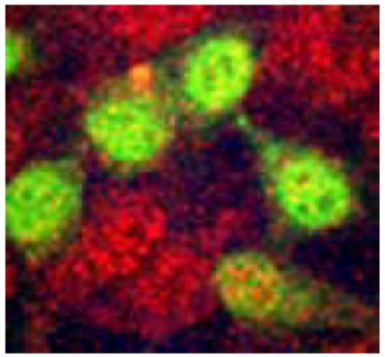

RED: cyclin A, indicating proliferating cells

GREEN: GFP, indicating infected cells;

BLUE: luciferase gene expression, indicating switching on of transgene expression

Figure 5.3. Luciferase expression is only observed in proliferating glial cells.
Immunofluorescence staining of cells infected by pG8-18 amplicon viral vectors are represented in (a) dGli36 and (b) HeLa cells. Both HeLa and dGli36 cells were actively proliferating, as indicated by the presence of endogenous cyclin A protein. Among these cells, only a proportion of cells was infected by pG8-18 amplicon viral vectors, as indicated by the expression of the exogenous green fluorescent protein. Luciferase expression (immunostained blue) could only be detected in proliferating cells infected by pG8-18 of glial origin.

dGli36 cells, as shown by the presence of exogenous eGFP expression, were positively stained for luciferase (blue) and endogenous cyclin A (red). In contrast, luciferase expression was not detected in proliferating but untransduced cells, as indicated by the absence of eGFP expression, and yet were positively stained for endogenous cyclin A. Most importantly, no luciferase expression could be detected in pG8-18 amplicon viral vector-infected HeLa cells (Figure 5.3b) even though the cells were clearly transduced by the viral vectors and were proliferating.

5.3.1.1 Cell type-specific and cell cycle-regulated transgene expression mediated by HSV-1 amplicon vectors in vivo

We further investigated the dual-specific regulation in an *in vivo* setting. A total of 2 x 10^6 TU of either pG8-18 or control pIH8GalLuc amplicon viral vector was administered intratumorally to immunodeficient animals harboring s.c. dGli36 tumor xenografts (~80-100 mm^3 in volume). Luciferase activity was found to be 10-fold higher (Figure 5.4a) in tumors injected with pG8-18 amplicon viral vector (3954 RLU/mg) rather than the control virus, pIH8GalLuc (380 RLU/mg). Similarly, luciferase activity was found to be 9-fold higher in dGli36-derived tumor (3954 RLU/mg) when compared with HeLa-derived tumor (440 RLU/mg) (Figure 5.4b). These results demonstrated that pG8-18 amplicon viral vectors could mediate transgene expression in a cell cycle- and cell type-specific manner *in vivo*.

5.3.1.2 Glial cell specific expression of FasL

To evaluate the efficacy of an apoptotic inducing gene in the context of HSV-1 amplicon viral vectors, the FasL gene was incorporated into pG8-18 to generate pG8-FasL. Human glioma dGli36 cells and nonglioma HeLa cells were infected with pG8-FasL at MOI of 1.0 (Figure 5.5). pIH8GalFasL vector was used as negative control. In section 4.3.2 (refer Figure 4.3b), we have shown that expression of FasL induced apoptosis in dGli36 cells by the presence of pyknotic nuclei. The percentage of apoptosis was determined using trypan blue exclusion assay at 72 h post-infection. In dGli36 cells infected with pG8-FasL, 50 % cytotoxicity was

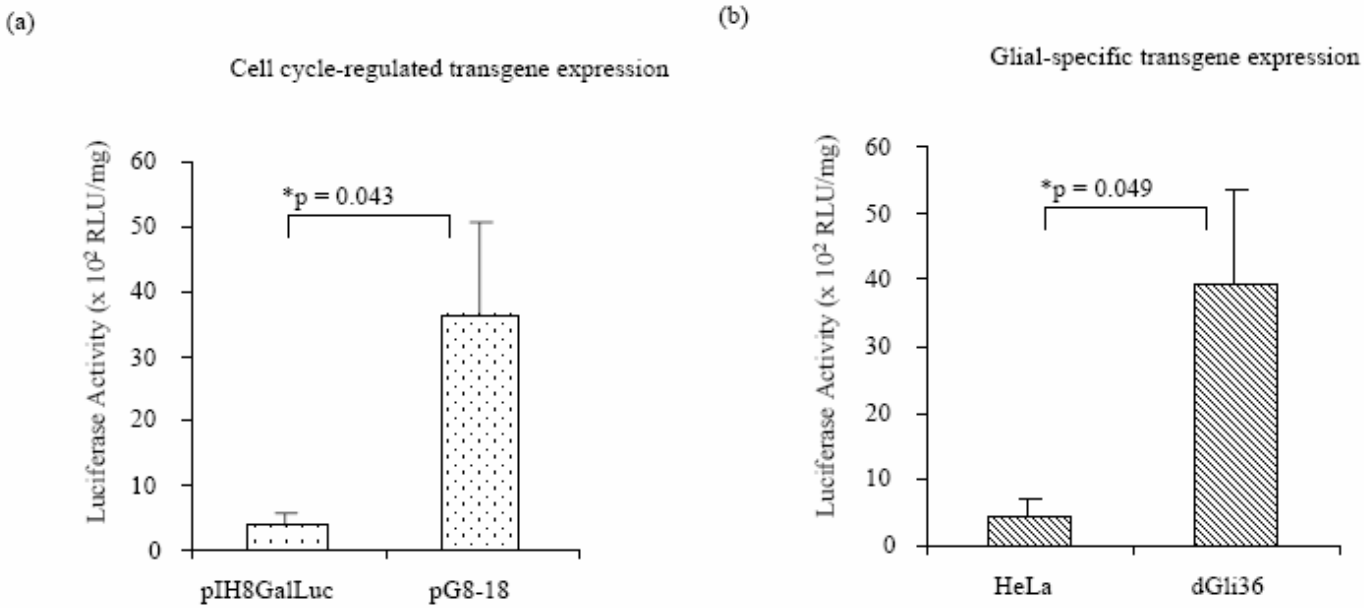

Figure 5.4. Cell cycle- and glial cell-specific transgene regulation mediated by HSV-1 amplicon viral vectors *in vivo*
(a) SCID mice harboring s.c. dGli36 tumor were injected with either pIH8GalLuc or pG8-18 amplicon virus vectors and analyzed for proliferation-dependent transgene via luciferase assay. (b) Glial cell-specific transgene regulation was analyzed in pG8-18 amplicon viral vector-transduced s.c. dGli36 and HeLa tumors. Luciferase expression for both experiments was determined 24 h post-infection. Data shown are averages of 5 mice ± SEM.

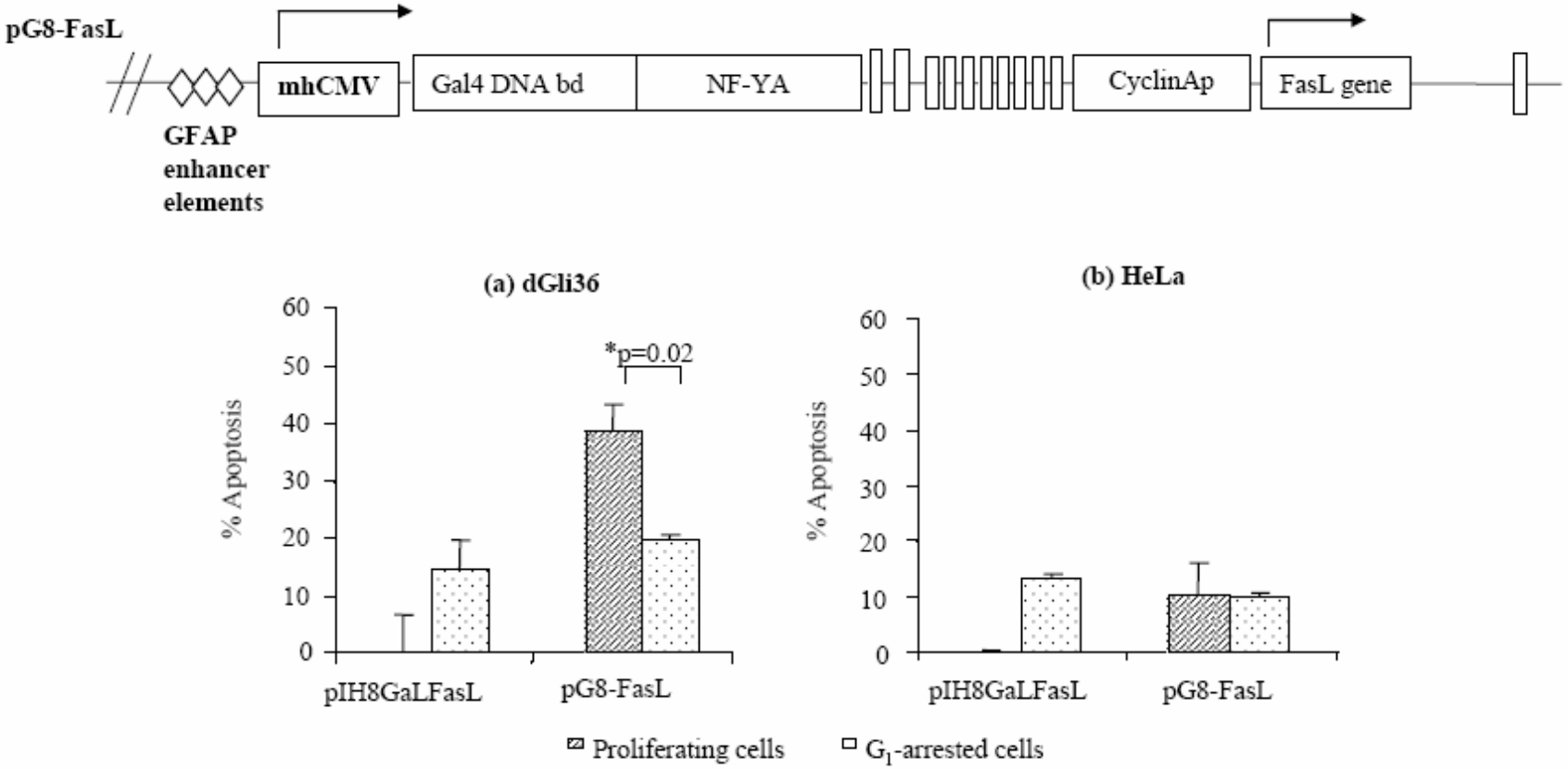

Figure 5.5. Cell death mediated by pG8-FasL vector is dual specific .
Proliferation-dependent as well as cell type-specific induction of apoptosis was determined in (a) dGli36 and (b) HeLa. Both dGli36 and HeLa were infected with pIH8GalFasL and pG8-FasL at MOI of 1.0. The apoptotic effect was measured as a reduction in cell viability 72 h post-transduction. Data shown are averages of triplicate experiments ± SEM.

observed in the proliferating populations compared with the G_1-arrested populations (p=0.02; Figure 5.5a). In contrast, no significant cell death was detected in pG8-FasL-transduced proliferating and G_1-arrested HeLa cells (Figure 5.5b) although the transduction efficiency for both cell lines is similar. To determine if the percentage of cell death observed is indeed due to the apoptotic effect of FasL, infected cells were examined for the level of FasL protein expression using ELISA assay. Our results showed that FasL expression in proliferating, pG8-FasL-transduced dGli36 cells was ~ 2.5-fold higher compared with that of the corresponding G_1-arrested cells (p=0.03). The level of FasL expression was similar to that of pG8-FasL-transduced HeLa cells; however, this did not correspond to the extent of apoptosis observed in the two cell lines (Figure 5.6). Taken together, the results suggest that cell death mediated by pG8-FasL is cell type-specific as well as cell cycle-regulated.

5.3.1.3 Suppression of tumor growth is observed in glioma only

The ability of FasL gene to suppress tumor growth has been demonstrated in pC8-FasL infected cells (refer section 4.3.7; Figure 4.9). In this section, the glioma specific expression of the FasL gene in suppressing tumor growth will be explored in SCID mice harboring either HeLa- or dGli36-SCID8-derived tumors on its right flank. The mice were divided into eight groups bearing either HeLa- or dGli36-SCID8-derived tumors, and injected with four different amplicon vectors, namely, pC8-36, pC8-FasL, pG8-18 and pG8-FasL. pC8-FasL was used as positive control; while pC8-36 and pG8-18 were negative controls. All mice were subjected to injection of viral vectors every ten days. At all time points when the tumor volumes were measured, the tumor sizes in both dGli36-SCID8 and HeLa injected with pC8-FasL vector were significantly smaller than the controls, pC8-36 (Figure 5.7). This indicated that the expression of FasL gene is able to suppress growth of both glioma and cervical carcinoma *in vivo*. In consensus with results observed from the *in vitro* studies (Figure 5.5), expression of FasL protein mediated by pG8-FasL could not inhibit the growth of HeLa cells *in vivo,* resulting in tumor volume similar to the controls injected with pG8-18 viral vectors (Figure 5.7b). In contrast, effective suppression of tumor growth was observed in mice

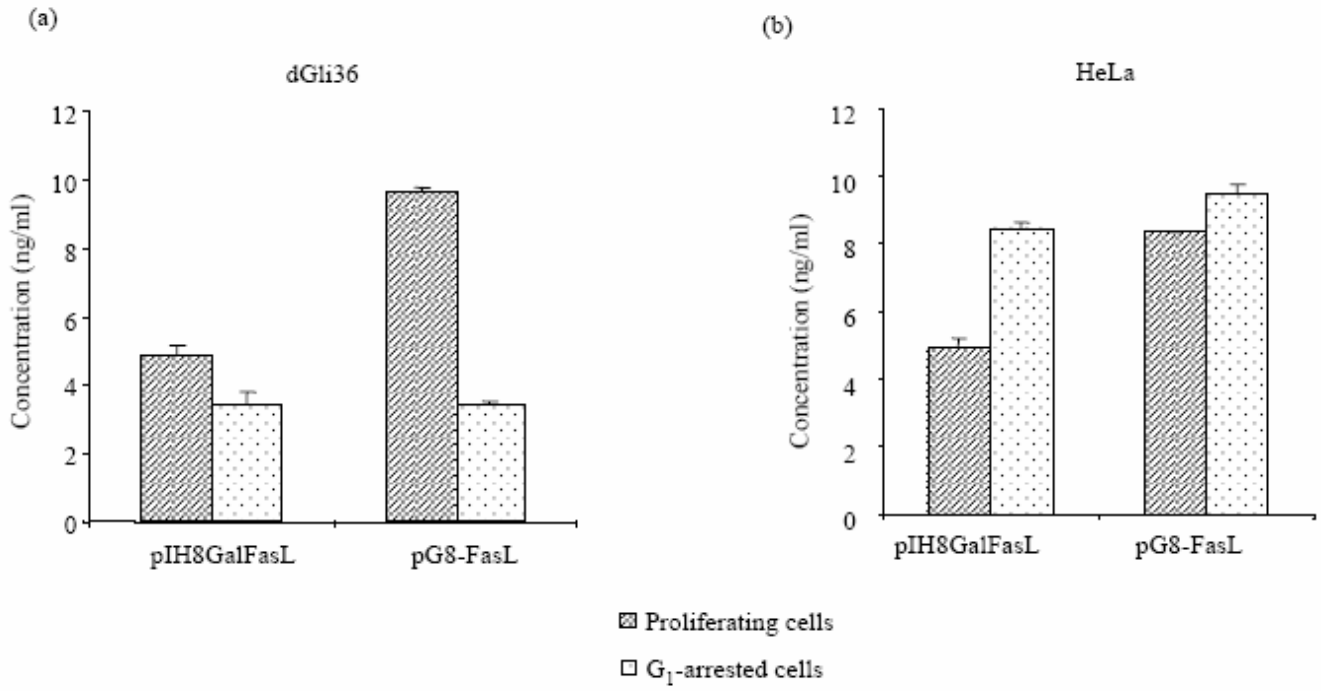

Figure 5.6. Expression of FasL is specific for proliferating glial cells
Proliferation-dependent as well as cell type-specific expression was determined in dGli36 and HeLa cells. Both dGli36 and HeLa cells were infected with pIH8GalFasLand pG8-FasL at MOI of 1.0. Value were normalized to cells alone. Data shown are averages of triplicate experiments ± SEM.

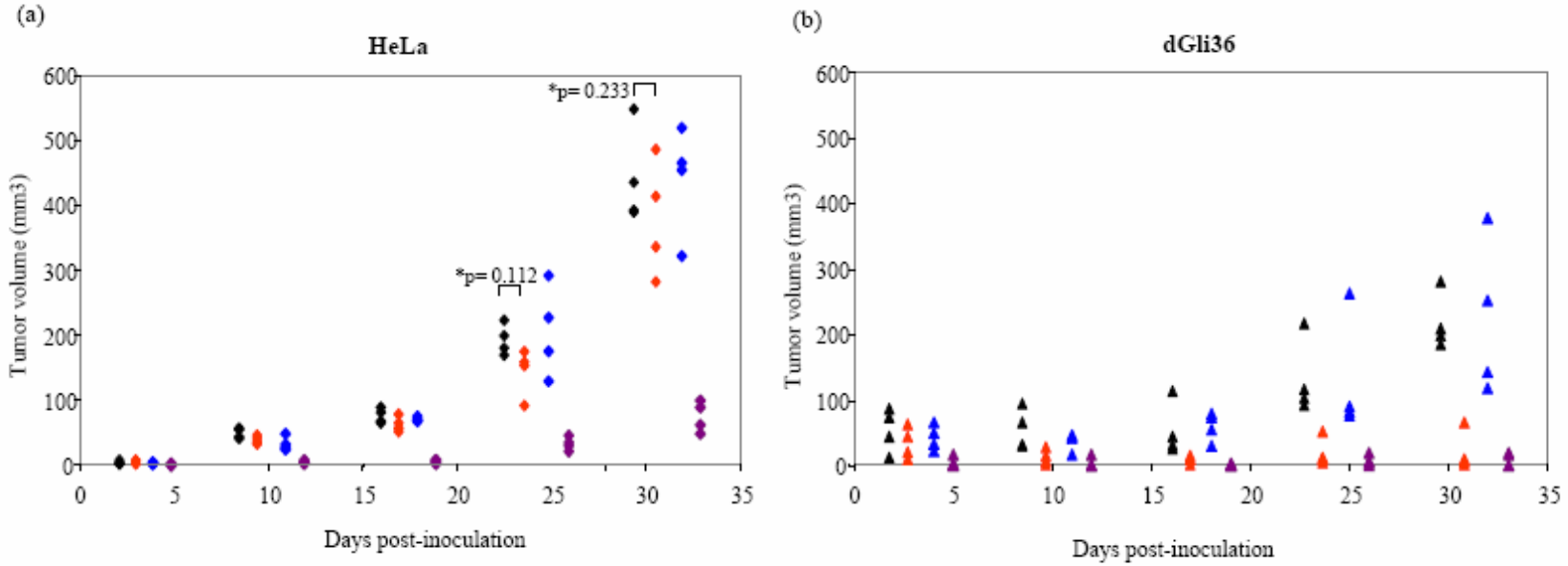

Figure 5.7 Expression of FasL mediated by pG8-FasL suppresses growth of glioma xenograft *in vivo*.
SCID mice harboring (a) HeLa or (b) dGli36 were injected with pC8-FasL, pC8-36, pG8-FasL and pG8-18 vectors. The effect of FasL was determined by measuring the tumor volume.

harboring human glioma xenografts and injected with pG8-FasL, which was significantly smaller than those injected with the pG8-18 vector (p=0.007; Figure 5.7a). The tumor volume in pG8-FasL-transduced-dGli36-SCID8 cells ranges between 0.0 mm^3 to 69.06 mm^3, whereas the tumor volume in pG8-FasL-transduced HeLa cells ranges between 282.52 mm^3 to 500.09 mm^3 during the final measurement. These results thus demonstrated that cell death mediated by FasL is specific for tumor of glial origins.

The effect of FasL overexpression was also investigated in an intracranial tumor model. We have previously demonstrated that the cell cycle-regulation of the vector is dependent on the input viral dosage (refer section 3.3.12; Figure 3.15). To maximize the effect of the therapeutic gene, dGli36 cells were infected with pG8-FasL at MOI of 2.0, to achieve infectivity of approximately 98 % by FACS analysis (data not shown). TUNEL staining indicated that none of the transduced cells (Figure 5.8a, part i) are apoptotic at the time of tumor implantation (Figure 5.8a, part ii). The transduced cells were then implanted stereotactically into the right hemisphere [bregma (0,0); lateral 2mm; depth 2.5 mm] of immunodeficient nude mice. pG8-18-infected-dGli36 cells were used as negative controls. We observed that the median survival time for FasL-injected mice was longer than that of the pG8-18-infected group. The median survival time for mice injected with pG8-18 is 8 days compared with 27 days in the pG8-FasL-infected group (Figure 5.8b). This difference is survival time is statistically significant when examined by Kaplan-Meier survival analysis, p=0.042 by log-rank, thus indicating that expression FasL gene is sufficient to induce an anti-tumor response in an intracranial glioma model.

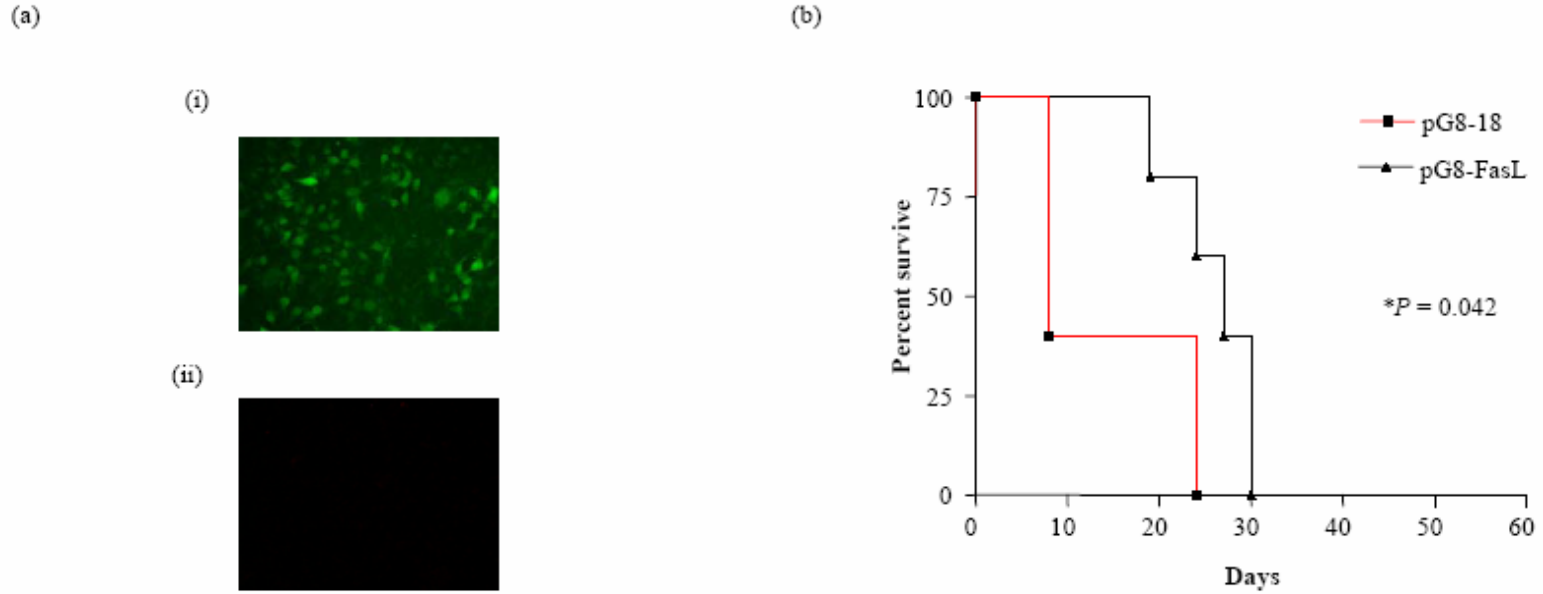

Figure 5.8 Expression of FasL prolonged the survival of mice harboring i.c. dGli36 tumor.
(a) (i) pG8-FasL-transduced cells as indicated by the expression of GFP. (ii) TUNEL assay indicates the absence of apoptotic cells prior to tumor-implantation. (b)pG8-18- and pG8-FasL-infected dGli36 cells were stereotactically inoculated into the right hemisphere of 6-week old nude mice (n=5). The effect of FasL was determined by measuring the percentage of survival at different time points. Survival curve was generated using Kaplan-Meier survival analysis.

5.3.1.4 Effect of TMZ on dGli36 human glioma cells

5.3.1.4.1 TMZ caused accumulations of cells at G2/M phase

The effect of TMZ on dGli36 cells was assessed at 24 h and 48 h following treatment with TMZ at various concentrations (25 μM, 50 μM, 75 μM, and 100 μM). Only minor cell death was observed at the varying concentrations with respect to the untreated control (data not shown). After 24 h of treatment, we noticed that more cells accumulated at the G_2/M phase in cells treated with 75 μM of TMZ (Figure 5.9), which is in agreement with a published report stating that cells treated with TMZ arrest at the G_2/M phase (Kanzawa et al., 2003). The percentage of G_2/M cells treated with 75 μM of TMZ after 48 h increased to approximately 40 %, with a reduction in both the G_0/G_1 and S phase (Figure 5.9). Since the effect of TMZ at 75 μM after 48 h of treatment is much stronger than 100 μM, this concentration was chosen for subsequent experiments.

5.3.1.4.2 Effect of TMZ on transgene expression mediated by pG8-18 in dGli36 cells

To determine whether luciferase gene expression can be activated in TMZ-treated cells, dGli36 was first treated with 75 μM of TMZ for 1 h, followed by infection with pG8-18 at MOI of 1.0 and pIH8GalLuc vector after 48 h. At the time of infection (48 h post-TMZ treatment), the percentage of S phase cells was approximately 40 %, which is similar to the untreated but transduced-dGli36 cells, and the percentage of G_2/M cells is approximately 50 %. Luciferase expression was analyzed 24 h post-transduction. No significant difference in luciferase expression could be detected between the asynchronized untreated pG8-18-transduced cells (1831.1 RLU/μg) and the TMZ-treated cells (1468.4 RLU/μg) ($p=0.38$; Figure 5.10a), suggesting that the effect of TMZ on transgene activities conferred by pG8-18 is minimal.

To mimic the clinical scenario, dGli36 glioma cells were first infected with either pG8-18 or pIH8GalLuc amplicon vector. After 6 h of infection, a portion of the cells was treated with 75μM of TMZ for 1 h at 37 °C, followed by incubating in fresh complete medium for another

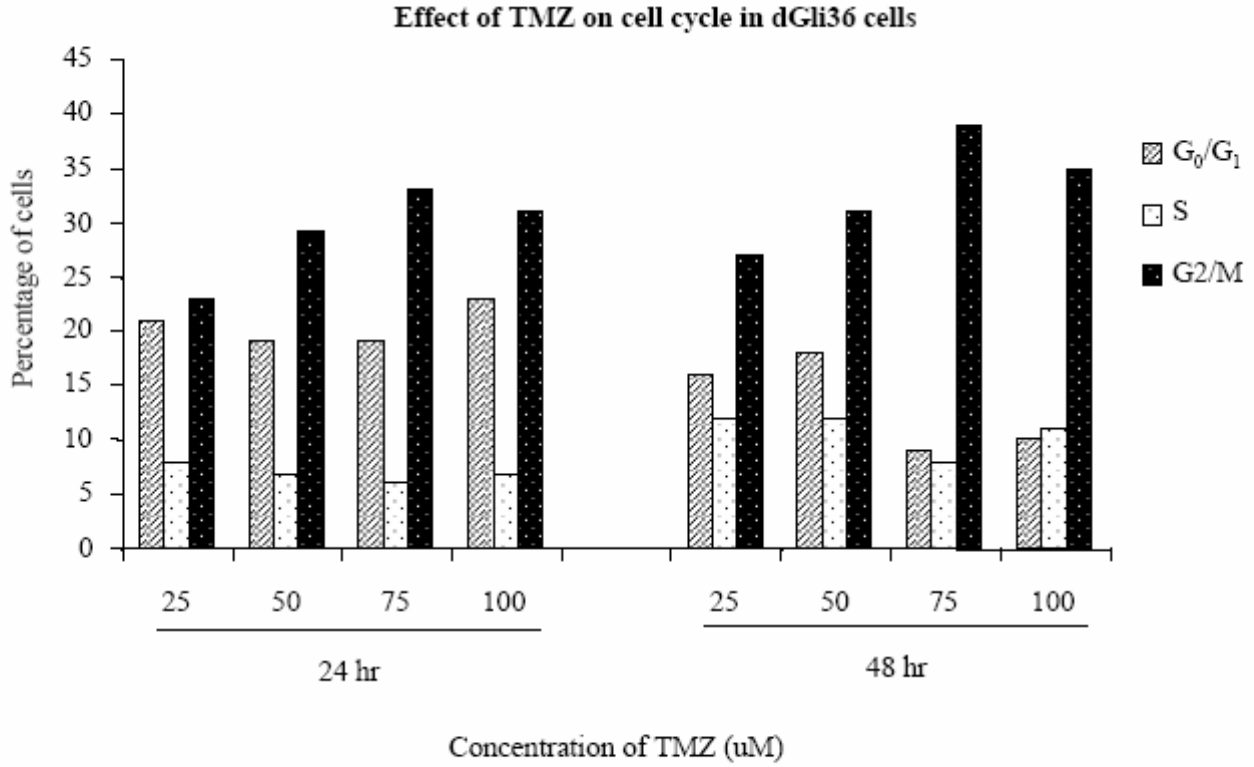

Figure 5.9 Effect of TMZ on cell cycle was analyzed in dGli36 cells.
dGli36 cells were treated with TMZ for 1 h. Fresh complete medium was replenished and the cells were cultured for either 24 h or 48 h. Cells were analyzed by flow cytometry and the cell cycle profile was generated using Modfit cell cycle software.

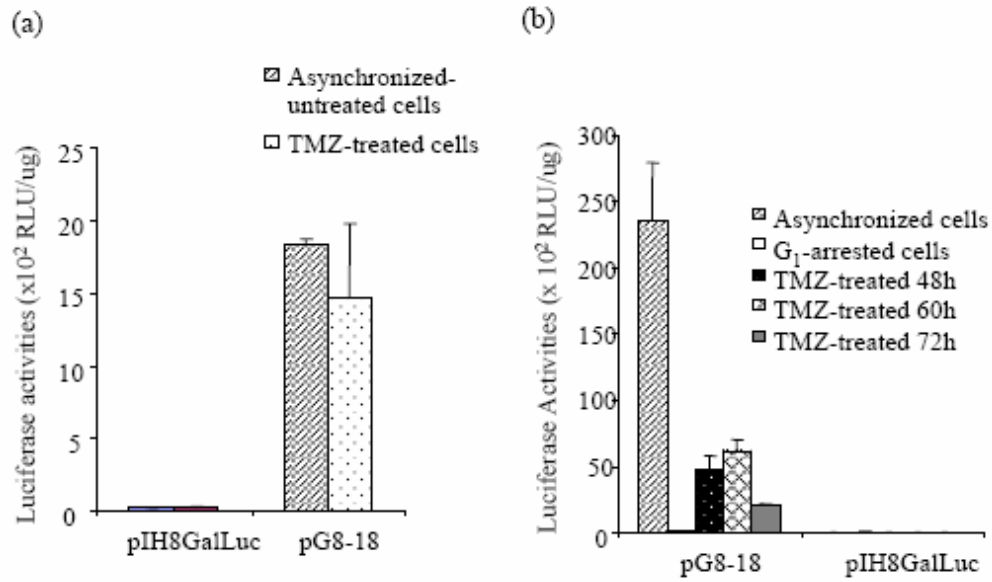

	G_0/G_1	S	G_2/M
Asynchronized	47	29	24
G_1-arrested	83	12	6
TMZ 48h	9	61	30
TMZ 60h	16	30	54
TMZ 72 h	22	28	50

Figure 5.10 Effect of TMZ on luciferase expression mediated by pG8-18
(a) dGli36 cells were treated with TMZ, after 48 h, the cells were infected with either pIH8GalLuc or pG8-18. Luciferase expression was measured after 48 h. (b) dGli36 cells were infected with either pG8-18 or pIH8GalLuc vector for 6 h prior to treatment with TMZ. Cells were treated with TMZ for 48 h, after which a portion of the treated cells was harvested for analyzing the luciferase expression. The other two portions were replenished with fresh medium without TMZ and harvested at 60 h or 72 h post-TMZ treatment for analyzing the luciferase activities. As comparison, luciferase gene expression was also analyzed in proliferating cells and G_1-arrested cells (treated with lovastatin). The cell cycle profile of TMZ treatment in pG8-18 transduced cells at the respective time points are indicated in the table.

48 h, 60 h, and 72 h. For comparison purposes, vector transduced-cells were also incubated in the presence of fresh complete medium for asynchronized cell populations; and treated with lovastatin to induce G_1-arrest. Luciferase activities were compared with those transduced with the control vector, pIH8GalLuc. Luciferase activities can be detected in all cells treated with TMZ, with the level of expression highest at 60 h post-treatment (6178.1 RLU/μg) (Figure 5.10b). Approximately 54 % of the cells are in the G_2/M phase of the cell cycle at this particular time point. These two experiments demonstrate that luciferase expression can be activated in proliferating glioma cells that are treated with chemotherapeutic drugs.

5.3.1.5 In vivo stability of the dual specific amplicon vector

The presence of the viral DNA and the expression of luciferase reporter gene at different time points post-injection were studied to determine the stability of pG8-18 amplicon viral vector *in vivo*. dGli36 human glioma cells were implanted via stereotactic injection into the brain of SCID mice at the right hemisphere, followed by inoculation of the pG8-18 amplicon viral vector into both hemispheres. To determine the stability of the viral vector, the mice were sacrificed on 4 days, 10 days and 28 days postinoculation, and the brains were harvested for PCR analysis as well as luciferase reporter gene assay.

Viral DNA was extracted from both the tumor bearing region and the normal brain (left side) of mice injected with pG8-18 amplicon viral vector. PCR analysis was performed to amplify the exogenous luciferase gene encoded on pG8-18. 18S rRNA was used as an internal control, luciferase cDNA were employed as the positive control, while uninfected mouse brain as the negative control. Vector DNA, as determined by the presence of the luciferase gene, was detected at 4 days, 10 days and at least 28 days after transduction in both the normal and the tumor bearing region (Figure 5.11). However, luciferase protein expression is only detectable at day 4 and day 10 post-injection (Figure 5.12a). By day 28, the level of luciferase protein expression has significantly reduced, although GFP is still detectable (Figure 5.12b).

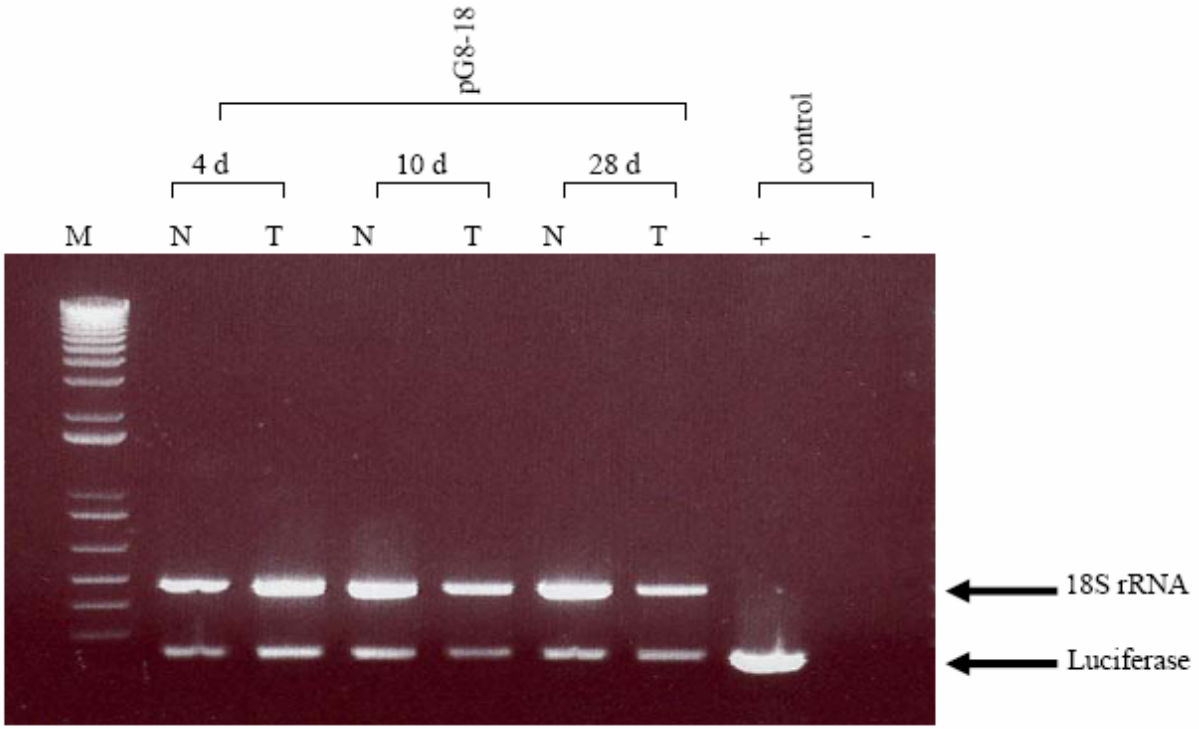

Figure 5.11 Stability of pG8-18 amplicon viral DNA *in vivo*.
Prior to inoculation of pG8-18 amplicon viral vector, immunodeficient mice were implanted with dGli36 tumor on the right hemistphere of the brain. The next day, 1 x 10^6 TU of pG8-18 vectors were inoculated to both the right side (T) and the left side (N) of the brain. At days 4, 10 and 28, the brains were harvested and Hirt's DNA was extracted for PCR analysis.

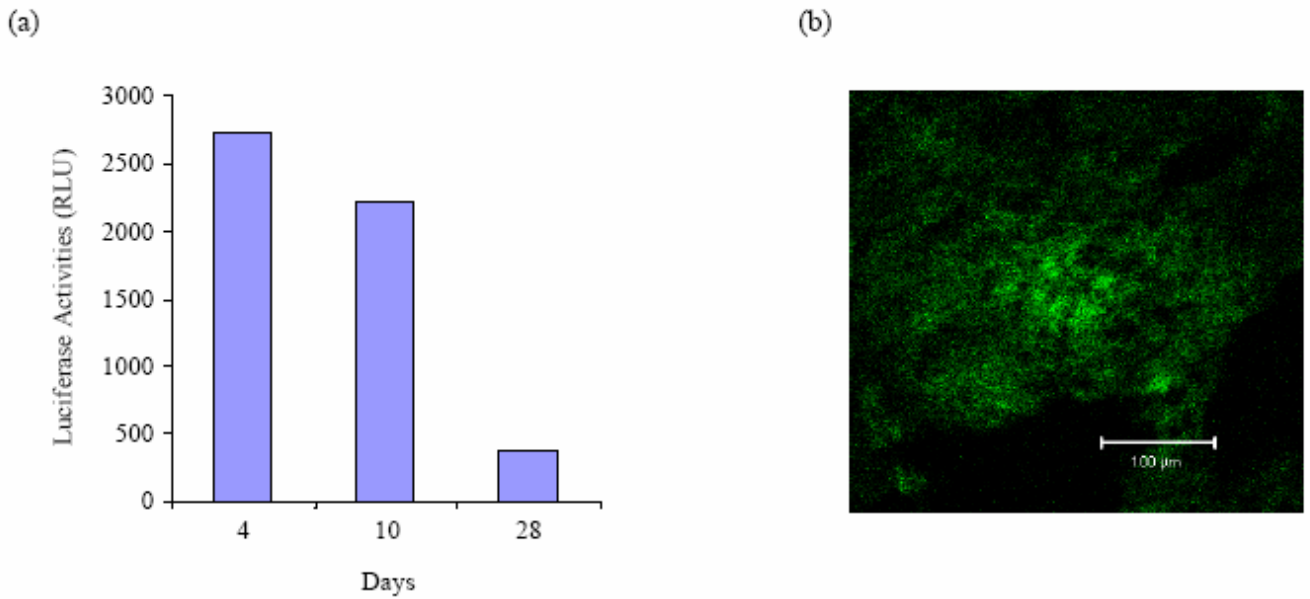

Figure 5.12 Stability of luciferase expression mediated by pG8-18 amplicon vector *in vivo*.
(a) Luciferase expression at day 4, 10 and 28 were analyzed. Data represents luciferase expression from the tumor region of the brain, i.e. right hemisphere. (b) GFP expression was detectable on day 28.

5.3.1.6 Transduction efficiency in vivo

To determine the percentage of transduced cells, pC8-36 and pG8-18 amplicon vectors were injected via stereotactic injection into the right side of the brain of normal mice. Twenty four hours following transduction, the mice were sacrificed and brains were harvested. Single cell suspensions were collected and the percentage of GFP positive cells in brains injected with pC8-36 and pG8-18 were determined to be 25.3 % $\pm$ 2.02 and 17.83 % $\pm$ 6.99, respectively (Figure 5.13). To confirm these findings, the experiment was repeated similarly in another group of mice. This time, the surface area of GFP positive cells in representative cryosections of brains injected with viral vectors was determined using confocal microscopy. The area of dispersion is determined by measuring the total surface area of each brain section (10 μm sections) positive for GFP expression (Table 5.1). The total area of dispersion is the sum of the GFP positive areas in all GFP positive sections. Therefore, the total surface area of GFP positive cells transduced by pC8-36 was determined to be 58.7 mm^2, and pG8-18 was 43.3 mm^2. By taking into account the thickness of each represented section, the volume of viral-transduced region was then calculated. Given that the volume of a 4-6 week old SCID mouse brain is approximately 358 mm^3, this would translate to a transduction efficiency of 16.4 % for pC8-36 and 12 % for pG8-18 (Table 5.1). The variation of ~6 % between the two methods may be due to the estimation involved in the latter approach when only representative cryosections were taken into account. Nevertheless, pC8-36 viral vectors exhibit higher transduction efficiency *in vivo* compared to pG8-18 viral vectors.

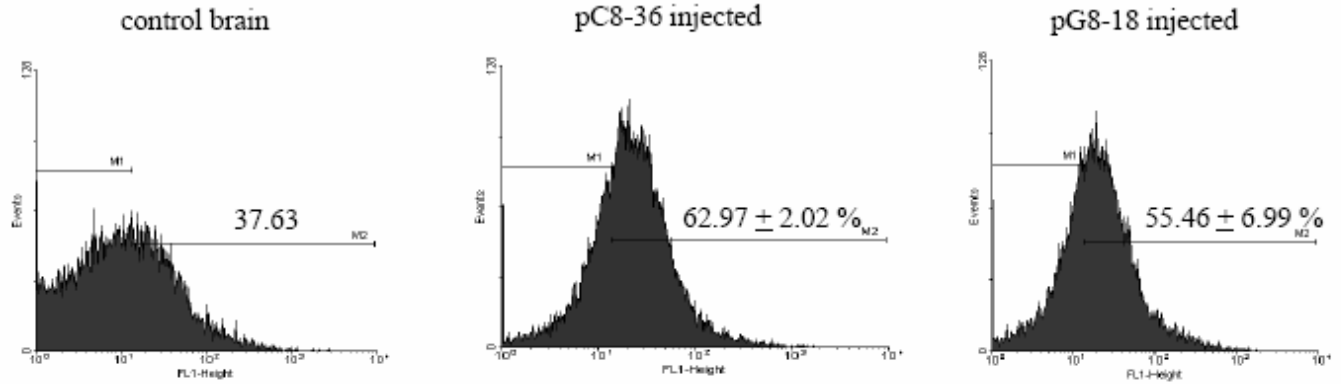

Figure 5.13 Transduction efficiency of pC8-36 and pG8-18 amplicon viral vectors *in vivo*.
Immunodeficient mice were inoculated with 1 x 10^6 TU of pC8-36 and pG8-18 amplicon vectors. The brains were harvested 24 h post-inoculation and single cell suspensions were acquired. The percentage of GFP positive cells was determined by FACS analysis.

Table 5.1. Determination of transduction efficiency of amplicon viruses *in vivo*

pC8-36	**Total number of slides**	**Total thickness (µm)**	**Surface area (µm)**	**Vol ($µm^3$)**	**Vol (mm^3)**
Slide 25-28	4	40	17502.79	700111.6	
Slide 29-32	4	40	118833	4753321.2	
Slide 33-38	6	60	118833	7129981.8	
Slide 39-42	4	40	329687.5	13187500	
Slide 43	10	100	329687.5	32968750	
Slide 46	1	10	6411.9	64119	
				58803783.6	**58.80**
pG8-18					
Slide 14-19	5	260	7652.18	1989566.8	
Slide 20-24	5	260	24657.61	6410978.6	
Slide 25-28	4	210	24657.61	5178098.1	
Slide 29-32	4	210	20895.96	4388151.6	
Slide 33-42	10	466.7	20895.96	9752144.53	
Slide 42-52	11	513.37	30240.09	15524355	
				43243294.6	**43.24**

5.3.1.7 Assessing the immunogenicity of the cell cycle-regulated vector

The cell cycle-regulated vectors contain transcriptional elements from the yeast Gal4 protein and the mouse NF-YA, which may generate antigenic peptides that might induce an immune response following *in vivo* gene transfer. Determination of the immunogenicity of these vectors is therefore important. We employed the AdGFP vector as positive control since recombinant Ad has been known to elicit immune response.

In order to have a fair comparison between the HSV-1 amplicon vectors and the positive control, AdGFP, the virus titer that gave similar percentage of infected cells by both viruses was predetermined by infecting permissive cell line, HeLa. The percentage of infectivity of AdGFP that is comparable to MOI of 1 of the HSV-1 amplicon vector was determined. HeLa cells (5×10^4) were infected with pC8-36 amplicon vector at MOI of 1.0. The transduction efficiency of pC8-36 at MOI of 1 was compared with MOI of 10, 10^2, 10^4, 10^6 and 10^8 pfu of AdGFP by analyzing for the percentage of GFP positive cells using FACS analysis. After incubating the viral supernatant with the cells for 6 h, the monolayer was washed once with PBS and replenished with complete medium containing 10 % serum. Twenty four hours post-infection, HeLa cells were harvested and the percentage of GFP positive cells was determined by FACs analysis. As shown in Table 5.2, the percentage of GFP in AdGFP infected cells at MOI of 10^2 (39 %) is approximately similar to that of pC8-36 infected cells (21 %).

Table 5.2: Comparison of percentage of GFP positive cells in both HSV-1 amplicon viral vectors infected and AdGFP infected HeLa cells.

Viral vectors	**% GFP**
pC8-36 MOI of 1.0	21
AdGFP 10^6	~ 95
AdGFP 10^4	69
AdGFP 10^2	39

The immunogenicity of pG8-18 amplicon vector was determined in immunocompetent mouse model. Six weeks old Balb/C mice were injected with the viral vector with comparable titers via stereotactic injection into the right brain [bregma (0, 0); lateral 2mm; depth 2.5 mm]. Saline injections were used as negative control, and AdGFP were used as the positive control. All mice were sacrificed either 1-day or 4-day post-transduction. The presence of innate immune response was determined by immnohistochemistry staining for the presence of T lymphocytes (CD4 and CD8) and microglia (CD11b) infiltration. On 1-day post inoculation, all injections induced inflammatory response due to the transient disruption of the BBB. CD4-, CD8- and CD11b-positive cells were observed in all animals injected with AdGFP, saline, pC8-36 and pG8-18 (Figure 5.14). On day 4, the expression levels of the CD4 and CD8 T lymphocytes in both pC8-36- and pG8-18-injected mice were comparable to that of the saline-injected mice (Figure 5.14). Similar results were observed in CD11b microglial infiltration. In contrast, mice injected with AdGFP elicited an enhanced immunologic response and microglia infiltration even on day 4 when compared to the saline-injected control. These results suggested that both pC8-36 and pG8-18 amplicon viral vectors packaged using the helper virus-free packaging system exhibited low immunogenicity and non-cytotoxicity.

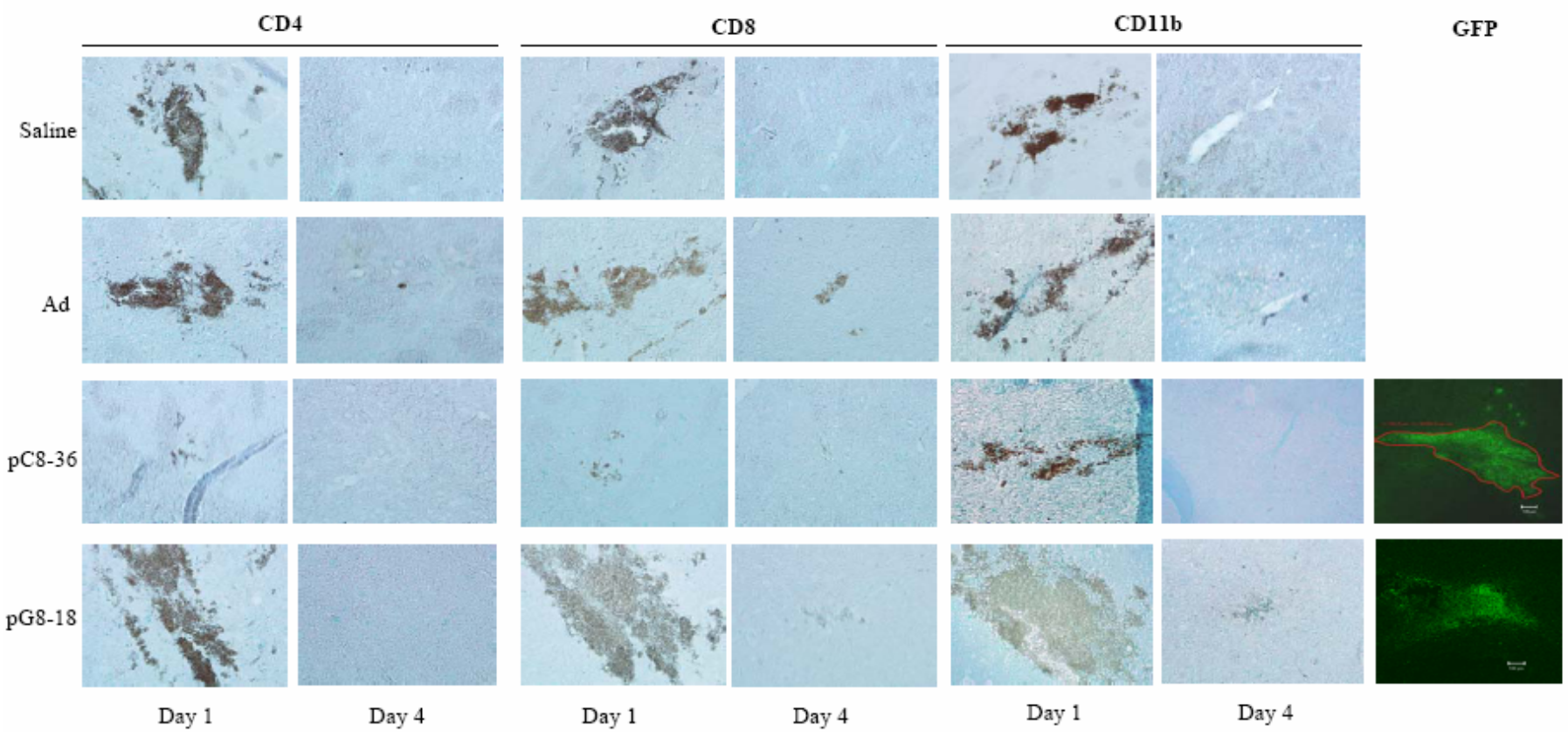

Figure 5.14 Immunogenicity of pC8-36 and pG8-18 amplicon viral vectors.
Balb/C mice were injected with 1 x 10^4 TU of pC8-36 and pG8-18 amplicon viral vectors, 1 x 10^2 pfu AdGFP and 10 µl saline, in the right brain. One day and 4 days post-injection, the brains were harvested, fixed and cryosectioned. Induction of immune response was detected using antibodies against CD4, CD8 and CD11b. GFP pictures indicate areas that were injected with the viral vectors.

5.3.2 Identification of glioma specific peptide

5.3.2.1 Enrichment of "glioma-specific" phage by in vitro biopanning

The Ph.D-12 phage display library, with a complexity of approximately 2 x 10^9 sequences, was employed for screening peptides that would bind specifically to human glioma cells. This library consists of 12-mer peptide sequences fused to the N terminus of the minor coat protein of the M13 phage, in a valency of 5 copies per virion. The library was screened against a mixture of human glioma cell lines including dGli36, SF767, U87MG, U251MG, and U373MG at 37 °C to increase the probability of obtaining sequences that could interact generically with most glioma cells (Figure 5.15). Phages rescued were further subjected to negative panning using nonglioma cell lines A549, CNE2, and HepG2, to eliminate nonspecific background binding (Figure 5.15). The amino acid sequences of the 79 phage clones obtained after such a selection revealed several dominant sequence motifs (Table 5.3). The sequence SGHQLLLNKMPN, designated MG2, was found in 24 % of the clones; and LWATFPPRPPWL, designated MG11, was found in 19 % of the clones (Table 5.3). A BLAST search of MG2 demonstrated 60 % sequence homology with the human mitogen-activated protein kinase kinase kinase 12 (MAP3K12). MAP3K12 was found to be highly expressed in brain and kidney, and has been implicated as an activator of the JNK/SAPK pathway (Su and Karin, 1996). Analysis of the second most frequently isolated phage-bearing peptide sequence, designated MG11, showed it to be 64 % homologous to semaphorin 4B precursor protein. Semaphorin 4B is a member of the semaphorin superfamily, which is involved in the inhibition of axonal extension by providing local signals to specify territories inaccessible for growing axons (Rieger et al., 2003). In addition to phage-bearing the MG11 peptide sequence, we have also isolated two other phage clones harboring peptide sequences that match to the semaphorin family of proteins. One of the sequences, HHGHSPTSPQVR, matches perfectly to the protein sequence of semaphorin 3A precursor protein, whereas the other peptide sequence, LPYGTSNRHAPV, showed 64 % homology with semaphorin 6B precursor protein. Semaphorin 3A, which binds with high affinity to neurophilin-1, induces the collapse and paralysis of neuronal growth cones.

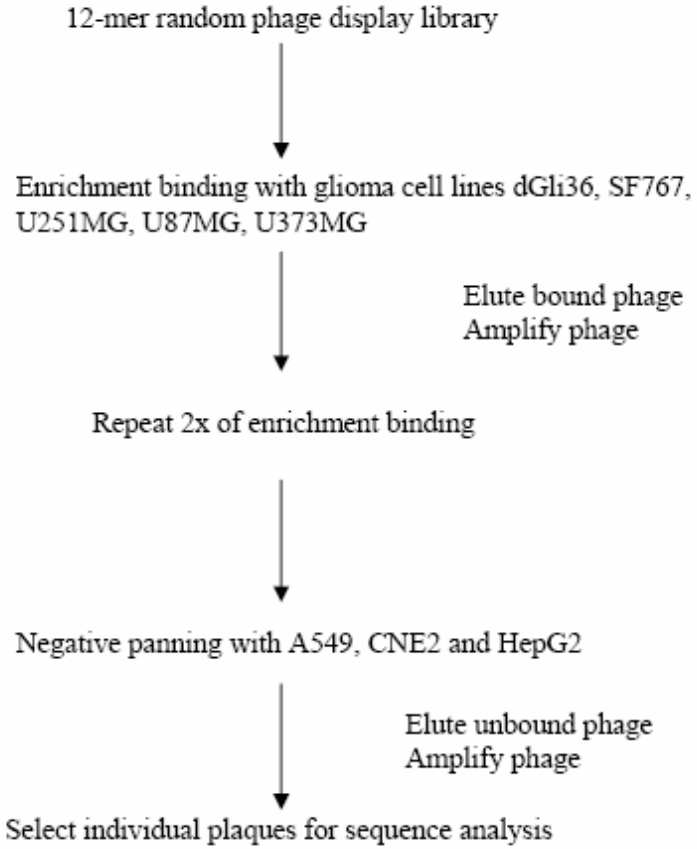

Figure 5.15 Biopanning of glioma targeted phage

Table 5.3. Lists of peptides isolated from biopanning of human glioma cell lines.

	Sequences	Frequency of occurrence	Homology to known human proteins	Alignment	% homology
1	SGHQLLLNKMPN (MG2)	24%	Mitogen-activated protein kinase kinase kinase 12	* *** ** [c] Db[a] 599 HDLLLRKMSS 608 Qy[b] 3 HQLLLNKMPN 12	60
2	LWATFPPRPPWL (MG11)	19%	Semaphorin 4B precursor	* ***** * Db 11 WGALPPRPPLL 21 Qy 2 WATFPPRPPWL 12	64
3	WSAAPTKPPYHT	6%	Voltage-dependent L-type calcium channel alpha-1D subunit	* * *** Db 1981 WATPPATPPYR 1991 Qy 1 WSAAPTKPPYH 11	46
4	ILANDLTAPGPR	5%	None		
5	HHGHSPTSPQVR	4%	Semaphorin 3A precursor	****** Db 575 HHGHSP 580 Qy 1 HHGHSP 6	100
6	LPYGTSNRHAPV	4%	Semaphorin 6B precursor (Sema Z)	**** * ** Db 435 LPYGGADRTAP 444 Qy 1 LPYGTSNRHAP 11	64
7	YVQGWNYHDLTR	4%	None		
8	LWAAFPPQASVA	4%	Synaptojanin 1	****** * Db 1245 AAFPPQSSLP 1254 Qy 3 AAFPPQASVA 12	70
9	FDTPHTLTWFHG	3%	None		

(a) Db represents sequence from database. (b) Qy is the query sequence from phage. (c) "*" represents identical amino acid.

Neuropilin-1 is a receptor for the vascular endothelial growth factor family and has been implicated in blood vessel formation. It also functions as a co-receptor with the Flk-1/KDR receptor tyrosine kinase (Gluzman-Poltorak et al., 2000). We noticed that several groups of the peptides selected are homologous to members of the semaphorin superfamily. It has been previously reported that the semaphorin family of proteins play important roles during neural development (Rieger et al., 2003; Schumacher et al., 2002), because MG11 is the most common sequence identified among the group of phages isolated, MG11 was thus chosen for subsequent studies.

5.3.2.2 Characterization of the binding epitopes of MG11 phage in vitro

To determine whether MG11 phage binds specifically to glioma cells, tumor cell lines of various histotypes were incubated with the phage. These include dGli36, SF767, U87MG, U251MG, U373MG, and T98G glioma cells, and A549, CNE2, HeLa, HepG2, KOSC-3, KZ2, and WT18 nonglioma cells as shown in Figure 5.15. The efficiency of MG11 phage binding to glioma cells (range, from 2 x 10^6 to 2.2 x 10^7 pfu/ml) was at least 3-fold higher than that of nonglioma cells (Figure 5.16). None of the nonglioma origin tumor cell lines tested exhibited considerable binding (range, from 1.5 x 10^4 to 9.6 x 10^5 pfu/ml). Thus, the *in vitro* phage binding assay indicated that MG11 phage binds specifically to glioma cells.

5.3.2.3 MG11 phage targets to human glioma xenograft in vivo

To determine whether phage bearing the MG11 binding motif can target specifically *in vivo* to human glioma xenografts, 10^{12} pfu MG11 phage was injected via tail vein to immunodeficient SCID mice harboring s.c. dGli36-derived glioma xenograft. Recovery of phage particles from tissues as well as xenografted dGli36 tumor indicated that MG11 phage is specific for tumor only (7.94 x 10^4 pfu/mg), whereas other tissues including brain, heart, kidney, liver, lung, and spleen gave only background binding (Figure 5.17). Minimal binding was observed in all tissues when control unselected phage was employed (Figure 5.17). The tumor specificity of MG11 was also examined by administering MG11 phage via tail vein to

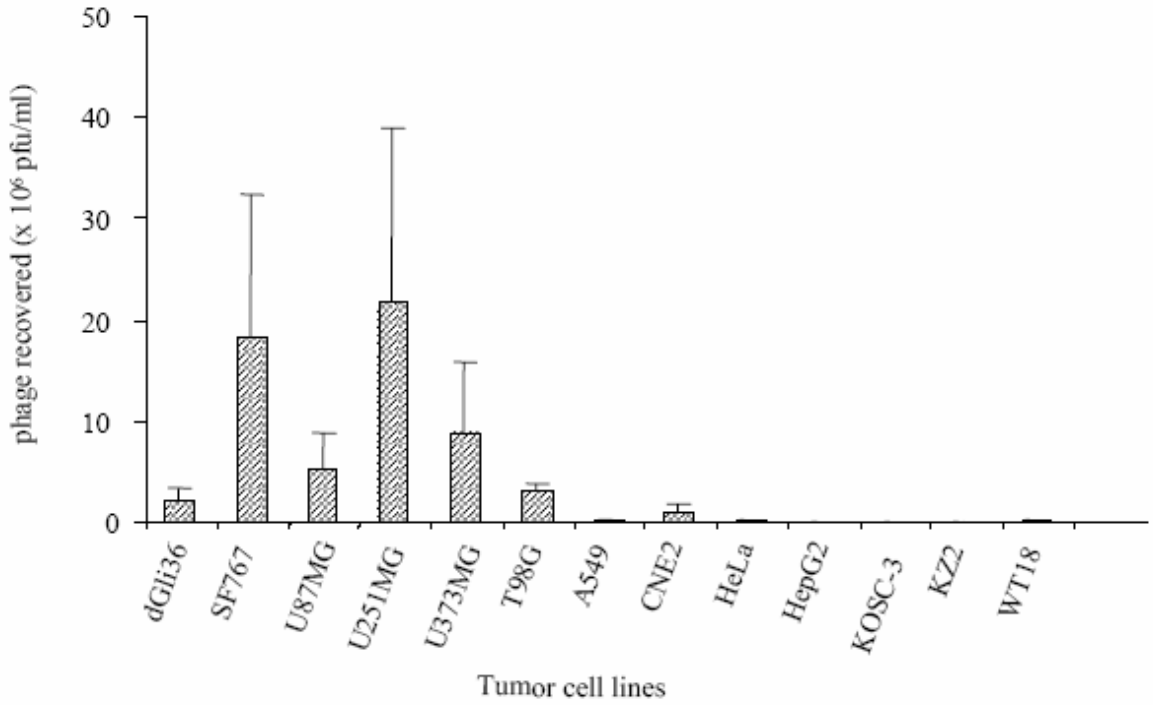

Figure 5.16 *In vitro* specificity of MG11 phage to a panel of human glioma cell lines.
Tumor cell lines of various origins were incubated with 10^{12} pfu/µl of MG11 phage at 37° C for 2 hours. Mean value for phage recovered from the binding assay and the SEM from triplicate experiments are shown.

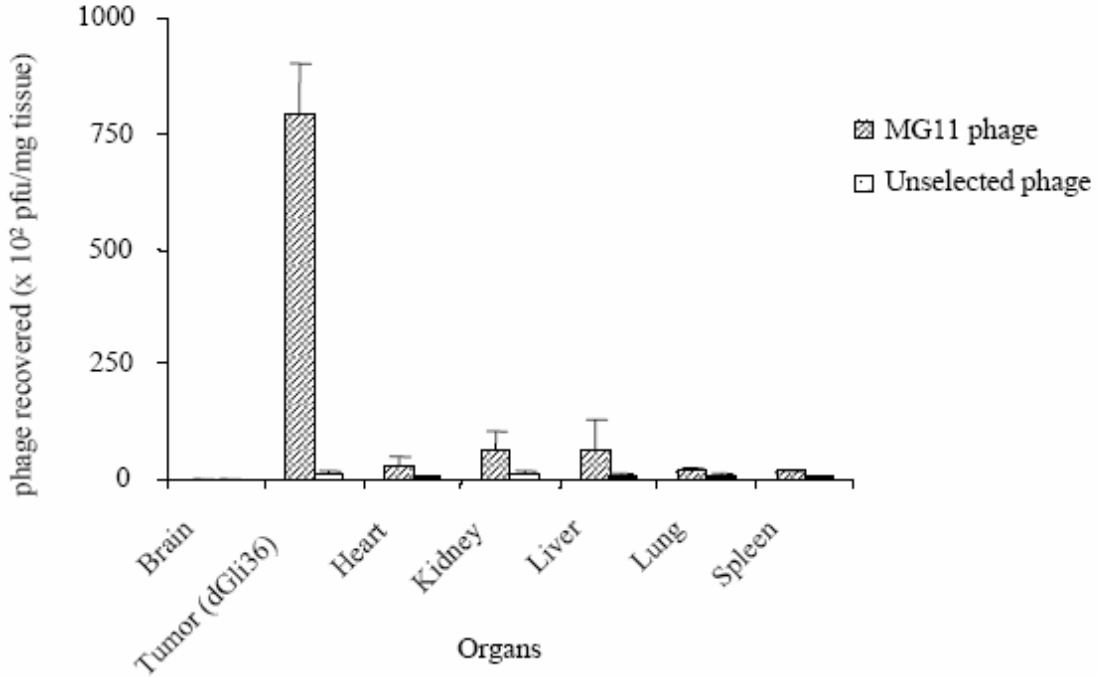

Figure 5.17 *In vivo* targeting of MG11 phage to glioma cells.
Binding of MG11 phage to different tissues was analyzed and compared with those injected with the unselected control phage.

immunodeficient mice bearing s.c. glioma xenograft (dGli36) and nonglioma xenograft (CNE2) on the right and left hind thigh, respectively. The enrichment factor in homing to the s.c. dGli36 glioma xenograft (7.9 x 10^4 pfu/mg), compared with the s.c. CNE2 tumor (1.67 x 10^4 pfu/mg), was 5-fold, (p=0.03; Figure 5.18a, part i). Similar results were obtained when another human glioma, SF767, was used. The enrichment factor in homing of MG11 phage to SF767-derived tumor (8.34 x 10^3 pfu/mg) was 4-fold higher when compared with the CNE2-derived tumor (2.21 x 10^3 pfu/mg), (p=0.02; Figure 5.18a, part ii), indicating that the binding of MG11 to human gliomas cell lines is specific.

5.3.2.4 MG11 phage does not bind to normal brain tissue

The specificity of MG11 phage binding to human glioma cells in the context of normal mouse astrocytes was investigated. Phage (10^{12}) was injected via tail vein into immunodeficient nude mice bearing an intracranial xenograft of dGli36 human glioma cells in the right hemisphere. Phage recovered from the right hemisphere bearing the xenografted tumor (9.2 x 10^2 pfu/mg) in mice injected with the MG11 phage gave an enrichment of 20-fold compared with those recovered from the normal side of the brain (0.5 x 10^2 pfu/mg) (left hemisphere) (p=0.013; Figure 5.18b). No significant difference could be detected between tumor-bearing mice and normal mice in the control groups injected with unselected phage (Figure 5.18b). These results demonstrated that phage bearing the MG11 epitope target specifically to cells of glial origin and do not bind to normal brain cells.

5.3.2.5 In vitro binding of **(K_{16})-MG11** *to human glioma cells*

The amino acid residues that make up the MG11 peptide sequence are very hydrophobic and could not be easily purified. To facilitate the purification procedure, we have inserted 16 lysine residues into the sequence. The addition of polylysine residues has been demonstrated to enhance the potential of the peptide to interact with the negatively charged plasmid DNA as demonstrated by Patel et al. (2001). In addition, a spacer sequence identical to that used by Patel et al. (2001) was also included to facilitate the movement of the peptide.

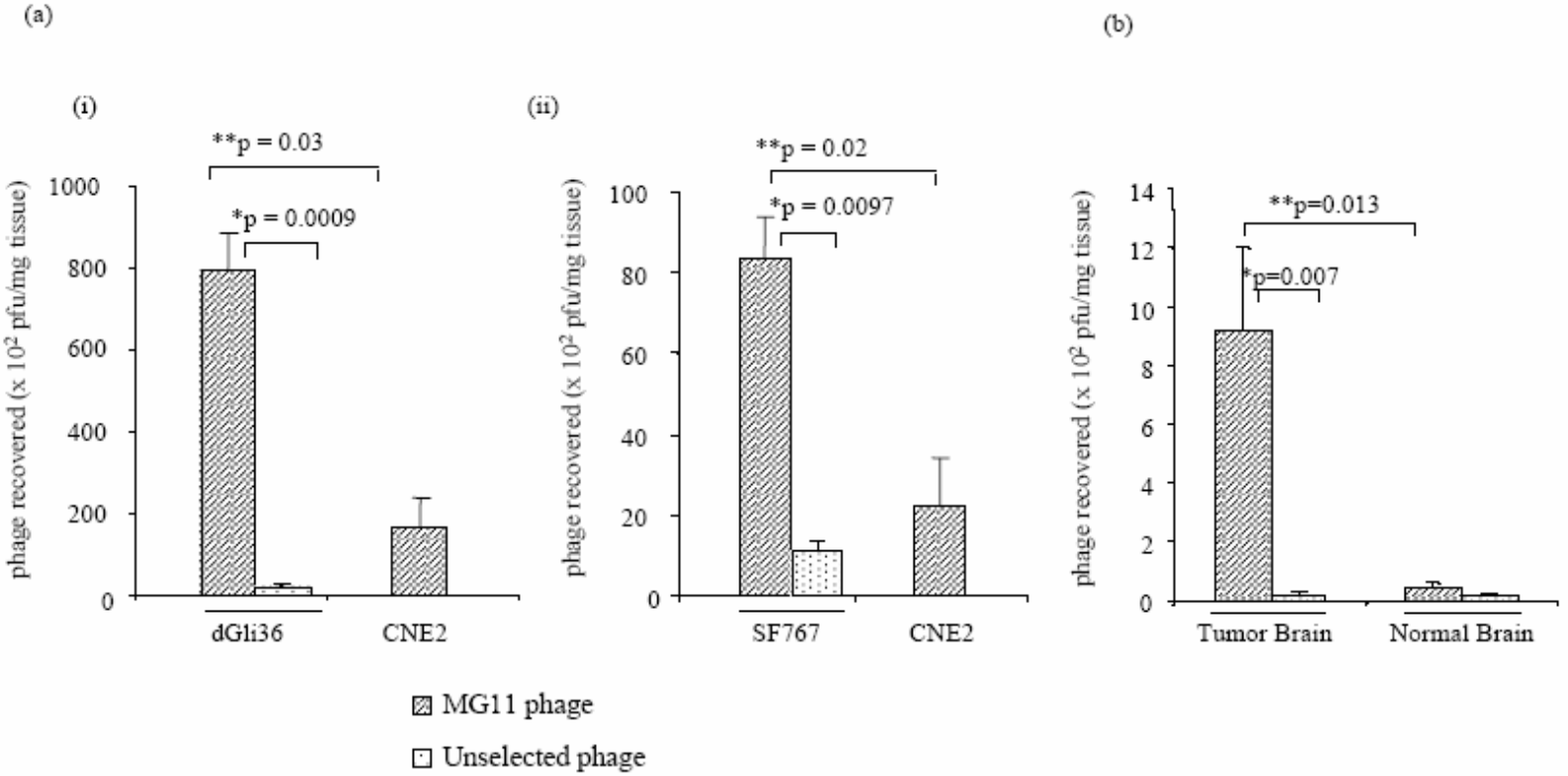

Figure 5.18 *In vivo* specificity of MG11 phage to panel of human glioma cell *in vivo*.
(a) Specific binding of MG11 phage to (i) dGli36 or (ii) SF767 human glioma xenograft as compared to a non-glioma xenograft, CNE2. Bars showed SEM of 3 mice. (b) Targeting of MG11 phage to intracranial dGli36 human glioma xenograft as compared to the normal region of the brain. Data shown are averages of 4 mice. *p≤0.05 (paired t-test).

The (K_{16})-MG11 peptide was chemically synthesized and complexed with a luciferase reporter plasmid, pNGVL-Luciferase (pNGVL-Luc). To determine the optimal concentration that would allow DNA and peptide interactions, and to maximize the efficiency of gene uptake, various peptides:DNA ratios were used in the transfection of SF767 cells. Various ratios of the pNGVL-Luc plasmid and (K_{16})-MG11 peptide were complexed, followed by incubation in SF767 glioma cells in the presence of chloroquine. Chloroquine was added as it has been previously demonstrated to prevent lysosomal DNA degradation (Zauner et al., 1997). After 24 h, luciferase expression was detected at peptide: DNA ratio (w/w) of 2:1 (39803 RLU/μg protein) (Figure 5.19a). The level of luciferase expression increased with escalating ratios of peptide to DNA (Figure 5.19a). This suggests that the abundance of lysine residues could facilitate the interaction of the peptide with the DNA molecules; hence ensuring the majority of the DNA molecules are complexed with the peptide. At peptide: DNA ratios of 10:1 and 20:1, toxicity could be detected as the treated SF767 glioma cells were not as healthy as the untreated controls. This could be due to the presence of high concentration of polylysine, which is known to be toxic to cells (Zauner et al., 1997). For subsequent experiments, we therefore adopted the optimal peptide: DNA ratio of 2:1.

To rule out the possibility that the binding of the peptide to the cells is due to the lysine residues inserted, we synthesized a control peptide in our experiment to confirm that the luciferase activities observed were a consequence of targeting. A control peptide, comprising of the 16 lysine residue followed by 12 amino acid sequence derived from biopanning of a nonglioma cell line, (K_{16})-H42, was also synthesized. H42 bears the sequence GGPTKEWELYLF. Similar experiments were carried out with the luciferase DNA and (K_{16})-H42 at various peptides to DNA ratios and no significant binding could be detected when analyzed 24 h post-transfection (Figure 5.19b).

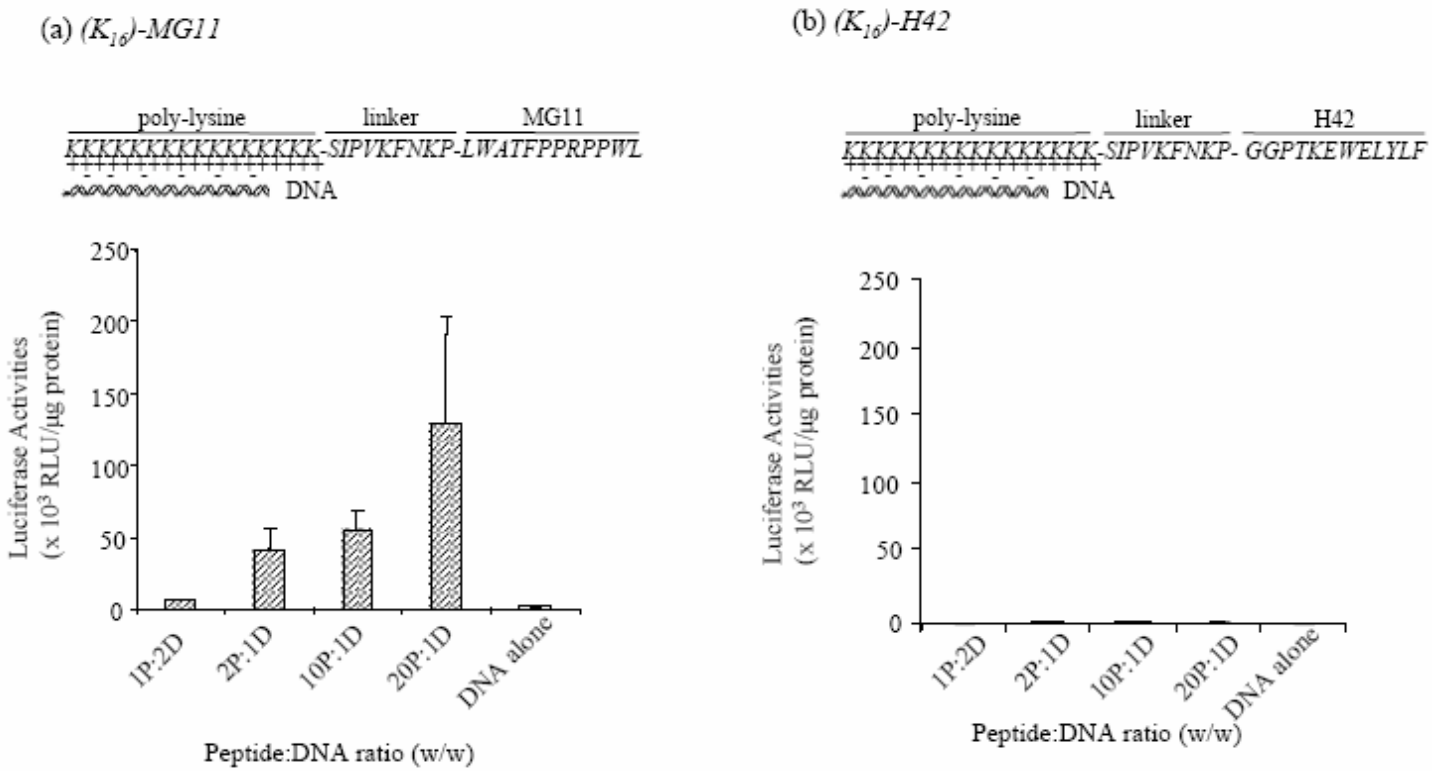

Figure 5.19 *In vitro* binding of (K_{16})-MG11 peptide to glioma cells.
(a) Proposed interaction of (K_{16})-MG11 and (b)(K_{16})-H42 peptide sequence with DNA and their effects on luciferase transgene expression. $3x10^5$ cells were transfected with peptide: DNA ratio of 1:2, 2:1, 10:1 and 20:1, for 24 h. Mean value for luciferase activities and SEM from triplicate experiments were shown.

5.3.2.6 (K_{16})-MG11 mediates expression of luciferase reporter gene to glioma cells

To further demonstrate the specificity of (K_{16})-MG11 peptide for glioma cells and to determine the optimal time point of luciferase transgene expression, peptide/DNA complex, prepared by mixing (K_{16})-MG11 peptide to pNGVL-Luc DNA at 2:1 (w/w) ratio, was added to tumor cell lines of different histotypes. These included dGli36, SF767, U251MG, A549, HeLa, HepG2, and CNE2 cells. Binding of peptide/DNA complexes was performed in the presence of 100 μM chloroquine, and luciferase expression was assayed 24 h and 48 h after transfection. Luciferase activities in SF767 glioma cell line (85473 RLU/μg) were at least 4-fold higher than in the CNE2 cell lines (19849 RLU/μg) at 24 h post-transfection. The level of gene expression at 48 h post-delivery is much higher than that at 24 h (Figure 5.20a, part i). The level of luciferase expression detected in U251MG, dGli36 and SF767 glioma cell lines increased dramatically by 48 h after transfection (Figure 5.20a, part i). Experiments using (K_{16})-MG11 peptide complexed with the reporter gene encoding eGFP also gave similar results (Figure 5.20a, part ii). Strong green fluorescence could be detected in U251MG glioma cells but not in HepG2 human hepatocellular carcinoma cells.

Furthermore, when peptide/DNA complexes prepared from (K_{16})-MG11 or (K_{16})-H42 peptide with pNGVL-Luc were mixed and added to SF767 and CNE2 cells, the luciferase expression in SF767 glioma cells transfected with (K_{16})-MG11: pNGVL-Luc (716940 RLU/μg) was 84-fold higher than that of (K_{16})-H42: pNGVL-Luc (8444 RLU/μg) control peptide transfected cells. The result thus demonstrate that the binding of (K_{16})-MG11 peptide is specific, and not due to the presence of positively charge lysine residues (Figure 5.20b). When compared with CNE2 nonglioma cell line, the level of luciferase expression observed in SF767 glioma cells transfected with pNGVL:Luc/(K_{16})-MG11 is 151-fold higher (Figure 5.20b). These results clearly illustrate that (K_{16})-MG11 is specific for glioma cells.

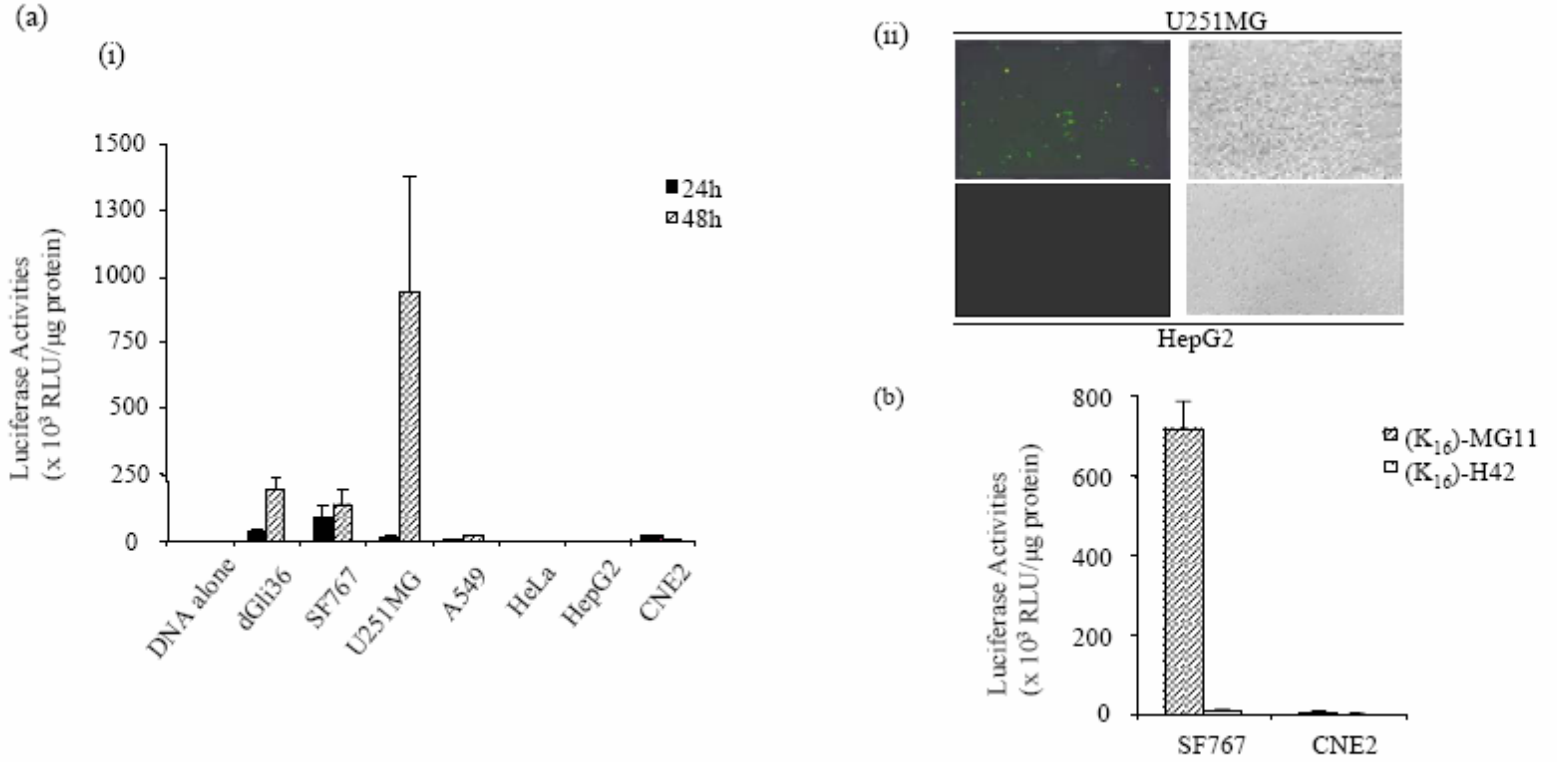

Figure 5.20 (K_{16})-MG11 peptide mediate transgene expression to a panel of human glioma cell lines .
(a)(i) Peptide/DNA (2:1; weight: weight ratio) complexes prepared from (K_{16})-MG11 were used to transfect pNGVL-Luc into various tumor cell lines. Luciferase activities were analyzed 24 h and 48 h post-transfection. (ii) 2:1 (weight: weight) ratio of peptide: DNA complexes prepared from (K_{16})-MG11 were used to transfect pEGFP-N1 into U251MG human glioma cells and HepG2 hepatoma cells. Fluorescence pictures were taken 48 h post-transfection. (b) Specificity of (K_{16})-MG11 when compared with (K_{16})-H42 control peptide. Peptide/DNA complexes prepared from (K_{16})-MG11 and (K_{16})-H42 were complexed with pNGVL-Luc and transfected into SF767 and CNE2 tumor cell lines. Luciferase activities were analyzed 48 h post-transfection. The luciferase activities shown are ±SEM of triplicates.

5.3.2.7 Characterization of (K_{16})-MG11 peptide targeted delivery in vitro and in vivo

To determine the direct specific binding of the (K_{16})-MG11 peptide to the cell surface of glioma cells, (K_{16})-MG11 peptide was conjugated to Lissamine rhodamine. After incubating the various tumor cell lines (SF767, U251MG, M059K, A549, HepG2, and HK1) with the Lissamine rhodamine-conjugated (K_{16})-MG11 peptide, the cells were examined under confocal microscopy and the levels of fluorescence detected were compared. SF767, U251MG, and M059K human glioma cell lines exhibited detectable fluorescence as shown by the presence of rhodamine on the surface of the cells (Figure 5.21 top). Little or no fluorescence was observed with nonglioma cell lines (Figure 5.21 bottom). In contrast, nonspecific red fluorescence was observed in all cell lines studied when incubated with (K_{16})-H42 control peptide under similar conditions (data not shown). Unlike the (K_{16})-MG11 peptide, no discrimination between glioma and nonglioma cells could be ascertained with the rhodamine-conjugated (K_{16})-H42 peptide (data not shown).

The binding specificity of (K_{16})-MG11 peptide to primary human glioma cells and normal primary human astrocytes was subsequently determined (Figure 5.22). Primary human glioma cells derived from biopsy or normal primary human astrocytes were incubated with Lissamine rhodamine-conjugated (K_{16})-MG11 peptide at 37 °C for 20 min. Significant binding of the (K_{16})-MG11 peptide was observed only in primary human glioma cells (Figure 5.22a). This binding specificity is comparable to that observed in SF767 human glioma cell line (Figure 5.22b). In contrast, no fluorescence could be detected with normal primary human astrocytes under similar conditions (Figure 5.22c). These results clearly demonstrated that the MG11 peptide is specific for human glioma cells and does not bind to normal human astrocytes.

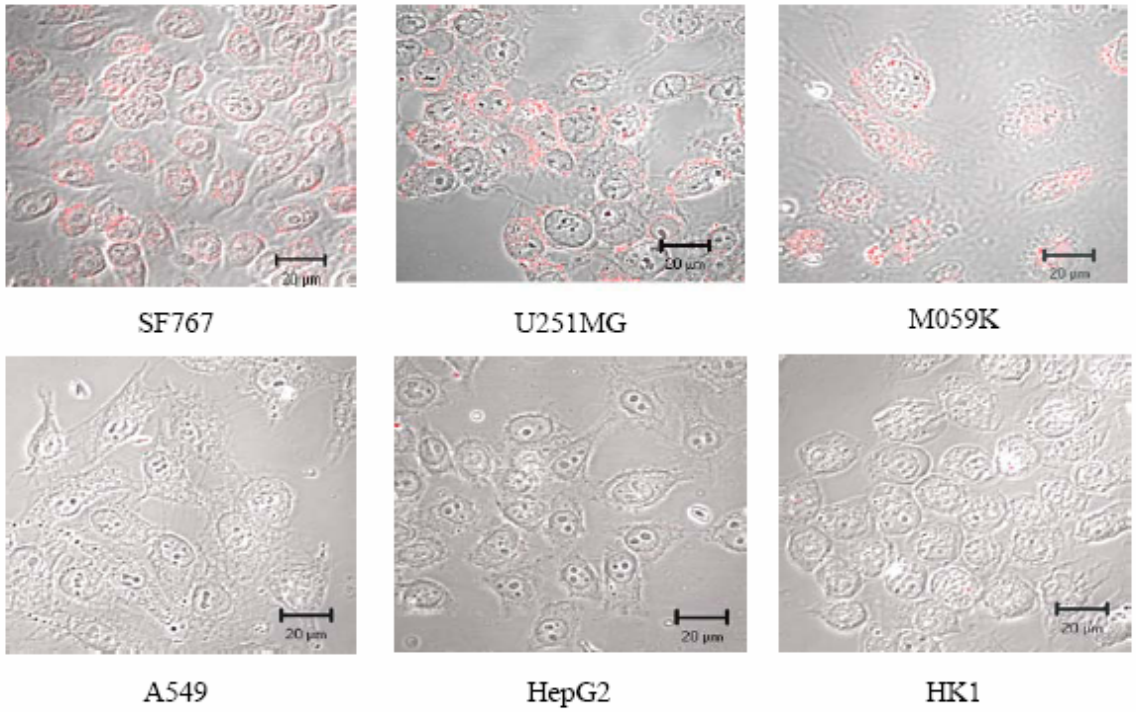

Figure 5.21 *In vitro* specificity of the lissamine rhodamine-labeled (K_{16})-MG11 peptide.
Tumor cell lines of various origins were incubated with 100 ng of (K_{16})-MG11 peptide for 20 min at 37 ° C. Cells were subsequently fixed and mounted as described in Materials and Methods. Fluorescence images were studied using the LSM 510 Meta confocal microscopy system.

(a) Primary GBM

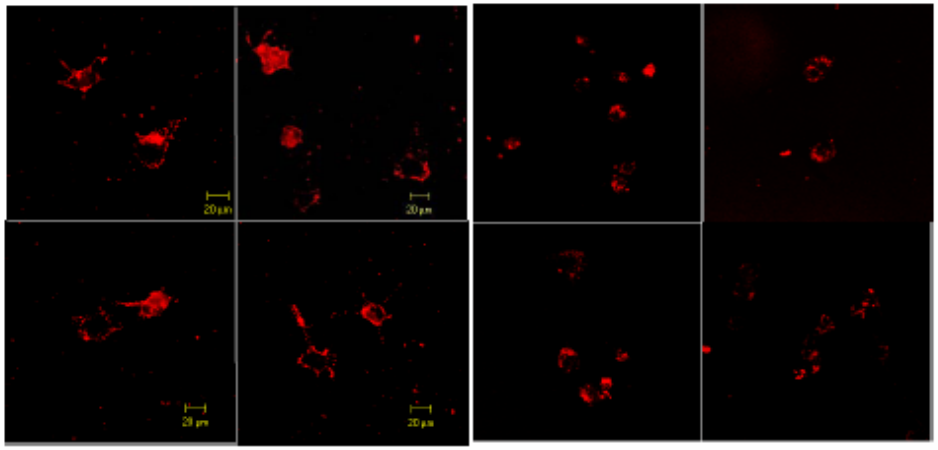

(b) SF767 human glioma cells

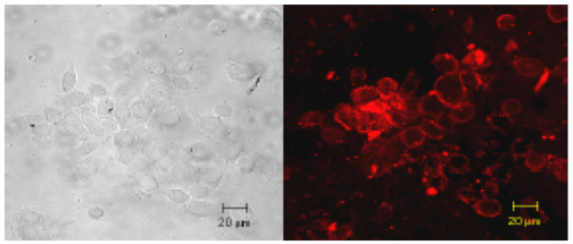

(c) Normal primary human astrocytes

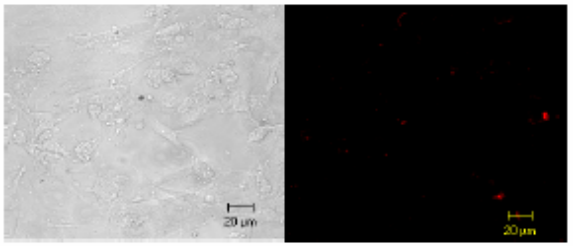

Figure 5.22 Binding of lissamine rhodamine-labeled (K_{16})-MG11 peptide to primary human glioma culture.
(a) Primary human glioma culture, (b) SF767 human glioma cells, and (c) normal human astrocytes were incubated with 100 ng of (K_{16})-MG11 for 20 min at 37 ° C. Cells were subsequently fixed and mounted as described in Materials and Methods. Fluorescence images were studied using the LSM 510 Meta confocal microscopy system.

To further demonstrate the tumor specificity of the (K_{16})-MG11 peptide on glioma xenograft, SCID mice harboring s.c.-established SF767-derived xenograft were injected intratumorally with Lissamine rhodamine-conjugated (K_{16})-MG11 peptide and (K_{16})-H42 peptide. After 20 min of circulation, the mouse bearing the SF767 glioma xenograft was perfused and tumor was harvested. The tumor sections were counterstained with FITC-labeled phalloidin, which stains F-actin, to show the cell surface. Cryostat sections of the tumors showed red fluorescence binding in SF767 glioma xenograft injected with (K_{16})-MG11 peptide (Figure 5.23a), demonstrating the binding of the (K_{16})-MG11 peptide. This binding, as observed in the inset (I), indicated that the (K_{16})-MG11 peptide interacted with cell surface receptors on the tumor cells. In contrast, red fluorescence was not detected in the SF767 tumor injected with (K_{16})-H42 peptide (Figure 5.23b). Although the staining obtained with FITC-labeled phalloidin (green) and Lissamine rhodamine-conjugated (K_{16})-MG11 peptide (red) was in close proximity, they did not colocalize. This reflects the fact that the receptors for MG11 peptide are located on the external side of the plasma membrane, whereas F-actin is situated just below this external periphery membrane layer. Taken together, our results suggested that the observed fluorescence can be attributable to the specific binding and subsequent uptake of the (K_{16})-MG11 peptide.

(a) MG11 (b) H42

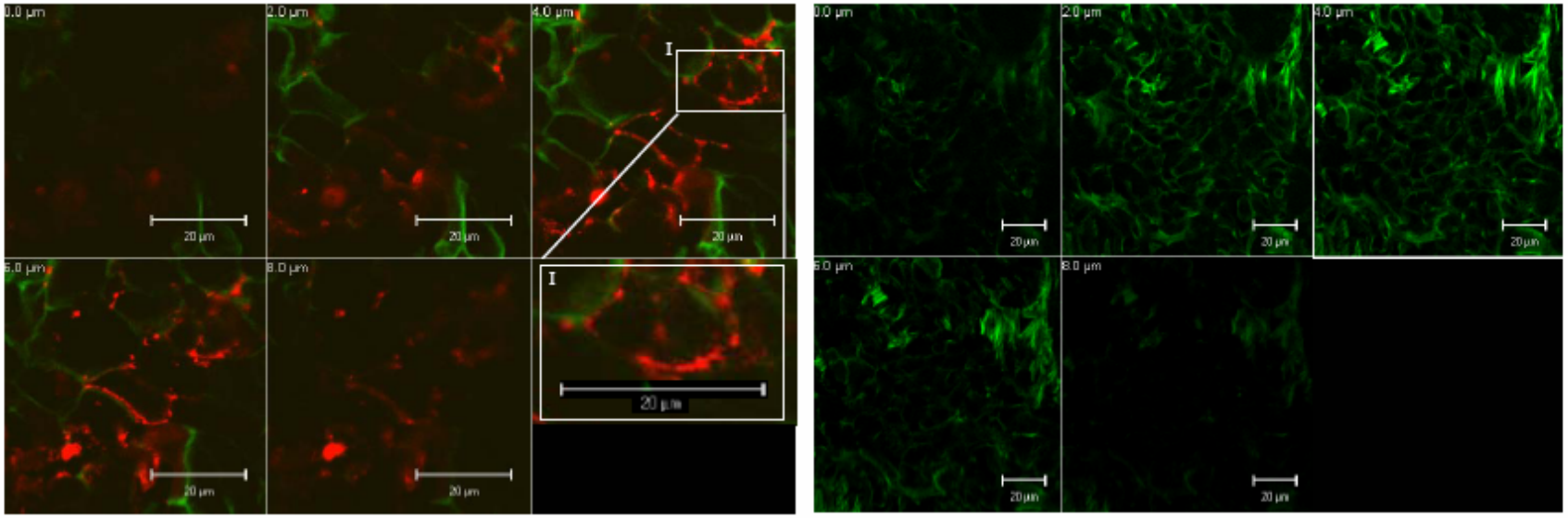

Figure 5.23 *In vivo* targeting of the (K_{16})-MG11 fluorescent-labeled peptide.
SF767 human glioma cells were inoculated into the right flank of immunodeficient mice to form a tumor xenograft. 100 ug of lissamine-rhodamine (a) (K_{16})-MG11 peptide or (b) (K_{16})-H42 peptide were injected intratumorally into separate mice bearing the SF767 human glioma xenograft and the peptides were allowed to circulate for 20 min. After which, the tumors were harvested and cryosectioned. Fluorescence images were studied using the LSM 510 Meta confocal microscopy system. "I" denotes inset.

5.4 Discussion

In this chapter, we have constructed a glioma-specific and cell cycle-regulated amplicon vector. We have shown that incorporation of the GFAP enhancer element will limit the luciferase reported gene expression to proliferating glioma cells, and when FasL was used as a therapeutic gene, the percentage of cell death of observe only in proliferating dGli36 glioma cells, but were absent in infected-proliferating-HeLa cells. Once the functionality of the vector was determined, the issues of immunogenicity, stability and transduction efficiency of the cell cycle-regulated amplicon vector need to be addressed. These are important issues as the success of gene therapy protocol is highly dependent on a safe and stable vector with high transduction efficiency. The earlier part of the thesis is focus on the cell cycle-regulated vector but not the dual-specific vector. Therefore, the topics on immunogenicity, stability and transduction efficiency was not included.

Gene transfer to malignant gliomas has been extensively pursued both in cell culture as well as in animal models. However, clinical gene therapy trials for recurrent gliomas have not fulfilled the high expectations suggested by preclinical laboratory results. One of the significant pitfalls is the low transduction efficiency of tumor cells observed *in vivo*, resulting in insufficient expression of therapeutic gene products to efficiently eradicate the tumor cells (Rainov and Kramm, 2001; Rainov and Ren, 2003; Weyerbrock and Oldfield, 1999). Retrovirus vector was one of the earliest viral vectors to be employed for the delivery of therapeutic genes to gliomas in the clinical settings (Rainov and Ren, 2003). Although both phase I and II clinical studies showed favorable safety profiles and some efficacy, the phase III study failed to demonstrate significant progression-free or extension of overall survival (Rainov and Ren, 2003). The use of adenovirus vectors, as well as HSV-based vectors, has also been actively pursued both in the laboratory and clinic (Bansal and Engelhard, 2000).

The major challenge of cancer gene therapy is the ability to restrict transgene expression to a particular tumor cell type. To circumvent this problem, tissue-specific promoter has been

employed to direct cell type-specific gene expression, thus lessen the potential toxicity to non-target cells. In this study, we have engineered a novel HSV-1 amplicon viral vector that incorporates both cell cycle- and cell type-specific regulatory elements. We incorporated the glial-specific promoter, GFAP, into the cell cycle-regulated amplicon vector. The insertion of this glial-specific element enables the transgene to be active only in proliferating glial cells. We did not incorporate the entire human GFAP promoter into our amplicon virus system. Instead, we incorporated the GFAP enhancer element in three tandem repeats and placed it upstream of a PCR-amplified hCMV minimal promoter. This glial cell-specific transcriptional element has been shown to be transcriptionally selective for astrocytic cells such as T98G glioma cells, which do not express GFAP (Chen et al., 1998). We have shown that the transcriptional activity is indeed specific to astrocytic cell lines such as dGli36, U251MG and SF767 cells (see Figure 5.2) and not present in nonastrocytic cell lines such as HeLa and HepG2. Similarly, when the FasL gene was incorporated into pG8-18 to generate pG8-FasL, the expression of FasL was only detectable in proliferating glioma cells (dGli36) but not in nonglioma cells (HeLa) cells. In addition, FasL expression mediated by pG8-FasL vector *in vivo* is shown to suppress the growth of s.c. glioma tumor (Figure 5.7) as well as to prolong the survival of mice harboring intracranial dGli36 tumor (Figure 5.8). These results thus suggested that the expression of FasL is indeed regulated in a cell type-specific and cell cycle-dependent manner. This observation is of great importance since the expression of FasL in non-target tissue such as liver, has been shown to be detrimental with FasL associated-apoptosis, resulting in liver failure (Aoki et al., 2000; Schlosser et al., 2000; Schneider et al., 1998).

Targeting of gene delivery vectors to specific tissues is dependent on the identification of ligands that interact with cell surface receptor molecules. For the targeting of HSV-1 vector, it is important to select for ligands that bind with high affinity, yet does not enhance receptor mediated endocytosis which will impede the delivery of the HSV-1 DNA to the nucleus, resulting in the degradation of the amplicon vector in the lysosome. It is preferable to insert

small targeting epitopes to the HSBD region (amino acid 33-123; Tal-Singer et al., 1995) to reduce potential interference of the chimeric protein on the virion surface.

We employed a phage display peptide library to isolate and characterize phage bearing peptide sequences that bind specifically to a wide array of human glioma cell lines. Analysis of the 79 phage clones obtained after biopanning of the Ph.D.-12 phage library revealed several dominant sequence motifs (Table 5.3). The sequence SGHQLLLNKMPN, encoded by the phage MG2 was found in 24 % of the clones and this sequence was shown to have 60 % homology with the human mitogen-activated protein kinase kinase kinase 12 (MAP3K12). The second most frequently isolated phage clone, MG11, bears the sequence LWATFPPRPPWL, which matches that of semaphorin 4B precursor, a membrane-bound semaphorin. Interestingly, two other phage clones that harbor peptide sequences with homology for the semaphorin family of proteins were also identified (Table 5.3). The sequence HHGHSPTSPQVR matches the protein sequence of secreted semaphorin 3A precursor protein, whereas the sequence LPYGTSNRHAPV is homologous to that of membrane-bound semaphorin 6B precursor protein. Semaphorin 3A has been reported to bind with high affinity to neuropilin-1 (Rieger et al., 2003), a receptor for the vascular endothelial growth factor family (Miao et al., 2000). Neuropilin-1, together with plexin, a receptor for the transmembrane-bound semaphorins (Rieger et al., 2003), form complexes with the class 3 semaphorins that are able to direct growing axons to their targets (Tamagnone et al., 1999). Besides modulating the extension of the axonal cones, semaphorins also regulate the migration of neural progenitor cells (Marin et al., 2001). One of the clinical features of gliomas is their ability to infiltrate and migrate to distant sites within the brain; it is therefore speculated that semaphorins could play a role in the carcinogenesis of glioma. This suggestion is consistent with reports of the presence of semaphorins in the progression of mouse mammary tumor and metastatic human lung adenocarcinoma (Martín-Satué and Blanco, 1999). Consistently, it has also been reported that both semaphorin 3 and semaphorin

6B could be detected by RT-PCR analysis of human glioma cell lines (Correa et al., 2001; Rieger et al., 2003).

Previous peptide sequences that target to human malignant glioma cells have been isolated (Spear et al., 2001; Zhang et al., 2001). However, the reported specificity is limited and confined to a single glioma cell line. Spear *et al* reported a peptide, having the sequence MCPKHPLGC that binds only to U87MG glioma cell line (Spear et al., 2001). Zhang *et al* also reported a sequence that binds to glioma cells. However, this sequence is not glioma specific, as it also binds to other cancer cell lines (Zhang et al., 2001). In our study, phage bearing the MG11 sequence showed a binding enrichment of more than 5-fold for glioma cells in comparison to nonglioma cells (Figure 5.16). Consistent with the *in vitro* data, the MG11 peptide-encoding phages were able to target specifically to dGli36 and SF767 human glioma xenografts, with a 5-fold binding enrichment over that of a nonglioma tumor xenograft under similar conditions (Figure 5.18a and b). Furthermore, the MG11 peptide was able to direct and confine the gene expression of the luciferase DNA specifically to human glioma cells (Figure 5.20). Currently, the lack of selectivity of cancer chemotherapeutic drugs results in high toxicities. As MG11 offers selective binding, it could potentially be useful as a targeting molecule. However, to enhance the effectiveness of targeting, the therapeutic index (ratio of binding to target glioma tissue versus binding to normal tissues) for each and every toxic molecule that may be conjugated to MG11 need to be determined. One of the challenges for *in vivo* targeting is to be able to direct the binding of the targeting peptide to tumor cells. We have shown that the MG11 peptide binds only to human glioma-derived cell lines (Figure 5.21) and primary human glioma cells (Figure 5.22a) but not to normal human brain cells (Figure 5.22c) or other nonglioma cells (Figure 5.21). These observations would be of great relevance for designing strategies to treat gliomas.

Viral vectors confer higher efficiency of gene transfer *in vivo* in comparison to non-viral vectors. However, components from HSV particles or cellular debris co-purified from viral

packaging or the transgene have been known to induce host immune response (Bowers et al., 2003). In our study (Figure 5.14) and a study performed by Olschowka et al. (2003), a transient immune response was observed in the brain following infusion of helper virus-free HSV-1 amplicon vectors with level of activated T lymphocytes and microglial cells returned to normal after four days. Similarly, the level of proinflammatory cytokine (IL-1β, TNF-α, IFN-γ), chemokines (MCP-1, IP-10) and adhesion molecules (ICAM-1) also returned to normal in the following day. This transient immune response was monitored by immunohistological staining for the expression of CD4, CD8, and CD11b in our study. However, dorsal foot pad analysis, or activation of cytotoxic T-lymphocyte (CTL) has been reported to investigate the activation of immune response.

One of the major problems of the HSV-1 vector system is the instability of the transgene expression. Viruses packaged in the presence of the helper viruses produce less stable gene expression when compared with those packaged using the helper virus-free system. Ho et al. (1993) reported that the lacZ expression mediated by helper-virus-dependent pIE1βgalori amplicon vector in the rat hippocampus declined to zero by day 7 post-transduction. In contrast, when packaged using helper-virus free system, the percentage of lacZ-positive cells was approximately 15 % of that observed at day 4. Our data demonstrated the persistence of the viral DNA in the mouse brain for at least 28 days with a significant reduction in luciferase gene expression one month after gene transfer (Figure 5.11 and 5.12). We have not determined the cause of the loss of luciferase gene expression 10 days post-infection. It is possible that the loss of luciferase expression is due to the short half-life of the protein, which has been demonstrated to be approximately 2-3 h (Ignowski and Schaffer, 2004; Thompson et al., 1991). Using BrdU incorporation assay, we have determine that the percentage of S phase cells in 7 day-old intracranial tumor is approximately 8 % (data not shown). Because only tumor cells that are situated at the periphery of the tumor mass are rapidly proliferating while those in the center core are not, we speculate that the significant reduction in luciferase

expression could also be due to the lack of proliferating cells resulting in the transgene not being activated. Since the HSV-1 genome is largely extrachromosal, the presence of the viral DNA would eventually diminish as more cell divisions take place. To increase the stability of the transgene expression in dividing cells, the HSV-1 amplicons have been modified to contain the *EBNA1* gene and *oriP* from the EBV genome, which allow the replication of the amplicon DNA together with the host cell DNA (Wang and Vos, 1996). This would ensure equal distribution of the amplicon DNA to daughter cells during mitosis. Incorporation of AAV elements into the HSV-1 amplicon would enhance transgene stability, most likely due to the integration of the transgene into the nucleus of the host cells (Constantini et al., 1999; Lam et al., 2002; Fraefel et al., 1997; Heister et al., 2002; Johnston et al., 1997). When the *gag* and *pol* gene from the retrovirus is incorporated in to the HSV-1 amplicon, the efficiency of transgene integration is 50-fold higher in comparison with HSV-1 amplicon (de Felipe et al., 2001). Other strategies employed include the development of the Cre/lox P system (Rinaldi et al., 1999) and the inclusion of a Tc1-like transposon, *sleeping beauty* (Ivics et al., 2004; Yant et al., 2002).

Conventional treatment of GBM involves a combination of surgery, chemotherapy and radiotherapy. Multiple cellular signals in the tumor cells are activated following exposure to radiation or chemotherapy which may interfere with our cell cycle-regulated amplicon vector. Our proposed strategy would serve as an "adjuvant" therapy to complement craniotomy in destroying any residual tumor cells that may remain at the resected tumor region. The cell cycle-regulated amplicon vector can be injected directly into the tumor bed following surgical resection of the core tumor mass. The patient might be subjected to chemotherapy, in which case, we are interested to know whether this treatment will affect the viral vector and the transgene activation. We have demonstrated that treatment with TMZ, the most common chemotherapeutic drug for GBM treatment, induces G_2/M arrest in dGli36 cells, but it does not affect the cell cycle-regulated transgene expression (Figure 5.10). On the other hand, ionizing radiation (IR) has been shown to induce transient G_2/M accumulation in

radiosensitive glioma cells, such as p53 mutated M059K cells that have the ability to repair DNA double-strand break (Xu et al., 2002; Holgersson et al., 2005). However, IR does not affect HSV-1 amplicon vector. In fact, it has been shown that IR provides a conducive local environment for the replication of HSV-1 viral vector (Advani et al., 1998, Bradley et al., 1999). In addition, IR can target enhanced viral replication specifically to the irradiated tumor bed, possibly by inducing expression of genes from the glioma cells that stimulates viral replication (Advani et al., 1998). Thus, cell cycle-regulated HSV-1 amplicon-transduced cells that survive IR may continue to divide.

In summary, transgene expression mediated by the amplicon vector can be restricted to glioma-cells by the incorporation of the GFAP promoter and the use of the MG11 targeting peptide. This approach would significantly enhance the efficiency of gene transfer and at the same time, increase the safety profile of the gene therapy protocol.

Chapter 6

Future Directions

Vector targeting is one of the most unambiguous lessons to derive from human clinical trials. Most current modes of vector entry into cells are not specific to cell type, and rely on the route of delivery to target certain cell populations. In the present study, focus has been placed on generating a viral vector that confers transgene expression in a cell type-dependent manner, and later, "fine-tuning" it to be cell type-specific by adopting a glial-cell specific promoter. This vector, denoted as pG8-18, is studied with respect to its ability to confer stable transgene expression, its infectability and mobility of the pG8-18 HSV virions are explored intracranially and more importantly, the amount of immune responses elicited by these viruses are also determined. To envisage the behavior of these viruses in a clinical setting, pG8-18 viral vectors are further evaluated in the presence of a chemotherapy drug commonly used for the treatment of human gliomas. Last but not least, the pursuit of a glioma-specific sequence is also presented, with the ultimate goal of incorporating the peptide sequence into the enveloped coat protein of pG8-18 amplicon vectors for targeting purposes. Currently, we have demonstrated that the vector is stable *in vivo*, relatively non-immunogenic and that the dual-specific regulation is retained even after treatment with drug, indicating that this vector may potentially be of clinical relevance for gene delivery. Despite of these encouraging findings, the system nonetheless has its limitations. Unlike the tetracycline or the dimerizer-regulated system, the cell cycle-regulated transcriptional activation system does not require the application of exogenous drugs or dimerizations of two protein domains. Instead, this system is strictly dependent on the activation of cellular proliferation, which in turns will activate transgene expression. This ensures that infected but "dormant" tumor cells will be killed once the cells enter the cell cycle, thus switching-on the therapeutic gene expression. However, the transgene regulation needs to be enhanced to ensure only proliferating tumor cells are affected. In addition, new avenues relating to the choice of therapeutic genes and promoters remain to be explored.

6.1 Enhanced transgene regulation

We have demonstrated that transgene expression regulated by the cell cycle-dependent vector is specific for proliferating cells (Chapter 3). The degree of cell cycle regulation, measured as a ratio of luciferase activity (expressed as RLU/ug) of the proliferating and G_1-arrested cells, ranges between 0.2-3.7 and 4.3-57.6 fold in pIH8GalLuc and pC8-36 constructs, respectively. To further increase the tightness of regulation, we propose to multimerize the binding sites (CDE/CHR elements) for CDF-1 located within cyclin A promoter. We hypothesize that the availability of more binding sites for CDF-1 repressor binding would tighten the transgene regulation during G_0/G_1 arrested stage. This is supported by preliminary findings that cell cycle-dependent transgene expression can be regulated in a viral dosage dependent manner (section 3.3.12). In parallel, other promoters, which contain the CDE/CHR elements, will be tested for their promoter strength in comparison to cyclin A promoter for stronger transactivation capability. Promoter such as *cyclin B* is a potential candidate. Cyclin B forms a complex with cdc2, which is required for cells to undergo mitosis. The expression level of cyclin B is maximal in G_2 phase of the cell cycle. In addition, the *cyclin B* promoter contains three CCAAT-boxes that can bind to and activated by NF-Y (Wasner et al., 2003). Moreover, overexpression of cyclin B has been associated with colorectal cancer (Sarafan-Vasseur et al., 2002) and lung carcinoma (Hofmann et al., 2004).

6.2 Alternative therapeutic genes and glioma-specific promoters

Currently, we have employed the *FasL* and *FADD* genes to assess the therapeutic efficacy of our system. The level of cytotoxicity induced by these two molecules using either the pC8-36 or pG8-18 based vector is not strong enough to achieve 100 % killing. In addition, the apoptotic effect of soluble FasL could be undesirable due to possible toxicity to normal tissue that expressed the Fas receptor. To circumvent this problem, multiple therapeutic gene cassettes such as p53 and FasL (Shinoura *et al*., 2000), p53 and Bax, FasL and FADD, FasL and TRAIL (Rubinchik et al., 2003), caspase-1 and interferon γ could also be evaluated. In addition, non-cleavable FasL which contains mutations in the metalloproteinase cleavage sites

has been demonstrated to induce potent apoptotic effect, and at the same time, reduce by-stander effect (Knox et al., 2003). The incorporation of these genes into one single vector would not only increase the therapeutic efficiency of the target cells, it would also overcome the low viral titer limitation of the HSV-1 amplicon vector.

The utilization of GFAP promoter to drive luciferase gene expression in pG8-18 is promising. However, one of the anticipated problems *in vivo* would be the expression of GFAP in normal human astrocytes and neural progenitor cells (Johansson et al., 1999; Laywell et al., 2000). Since our vector is capable of infecting normal astrocytes, the transgene could be activated during reactive gliosis, resulting in the elimination of these proliferating cells in addition to the tumor cells. The system could be improved by the use of tumor-specific promoter such as the telomerase promoter which is highly expressed in malignant tumor cells but not in normal cells. The activation of telomerase is regulated at the transcription level by the telomerase catalytic subunit, human telomerase reverse transcriptase (hTERT). Several groups have demonstrated the use of hTERT promoter to regulate the expression of apoptotic gene such as FADD (Koga et al., 2001), caspase 8 (Komata et al., 2002), caspase 6 (Komata et al., 2001) and HSV-tk (Takeda et al., 2003). Although this approach may have added advantage to restricting transgene expression in proliferating tumor cells, it does not overcome the non-selective bystander effect of FasL (as shown in Figure 4.4) and may be hazardous to the untransduced cells surrounding the tumor border regions. Numerous studies have reported on the over-expression of the interleukin-13 receptors (IL-13R) on human glioma cell lines and virtually all high-grade human glioma samples (Debinski et al., 1995; Joshi et al., 2000; Husain et al., 2001). Analysis of the subunit composition of IL-13R in primary explants of malignant glioma cells has demonstrated that IL-13R composed of three different chains namely; IL-13Rα1 (also known as IL-13Rα'); IL-13Rα2 (also known as IL-13Rα) and IL-4Rα (also known as IL-4Rβ) (Husain et al., 2003). Human glioma cells overexpress IL-13Rα2, which is only marginally expressed or completely deficient in normal brain tissues, B

cells, monocytes, T lymphocytes and endothelial cells (Joshi et al., 2000; Husain et al., 2003). We have confirmed the over-expression of IL-13Rα2 transcripts in some of the human glioma cell lines (data not shown) and would like to further examine the expression level in primary human glioma cells. To target IL-13R, IL-13 cytotoxin (IL13-PE38QQR) composed of IL-13 and a mutated short form of *Pseudomonas* exotoxin moiety (PE_A) have been shown to be highly selective and lethal for glioma cells (Debinski et al., 1995). Normal cells including immune cells, endothelial cells and normal brain cells are spared from the cytotoxic effect of the IL-13 cytotoxin (Husain et al., 2003; Souweidane et al., 2004). Cytotoxicity could be demonstrated in glioma cells at concentrations as low as 0.001 μg/ml (Debinski et al., 1995; Liu et al, 2000). Due to the tumor specificity and large therapeutic index, the IL-13 cytotoxin is currently being tested in PhaseI/II studies for recurrent supratentorial malignant gliomas in adults. We hypothesize that the use of IL13-PE38QQR could potentially enhance the specificity of the therapeutic gene expression.

6.3 Clinical application of the cell cycle-regulated amplicon vector

Our proposed strategy would serve as an "adjuvant" therapy to complement craniotomy in destroying any residual tumor cells that may remain at the resected tumor region. The cell cycle-regulated amplicon vector can be injected directly into the tumor bed following surgical resection of the core tumor mass. Since majority of the tumor mass has been removed, the dose of viral vectors required to eradicate residual tumor cells is expected to be correspondingly small. By doing so, one would minimize the likelihood of harming distant normal, dividing cells. In fact, this treatment protocol mimic gliadel wafers which have been clinically applied for implantation into the tumor sites at the time of surgery to slowly release a chemotherapy drug such as BCNU (Brem and Gabikian, 2001). Thus, the 10-fold difference observed *in vivo* (Figure 5.4) would have a significant impact considering that these viruses will be inoculated into the resected cavity rim, harboring mainly replicating malignant cells rather than administering to a mass of tumor cells. This method overcomes

the problems associated with implantation of vector producing cells (VPC), such as the inability to distribute the VPC and the instability of the VPC (Rainov and Ren, 2003). However, the low percentage of transduced cells *in vivo* would still pose a problem. Therefore, injections at multiple sites need to be carried out to ensure majority of the residual tumor cells are infected by the amplicon viral vectors.

6.4 Combining vector targeting with transcriptional targeting

The HSV-1 genome contains more than 80 genes with one-fifth of the genes encoding for virion surface proteins and the envelope glycoproteins. Initial attachment and subsequent entry of the virus to the host cells are dependent upon 5 major glycoproteins, namely, gC, gB, gH, gL and gD. To retarget HSV, the membrane glycoproteins can be modified such that the natural tropism of the virion is reduced, and the modified glycoproteins that contain those new ligands are able to infect and penetrate target cells. During the infection process, binding of HSV to the cell surface heparan sulfate (HS) is primarily mediated through gC, which is located in the U_L segment of the HSV-1 genome and encoded by the *U_L44* gene. gC contains a well characterized heparan sulfate binding domain (HSBD) which can be modified with ligands that target to specific cell types (Tal-Singer et al., 1995). Deletion in the HSBD in gC resulted in significant reduction in infectivity to HSV-1 natural target cells.

Several groups have created chimeric gC that carries insertion in the HSBD between amino acids 33 and 123 (Grandi et al., 2003; Laquerre et al., 1998; Spear et al., 2003). Laquerre *et al*. (1998) inserted the erythropoietin binding domain into the HSBD region of gC in a gB-deleted mutant. The results demonstrated that this modified HSV is targeted to murine cells expressing the erythropoietin receptor. However, deletion of gB, which is required for membrane fusion, resulted in endocytosis of the vector leading to aborted infection. In 2003, Spear et al. constructed a novel amplicon vector, pCONGAH, which has a higher affinity to cells expressing the pseudo-histidine (his) tag. This vector contains the standard amplicon packaging as well as origin of replication components (Spear et al., 2003). The pCONGAH

also contains the gene encoding for *gC*, which was modified to contain 6 successive his-residues (Spear et al., 2003). The authors demonstrated at least 4-fold higher affinity of pCONGAH viral vector to cells that expresses the pseudo-his tag *in vitro* compared to the parental cell line that does not overexpress the pseudo-his tag (Grandi et al., 2004; Grandi et al., 2003). Unlike the erythropoietin-targeting HSV, the infectivity of pCONGAH is not affected (Grandi et al., 2004; Grandi et al., 2003). This is the first attempt at modifying the envelope of a HSV-1 amplicon vector.

Thus, the generation of pCONGA-MG11 will allow us to test the homing potential of MG11 in the context of a HSV-1 amplicon peptide display vector. Once the targeting ability of MG11 peptide sequence mediated by amplicon vector is determined *in vivo*, modification of the envelope glycoprotein of the cell cycle regulated HSV-1 amplicon vector, pG8-18, to express the MG11 peptide sequence, will be attempted to enhance homing specificity and potentially target the infiltrated invasive cells. The combination of the two targeting systems would ensure only those rapidly proliferating glioma cells that express the receptor for the MG11 peptide be infected by pG8-18. More importantly, the amount of viruses needed to achieve a therapeutic response would be significantly reduced, hence minimize potential side effects.

6.5 Conclusion

In summary, we have designed a HSV-1 amplicon based "ideal" gene delivery system that is (i) capable of incorporating a large transgene; (ii) stable; (iii) safe; (iv) regulatable; (v) capable of targeting to a specific cell type. Transgene expression mediated by this vector can be regulated in glioma-specific and cell cycle-regulated manner. Coupling of this vector system with the targeting peptide could potentially be useful in the removal of the residual, infiltrative tumor cells.

Bibliography

Ace, C.I., McKee, T.A., Ryan, J.M., Cameron, J.M., and Preston, C.M. (1989). Construction and characterization of a herpes simplex virus type 1 mutant unable to transinduce immediate-early gene expression. J Virol *63*, 2260-2269.

Agha-Mohammadi, S., and Lotze, M. T. (2000). Regulatable systems: applications in gene therapy and replicating viruses. J Clin Invest *105*, 1177-1183.

Aghi, M., Hochberg, F., and Breakefield, X. O. (2000). Prodrug activation enzymes in cancer gene therapy. J Gene Med *2*, 148-164.

Advani, S. J., Kataoka, Y., Sibley, G. S., Song, P.Y., Hallahan, D. E., Roizman, B., and Weichselbaum, R. R. (1998). Enhancement of replication of genetically engineered herpes simplex viruses by ionizing radiation: a new paradigm for destruction of therapeutically intractable tumors. Gene Ther *5*, 160-165.

Albertoni, M., Daub, D., Arder, K., Viars, C., Powell, C., and Van Meir, E. (1998). Genetic instability leads to loss of both p53 alleles in a human glioblastoma. Oncogene *16*, 321-326.

Alemany, R., Gomez-Manzano, C., Balagué, C., Yung, W., Curiel, D., Kyritsis, A., and Fueyo, J. (1999). Gene Therapy for Gliomas: molecular target, adenoviral vectors, and oncolytic adenoviruses. Exp Cell Res *252*, 1-12.

Ambar, B. B., Frei, K., Malipiero, U., Morelli, A. E., Castro, M. G., Lowenstein, P. R., and Fontana, A. (1999). Treatment of experimental glioma by administration of adenoviral vectors expressing Fas ligand. Hum Gene Ther *10*, 1641-1648.

Aoki, K., Akyurek, L.M., San, H., Leung, K., Parmacek, M.S., Nabel, E.G., and Nabel, G.J. (2000). Restricted expression of an adenoviral vector encoding Fas ligand (CD95L) enhances safety for cancer gene therapy. Mol Ther *1*, 555-565.

Arap, W., Pasqualini, R., and Ruoslahti, E. (1998). Cancer treatment by targeted drug delivery to tumor vasculature in a mouse model. Science *279*, 377-380.

Arap, W., Haedicke, W., Bernasconi, M., Kain, R., Rajotte, D., Krajewski, S., Ellerby, H. M., Bredesen, D. E., Pasqualini, R., and Ruoslahti, E. (2002a). Targeting the prostate for destruction through a vascular address. Proc Natl Acad Sci U S A *99*, 1527-1531.

Arap, W., Kolonin, M. G., Trepel, M., Lahdenranta, J., Cardo-Vila, M., Giordano, R. J., Mintz, P. J., Ardelt, P. U., Yao, V. J., Vidal, C. I.*, et al.* (2002b). Steps toward mapping the human vasculature by phage display. Nat Med *8*, 121-127.

Ausubel, F., Brent, R., Kingston, R., Moore, D., Seidman, J., Smith, J., and Struhl, K. (1987). Current protocols in molecular biology, Vol I. (New York, Wiley).

Baekelandt, V., Claeys, A., Eggermont, K., Lauwers, E., Strooper, B. D., Nuttin, B., and Debyser, Z. (2002). Characterization of lentiviral vector-mediated gene transfer in adult mouse brain. Hum Gene Ther *13*, 841-853.

Bansal, K., and Engelhard, H. (2000). Gene therapy for brain tumors. Curr Oncol Rep *2*, 463-472.

Baringer, J. R., and Swoveland, P. (1973). Recovery of herpes-simplex virus from human trigeminal ganglions. N Engl J Med *288*, 648-650.

Barry, M., Dower, W., and Johnston, S. (1996). Toward cell-targeting gene therapy vectors: selection of cell-binding peptides from random peptide-presenting phage libraries. Nat Med *2*, 299-305.

Batterson, W., and Roizman, B. (1983). Characterization of the herpes simplex virion-associated factor responsible for the induction of alpha genes. J Virol *46*, 371-377.

Bergers, G., Javaherian, K., Lo, K.M., Folkman, J., and Hanahan, D. (1999). Effects of angiogenesis inhibitors on multistage carcinogenesis in mice. Science *284*, 808-812.

Besnard, F., Brenner, M., Nakatani, Y., Chao, R., Purohit, H. J., and Freese, E. (1991). Multiple interacting sites regulate astrocyte-specific transcription of the human gene for glial fibrillary acidic protein. J Biol Chem *266*, 18877-18883.

Biernat, W., Kleihues, P., Yonekawa, Y., and Ohgaki, H. (1997). Amplification and overexpression of MDM2 in primary (de novo) glioblastomas. J Neuropathol Exp Neurol *56*, 180-185.

Black, A. R., and Azizkhan-Clifford, J. (1999). Regulation of E2F: a family of transcription factors involved in proliferation control. Gene *237*, 281-302.

Bonapace, I. M., Addeo, R., Altucci, L., Cicatiello, L., Bifulco, M., Laezza, C., Salzano, S., Sica, V., Bresciani, F., and Weisz, A. (1996). 17 beta-Estradiol overcomes a G_1 block induced by HMG-CoA reductase inhibitors and fosters cell cycle progression without inducing ERK-1 and -2 MAP kinases activation. Oncogene *12*, 753-763.

Boviatsis, E. J., Park, J. S., Sena-Esteves, M., Kramm, C. M., Chase, M., Efird, J. T., Wei, M. X., Breakefield, X. O., and Chiocca, E. A. (1994a). Long-term survival of rats harboring brain neoplasms treated with ganciclovir and a herpes simplex virus vector that retains an intact thymidine kinase gene. Cancer Res *54*, 5745-5751.

Boviatsis, E. J., Scharf, J. M., Chase, M., Harrington, K., Kowall, N. W., Breakefield, X. O., and Chiocca, E. A. (1994b). Antitumor activity and reporter gene transfer into rat brain neoplasms inoculated with herpes simplex virus vectors defective in thymidine kinase or ribonucleotide reductase. Gene Ther *1*, 323-331

Bowers, W., Olschowka, J., and Federoff, H. (2003). Immune responses to replication-defective HSV-1 type vectors within the CNS: implications for gene therapy. Gene Ther *10*, 941-945.

Bradley, J. D., Yasuhsi, K., Advani, S., Chung, S. M., Arani, R. B., Gillespie, G. Y., Whitley, R. J., Markert, J. M., Roizman, B., and Weichselbaum, R. R. (1999). Ionizing radiation improves survival in mice bearing intracranial high-grade gliomas injected with genetically modified herpes simplex virus. Clin Cancer Res *5*, 1517-1522.

Brem, H., and Gabikian, P. (2001) Biodegradable polymer implants to treat brain tumor. J Control Release *74*, 63-67.

Brenner, M., Kisseberth, W. C., Su, Y., Besnard, F., and Messing, A. (1994). GFAP promoter directs astrocyte-specific expression in transgenic mice. J Neurosci *14*, 1030-1037.

Bridgewater, J.A., Springer, C.J., Knox, R.J., Minton, N.P., Michael, N.P., and Collins, M.K. (1995). Expression of the bacterial nitroreductase enzyme in mammalian cells renders them selectively sensitive to killing by the prodrug CB1954. Eur J Cancer *31A*, 2362-2370.

Bridgewater, J.A., Knox, R.J., Pitts, J.D., Collins, M.K., and Springer, C.J. (1997). The bystander effect of the nitroreductase/CB1954 enzyme/prodrug system is due to a cell-permeable metabolite. Hum Gene Ther *8*, 709-717.

Brooks, A.I., Halterman, M.W., Chadwick, C.A., Davidson, B.L., Haak-Frendscho, M., Radel, C., Porter, C., and Federoff, H.J. (1998). Reproducible and efficient murine CNS gene delivery using a microprocessor-controlled injector. J Neurosci Methods *80*, 137-147.

Burger, P. C., Dubois, P. J., Schold, S. C., Jr., Smith, K. R., Jr., Odom, G. L., Crafts, D. C., and Giangaspero, F. (1983). Computerized tomographic and pathologic studies of the untreated, quiescent, and recurrent glioblastoma multiforme. J Neurosurg *58*, 159-169.

Burton, E. A., Wechuck, J. B., Wendell, S. K., Goins, W. F., Fink, D. J., and Glorioso, J. (2001). Multiple applications for replication-defective herpes simplex virus vectors. Stem Cells *19*, 358-377.

Cameron, J. M., McDougall, I., Marsden, H. S., Preston, V. G., Ryan, D. M., and Subak-Sharpe, J. H. (1988). Ribonucleotide reductase encoded by herpes simplex virus is a determinant of the pathogenicity of the virus in mice and a valid antiviral target. J Gen Virol *69 (Pt 10)*, 2607-2612.

Campa, M., Serlin, S., and Patz, E. J. (2002). Development of novel tumor imaging agents with phage-display combinatorial peptide libraries. Acad Radiol *9*, 927-932.

Cascino, I. I., Papoff, G., Eramo, A., and Ruberti, G. (1996). Soluble Fas/Apo-1 splicing variants and apoptosis. Front Biosci *1*, d12-18.

Castro, M., Cowen, R., Williamson, I., David, A., Jimenex-Dalmaroni, M., Yuan, X., Bigliari, A., Williams, J., Hu, J., and Lowenstein, P. (2003a). Current and future strategies for the treatment of malignant brain tumors. Pharmacol Ther *98*, 71-108.

Castro, M., Goverdhana, S., Hu, J., Jovel, N., Yuan, X., and Lowenstein, P. (2003b). Gene therapy for pituitary tumors: from preclinical models to clinical implementation. Front Neuroendocrinol *24*, 62-77.

Chang, S. M., Lamborn, K. R., Malec, M., Larson, D., Wara, W., Sneed, P., Rabbitt, J., Page, M., Nicholas, M. K., and Prados, M. D. (2004a). Phase II study of temozolomide and thalidomide with radiation therapy for newly diagnosed glioblastoma multiforme. Int J Radiat Oncol Biol Phys *60*, 353-357.

Chang, S. M., Seiferheld, W., Curran, W., Share, R., Atkins, J., Choucair, A., Kresl, J., Thoron, L., Cairncross, G., Gilbert, M.*, et al.* (2004b). Phase I study pilot arms of radiotherapy and carmustine with temozolomide for anaplastic astrocytoma (Radiation Therapy Oncology Group 9813): implications for studies testing initial treatment of brain tumors. Int J Radiat Oncol Biol Phys *59*, 1122-1126.

Chen, D., Murphy, B., Sung, R., and Bromberg, J. (2003). Adaptive and innate immune responses to gene transfer vectors: role of cytokines and chemokines in vector function. Gene Ther *10*, 991-998.

Chen, J., Bezdek, T., Chang, J., Kherzai, A. W., Willingham, T., Azzara, M., and Nisen, P. D. (1998). A glial-specific, repressible, adenovirus vector for brain tumor gene therapy. Cancer Res *58*, 3504-3507.

Cheney, W., Johnson, D., Vaillancort, M., Avanzini, J., Morimoto, A., Demers, G., Wills, K., Shabarm, P., Bolen, J., Tavtigian, S., and Bookstein, R. (1998). Suppression of tumorigenicity of glioblastoma cells by adenovirus mediated MMAC1/PTEN gene transfer. Cancer Res *58*, 2331-2334.

Chinnaiyan, A., O'Rourke, K., Tewari, M., and Dixit, V. (1995). FADD, a novel death domain-containing protein, interacts with the death domain of FAS and initiates apoptosis. Cell *81*, 505-512.

Chinnaiyan, A., Tepper, C., Seldin, M., O'Rourke, K., Kischkel, F., Hellbardt, S., Krammer, P., Peter, M., and Dixit, V. (1996). FADD/MORT1 is a common mediator of CD95 (Fas/APO-1) and tumor necrosis factor receptor-induced apoptosis. J Bio Chem *271*, 4961-4965.

Choi, C., and Benveniste, E. N. (2004). Fas ligand/Fas system in the brain: regulator of immune and apoptotic responses. Brain Res Brain Res Rev *44*, 65-81.

Chou, J., and Roizman, B. (1992). The γ34.5 gene of herpes simplex virus 1 precludes neuroblastoma cells from triggering total shutoff of protein synthesis characteristic of programmed cell death in neuronal cells. Proc Natl Acad Sci USA *89*, 3266-3270.

Clark, A. S., Deans, B., Stevens, M. F., Tisdale, M. J., Wheelhouse, R. T., Denny, B. J., and Hartley, J. A. (1995). Antitumor imidazotetrazines. 32. Synthesis of novel

imidazotetrazinones and related bicyclic heterocycles to probe the mode of action of the antitumor drug temozolomide. J Med Chem *38*, 1493-1504.

Cohen, K., Liu, T., Bissonette, R., Puri, R., and Frankel, A. (2003). DAB389EGF fusion protein therapy of refractory glioblastoma multiforme. Curr Pharm Biotechnol *4*, 39-49.

Constantini, L. C., Bakowska, J. C., Breakefield, X. O., and Isacson, O. (2000). Gene therapy in the CNS. Gene Ther *17*, 93-109.

Constantini, L. C., Jacoby, D. R., Wang, S., Fraefel, C., Breakefield, X. O., and Isacson, O. (1999). Gene transfer to the nigrostriatal system by hybrid herpes simplex virus/adeno-associated virus amplicon vectors. Hum Gene Ther *10*, 2481-2494.

Cooper, M. (2001). Non-infectious gene transfer and expression systems for cancer gene therapy. In Gene Therapy of Cancer, E. Lattime, and S. Gersm, eds. (CA, Academic Press).

Corey, L., and Spear, P. G. (1986). Infections with herpes simplex viruses (2). N Engl J Med *314*, 749-757.

Correa, R., Sasahara, R., Bengtson, M., Katayama, M., Salim, A., Brentani, M., Sogayar, M., De Souza, S., and Simpson, A. (2001). Human semaphorin 6B [(HSA)SEMA6B], a novel human class 6 semaphorin gene: alternative splicing and all-trans-retinoic acid-dependent downregulation in glioblastoma cell lines. Genomics *73*, 343-348.

Cortez, N., Trejo, F., Vergara, P., and Segovia, J. (2000). Primary astrocytes retrovirally transduced with a tyrosine hydroxylase transgene driven by a glial-specific promoter elicit behavioral recovery in experimental parkinsonism. J Neurosci Res *59*, 39-46.

Cosman, D. (1994). A family of ligands for the TNF receptor superfamily. Stem Cells *12*, 440-455.

Culver, K., Ram, Z, Wallbridge, S, Ishii, H, Oldfield, EH, Blaese, RM. (1992). In vivo gene transfer with retroviral vector-producer cells for treatment of experimental brain tumors. Science *256*, 1550-1552.

Cunningham, C., and Davidson, A. J. (1983). A cosmid-based system for constructing mutants of herpes simplex virus type 1. Virology *197*, 115-124.

Damek, D. M., and Hochberg, F. H. (1997). Clinical aspects of brain tumor. Curr Opin Neurol *10*, 452-458.

Das, A., Tan, W. L., Teo, J., and Smith, D. R. (2002). Glioblastoma multiforme in an Asian population: evidence for a distinct genetic pathway. J Neurooncol *60*, 117-125.

de Felipe, P., Izquierdo, M., Wandosell, F., and Lim, F. (2001). Integrating retroviral cassette extends gene delivery of HSV-1 expression to dividing cells. Biotechniques *31*, 394-402, 404-405.

Debinski, W., Obiri, N.I., Powers, S.K., Pastan, I., and Puri, R.K. (1995). Human glioma cells overexpress receptors for interleukin 13 and are extremely sensitive to a novel chimeric protein composed of interleukin 13 and pseudomonas exotoxin. Clin Cancer Res *1*, 1253-1258.

Debinski, W., Gibo, D. M., Slagle, B., Powers, S. K., and Gillespie, G. Y. (1999). Receptor for interleukin 13 is abundantly and specifically over-expressed in patients with glioblastoma multiforme. Int J Oncol *15*, 481-486.

Delaney, C.L., Brenner, M., and Messing, A. (1996). Conditional ablation of cerebellar astrocytes in postnatal transgenic mice. J Neurosci *16*, 6908-6918.

DeLuca, N.A., McCarthy, A.M., and Schaffer, P.A. (1985). Isolation and characterization of deletion mutants of herpes simplex virus type 1 in the gene encoding immediate-early regulatory protein ICP4. J Virol *56*, 558-570.

Drewinko, B., Patchen, M., Yang, L. Y., and Barlogie, B. (1981). Differential killing efficacy of twenty antitumor drugs on proliferating and nonproliferating human tumor cells. Cancer Res *41*, 2328-2333.

Dunn, I. F., Heese, O., and Black, P. M. (2000). Growth factors in glioma angiogenesis: FGFs, PDGF, EGF, and TGFs. J Neurooncol *50*, 121-137.

Dutta, A., and Stillman, B. (1992). cdc2 family kinases phosphorylate a human cell DNA replication factor, RPA, and activate DNA replication. Embo J *11*, 2189-2199.

Eddleston, M., and Mucke, L. (1993). Molecular profile of reactive astrocytes--implications for their role in neurologic disease. Neuroscience *54*, 15-36.

Elledge, S. J., Richman, R., Hall, F. L., Williams, R. T., Lodgson, N., and Harper, J. W. (1992). CDK2 encodes a 33-kDa cyclin A-associated protein kinase and is expressed before CDC2 in the cell cycle. Proc Natl Acad Sci U S A *89*, 2907-2911.

Elshami, A. A., Saavedra, A., Zhang, H., Kucharczuk, J. C., Spray, D. C., Fishman, G. I., Amin, K. M., Kaiser, L. R., and Albelda, S. M. (1996). Gap junctions play a role in the 'bystander effect' of the herpes simplex virus thymidine kinase/ganciclovir system in vitro. Gene Ther *3*, 85-92.

Enam S.A., Eisenberg A.D., Norman D., Rosenblum M.L. (1998). Patterns of spread and recurrence of glioma: studies by neuroimaging. In Brain Tumor Invasion: Biological, Clinical and Therapeutic Considerations. T Mikkelsen, R Bjerkvig, OD Lairum, and ML Rosenblum, eds. Wiley-Liss, Inc. pp. 133-159.

Eng, L. F., Vanderhaeghen, J. J., Bignami, A., and Gerstl, B. (1971). An acidic protein isolated from fibrous astrocytes. Brain Res *28*, 351-354.

Eng, L. F. (1985). Glial fibrillary acidic protein (GFAP): the major protein of glial intermediate filaments in differentiated astrocytes. J Neuroimmunol *8*, 203-214.

Eng, L. F., Ghirnikar, R. S., and Lee, Y. L. (2000). Glial fibrillary acidic protein: GFAP-thirty-one years (1969-2000). Neurochem Res *25*, 1439-1451.

Essler, M., and Ruoslahti, E. (2002). Molecular specialization of breast vasculature: a breast-homing phage-displayed peptide binds to aminopeptidase P in breast vasculature. Proc Natl Acad Sci U S A *99*, 2252-2257.

Eszterhas, S.K., Bouhassira, E.E., Martin, D.I., and Fiering, S. (2002). Transcriptional interference by independently regulated genes occurs in any relative arrangement of the genes and is influenced by chromosomal integration position. Mol Cell Biol *22*, 469-479.

Evans, T., Rosenthal, E. T., Youngblom, J., Distel, D., and Hunt, T. (1983). Cyclin: a protein specified by maternal mRNA in sea urchin eggs that is destroyed at each cleavage division. Cell *33*, 389-396.

Folkman, J. (1972). Anti-angiogenesis: New concept for therapy of solid tumors. Ann Surg *175*, 409-416.

Fraefel, C., Song, S., Lim, F., Lang, P., Yu, L., Wang, Y., Wild, P., and Geller, A. I. (1996). Helper virus-free transfer of herpes simplex virus type 1 plasmid vectors into neural cells. J Virol *70*, 7190-7197.

Fraefel, C., Jacoby, D. R., Lage, C., Hilderbrand, H., Chou, J. Y., Alt, F. W., Breakefield, X. O., and Majzoub, J. A. (1997). Gene transfer into hepatocytes mediated by helper virus-free HSV/AAV hybrid vectors. Mol Med *3*, 813-825.

Freeman, S. M., Abboud, C., Whartenby, K., Packman, C., Koeplin, D., Moolten, F., and Abraham, G. (1993). The "bystander effect": Tumor regression when a fraction of the tumor mass is genetically modified. Cancer Res *53*, 5274-5283.

Fueyo, J., Gomez-Manzano, C., Bruner, J. M., Saito, Y., Zhang, B., Levin, V. A., Yung, W. K. A., and Kyritsis, A. P. (1996). Hypermethylation of the CpG island of p16/CDKN2 correlates with gene inactivation in gliomas. Oncogene *13*, 1615-1619.

Fukuyama, K., Matsuzawa, K., Hubbard, S. L., Dirks, P. B., Murakami, M., and Rutka, J. T. (1996). Analysis of glial fibrillary acidic protein gene methylation in human malignant gliomas. Anticancer Res *16*, 1251-1257.

Gao, H., and Hui, K.M. (2001). Synthesis of a novel series of cationic lipids that can act as efficient gene delivery vehicles through systematic heterocyclic substitution of cholesterol derivatives. Gene Ther *8,* 855-863.

Gaspar, L. E., Fisher, B. J., Macdonald, D. R., LeBer, D. V., Halperin, E. C., Schold, S. C., Jr., and Cairncross, J. G. (1992). Supratentorial malignant glioma: patterns of recurrence and implications for external beam local treatment. Int J Radiat Oncol Biol Phys *24*, 55-57.

Georges, P., Przedborski, S., Brotchi, J., Chatel, M., Gedouin, D., and Hildebrand, J. (1988). Effect of HECNU in malignant supratentorial gliomas--a phase II study. J Neurooncol *6*, 211-219.

Gerolami, R., Uch, R., Jordier, F., Chapel, S., Bagnis, C., Brechot, C., and Mannoni, P. (2000). Gene transfer to hepatocellular carcinoma: transduction efficacy and transgene expression kinetics by using retroviral and lentiviral vectors. Cancer Gene Ther *7*, 1286-1292.

Giese A., Westphal M. (2001). Treatment of malignant glioma: a problem beyond the margins of resection. J Cancer Res Clin Oncol *127*, 217-225.

Gluzman-Poltorak, Z., Cohen, T., Herzog, Y., and Neufeld, G. (2000). Neuropilin-2 and Neuropilin-1 are receptors for the 165-amino acid form of vascular endothelial growth factor (VEGF) and of placenta growth factor-2, but only neuropilin-2 functions as a receptor for the 145-amino acid form of VEGF. J Biol Chem *275*, 18040-18045.

Gossen, M., and Bujard, H. (1992). Tight control of gene expression in mammalian cells by tetracycline-responsive promoters. Proc Natl Acad Sci U S A *89*, 5547-5551.

Grandi, P., Wang, S., Schuback, D., Krasnykh, V., Spear, M., Curiel, D., Manservigi, R., and Breakefield, X. (2003). HSV-1 virions engineered for specific binding to cell surface receptors. Mol Ther *9*, 419-427.

Grandi, P., Spear, M., Breakefield, X., and Wang, S. (2004). Targeting HSV amplicon vectors. Methods *33*, 179-186.

Grimm, S., Stanger, B., and Leder, P. (1996). RIP and FADD: Two "death domain" -containing proteins can induce apoptosis by convergent, but dissociable, pathways. Proc Natl Acad Sci U S A *93*, 10923-10927.

Hampl, J. A., Camp, S. M., Mydlarz, W. K., Hampl, M., Ichikawa, T., Chiocca, E. A., Louis, D. N., Sena-Esteves, M., and Breakefield, X. O. (2003). Potentiated gene delivery to tumors using herpes simplex virus/Epstein-Barr virus/RV tribrid amplicon vectors. Hum Gene Ther *14*, 611-626.

Hao, C., Beguinot, F., Condorelli, G., Trencia, A., Van Meir, E. G., Yong, V. W., Parney, I. F., Roa, W. H., and Petruk, K. C. (2001). Induction and intracellular regulation of tumor necrosis factor-related apoptosis-inducing ligand (TRAIL) mediated apoptosis in human malignant glioma cells. Cancer Res *61*, 1162-1170.

Harrow, S., Papanastassiou, V., Harland, J., Mabbs, R., Petty, R., Fraser, M., Hadley, D., Patterson, J., Brown, S. M., and Rampling, R. (2004). HSV1716 injection into the brain adjacent to tumour following surgical resection of high-grade glioma: safety data and long-term survival. Gene Ther *11*, 1648-1658.

He, J., Olson, J. J., and James, C. D. (1995). Lack of p16INK4 or retinoblastoma protein (pRB), or amplification-associated overexpression of CDK4 is observed in distinct subsets of malignant glial tumors and cell lines. Cancer Res *55*, 4833-4836.

Heister, T., Heid, I., Ackermann, M., and Fraefel, C. (2002). Herpes simplex virus type 1/adeno-associated virus hybrid vectors mediate site-specific integration at the adeno-associated virus preintegration site, AAVS1, on human chromosome 19. J Virol *76*, 7163-7173.

Henglein, B., Chenivesse, X., Wang, J., Eick, D., and Brechot, C. (1994). Structure and cell cycle-regulated transcription of the human cyclin A gene. Proc Natl Acad Sci U S A *91*, 5490-5494.

Henson, J. W., Schnitker, B. L., Correa, K. M., von Deimling, A., Fassbender, F., Xu, H. J., Benedict, W. F., Yandell, D. W., and Louis, D. N. (1994). The retinoblastoma gene is involved in malignant progression of astrocytomas. Ann Neurol *36*, 714-721.

Herrlinger, U., Kramm, C. M., Aboody-Guterman, K. S., Silver, J. S., Ikeda, K., Johnston, K. M., Pechan, P. A., Barth, R. F., Finkelstein, D., Chiocca, E. A.*, et al.* (1998). Pre-existing herpes simplex virus 1 (HSV-1) immunity decreases, but does not abolish, gene transfer to experimental brain tumors by a HSV-1 vector. Gene Ther *5*, 809-819.

Herrlinger, U., Pechan, P. A., Jacobs, A. H., Woiciechowski, C., Rainov, N. G., Fraefel, C., Paulus, W., and Reeves, S. A. (2000). HSV-1 infected cell proteins influence tetracycline-regulated transgene expression. J Gene Med *2*, 379-389.

Higgins, G.M., and Anderson, R.M. (1931). Experimental pathology of the liver. Arch Pathol *12*, 186-201

Hirose, Y., Berger, M. S., and Pieper, R. O. (2001). p53 effects both the duration of G2/M arrest and the fate of temozolomide-treated human glioblastoma cells. Cancer Res *61*, 1957-1963.

Hirose, Y., Katayama, M., Berger, M. S., and Pieper, R. O. (2004). Cooperative function of Chk1 and p38 pathways in activating G2 arrest following exposure to temozolomide. J Neurosurg *100*, 1060-1065.

Hirsch, F.R., Varella-Garcia, M., Bunn, P.A. Jr., Di Maria, M.V., Veve, R., Bremnes, R.M., Baron, A.E., Zeng, C., and Franklin, W.A. (2003). Epidermal growth factor receptor in non-small-cell lung carcinomas: correlation between copy number and protein expression and impact on prognosis. J Clin Oncol *21*, 3798-3807.

Hirt, B. (1967). Selective extraction of polyoma DNA from infected mouse cell cultures. J Mol Bio *26*, 365-369.

Ho, D. Y., Mocarski, E. S., and Sapolsky, R. M. (1993). Altering central nervous system physiology with a defective herpes simplex virus vector expressing the glucose transporter gene. Proc Natl Acad Sci U S A *90*, 3655–3659.

Hofmann, H. S., Hansen, G., Burdach, S., Bartling, B., Silber, R. E., and Simm, A. (2004). Discrimination of human lung neoplasm from normal lung by two target genes. Am J Respir Crit Care Med *170*, 516-519.

Holgersson, A., Heiden, T., Castro, J., Edgren, M. R., Lewensohn R., and Meijer, A.E. (2005). Different G2/M accumulation in M059J and M059K cells after exposure to DNA double-strand break-inducing agents. Int J Radiation Oncology Biol Phys *61*, 915-921.

Holland, E. C. (2000). Glioblastoma multiforme: the terminator. Proc Natl Acad Sci U S A *97*, 6242-6244.

Hsich, G., Sena-Esteves, M., and Breakefield, X. O. (2002). Critical issues in gene therapy for neurologic disease. Hum Gene Ther *13*, 579-604.

Huber, B., Austin, E., Richards, C., Davis, S., and Good, S. (1994). Metabolism of 5-fluorocytosine to 5-fluorouracil in human colorectal tumor cells transduced with the cytosine deaminase gene: significant antitumor effects when only a small percentage of tumor cells express cytosine deaminase. Proc Natl Acad Sci U S A *91*, 8302-8306.

Huet, X., Rech, J., Plet, A., Vie, A., and Blanchard, J. M. (1996). Cyclin A expression is under negative transcriptional control during the cell cycle. Mol Cell Biol *16*, 3789-3798.

Hughes, B.W., King, S.A., Allan, P.W., Parker, W.B., and Sorscher, E.J. (1998). Cell to cell contact is not required for bystander cell killing by Escherichia coli purine nucleoside phosphorylase. J Biol Chem *273*, 2322-2328.

Hunter, W. D., Martuza, R. L., Feigenbaum, F., Todo, T., Mineta, T., Yazaki, T., Toda, M., Newsome, J. T., Platenberg, R. C., Manz, H. J., *et al.* (1999). Attenuated, replication-competent herpes simplex virus type 1 mutant G207: safety evaluation of intracerebral injection in nonhuman primates. J Virol *73*, 6319-6326.

Husain, S.R., Joshi, B.H., and Puri, R.K. (2001). Interleukin-13 receptor as a unique target for anti-glioblastoma therapy. Int J Cancer. *92*, 168-175.

Husain, S.R. and Puri, R.K. (2003). Interleukin-13 receptor-directed cytotoxin for malignant glioma therapy: from bench to bedside. J Neurooncol. *65*, 37-48.

Igney, F.H., and Krammer, P.H. (2002). Death and anti-death: tumour resistance to apoptosis. Nat Rev Cancer *2*, 277-288.

Ignowski, J. M., and Schaffer, D. V. (2004). Kinetic analysis and modeling of firefly luciferase as a quantitative reporter gene in live mammalian cells. Biotechnol Bioeng *86*, 827-834.

Ilsey, D. D., Lee, S. H., Miller, W. H., and Kutcha, R. D. (1995). Acyclic guanosine analogs inhibit DNA polymerase alpha, delta and epsilon with very different potencies and have unique mechanism of action. Biochemistry *34*, 2504-2510.

Ivics, Z., Kaufman, C. D., Zayed, H., Miskey, C., Walisko, O., and Izsvak, Z. (2004). The Sleeping Beauty transposable element: evolution, regulation and genetic applications. Curr Issues Mol Biol *6*, 43-55.

Jäättelä, M. (2004). Multiple cell death pathways as regulators of tumour initiation and progression. Oncogene *23*, 2746-2756.

Jakobsson, J., Ericson, C., Jansson, M., Bjork, E., and Lundberg, C. (2003). Targeted transgene expression in rat brain using lentiviral vectors. J Neurosci Res *73*, 876-885.

Jerome, V., and Müller, R. (1998). Tissue-specific, cell cycle-regulated chimeric transcription factors for the targeting of gene expression to tumor cells. Hum Gene Ther *9*, 2653-2659.

Jiang, Z., Zheng, X., Lytle, R. A., Higashikubo, R., and Rich, K. M. (2004). Lovastatin-induced up-regulation of the BH3-only protein, Bim, and cell death in glioblastoma cells. J Neurochem *89*, 168-178.

Johansson, C. B., Svensson, M., Wallstedt, L., Janson, A. M., and Frisen, J. (1999). Neural stem cells in the adult human brain. Exp Cell Res *253*, 733-736.

Johnston, K. M., Jacoby, D., Pechan, P. A., Fraefel, C., Borghesani, P., Schuback, D., Dunn, R. J., Smith, F. I., and Breakefield, X. O. (1997). HSV/AAV hybrid amplicon vectors extend transgene expression in human glioma cells. Hum Gene Ther *8*, 359-370.

Joshi, B.H., Husain, S.R., and Puri, R.K. (2000). Preclinical studies with IL-13PE38QQR for therapy of malignant glioma. Drug News Perspect. *13*, 599-605.

Jounaidi, Y., and Waxman, D.J. (2004). Use of replication-conditional adenovirus as a helper system to enhance delivery of P450 prodrug-activation genes for cancer therapy. Cancer Res *64*, 292-303.

Juo, P., Kuo, C. J., Yuan, J., and Blenis, J. (1998). Essential requirement for caspase-8/FLICE in the initiation of the Fas-induced apoptotic cascade. Curr Biol *8*, 1001-1008.

Kanzawa, T., Germano, I.M., Kondo, Y., Ito, H., Kyo, S., and Kondo, S. (2003). Inhibition of telomerase activity in malignant glioma cells correlates with their sensitivity to temozolomide. Br J Cancer *89*, 922-929.

Karlsson, T., Henriksson, R., and Hedman, H. (2004). Induction of apoptosis in resistant glioma cells by synthetic caspase-activation. J Neuro-Oncol *66*, 71-79.

Kayagaki, N., Kawasaki, A., Ebata, T., Ohmoto, H., Ikeda, S., and Inoue, S. (1995). Metalloproteinase-mediated release of human Fas ligand. J Exp Med *182*, 1777-1783.

Kleihues, P., Louis, D., Scheithauer, B., Rorke, L., Reifenberger, G., Burger, P., and Cavenee, W. (2002). The WHO classification of tumors of the nervous system. J Neuropathol Exp Neurol *61*, 215-225.

Knight, M.J., Riffkin, C.D., Muscat, A.M., Ashley, D.M., and Hawkins, C.J. (2001). Analysis of FasL and TRAIL induced apoptosis pathways in glioma cells. Oncogene *20*, 5789-5798.

Knox, P.G., Milner, A.E., Green, N.K., Eliopoulos, A.G., and Young, L.S. (2003). Inhibition of mellatoproteinase cleavage enhances the cytotoxicity of Fas ligand. J Immunol *170*, 677-685.

Koga, S., Hirohata, S., Kondo, Y., Komata, T., Takakura, M., Inoue, M., Kyo, S., and Kondo, S. (2001). FADD gene therapy using the human telomerase catalytic subunit (hTERT) gene promoter to restrict induction of apoptosis to tumors in vitro and in vivo. Anticancer Res *21*, 1937-1943.

Koivunen, E., Arap, W., Rajotte, D., Lahdenranta, J., and Pasqualini, R. (1999). Identification of receptor ligands with phage display peptide libraries. J Nucl Med *40*, 883-888.

Kolberg, M., Strand, K.R., Graff, P., and Andersson, K.K. (2004). Structure, function, and mechanism of ribonucleotide reductases. Biochim Biophys Acta *1699*, 1-34.

Komata, T., Kondo, Y., Kanzawa, T., Hirohata, S., Koga, S., Sumiyoshi, H., Srinivasula, S. M., Barna, B. P., Germano, I. M., Takakura, M.*, et al.* (2001). Treatment of malignant glioma cells with the transfer of constitutively active caspase-6 using the human telomerase catalytic subunit (human telomerase reverse transcriptase) gene promoter. Cancer Res *61*, 5796-5802.

Komata, T., Kondo, Y., Kanzawa, T., Ito, H., Hirohata, S., Koga, S., Sumiyoshi, H., Takakura, M., Inoue, M., Barna, B. P.*, et al.* (2002). Caspase-8 gene therapy using the human telomerase reverse transcriptase promoter for malignant glioma cells. Hum Gene Ther *13*, 1015-1025.

Kondo, S., Ishizaka, Y., Okada, T., Kondo, Y., Hitomi, M., Tanaka, Y., Haqqi, T., Barnett, G., and Barna, B. (1998). FADD gene therapy for malignant gliomas in vitro and in vivo. Hum Gene Ther *9*, 1599-1608.

Krisky, D. M., Wolfe, D., Goins, W. F., Marconi, P. C., Ramakrishnan, R., Mata, M., Rouse, R. J., Fink, D. J., and Glorioso, J. C. (1998). Deletion of multiple immediate-early genes from herpes simplex virus reduces cytotoxicity and permits long-term gene expression in neurons. Gene Ther *5*, 1593-1603.

Kumar-Singh, R., and Farber, D. B. (1998). Encapsidated adenovirus mini-chromosome-mediated delivery of genes to the retina: application to the rescue of photoreceptor degeneration. Hum Mol Genet *7*, 1893-1900.

Kuriyama, N., Kuriyama, H., Julin, C.M., Lamborn, K., Israel, M.A. (2000). Pretreatment with protease is a useful experimental strategy for enhancing adenovirus-mediated cancer gene therapy. Hum Gene Ther *11*, 2219-2230.

Kwong, A. D., J.A., K., and Frenkel, N. (1988). Herpes simplex virus virion host shut-off function. J Virol *62*, 912-921.

Lachmann, R. H. (2004). Herpes Simplex Virus-based Vectors. Int J Exp Path *85*, 177-190.
Lam, P. Y., and Breakefield, X. O. (2001). Potential of gene therapy for brain tumors. Hum Mol Genet *10*, 777-787.

Lam, P. Hui, K.M., Wang, Y., Allen, P.D., Louis, D.N., Yuan, C.J., and Breakefield, X.O. (2002). Dynamics of transgene expression in human glioblastoma cells mediated by herpes simplex virus/adeno-associated virus amplicon vectors. Hum Gene Ther *13*, 2147-2159.

Laquerre, S., Anderson, D. B., Stolz, D. B., and Glorioso, J. C. (1998). Recombinant herpes simplex virus type 1 engineered for targeted binding to erythropoietin receptor-bearing cells. J Virol *72*, 9683-9697.

Laywell, E. D., Rakic, P., Kukekov, V. G., Holland, E. C., and Steindler, D. A. (2000). Identification of a multipotent astrocytic stem cell in the immature and adult mouse brain. Proc Natl Acad Sci U S A *97*, 13883-13888.

Leibel, S.A., Scott, C.B., and Loeffler, J.S. (1994). Contemporary approaches to the treatment of malignant gliomas with radiation therapy. Semin Oncol *21*, 198-219.

Li, J., Yen, C., Liaw, D., Podsypanina, K., Bose, S., Wang, S. I., Puc, J., Miliaresis, C., Rodgers, L., McCombie, R.*, et al.* (1997). PTEN, a putative protein tyrosine phosphatase gene mutated in human brain, breast and prostate cancer. Science *275*, 1943-1946.

Lieber, A., He, C. Y., and Kay, M. A. (1997). Adenoviral preterminal protein stabilizes mini-adenoviral genomes in vitro and in vivo. Nat Biotechnol *15*, 1383-1387.

Liu, H., Jacobs, B.S., Liu, J., Prayson, R.A., Estes, M.L., Barnett, G.H., and Barna, B.P. (2000). Interleukin-13 sensitivity and receptor phenotypes of human glial cell lines: non-neoplastic glia and low-grade astrocytoma differ from malignant glioma. Cancer Immunol Immunother *49*, 319-324.

Liu, N., Lucibello, F. C., Korner, K., Wolfraim, L. A., Zwicker, J., and Müller, R. (1997). CDF-1, a novel E2F-unrelated factor, interacts with cell cycle-regulated repressor elements in multiple promoters. Nucleic Acids Res *25*, 4915-4920.

Liu, N., Lucibello, F. C., Engeland, K., and Müller, R. (1998). A new model of cell cycle-regulated transcription: repression of the cyclin A promoter by CDF-1 and anti-repression by E2F. Oncogene *16*, 2957-2963.

Liu, R., Enstrom, A., and KS, L. (2003). Combinatorial peptide library methods for immunobiology research. Exp Hematol *31*, 11-30.

Louis, D. N., and Gusella, J. F. (1995). A tiger behind many doors: multiple genetic pathways to malignant glioma. Trends Genet *11*, 412-415.

Lucibello, F. C., Truss, M., Zwicker, J., Ehlert, F., Beato, M., and Müller, R. (1995). Periodic cdc25C transcription is mediated by a novel cell cycle-regulated repressor element (CDE). Embo J *14*, 132-142.

Madhankumar, A. B., Mintz, A., and Debinski, W. (2004). Interleukin 13 mutants of enhanced avidity toward the glioma-associated receptor, IL13Ralpha2. Neoplasia *6*, 15-22.

Maleniak, T. C., Darling, J. L., Lowenstein, P. R., and Castro, M. G. (2001). Adenovirus-mediated expression of HSV1-TK or Fas ligand induces cell death in primary human glioma-derived cell cultures that are resistant to the chemotherapeutic agent CCNU. Cancer Gene Ther *8*, 589-598.

Manickan, E., Yu, Z., Rouse, R. J., Wire, W. S., and Rouse, B. T. (1995). Induction of protective immunity against herpes simplex virus with DNA encoding the immediate early protein ICP 27. Viral Immunol *8*, 53-61.

Marin, O., Yaron, A., Bagri, A., Tessier-Lavigne, M., and Rubenstein, J. (2001). Sorting of striatal and cortical interneurons regulated by semaphorin-neuropilin interactions. Science *293*, 872-875.

Martín-Satué, M., and Blanco, J. (1999). Identification of semaphorin E gene expression in metastatic human lung adenocarcinoma cells by mRNA differential display. J Surg Oncol *72*, 18-23.

Martuza, R., Malick, A., Markert, J.M., Ruffner, K.L., Coen, D.M. (1991). Experimental therapy of human glioma by means of a genetically engineered virus mutant. Science *252*, 854-856.

Masood, K., Besnard, F., Su, Y., and Brenner, M. (1993). Analysis of a segment of the human glial fibrillary acidic protein gene that directs astrocyte-specific transcription. J Neurochem *61*, 160-166.

Matthews, T., and Boehme, R. (1988). Antiviral activity and mechanism of action of ganciclovir. Rev Infect Dis *10 Suppl 3*, S490-494.

McKie, E. A., Graham, D. I., and Brown, S. M. (1998). Selective astrocytic transgene expression in vitro and in vivo from the GFAP promoter in a HSV RL1 null mutant vector--potential glioblastoma targeting. Gene Ther *5*, 440-450.

Medzhitov, R., and Janeway Jr, C. (1997). Innate immunity: impact on the adaptive immune response. Curr Opin Immunol *9*, 4-9.

Miao, H., Lee, P., Lin, H., Soker, S., and Klagsbrun, M. (2000). Neuropilin-1 expression by tumor cells promotes tumor angiogenesis and progression. Faseb J *14*, 2532-2539.

Michalopoulos, G. K., and DeFrances, M. C. (1997). Liver Regeneration. Science *276*, 60-66.

Millauer, B., Shawver, L. K., Plate, K. H., Risau, W., and Ullrich, A. (1994). Glioblastoma growth inhibited in vivo by dominant-negative Flk-1 mutant. Nature *367*, 576-579.

Mineta, T., Rabkin, S. D., and Martuza, R. L. (1994). Treatment of malignant gliomas using ganciclovir-hypersensitive, ribonucleotide reductase-deficient herpes simplex viral mutant. Cancer Res *54*, 3963-3966.

Mintz, A., Gibo, D. M., Slagle-Webb, B., Christensen, N. D., and Debinski, W. (2002). IL-13Ralpha2 is a glioma-restricted receptor for interleukin-13. Neoplasia *4*, 388-399.

Mischel, P., and Cloughesy, T. (2003). Targeted molecular therapy of GBM. Brain Pathol *13*, 52-61.

Moolten, F. L., and Wells, J. M. (1990). Curability of tumors bearing herpes thymidine kinase genes transferred by retrovirus vectors. J Natl Cancer Inst *82*, 297-300.

Morelli, A.E., Larregina, A.T., Smith-Arica, J., Dewey, R.A., Southgate, T.D., Ambar, B., Fontana, A., Castro, M.G., and Lowenstein, P.R. (1999). Neuronal and glial cell type-specific promoters within adenovirus recombinants restrict the expression of the apoptosis-inducing molecule Fas ligand to predetermined brain cell types, and abolish peripheral liver toxicity. J Gen Virol *80*, 571-583.

Morsy, M. A.,Gu, M., Motzel, S., Zhao, J., Lin, J., Su, Q., Allen, H., Franlin, L., Parks, R. J., Graham, F. L.*, et al.* (1998). An adenoviral vector deleted for all viral coding sequences results in enhanced safety and extended expression of a leptin transgene. Proc Natl Acad Sci U S A *95*, 7866-7871.

Nagane, M., Coufal, F., Lin, H., Bogler, O., Cavenee, W. K., and Huang, H. J. (1996). A common mutant epidermal growth factor receptor confers enhanced tumorigenicity on human glioblastoma cells by increasing proliferation and reducing apoptosis. Cancer Res *56*, 5079-5086.

Nettelbeck, D. M., Jerome, V., and Müller, R. (1999). A dual specificity promoter system combining cell cycle-regulated and tissue-specific transcriptional control. Gene Ther *6*, 1276-1281.

Newlands, E. S., Foster, T., and Zaknoen, S. (2003). Phase I study of temozolamide (TMZ) combined with procarbazine (PCB) in patients with gliomas. Br J Cancer *89*, 248-251.

Ng, H. K., and Lam, P. Y. (1998). The molecular genetics of central nervous system tumors. Pathology *30*, 196-202.

Nigro, J. M., Baker, S. J., and Preisinger, A. C. (1989). Mutations in the p53 gene occur in diverse human tumor types. Nature *342*, 705-708.

Nilaver, G., Muldoon, L., Kroll, R., Pagel, M., Breakefield, X., Davidson, B., and Neuwelt, E. (1995). Delivery of herpesvirus and adenovirus to nude rat intracerebral tumors after osmotic blood-brain barrier disruption. Proc Natl Acad Sci U S A *92*, 9829-9833.

O'Connell, J., O'Sullivan, G., Collins, J., and F, S. (1996). The Fas counterattack: Fas-mediated T cell killing by colon cancer cells expressing Fas ligand. J Exp Med *184*, 1075-1082.

Oehmig, A., Fraefel, C., and Breakefield, X.O. (2004). Update on herpesvirus amplicon vectors. Mol Ther *10*, 630-643.

Oh, M., Choi, J., Kim, I.H., Lee, Y.H., Huh, J.Y., Park, Y. K., Lee, K. W., Chough, S.Y., Joo, K.S., Ku, B.S., *et al.* (2000). Detection of epidermal growth factor receptor in the serum of patients with cervial carcinoma. Clin Cancer Res *6*, 4760-5763.

Olschowka, J. A., Bowers, W. J., Hurley, S. D., Mastrangelo, M. A., and Federoff, H. J. (2003). Helper-free HSV-1 amplicons elicit a markedly less robust innate immune response in the CNS. Mol Ther *7*, 218-227.

Papanastassiou, V., Rampling, R., Fraser, M., Petty, R., Hadley, D., Nicoll, J., Harland, J., Mabbs, R., and Brown, M. (2002). The potential for efficacy of the modified (ICP 34.5 (-)) herpes simplex virus 1716 following intratumoral injection into human malignant glioma: a proof of principle study. Gene Ther *9*, 198-406.

Parmley, S., and Smith, G. (1989). Antibody-selectable filamentous fd phage vectors: affinity purification of target genes. Gene *73*, 305-318.

Pasqualini, R., and Ruoslahti, E. (1996). Organ targeting in vivo using phage display peptide libraries. Nature *380*, 364-366.

Pasqualini, R., Koivunen, E., Kain, R., Lahdenranta, J., Sakamoto, M., Stryhn, A., Ashmun, R. A., Shapiro, L. H., Arap, W., and Ruoslahti, E. (2000). Aminopeptidase N is a receptor for tumor-homing peptides and a target for inhibiting angiogenesis. Cancer Res *60*, 722-727.

Patel, S., Zhang, X., Collins, L., and Fabre, J.W. (2001). A small, synthetic peptide for gene delivery via the serpin-enzyme complex receptor. J Gene Med *3*, 271-279.

Paul, D. B., and Kruse, C. A. (2001). Immunologic approaches to therapy for brain tumors. Curr Neurol Neurosci Rep *1*, 238-244.

Pekny, M., Eliasson, C., Chien, C.L., Kindblom, L.G., Liem, R., Hamberger, A., and Belsholtz, C. (1998). GFAP-deficient astrocytes are capable of stellation in vitro when cocultured with neurons and exhibit a reduced amount of intermediate filaments and an increased cell saturation density. Exp Cell Res *239*, 332-343.

Pines, J., and Hunter, T. (1990). p34cdc2: the S and M kinase? New Biol *2*, 389-401.

Plate, K. H., and Risau, W. (1995). Angiogenesis in malignant gliomas. Glia *15*, 339-347.

Pollock, R., and Clackson, T. (2002). Dimerizer-regulated gene expression. Curr Opin Biotechnol *13*, 459-467.

Powell, W. C., Fingleton, B., Wilson, C. L., Boothby, M., and Matrisian, L. M. (1999). The metalloproteinase matrilysin proteolytically generates active soluble Fas ligand and potentiates epithelial cell apoptosis. Curr Biol *9*, 1441-1447.

Preston, C.M., Mabbs, R., and Nicholl, M.J. (1997). Construction and characterization of herpes simplex virus type 1 mutants with conditional defects in immediate early gene expression. Virology *229*, 228-239.

Preston, C.M., Rinaldi, A., and Nicholl, M.J. (1998). Herpes simplex virus type 1 immediate early gene expression is stimulated by inhibition of protein synthesis. J Gen Virol *79*, 117-124.

Quintana, J. G., Lopez-Colberg, I. I., and Cunningham, L. A. (1998). Use of GFAP-lacZ transgenic mice to determine astrocyte fate in grafts of embryonic ventral midbrain. Brain Res Dev Brain Res *105*, 147-151.

Qureshi, N., Bankiewicz, K., Louis, D., Hochberg, F., Chiocca, E., and Harsh, G. T. (2000). Multicolumn infusion of gene therapy cells into human brain tumors: technical report. Neurosurgery *46*, 663-668.

Rainov, N., Zimmer, C., Chase, M., Kramm, C., Chiocca, E., Weissleder, R., and Breakefield, X. (1995). Selective uptake of viral and monocrystalline particles delivered intra-arterially to experimental brain neoplasms. Hum Gene Ther *6*, 1543-1552.

Rainov, N. (2000). A phase III clinical evaluation of herpes simplex virus type 1 thymidine kinase and ganciclovir gene therapy as an adjuvant to surgical resection and radiation in adults with previously untreated glioblastoma multiforme. Hum Gene Ther *11*, 2389-2401.

Rainov, N., and Kramm, C. (2001). Vector delivery methods and targeting strategies for gene therapy of brain tumors. Curr Gene Ther *1*, 367-383.

Rainov, N., and Ren, H. (2003). Gene therapy for human malignant brain tumors. Cancer J *9*, 180-188.

Rajcani, J., and Vojvodova, A. (1998). The role of herpes simplex virus glycoproteins in the virus replication cycle. Acta Virol *42*, 103-118.

Rajotte, D., Arap, W., Hagedorn, M., Koivunen, E., Pasqualini, R., and Ruoslahti, E. (1998). Molecular heterogeneity of the vascular endothelium revealed by in vivo phage display. J Clin Invest *102*, 430-437.

Ralph, G. S., Bienemann, A., Harding, T. C., Hopton, M., Henley, J., and Uney, J. B. (2000). Targeting of tetracycline-regulatable transgene expression specifically to neuronal and glial cell populations using adenoviral vectors. Neuroreport *11*, 2051-2055.

Rasmussen, U., Schreiber, V., Schultz, H., Mischler, F., and Schughart, K. (2002). Tumor cell-targeting by phage-displayed peptides. Cancer Gene Ther *9*, 606-612.

Ravi, D., Ramadas, K., Mathew, B. S., Nalinakumari, K. R., Nair, M. K., and Pillai, M. R. (1998). Angiogenesis during tumor progression in the oral cavity is related to reduced apoptosis and high tumor cell proliferation. Oral Oncol *34*, 543-548.

Read, G. S., and Frenkel, N. (1983). Herpes simplex virus mutants defective in the virion associated shut-off of host polypeptide synthesis and exhibiting abnormal synthesis of alpha (immediate early) viral polypeptides. J Virol *46*, 498-512.

Rieger, J., Wick, W., and Weller, M. (2003). Human malignant glioma cells express semaphorins and their receptors, neuropilins and plexins. Glia *42*, 379-389.

Rinaldi, A., Marshall, K., and Preston, C. (1999). A non-cytotoxic herpes simplex virus vector which expresses Cre recombinase directs efficient site specific recombination. Virus Res *65*, 11-20.

Rodriguez, L. A., and Levin, V. A. (1987). Does chemotherapy benefit the patient with a central nervous system glioma? Oncology (Huntingt) *1*, 29-36, 40-21.

Roizman, B., and Sears, A. (1996). Herpes simplex viruses and their replication. In Fields Virology, B. N. Fields, D. M. Knipe, and P. M. Howley, eds. (Philadelphia, Lippincott-Raven), pp. 2231-2295.

Roth, W., Isenmann, S., Nakamura, M., Platten, M., Wick, W., Kleihues, P., Bahr, M., Ohgaki, H., Ashkenazi, A., and Weller, M. (2001). Soluble decoy receptor 3 is expressed by malignant gliomas and suppresses CD95 ligand-induced apoptosis and chemotaxis. Cancer Res *61*, 2759-2765.

Rubinchik, S., Wang, D., Yu, H., Fan, F., Luo, M., Norris, J., and Dong, J. (2001). A complex adenovirus vector that delivers FasL-GFP with combined prostate-specific and tetracycline-regulated expression. Mol Ther *4*, 416-426.

Rubinchik, S., Yu, H., Woraratanadharm, J., Voelkel-Jonson, C., Norris, J.S., and Dong, J.Y. (2003). Enhanced apoptosis of glioma cell lines is achieved by co-delivering FasL-GFP and TRAIL with a complex Ad5 vector. Cancer Gene Ther *10*, 814-822.

Rutka, J. T., and Smith, S. L. (1993). Transfection of human astrocytoma cells with glial fibrillary acidic protein complementary DNA: analysis of expression, proliferation, and tumorigenicity. Cancer Res *53*, 3624-3631.

Rutka, J. T., Hubbard, S. L., Fukuyama, K., Matsuzawa, K., Dirks, P. B., and Becker, L. E. (1994). Effects of antisense glial fibrillary acidic protein complementary DNA on the growth, invasion, and adhesion of human astrocytoma cells. Cancer Res *54*, 3267-3272.

Rutka, J. T., Murakami, M., Dirks, P. B., Hubbard, S. L., Becker, L. E., Fukuyama, K., Jung, S., Tsugu, A., and Matsuzawa, K. (1997). Role of glial filaments in cells and tumors of glial origin: a review. J Neurosurg *87*, 420-430.

Saas, P., Walker, P., Hahne, M., Quiquerez, A., Schnuriger, V., Perrin, G., French, L., Van Meir, E., de Tribolet, N., Tschopp, J., *et al.* (1997). Fas ligand expression by astrocytoma in vivo: maintaining immune privilege in the brain? J Clin Invest *99*, 1173-1178.

Sacks, W. R., Greene, C. C., Aschman, D. P., and Schaffer, P. A. (1985). Herpes simplex virus type 1 ICP27 is an essential regulatory protein. J Virol *55*, 796-805.

Saeki, Y., Ichikawa, T., Saeki, A., Chiocca, E. A., Tobler, K., Ackermann, M., Breakefield, X. O., and Fraefel, C. (1998). Herpes simplex virus type 1 DNA amplified as bacterial artificial chromosome in Escherichia coli: rescue of replication-competent virus progeny and packaging of amplicon vectors. Hum Gene Ther *9*, 2787-2794.

Saeki, Y., Fraefel, C., Ichikawa, T., Breakefield, X. O., and Chiocca, E. A. (2001). Improved helper virus-free packaging system for HSV amplicon vectors using an ICP27-deleted, oversized HSV-1 DNA in a bacterial artificial chromosome. Mol Ther *3*, 591-601.

Saeki, Y., Breakefield, X. O., and Chiocca, E. A. (2003). Improved HSV-1 amplicon packaging system using ICP27-deleted, oversized HSV-1 BAC DNA. Methods Mol Med *76*, 51-60.

Saleh, M., Stackeer, S. A., and Wilks, A. F. (1996). Inhibition of growth of C6 glioma cells in vivo by expression of antisense vascular endothelial growth factor sequence. Cancer Res *56*, 393-401.

Sallot, M., Ordener, C., Lascombe, I., Propper, A., Adessi, G. L., and Jouvenot, M. (1996). Differential EGF action on nuclear protooncogenes in human endometrial carcinoma RL95-2 cells. Anticancer Res *16*, 401-406.

Samaniego, L.A., Wu, N., and DeLuca, N.A. (1997). The herpes simplex virus immediate-early protein ICP0 affects transcription from the viral genome and infected-cell survival in the absence of ICP4 and ICP27. J Virol *71*, 4614-4625.

Samaniego, L.A., Neiderhiser, L., and DeLuca, N.A. (1998). Persistence and expression of the herpes simplex virus genome in the absence of immediate-early proteins. J Virol *72*, 3307-3320.

Sambrook J., Fritsch, E.F., and Maniatis, T. (1989). Molecular Cloning: a laboratory manual. (New York, Cold Spring Harbor Lab Press).

Samoylova, T., Morrison, N., and Cox, N. (2003). Molecular markers of glial tumors: current targeting strategies. Curr Med Chem *10*, 831-843.

Sandberg-Wollheim, M., Malmstrom, P., Stromblad, L. G., Anderson, H., Borgstrom, S., Brun, A., Cronqvist, S., Hougaard, K., and Salford, L. G. (1991). A randomized study of chemotherapy with procarbazine, vincristine, and lomustine with and without radiation therapy for astrocytoma grades 3 and/or 4. Cancer *68*, 22-29.

Sandler, V. M., Wang, S., Angelo, K., Lo, H. G., Breakefield, X. O., and Clapham, D. E. (2002) Modified herpes simplex virus delivery of enhanced GFP into the central nervous sytem. J Neurosci Methods *121,* 211-219

Sarafan-Vasseur, N., Lamy, A., Bourguignon, J., Pessot, F. L., Hieter, P., Sesboue, R., Bastard, C., Frebourg, T., and Flaman, J. M. (2002). Overexpression of B-type cyclins alters chromosomal segregation. Oncogene *21*, 2051-2057.

Schlosser, S.F., Azzaroli, F., Dao, T., Hingorani, R., Nicholas Crispe, I., and Boyer, J.L. (2000). Induction of murine hepatocyte death by membrane-bound CD95 (Fas/APO-1)-ligand: characterization of an in vitro system. Hepatology *32*, 779-785.

Schmidt, F., Groscurth, P., Kermer, M., Dichgans, J., and Weller, M. (2001). Lovastatin and phenylacetate induce apoptosis, but not differentiation, in human malignant glioma cells. Acta Neuropathol (Berl) *101*, 217-224.

Schneider, P., Holler, N., Bodmer, J., Hahne, M., Frei, K., Fontana, A., and Tschopp, J. (1998). Conversion of membrane-bound Fas (CD95) ligand to its soluble form is associated with downregulation of its proapoptotic activity and loss of liver toxicity. J Exp Med *187*, 1205-1213.

Schnell, M. A., Zhang, Y., Tazelaar, J., Gao, G. P., Yu, Q. C., Qian, R., Chen, S. J., Varnavski, A. N., LeClair, C., Raper, S. E., *et al.* (2001). Activation of innate immunity in nonhuman primates following intraportal administration of adenoviral vectors. Mol Ther *3*, 708-722.

Schumacher, T., Hofer, S., Eichhorn, K., Wasner, M., Zimmerer, S., Freitag, P., Probst, A., Gratzl, O., Reubi, J., Maecke, H., *et al.* (2002). Local injection of the 90Y-labelled peptidic vector DOTATOC to control gliomas of WHO grades II and III: an extended pilot study. Eur J Nucl Med Mol Imaging *29*, 486-493.

Schwartz, B., Benoist, C., Abdallah, B., Rangara, R., Hassan, A., Scherman, D., and Demeneix, B.A. (1996). Gene transfer by naked DNA into adult mouse brain. Gene Ther *3*, 405-411.

Sena-Esteves, M., Saeki, Y., Fraefel, C., and Breakefield, X. O. (2000). HSV-1 amplicon vectors--simplicity and versatility. Mol Ther *2*, 9-15.

Shibata, T., Giaccia, A., and Brown, J. (2000). Development of a hypoxia-responsive vector for tumor-specific gene therapy. Gene Ther *7*, 493-498.

Shinohara, H., Yagita, H., Ikawa, Y., and Oyaizu, N. (2000). Fas drives cell cycle progression in glioma cells via extracellular signal-regulated kinase activation. Cancer Res *60*, 1766-1772.

Shinoura, N., Yoshida, Y., Asai, A., Kirino, T., and Hamada, H. (2000). Adenovirus-mediated transfer of p53 and Fas ligand drastically enhances apoptosis in gliomas. Cancer Gene Ther *7*, 732-738.

Short, M. P., Choi, B. C., Lee, J. K., Malick, A., Breakefield, X. O., and Martuza, R. L. (1990). Gene delivery to glioma cells in rat brain by grafting of a retrovirus packaging cell line. J Neurosci Res *27*, 427-439.

Sidransky, D., Mikkelsen, T., Schwechheimer, K., Rosenblue, M. L., Cavanee, W., and Vogelstein, B. (1992). Clonal expansion of p53 mutant cells is associated with brain tumor progression. Nature *355*, 846-847.

Silbergeld, D. L., and Chicoine, M. R. (1997). Isolation and characterization of human malignant glioma cells from histologically normal brain. J Neurosurg *86*, 525-531.

Simmons, M.L., Lamborn, K.R., Takahashi, M., Chen, P., Israel, M.A., Berger, M.S., Godfrey, T., Nigro, J., Prados, M., Chang, S., *et al.* (2001). Analysis of complex relationship between age, p53, epidermal growth factor receptor, and survival in glioblastoma patients. Cancer Res *61*, 1122-1128.

Smibert, C., Johnson, D., and Smiley, J. (1992). Identification and characterization of the virion-induced host shutoff product of herpes simplex virus gene UL41. J Gen Virol *73*, 467-470.

Smith-Arica, J. R., Morelli, A. E., Larregina, A. T., Smith, J., Lowenstein, P. R., and Castro, M. G. (2000). Cell-type-specific and regulatable transgenesis in the adult brain: adenovirus-encoded combined transcriptional targeting and inducible transgene expression. Mol Ther *2*, 579-587.

Song, S., Wang, Y., Bak, S.Y., Lang, D., Ullrey, D., Neve, R.L., O'Malley, K.L., and Geller, A.I. (1997). An HSV-1 vector containing the rat tyrosine hydroxylase promoter enhaces both long-term and cell type-specific expression in the midbrain. J Neurochem *68*, 1792-1803.

Souweidane, M.M., Occhiogrosso, G., Mark, E.B., and Edgar, M.A. (2004). Interstitial infusion of IL13-PE38QQR in the rat brain stem. J Neurooncol. *67*, 287-293.

Spaete, R., and Frenkel, N. (1982). The herpes virus amplicon: A new eucaryotic defective-virus cloning-amplifying vector. Cell *30*, 295-304.

Spaete, R. R., and Frenkel, N. (1985). The herpes simplex virus amplicon: analyses of cis-acting replication functions. Proc Natl Acad Sci U S A *82*, 694-698.

Spear, P. G. (1993). Entry of alpha herpesviruses into cells. Semin Virol *4*, 167-180.

Spear, M. A., Sun, F., Eling, D. J., Gilpin, E., Kipps, T. J., Chiocca, E. A., and Bouvet, M. (2000). Cytotoxicity, apoptosis, and viral replication in tumor cells treated with oncolytic ribonucleotide reductase-defective herpes simplex type 1 virus (hrR3) combined with ionizing radiation. Cancer Gene Ther *7*, 1051-1059.

Spear, M., Breakefield, X., Beltzer, J., Schuback, D., Weissleder, R., Pard, F., and Ladner, R. (2001). Isolation, characterization, and recovery of small peptide phage display epitopes selected against viable malignant glioma cells. Cancer Gene Ther *8*, 506-511.

Spear, M. A., Schuback, D., Miyata, K., Grandi, P., Sun, F., Yoo, L., Nguyen, A., Brandt, C. R., and Breakefield, X. O. (2003). HSV-1 amplicon peptide display vector. J Virol Methods *107*, 71-79.

Stavropoulos, T. A., and Strathdee, C. A. (1998). An enhanced packaging system for helper-dependent herpes simplex virus vectors. J Virol *72*, 7137-7143.

Steck, A., Pershouse, M. A., Jasser, S. A., Yung, W. K., Lin, H., Lig, A. H., Lanford, L., Baumgard, M. L., Hattier, T., Davis, T.*, et al.* (1997). Identification of a candidate tumor suppressor gene, MMAC1, at chromosome 10q23.3 that is mutated in multiple advanced cancers. Nat Genet *15*, 356-362.

Stewart, L. (2002). Chemotherapy in adult high-grade glioma: a systematic review and meta-analysis of individual patient data from 12 randomised trials. Lancet *359*, 1011-1018.

Su, B., and Karin, M. (1996). Mitogen-activated protein kinase cascades and regulation of gene expression. Curr Opin Immunol *8*, 402-411.

Suda, T., Hashimoto, H., Tanaka, M., Ochi, T., and Nagata, S. (1997). Membrane Fas ligand kills human peripheral blood T lymphocytes, and soluble Fas ligand blocks the killing. J Exp Med *186*, 2045-2050.

Sundaresan, P., Hunter, W. D., Martuza, R. L., and Rabkin, S. D. (2000). Attenuated, replication-competent herpes simplex virus type 1 mutant G207: safety evaluation in mice. J Virol *74*, 3832-3841.

Sunpaweravong, P., Sunpaweravong, S., Puttawibul, P., Mitarnun, W., Zeng, C., Baron, A.E., Franklin, W., Said, S., and Varella-Garcia, M. (2004). Epidermal growth factor receptor and cyclin D1 are independently amplified and overexpressed in esophageal squamous cell carcinoma. J Cancer Res Clin Oncol. *Epub*.

Swenson, K. I., Farrell, K. M., and Ruderman, J. V. (1986). The clam embryo protein cyclin A induces entry into M phase and the resumption of meiosis in Xenopus oocytes. Cell *47*, 861-870.

Szardenings, M., Tornroth, S., Mutulis, F., Muceniece, R., Keinanen, K., Kusinene, A., and Wikberg, J. (1997). Phage display selection on whole cells yields a peptide specific for melanocortin receptor 1. J Biol Chem *272*, 27943-27948.

Tai, C., Logg, C., Park, J., Anderson, W., Press, M., and Kasahara, N. (2003). Antibody-mediated targeting of replication-competent retroviral vectors. Hum Gene Ther *14*, 789-802.

Takamiya, Y., Short, M. P., Moolten, F. L., Fleet, C., Mineta, T., Breakefield, X. O., and Martuza, R. L. (1993). An experimental model of retrovirus gene therapy for malignant brain tumors. J Neurosurg *79*, 104-110.

Takeda, T., Inaba, H., Yamazaki, M., Kyo, S., Miyamoto, T., Suzuki, S., Ehara, T., Kakizawa, T., Hara, M., DeGroot, L. J., *et al.* (2003). Tumor-specific gene therapy for undifferentiated thyroid carcinoma utilizing the telomerase reverse transcriptase promoter. J Clin Endocrinol Metab *88*, 3531-3538.

Takemoto, M., Kuroda, M., Urano, M., Nishimura, Y., Kawasaki, S., Kato, H., Okumura, Y., Akaki, S., Kanazawa, S., Asaumi, J.*, et al*. (2003). The effect of various chemotherapeutic agents given with mild hyperthermia on different types of tumours. Int J Hyperthermia *19*, 193-203.

Tal-Singer, R., Peng, C., Ponce De Leon, M., Abrams, W. R., Banfield, B. W., Tufaro, F., Cohen, G. H., and Eisenberg, R. J. (1995). Interaction of herpes simplex virus glycoprotein gC with mammalian cell surface molecules. J Virol *69*, 4471-4483.

Tamagnone, L., Artigiani, S., Chen, H., He, Z., Ming, G., Song, H., Chedotal, A., Winberg, M., Goodman, C., Poo, M.*, et al.* (1999). Plexins are a large family of receptors for transmembrane, secreted, and GPI-anchored semaphorins in vertebrates. Cell *99*, 71-80.

Tanaka, M., Itai, T., Adachi, M., and Nagata, S. (1998). Downregulation of Fas ligand by shedding. Nat Med *4*, 31-36.

Tanaka, M., Suda, T., Takahashi, T., and Nagata, S. (1995). Expression of the functional soluble form of human Fas ligand in activated lymphocytes. EMBO J *14*, 1129-1135.

Tanaka, T., Manome, Y., Wen, P., Kufe, D. W., and Fine, H. A. (1997). Viral vector-mediated transduction of a modified platelet factor 4 cDNA inhibits angiogenesis and tumor growth. Nat Med *3*, 437-442.

Thomas, C. E., Schiedner, G., Kochanek, S., Castro, M. G., and Lowenstein, P. R. (2000). Peripheral infection with adenovirus causes unexpected long-term brain inflammation in animals injected intracranially with first-generation, but not with high-capacity, adenovirus

vectors: Toward realistic long-term neurological gene therapy for chronic diseases. Proc Natl Acad Sci U S A *97*, 7482-7487.
Thompson, J. F., Hayes, L. S., and Lloyd, D. B. (1991). Modulation of firefly luciferase stability and impact on studies of gene regulation. Gene *103*, 171-177.

Toniatti, C., Bujard, H., Cortese, R., and Ciliberto, G. (2004). Gene therapy progress and prospects: transcription regulatory systems. Gene Ther *11*, 649-657.

Trepel, M., Arap, W., and Pasqualini, R. (2002). In vivo phage display and vascular heterogeneity: implications for targeted medicine. Curr Opin Chem Biol *6*, 399-404.

Ueki, K., Ono, Y., Henson, J. W., Efird, J. T., von Deimling, A., and Louis, D. N. (1996). CDKN2/p16 or RB alterations occur in the majority of glioblastomas and are inversely correlated. Cancer Res *56*, 150-153.

Ueno, M., Koyama, F., Yamada, Y., Fujimoto, H., Takayama, T., Kamada, K., Naito, A., Hirao, S., Mukogawa, T., Hamada, H., *et al*. (2001). Tumor-specific chemo-radio-gene therapy for colorectal cancer cells using adenovirus vector expressing the cytosine deaminase gene. Anticancer Res *21*, 2601-2608.

Van Beusechem, V., Grill, J., Mastenbroek, D., Wickham, T., Roelvink, P., Haisma, H., Lamfers, M., Dirven, C., Pinedo, H., and Gerritsen, W. (2002). Efficient and selective gene transfer into primary human brain tumors by using single-chain antibody-targeted adenoviral vectors with native tropism abolished. J Virol *76*, 2753-2762.

Vandier, D., Rixe, O., Brenner, M., Gouyette, A., and Besnard, F. (1998). Selective killing of glioma cell lines using an astrocyte-specific expression of the herpes simplex virus-thymidine kinase gene. Cancer Res *58*, 4577-4580.

Vandier, D., Rixe, O., Besnard, F., Kim, M., Rikiyama, T., Goldsmith, M., Brenner, M., Gouyette, A., and Cowan, K. H. (2000). Inhibition of glioma cells in vitro and in vivo using a recombinant adenoviral vector containing an astrocyte-specific promoter. Cancer Gene Ther *7*, 1120-1126.

Varghese, S., Newsome, J. T., Rabkin, S. D., McGeagh, K., Mahoney, D., Nielsen, P., Todo, T., and Martuza, R. L. (2001). Preclinical safety evaluation of G207, a replication-competent

herpes simplex virus type 1, inoculated intraprostatically in mice and nonhuman primates. Hum Gene Ther *12*, 999-1010.

Varghese, S., and Rabkin, S. D. (2002). Oncolytic herpes simplex virus vectors for cancer virotherapy. Cancer Gene Ther *9*, 967-978.

Verma, I. M. (2000). A tumultuous year for gene therapy. Mol Ther *2*, 415-416.

von Deimling, A., von Ammon, K., Schoenfeld, D., Wiestler, O. D., Seizinger, B. R., and Louis, D. N. (1993). Subsets of glioblastoma multiforme defined by molecular genetic analysis. Brain Pathol *3*, 19-26.

von Deimling, A. (1997). Molecular genetic classification of astrocytic and oligodendroglial tumors. Brain Pathol *7*, 1311-1313.

Wakimoto, H., Johnson, P., DM, K., and Chiocca, E. (2003). Effects of innate immunity on herpes simplex virus and its ability to kill tumor cells. Gene Ther *10*, 983-990.

Walter, K. A., Tarmago, R. J., Olivi, A., Burger, P., and Brem, H. (1995). Intratumoral chemotherapy. Neurosurgery *37*, 1128-1145.

Wang, S., and Vos, J. M. (1996). A hybrid herpesvirus infectious vector based on Epstein-Barr virus and herpes simplex virus type 1 for gene transfer into human cells in vitro and in vivo. J Virol *70*, 8422-8430.

Wang, S., Fraefel, C., and Breakefield, X. (2002). HSV-1 amplicon vectors. Methods Enzymol *346*, 593-603.

Wang, Y., Camp, S.M., Niwano, M., Shen, X., Bakowska, J.C., Breakefield, X.O., and Allen, P.D. (2002). Herpes simplex virus type 1/adeno-associated virus rep(+) hybrid amplicon vector improves the stability of transgene expression in human cells by site-specific integration. J Virol *76*, 7150-7162.

Wang, Y., Yu, L., and Geller, A. I. (1999). Diverse stabilities of expression in the rat brain from different cellular promoters in a helper virus-free herpes simplex virus type 1 vector system. Hum Gene Ther *10*, 1763-1771.

Wasner, M., Haugwitz, U., Reinhard, W., Tschop, K., Spiesbach, K., Lorenz, J., Mossner, J., and Engeland, K. (2003). Three CCAAT-boxes and a single cell cycle genes homology region (CHR) are the major regulating sites for transcription from the human cyclin B2 promoter. Gene *312*, 225-237.

Wejde, J., Carlberg, M., Hjertman, M., and Larsson, O. (1993). Isoprenoid regulation of cell growth: identification of mevalonate-labelled compounds inducing DNA synthesis in human breast cancer cells depleted of serum and mevalonate. J Cell Physiol *155*, 539-548.

Weller, M., Frei, K., Groscurth, P., Krammer, P., Yonekawa, Y., and Fontana, A. (1994). Anti-Fas/APO-1 antibody-mediated apoptosis of cultured human glioma cells, induction and modulation of sensitivity by cytokines. J Clin Invest *94*, 954-964.

Weller, M., Malipiero, U., Rensing-Ehl, A., Barr, P., and Fontana, A. (1995). Fas/APO-1 gene transfer for human malignant glioma. Cancer Res *55*, 2936-2944.

Weyerbrock, A., and Oldfield, E. (1999). Gene transfer technologies for malignant gliomas. Curr Opin Oncol *11*, 168-173.

White, S., Nicklin, S., Sawamura, T., and Baker, A. (2001). Identification of peptides that target the endothelial cell-specific LOX-1 receptor. Hypertension *27*, 449-455.

Wilcken, N. R., Musgrove, E. A., and Sutherland, R. L. (1997). Different points of action of retinoids and anti-estrogens in G1 phase identified in synchronized T-47D breast cancer cells. Int J Cancer *70*, 291-296.

Worgall, S., Wolff, G., Falck-Pedersen, E., and Crystal, R. G. (1997). Innate immune mechanisms dominate elimination of adenoviral vectors following in vivo administration. Hum Gene Ther *8*, 37-44.

Wu, G.Y., and Wu, C.H. (1987). Receptor-mediated in vitro gene transformation by a soluble DNA carrier system. J Biol Chem *262*, 4429-4432.

Wu, L., Timmers, C., Maiti, B., Saavedra, H. I., Sang, L., Chong, G. T., Nuckolls, F., Giangrande, P., Wright, F. A., Field, S. J., *et al*. (2001). The E2F1-3 transcription factors are essential for cellular proliferation. Nature *414*, 457-462.

Wysocka, J., and Herr, W. (2003). The herpes simplex virus VP16-induced complex: the makings of a regulatory switch. Trends Biochem Sci *28*, 294-304.

Xu, B., Kim, S. T., Lim, D. S., and Kastan, M. B. (2002). Two molecularly distinct G2/M checkpoints are induced by ionizing radiation. Mol Cell Biol *22*, 1049-1059.

Yamada, Y., Kimura, H., Morishima, T., Daikoku, T., Maeno, K., and Nishiyama, Y. (1991). The pathogenicity of ribonucleotide reductase-null mutants of herpes simplex virus type 1 in mice. J Infect Dis *164*, 1091-1097.

Yamini, B., Yu, X., Gillespie, G. Y., Kufe, D. W., and Weichselbaum, R. R. (2004). Transcriptional targeting of adenovirally delivered tumor necrosis factor alpha by temozolomide in experimental glioblastoma. Cancer Res *64*, 6381-6384.

Yant, S. R., Ehrhardt, A., Mikkelsen, J. G., Meuse, L., Pham, T., and Kay, M. A. (2002). Transposition from a gutless adeno-transposon vector stabilizes transgene expression in vivo. Nat Biotechnol *20*, 999-1005.

Yung, W. K., Prados, M. D., Yaya-Tur, R., Rosenfeld, S. S., Brada, M., Friedman, H. S., Albright, R., Olson, J., Chang, S. M., O'Neill, A. M.*, et al.* (1999). Multicenter phase II trial of temozolomide in patients with anaplastic astrocytoma or anaplastic oligoastrocytoma at first relapse. Temodal Brain Tumor Group. J Clin Oncol *17*, 2762-2771.

Yung, W. K., Albright, R. E., Olson, J., Fredericks, R., Fink, K., Prados, M. D., Brada, M., Spence, A., Hohl, R. J., Shapiro, W., *et al*. (2000). A phase II study of temozolomide vs. procarbazine in patients with glioblastoma multiforme at first relapse. Br J Cancer *83*, 588-593.

Zauner, W., Kichler, A., Schmidt, W., Mechtler, K., and Wagner, E. (1997). Glycerol and polylysine synergize in their ability to rupture vesicular membranes: a mechanism for increased transferrin-polylysine-mediated gene transfer. Exp Cell Res *232*, 137-145.

Zhang, J., Spring, H., and Schwab, M. (2001). Neuroblastoma tumor cell-binding peptides identified through random peptide phage display. Cancer Lett *171*, 153-164.

Zhang, G.R., Wang, X., Yang, T., Sun, M., Zhang, W., Wang, Y., and Geller, A.I. (2000). A tyrosine hydroxylase-neurofilament chimeric promoter enhances long-term expression in rat forebrain neurons from helper virus-free HSV-1 vectors. Brain Res Mol Brain Res *8*, 17-31.

Zwicker, J., Gross, C., Lucibello, F. C., Truss, M., Ehlert, F., Engeland, K., and Müller, R. (1995a). Cell cycle regulation of cdc25C transcription is mediated by the periodic repression of the glutamine-rich activators NF-Y and Sp1. Nucleic Acids Res *23*, 3822-3830.

Zwicker, J., Lucibello, F.C., Wolfraim, L.A., Gross, C., Truss, M., Engeland, K., and Müller, R. (1995b). Cell cycle regulation of the cyclin A, cdc25C and cdc2 genes is based on a common mechanism of transcriptional repression. EMBO J *14*, 4514-4522.

Zwicker, J., Lucibello, F. C., Jerome, V., Brusselbach, S., and Müller, R. (1997). CDF-1-mediated repression of cell cycle genes targets a specific subset of transactivators. Nucleic Acids Res *25*, 4926-4932.

Zwicker, J., Korner, K., and Müller, R. (1999). The SV40 large T oncoprotein disrupts DNA-binding of the cell cycle-regulated transcriptional repressor CDF-1. Oncogene *18*, 2023-2025.